Approved For Release 2009/05/01 : CIA-RDP80T00246A007500340002-0

25X1

Page Denied

Approved For Release 2009/05/01 : CIA-RDP80T00246A007500340002-0

Approved For Release 2009/05/01 : CIA-RDP80T00246A007500340002-0

One Flow Cascade Cycle

(in Schemes of Natural Gas Liquefaction and Separation)

A.P. KLEEMENKO, C.T.S.
Institute for Gas Research of the Academy of Sciences,
Kiev, U.S.S.R.

The use of a multi-component mixture in the capacity of a cooling agent in cycles of deep and moderate cooling cycles, as is shown in this paper, may present a considerable thermodynamic effect.

As is generally known, energy consumption in a refrigerating cycle is determined by the degree of irreversibility of separate processes constituting the cycle. In all the throttle cycles, which comprise all the steam compression cycles of moderate cold and the combined multi-flow cycle of deep cooling Picte cycle, the losses caused by the irreversibility of heat-exchange and throttling processes are major factors which determine the effectivity of deep cooling cycles.

The irreversibility of a heat-exchange process is determined by the temperature difference in that process.

An ideal heat-exchange process, which is characterized by a zero temperature difference, is theoretically possible only at a counter current, when equal regularities of alteration of heat exchange of cold bearer and consumer in the function of temperature occur:

$$G_1 C_{p1} \varphi_1 (t) = G_2 C_{p2} \varphi_2 (t) \qquad (1)$$

where: G_1 and G_2 - amounts of substance in straight and reverse flows

$C_{p1} \varphi_1 (t)$ and $C_{p2} \varphi_2 (t)$ - heat capacities of straight and reverse flows in the function of temperature

As a result of unequality of heat capacities of the substances involved in the heat exchange and the nonconformity of their relations to temperatures, it appears possible to create, in most cases, a temperature difference only at one end of the heat exchanger. The temperature difference at the other end appears to be rigidly fixed by physical properties of the substances involved in the heat exchange. The values of these temperature differences are sometimes very great in deep cooling. As a result of this phenomenon, the coefficient of thermodynamic reversibility of the heat exchanging apparatus decreases.

In order to reduce the losses during the heat exchange processes in cooling and liquation of gases, it appears necessary that the source of cold - the cooling agent, by means of which the cooling and liquation of gas is brought about, should have about the same relation $t = \varphi(i)$ as the gas that is being liquefied.

Approved For Release 2009/05/01 : CIA-RDP80T00246A007500340002-0

Approved For Release 2009/05/01 : CIA-RDP80T00246A007500340002-0

The use of one component cooling agents boiling at constant temperature predetermines high values of temperature differences at one end of the heat exchanger (or in the middle of it) and causes high values of losses on heat exchange and consequently higher energy consumption.

Multi-component mixtures have variable boiling temperatures. When using multi-component systems, it becomes possible to achieve the validity of the relation determined by the equation (1) for the gas which is being liquefied and the cooling agent of multi-component composition. In such a case the temperature differences along the entire "length" of the heat exchanger will be the smallest, whereas the coefficient of thermodynamic reversibility of the heat exchanging apparatus increases. Energy consumption in the refrigerating process will be lowered correspondingly.

According to our computations and data available in literature, the utilization of the propane-butane binary mixture, instead of ammonia, in a refrigerating cycle of moderate cold for achieving temperatures - 25° - - 30°C causes a decrease of energy consumption by 15 - 25 %.

The throttling of any substance without exception in the liquid state is always more effective than that of any substance in the gaseous state. The coefficient of thermodynamic reversibility of the throttling process of a fluid reaches very high values, amounting to a figure of the order of 0.8 - 0.9 in the zone of temperature beyond the critical.

The transition of a gas into the liquid state may take place not only as a result of the condensing of the gas, but because of its being solved in another fluid as well.

The presence of a solvent causes the transition of a gas into the liquid state at temperatures far above those of condensation and even at temperatures above the critical. This effect may be utilized in refrigerating cycles. When cooling a compressed binary or a multi-component gas mixture consisting of gases with various boiling points the first component to liquefy is that having the highest boiling point. The liquid thus formed dissolves the other components of the gas mixture; and as a result the liquid is transformed into low boiling components, which at the given temperature and in the absence of high boiling components cannot condensate. A low boiling component will be desorbed from such a multi-component mixture at the time of its being throttled (similarly as steam is evolved in the process of pure substance throttling).

The decrease of the temperature level of gas liquefaction processes as a result of absorption raises the thermodynamic reversibility of low temperature refrigerating cycles. The combining of both the compression and absorption cycles permits increasing the thermodynamic effectivity and simplifying the constructional design of the installation.

Approved For Release 2009/05/01 : CIA-RDP80T00246A007500340002-0

Approved For Release 2009/05/01 : CIA-RDP80T00246A007500340002-0

The one flow cascade cycle of deep cooling developed by the author and investigated by the author and his collaborators is based on the theoretical propositions listed in this paper: a multi-component mixture of hydrocarbons is being utilized as a cooling agent (other cooling agents forming ideal solutions, as freons, may be used).

The combining of the composition of hydrocarbon mixture and pressure permits obtaining cold at any temperature level in the range up to - 160°C and below that figure when operating under vacuum. The mixture composition and pressure are selected so as to satisfy the heat exchange at minimum temperature differences.

On the other hand, the mounting and the construction of the one flow cascade cycle are such that only the throttling of the liquid phase is being carried out in it. The latter phenomenon, as has been mentioned previously, predetermines the high value of the coefficient of the thermodynamic reversibility of the process.

The suggested one flow cascade cycle which has been investigated on a pilot scale, may be used in the following cases:

a) In the processes of methane liquefaction.

b) In cycles of air liquefaction and separation - in the capacity of an element of deep preliminary cooling up to the above mentioned temperatures.

c) In cycles of gas separation in cracking and pyrolysis.

d) In cold producing installations with parameters -80 - 100°C.

In addition to the aforementioned thermodynamic advantages of cycles with multi-component cooling agents, the one flow cascade cycle has the following peculiarity: heat emission at the low pressure side takes place in conditions of constant evaporation of the mixture components complicated by purely gaseous heat exchange. The heat emission coefficients are hereby increased just at the low pressure side.

Description of the One Flow Cascade Cycle Pilot Plant

The pilot plant for investigating the one flow cascade cycle consists of the following elements: a) a compressor, EC, with intermediate cooling arrangements and an end cooler, b) a first stage liquid separator, SL-I, and a second stage one, SL-II, c) a heat exchanger consisting of two sections, HE-I and HE-II, d) a receiver R and e) a system of throttling valves, EY-I, EY-2 and EY-3.

Investigations of two operating regimes were made at that plant: a) a half-closed cooling cycle for natural gas liquefaction and b) a closed cooling cycle for air liquefaction.

Approved For Release 2009/05/01 : CIA-RDP80T00246A007500340002-0

Approved For Release 2009/05/01 : CIA-RDP80T00246A007500340002-0

Using the regime for natural gas liquefaction, the installation operates as follows: natural gas, consisting chiefly of methane and containing 3.5% of ethane, propane, and butanes, enters the arrangement for gas drying and purification. The drying is carried out by means of alum silica gel up to the dew point -40 - 45°C. Purification from CO_2 is carried out by means of solid potassium hydroxide KOH. The dried and purified gas enters the three-stage compressor C. When experimenting with gases containing propane and butanes only, the condensate, as a rule, was precipitated after the end condenser E in the liquid separator SL-I. This condensate was throttled in the widener (Throttling) valve EY-I and discharged into the low pressure branch of the first section of the heat exchanger HE-I. The steam phase was directed under high pressure from the liquid separator SL-I into the high pressure branch of the same section. There at the expense of the reverse flow cold and that of the evaporation of the condensate it was cooled up to the temperature -40°C. In this way practically all the butanes and up to 80 - 90 % of the propane of the mixture are condensated and a considerable amount of propane and ethane was dissolved. The liquid obtained from the process described is separated from the steam phase in the separator SL-II and after having been throttled in the widening valve EY-2 is directed to the low pressure branch of the second section of the heat exchanger HE-II. The cold obtained on the evaporation of the liquid is transferred to the high pressure flow and as a result it is fully condensated and partly overcooled.

After having been throttled up to the pressure 1.2 atm. and separated from the steam phase, the liquefied natural gas is transferred into the storehouse along the pipeline LNG.

The operating conditions of the installation in respect of pressure, concentrations of hydrocarbons C_2, C_3, C_4 were so chosen as to bring their absolute amounts in the natural gas (in the pipeline LNG) to less than one half of their contents in the initial gas in the pipeline NG.

The installation works in a closed circuit under the operating conditions for air liquefaction (or for liquation of natural gas with a very low percentage of heavy hydrocarbons), with both pipelines NG and LNG detached. The cold was withdrawn from the system through heat exchanger A-LA and was spent for liquefaction of air (or natural gas containing 98.5% of methane and 1.2% of nitrogen.

Object and Procedure of Experiment

The object of the experiment was to determine the optimum parameters of the scheme: composition of cooling agent, pressure, temperature and position of condensate sampling. Temperature was measured by means of thermocouples located at sixteen points (see numeration in fig.1). Testing of the cooling agent was carried out by means of a gas-analyzer CIATIM-51. Experiments were performed on a binary mixture methane-propane and a triple one methane-ethane-propane. Results of the experiment with the binary mixture methane-

Approved For Release 2009/05/01 : CIA-RDP80T00246A007500340002-0

Approved For Release 2009/05/01 : CIA-RDP80T00246A007500340002-0

propane in closed circuit are shown in fig. 2. The relation - cooling agent composition $\gamma = \varphi(p)$ (as characterized by methane content) - working pressure is shown in curve "a". The relation: temperature of liquid after throttling from liquid separators SL-I and SL-II - in function of working pressure - is given in curves "b" and "c".

Energy consumption for obtaining 1000 kcal of cold at temperature level -156°C is shown in fig. 3. During experiments with that installation on a triple mixture methane-propane-butane somewhat lower energy consumption was obtained, the optimum being shifted to low pressure area. For that optimum: Working pressure: 60 - 65 ata., Mixture composition: C_1 - 65% mol, C_3 - 20%m, C_4 - 15%.

Temperature of liquid sampling from SL-II - from -50° C up to -30°C.

For obtaining cold at a temperature level -40 - 80° C. experiments were carried out in a conventional one-stage steam compressioned cooling cycle with a regenerative heat exchanger (i.e. with detached liquid separators SL-I and SL-II, fig. 1).

Results of the experiment at a temperature of cooling water + 13 - + 15°C are shown in fig. 4. As can be seen from the graph, energy consumption, when obtaining cold at the level -80 - -70°, constitutes from 1.7 to 1.4 kwh per 1000 kcal. This energy consumption is lower than that in two flow cascade installations (comparable in respect of cold production) and considerably lower than the energy consumption in an ammonia cycle with two stage compression and operating under vacuum.

Acknowledgement.

The author expresses his gratitude to engineer Visotsky, who carried out the experiments in the investigation of schemes developed by the author.

COPYRIGHT RESERVED

Approved For Release 2009/05/01 : CIA-RDP80T00246A007500340002-0

Approved For Release 2009/05/01 : CIA-RDP80T00246A007500340002-0

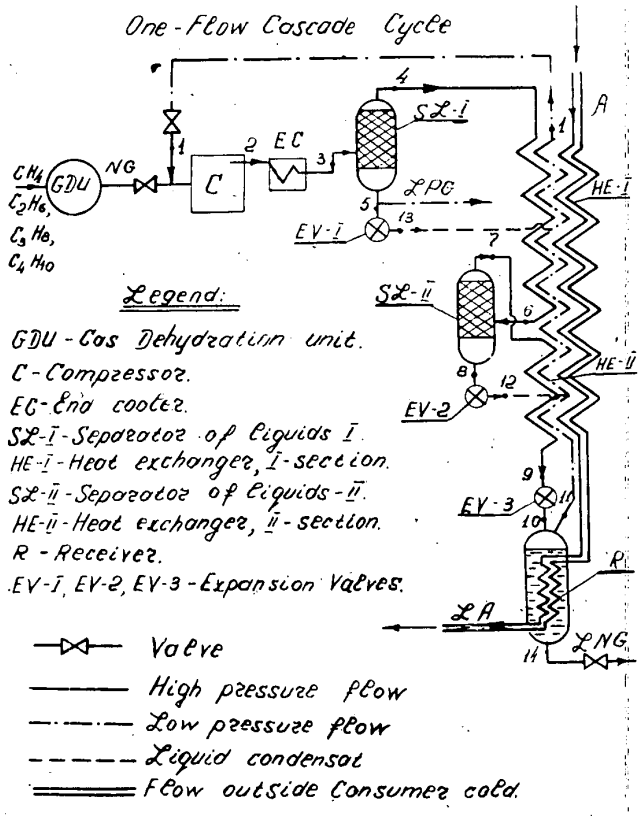

Fig. 1. One flow cascade cycle.

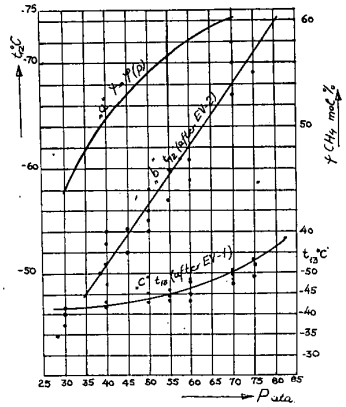

Fig. 2. Methane contents of cooling agent vs working pressure (temperature level ÷156° C.) and temperature regime of the liquid separators.

Approved For Release 2009/05/01 : CIA-RDP80T00246A007500340002-0

Approved For Release 2009/05/01 : CIA-RDP80T00246A007500340002-0

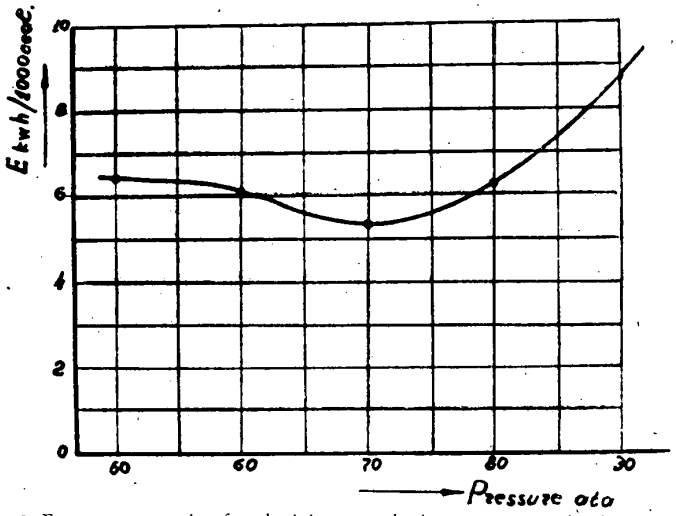

Fig. 3. Energy consumption for obtaining 1000 kcal at temperature level –150° C.

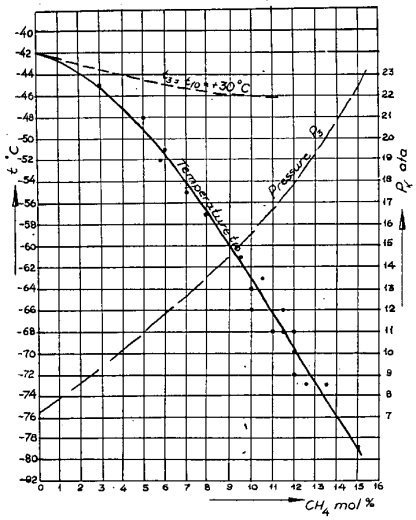

Fig. 4. Operating conditions of steam compressioned cycle with binary mixture methane–propane at temperature level –70 – –80° C.

Approved For Release 2009/05/01 : CIA-RDP80T00246A007500340002-0

Approved For Release 2009/05/01 : CIA-RDP80T00246A007500340002-0

DETERMINATION OF WORK OF COMPRESSION WITH REAL

THE DETERMINATION OF WORK OF COMPRESSION WITH REAL GASES

Détermination du travail de compression avec les fluides frigorigènes ou peu connus

H.S. WEINBERG
The Moscow Bauman Higher Technical School, Moscow, U.S.S.R.

SOMMAIRE. Pour déterminer le travail consommé dans un compresseur à compression adiabatique ou isotherme, il faut des diagrammes thermiques, des tables de vapeur surchauffée out les équations correspondantes. On ne dispose pas de ces renseignements pour les fluides frigorigènes nouveaux ou peu connus, il est conc nécessaire de trouver d'autres méthodes, telle que celle indiquée ci-dessous:

Pour les calculs, on utilise le coefficient de compressibilité $\xi = \frac{Pv}{RT}$ ou le coefficient Amagat $\rho = \frac{Pv}{P_o V_o}$

Ces coefficients peuvent être calculés avec une approximation suffisante par similitude avec les [illegible] utilisés et corrigés à l'aide du petit nombre de données expérimentales dont [illegible] dispose.

Le calcul est basé sur l'application de l'équation d'état $Pv = RT + \beta P$.

β est ici une variable, déterminée d'après les graphiques généraux dans le cas où l'on dispose des valeurs de la pression et la température critique ou analytiquement, si la valeur ξ est connue ainsi que les paramètres critiques.

Le volume du gaz [illegible] pressions élevées est plus grand que celui du gaz idéal, c'est-à-dire $\beta > 0$. Sur la courbe de saturation ou pour les vapeurs peu surchauffées son volume est inférieur à celui du gaz idéal ($\beta < 0$).

La méthode proposée pour le calcul du travail de compression consiste à comparer des diagrammes indicateurs d'une machine idéale comprimant le gaz donné et un compresseur comprimant un gaz idéal ayant la même valeur de R. La surface ou diagramme indicateur est facilement calculée d'après les formules connues.

La méthode est valable pour la compression isotherme comme pour la compression adiabatique.

Le travail absorbé est égal à:

$$\ell = \int v_w dP = \int v_{id} dP + \int \beta dP \quad \text{kgm/kg}$$

On donne une méthode de calcul approché assez précis pour le dernier élément de l'équation.

Approved For Release 2009/05/01 : CIA-RDP80T00246A007500340002-0

Approved For Release 2009/05/01 : CIA-RDP80T00246A007500340002-0

On donne des formules de calcul comprenant les coefficients ξ ou ρ au lieu de β, valables pour n'importe quelles conditions de P-v-T.

Des calculs types pour diverses substances indiquent que les calculs suivant la méthode proposée donnent sans peine la précision nécessaire.

Approved For Release 2009/05/01 : CIA-RDP80T00246A007500340002-0

Approved For Release 2009/05/01 : CIA-RDP80T00246A007500340002-0

Thermal diagrams, superheated vapour tables or respective equations are required for calculation of the work consumption of an ideal compressor. In the case of little studied substances there may be no such data available.

An approximate analytical method requiring only a minimum number of P-v-T data for the determination of work consumption in a compressor is discussed below.

The following dimensionless group numbers are used by the author in the calculation formulae: the coefficient $\xi = \frac{Pv}{RT}$ and the Amagat coefficient $\rho = \frac{Pv}{P_0 v_0}$

The coefficient $\rho' = \frac{Pv}{273{,}16 \cdot R}$ is recommended in the superheated vapour region instead of the Amagat coefficient. The coefficient $\rho_{cz} = \frac{Pv}{RT_{cz}}$, related to the critical temperature T_{cz} may be used in some cases.

Calculations of work consumption in a compressor are based on the utilization of the equation of state:

$$Pv = RT + \beta P$$

β - is here a variable estimating the difference between the volume of real gas and that of ideal gas having the same value of the gas constant value R

$$v = v_{id} + \beta = \frac{RT}{P} + \beta$$

In the high pressure region $v < v_{id}$ and $\beta > 0$ and in the superheated vapour region $v < v_{id}$ and $\beta < 0$.

Approved For Release 2009/05/01 : CIA-RDP80T00246A007500340002-0

Approved For Release 2009/05/01 : CIA-RDP80T00246A007500340002-0

The value β may be determined in accordance with the generalized graphs a (Fig.1) if the dimensionless value

$$\frac{\beta}{(v_{id})_{cr}} = \beta \frac{P_{cr}}{RT_{cr}}$$

is regarded instead of β.

$(v_{id})_{cr}$ is here the volume of the ideal gas with the same value of R at the critical pressure P_{cr} and the critical temperature T_{cr}

The upper boundary curves for some substances are given in graph b (Fig.1).

The values of β are connected with ξ and ρ by simple relations

$$\beta \frac{P}{RT} = \xi - 1$$

$$\beta \frac{P}{R} = 273{,}16\,\rho - T$$

$$\frac{\beta}{(v_{id})_{cr}} = \frac{\vartheta}{\pi}(\xi - 1)$$

Here $\vartheta = \frac{T}{T_{cr}}$ and $\pi = \frac{P}{P_{cr}}$

In the high pressure region β is termed 'surplus volume'. In the superheated vapour region β is termed 'lost volume'.

Method of calculations.

The suggested calculating method consists in comparing the theoretical indicator diagrams of the compressor at the compression of the particular real gas or vapour and at the compression of the ideal gas having an equal value of R.

The calculation is valid for any region of P-v-T (both in the superheated vapour and high pressure regions for isothermal and adiabatic compression).

Shown in Fig.2 are indicator diagrams (P-v -diagrams for 1 kg of a substance) for three P-v-T regions. The real gas indicator diagram is represented by 1-2-3-4. Diagram 1'-2'-3'-4' has the same area, the line 1'-2' being the line of compression of ideal gas

Approved For Release 2009/05/01 : CIA-RDP80T00246A007500340002-0

Approved For Release 2009/05/01 : CIA-RDP80T00246A007500340002-0

with the same value of R . Apparently, the sections 3-2 and 4-1 are respectively equal to 3'-2' and 4'-1', consequently the sections 3-3' and 4-4' are respectively equal to the sections 2-2' and 1-1' and determine the value of β . The positive value of β is measured leftwards.

While the calculation of the area 1-2-3-4 or its determination by means of a planimeter may be impossible, the calculation of the areas 1'-2'-3-4 and 4-3-3'-4' presents no difficulty.

When plotting the line of compression of an ideal gas 1'-2', it is assumed that its temperature varies in the same manner as a real gas does. If the real gas is compressed adiabatically, then it may be difficult to plot the lines of compression of the ideal gas. However, with the line 1'-2' plotted in accordance with the adiabatic curve of the ideal gas only a negligible error will appear as the temperature at the end of compression of the ideal gas is close to that of the real gas. In this case

$$\frac{T_2}{T_1} = \left(\frac{P_2}{P_1}\right)^{\frac{K_0 - 1}{K_0}}$$

The area 1'-2'-3-4 is calculated in accordance with the known formulae.

At isothermal compression

$$l_{id} = RT \cdot \ln \frac{P_2}{P_1} \quad \text{kgm/kg}$$

At adiabatic compression

$$l_{id} = \frac{K_0}{K_0 - 1} RT_1 \left[\left(\frac{P_2}{P_1}\right)^{\frac{K-1}{K_0}} - 1\right] \text{ kgm/kg}$$

The exponent of the adiabatic curve of the ideal gas is selected equal to

$$K_0 = \frac{C_{p0}}{C_{v0}}$$

If these data are not available, the choice is done in accordance with the number of atoms in the molecule and upon

Approved For Release 2009/05/01 : CIA-RDP80T00246A007500340002-0

Approved For Release 2009/05/01 : CIA-RDP80T00246A007500340002-0

the molecular weight.

The area of 4-3-3'-4' may be determined without a planimeter by various methods depending upon the fact whether the temperature in the point 2 is known.

If the temperature T_2 and consequently β_2, ξ_2 or ρ_2 are known, then the area 4-3-3'-4' may be conventionally determined as the area of a trapezium. Great precision is provided by such calculation, as the curvature of the line 3'-4' is insignificant. This method of calculation is referred to below as 'calculation by the trapezium area'.

With the temperature T_2 unknown for some reason or if the values β_2, ξ_2 or ρ_2 cannot be determined for some other reason, then the assumption can be made that $\beta_2 = \beta_1$, and the area 4-3-3'-4' be determined as the area of a rectangle plotted on the section 4-4'. This method of calculation is referred to in this paper as 'calculation by the rectangle area'.

Calculation by the trapezium area.

The work consumed in a compressor per 1 kg of working substance is expressed by

$$l = l_{id} + \frac{\beta_1 + \beta_2}{2}\left(P_2 - P_1\right) \qquad \text{kgm/kg} \qquad (1)$$

From the above relations the following calculation formulae are derived:

At adiabatic compression

$$l = l_{id} + \frac{RT_1}{2}\left[\frac{\xi_1 - 1}{P_1} - \frac{\xi_2 - 1}{P_2}\cdot\frac{T_2}{T_1}\right]\left(P_2 - P_1\right) \qquad \text{kgm/kg} \qquad (2)$$

or

$$l = l_{id} + \left[\frac{273,16R}{2}\left(\frac{\rho_1}{P_1} + \frac{\rho_2}{P_2}\right) - \frac{RT_1}{2}\left(\frac{1}{P_1} + \frac{1}{P_2}\,\frac{T_2}{T_1}\right)\right]\left(P_2 - P_1\right) \qquad (3)$$

At isothermal compression

$$l = l_{id} + \frac{RT}{2}\left(\frac{\xi_1 - 1}{P_1} + \frac{\xi_2 - 1}{P_2}\right)\cdot\left(P_2 - P_1\right) \qquad \text{kgm/kg} \qquad (4)$$

Approved For Release 2009/05/01 : CIA-RDP80T00246A007500340002-0

Approved For Release 2009/05/01 : CIA-RDP80T00246A007500340002-0

or

$$l = l_{id} + \left[\frac{273,16R}{2}\left(\frac{\rho_1}{P_1} + \frac{\rho_2}{P_2}\right) - \frac{RT}{2}\left(\frac{1}{P_1} + \frac{1}{P_2}\right)\right](P_2 - P_1) \text{ kgm/kg} \qquad (5)$$

Calculation by the rectangle area.

The expression for the work consumed in a compressor per 1 kg of working substance is

$$l = l_{id} + \beta_1(P_2 - P_1) \text{ kgm/kg} \qquad (6)$$

At adiabatic compression

$$l = l_{id} + \frac{RT_1}{P_1}(\xi_1 - 1)(P_2 - P_1) \text{ kgm/kg} \qquad (7)$$

or

$$l = l_{id} + \left(\frac{273,16R}{P_1}\rho_1 - \frac{RT_1}{P_1}\right)(P_2 - P_1) \text{ kgm/kg} \qquad (8)$$

At isothermal compression

$$l = l_{id} + \frac{RT}{P_1}(\xi_1 - 1)(P_2 - P_1) \text{ kgm/kg} \qquad (9)$$

or

$$l = l_{id} + \left(\frac{273,16R}{P_1}\rho_1 - \frac{RT}{P_1}\right)(P_2 - P_1) \qquad (10)$$

Results of calculation.

Control calculations were carried out for the determination of the error of the suggested method.

The parameters corresponding to the beginning of compression and to its end are given in tables 1 and 2 as well as a comparison of the results of calculation carried out according to the suggested method with the data calculated by the tables and diagrams. No calculations according to thermal diagrams were performed for air and the results of calculations by the area of the trapezium were taken as 100%.

Approved For Release 2009/05/01 : CIA-RDP80T00246A007500340002-0

Approved For Release 2009/05/01 : CIA-RDP80T00246A007500340002-0

Table 1

Results of control calculations at isothermal compression

Working substance	Freon-12	Water	Water	Air
Initial pressure, atm.	2.0	50	60	282
Final pressure, atm.	22.0	165	260	1000
Temperature, °C	+80	+350	+400	+100
Work consumption, %				
Determined by tables and diagrams	100.00	100.00	100.00	-
Work l_{id}				
Calculated by area of trapezium	99.05	100.31	98.81	100.00
" by area of rectangle	102.98	106.15	104.87	93.71

Table 2

Results of control calculations at adiabatic compression

Working substance	Ammonia	Freon-12	Water	Air
Initial pressure, atm.	3.0	5.0	80	282
Final pressure, atm	12.0	26.0	200	645
Initial temperature, °C	-5.0	+14.7	+320	+100
Work consumption, %				
Determined by tables and diagrams	100.00	100.00	100.00	-
Work l_{id}				
Calculated by area of trapezium	98.77	101.27	99.22	100.00
" by area of rectangle	95.87	105.14	89.30	93.58

Copyright reserved

Approved For Release 2009/05/01 : CIA-RDP80T00246A007500340002-0

Approved For Release 2009/05/01 : CIA-RDP80T00246A007500340002-0

SIMILARITY CRITERIA FOR THE DETERMINATION OF P-v-T PARAMETERS OF REFRIGERANTS

Critères de similitude pour la détermination des paramètres P-v-T des fluides frigorigènes

I.S. BADYLKES
The Scientific Research Institute of the Refrigerating Industry of the U.S.S.R., Moscow, U.S.S.R.

SOMMAIRE. Les progrès réalisés dans la chimie de synthèse et la possibilité d'appliquer de nouveaux agents dont les propriétés thermodynamiques sont peu étudiées a rendu urgente la mise au point d'une loi approchée des états correspondants:

$$f(\pi, \delta, \varphi) = 0$$

En rompant avec les méthodes de correction empiriques utilisées jusqu'à présent, un certain nombre d'auteurs ont essayé d'établir une loi généralisée en introduisant un critère de similitude supplémentaire:

$$f_1(\pi, \delta, \varphi, K) = 0$$

On a supposé qu'il serait ainsi possible d'approcher considerablement de la solution de ce problème complexe et que les propriétés d'un gaz imparfait quelconque, exprimées en fractions des paramètres critiques correspondants, seront vraiment identiques.

Il y avait cependant un point faible du fait qu'on choisissait K en se basant uniquement sur des principes généraux de caractère hypothétique. C'est pourquoi il y a encore une différence importante dans les dimensions physiques prises pour les quantités entrant dans le critère K et on n'est ainsi nullement certain qu'il soit possible de représenter par un seul critère supplémentaire les particularités de diverses structures thermodynamiques des substances normales et composées.

En partant d'une analyse purement théorique, l'A. propose deux critères supplémentaires, combinant les caractéristiques physiques de tous les critères proposés précédemment et étend la loi des états correspondants sous la forme de:

$$f_2(\pi; \delta; \varphi, K_1; K_2) = 0$$

où : $K_1 = \frac{\tau_s}{A R T_s} = \frac{426,94}{847,83} \frac{\eta T_s}{T_s}$; $K_2 = \frac{T_s}{T_c}$

$$\pi = \frac{P}{P_c} ; \quad \delta = \frac{T}{T_c} ; \quad \varphi = \frac{v}{v_c} \quad R = \frac{847,83}{\mu}$$

Signes utilisés:

A: $\frac{1}{426,94}$

τ: chaleur latente d'evaporation en kcal/kg

μ: poids moléculaire

T: température (^{o}K)

P: pression de vapeur saturée

v: volume spécifique de la vapeur .

Approved For Release 2009/05/01 : CIA-RDP80T00246A007500340002-0

Approved For Release 2009/05/01 : CIA-RDP80T00246A007500340002-0

L'indice "S" correspond aux températures d'evaporation normales, l'indice "C" aux températures critiques.

Un critère universel $K_{univ.}$ est proposé par l'A. pour la détermination du volume spécifique de la vapeur saturée sèche et de la vapeur surchaufée:

$$K_{univ.} = \left(\frac{v P_c}{R T_c}\right) \delta ; \pi ; K_1 ; K_2 = idem$$

(v est exprimé en m^3/kg, P en kg/m^2).

Ainsi, avec des valeurs similaires de δ ; π; K_1 et K_2, la valeur de $K_{univ.}$ est constante, indépendamment de la structure thermodynamique et de la nature chimique des agents.

De plus, la généralisation théorique permet de déterminer les paramètres P-v-T des substances non étudiées à l'aide de deux seuls résultats expérimentaux fondamentaux concernant la saturation, à savoir la température normale et la température critique.

Approved For Release 2009/05/01 : CIA-RDP80T00246A007500340002-0

Approved For Release 2009/05/01 : CIA-RDP80T00246A007500340002-0

It is well known that the properties of compounds in corresponding states /for equal $\pi = \frac{p}{p_c}$; $\vartheta = \frac{T}{T_c}$; $\varphi = \frac{v}{v_c}$ /, expressed as ratios of the critical parameters, should be identical and independent of their chemical nature. This law does not reflect molecular interaction in a real gas and may be corrected by introducing the additional criteria $K_1 \ldots K_m$ of which t e change in values characterizes the deviation from the similarity principle. Hence they must have constant values and the universal function assumes the form:

$$f(\pi; \vartheta; \varphi; K_1 \ldots K_m) = f(\pi; \vartheta; \varphi; idem) = 0 \qquad \text{(I)}$$

To determine the properties of compounds with recourse to minimum empirical data, it is necessary to determine the minimum number of criteria (dimensionless groups) $K_1 \ldots K_x$ that can incorporate the physical properties of all others $K_{x+1} \ldots K_m$. Hence

$$f(\pi; \vartheta; \varphi; K_1 \ldots K_x) = f(\pi; \vartheta; \varphi; K_{x+1} \ldots K_m) \qquad \text{(I-a)}$$

On the saturation curve it follows directly from the $f(\pi, \vartheta) = 0$ function that for $K_1 = \vartheta_s = \frac{T_s}{T_c}$ should be $K_2 = \pi_s = \frac{1}{p_c}$ or p_c is identical for thermodynamically similar groups of compounds. (The quantities with the subscripts s refer to I physical atm).

Approved For Release 2009/05/01 : CIA-RDP80T00246A007500340002-0

Approved For Release 2009/05/01 : CIA-RDP80T00246A007500340002-0

We shall prove on the basis of dimensionless analysis that the criteria K_1 ; K_2 incorporate the physical properties of all others and, consequently, in equation (I-a) $x = 2$

We shall note beforehand that among compounds there can naturally be no complete coincidence between K_1 and K_2 However, their values being close the utilization of most important additional criteria from the group $K_{x+1} \ldots K_m$ leads as it will be seen further to small errors which do not exceed the limits allowed in practice.

Since $f(\pi, \varphi'') = 0$

$$K_3 = \varphi_s'' = \ldots\ldots = \varphi_{s_n}'' = idem_3 \qquad (2)$$

The subscripts n designate the compound selected as reference.

Further, $\pi_s = \ldots = \pi_{s_n}$ and therefore

$$K_4 = \left(\frac{d \ln \pi}{d \ln \vartheta}\right)_{1atm} = \ldots\left(\frac{d \ln \pi_n}{d \ln \vartheta}\right)_{1atm} = idem_4 \qquad (3)$$

$$K_5 = \left(\frac{d\pi}{d\vartheta}\right)_{1atm} = \ldots\ldots = \left(\frac{d\pi_n}{d\vartheta}\right)_{1atm} = idem_5 \qquad (4)$$

From the Clapeyron-Clausius equation

$$\frac{r_s \Psi}{A P_s v_s^{id}} = \left(\frac{d \ln p}{d \ln T}\right)_{1atm} = \left(\frac{d \ln \pi}{d \ln \vartheta}\right)_{1atm} \qquad (5)$$

where

$$T - {}^\circ K \; ; \quad \Psi = \frac{v_s^{id}}{v_s'' - v_s'} \; ; \quad v_s^{id} = \frac{R T_s}{P_s} \; ; \quad R = \frac{848}{\mu}$$

The values of Ψ change within very small limits (1.02 ÷ 1.05). Proceeding from the Nernst equation we can write down /1/:

Approved For Release 2009/05/01 : CIA-RDP80T00246A007500340002-0

Approved For Release 2009/05/01 : CIA-RDP80T00246A007500340002-0

$$\Psi = \frac{1}{1 - \frac{1}{P_c}} = \frac{1}{1 - K_2} = idem' \qquad (6)$$

Taking into account equations (3), (5) and (6):

$$K_6 = \frac{\tau_s \Psi}{AR T_s} = \frac{426.24}{847.83} \frac{\mu \tau_s}{T_s} = idem_6 \qquad (7)$$

where $\frac{\mu \tau_s}{T_s}$ is the Trouton number; μ - the molecular weight.

As

$$\left[\frac{d \ln p}{d\left(-\frac{1}{T}\right)}\right]_{T=T_s} = T_s \left(\frac{d \ln \pi}{d \ln \vartheta}\right)_{T=T_s}$$

$$\left[\frac{d \ln p}{d\left(-\frac{T_s}{T}\right)}\right]_{T=T_s} = K_6^S \qquad (8)$$

In this case

$$\frac{d \ln p}{d\left(-\frac{T_s}{T}\right)} = K_6 \cdot f\left(\frac{T_s}{T}\right) \qquad (9)$$

At $T = T_s$ $\quad f\left(\frac{T_s}{T}\right) = 1$ and equation (9) becomes identical with equation (8). In the critical point

$$f\left(\frac{T_s}{T}\right) = f\left(\frac{T_s}{T_c}\right) = f(K_1) \qquad (10)$$

Then taking into account equations (7), (9) and (10):

$$K_7 = \left[\frac{d \ln p}{d\left(-\frac{T_s}{T}\right)}\right]_{\vartheta=1} = idem_7 \qquad (11)$$

Hence

$$K_8 = \left(\frac{d \ln \pi}{d \ln \vartheta}\right)_{\vartheta=1} = \left(\frac{d\pi}{d\vartheta}\right)_{\vartheta=1} = \frac{T_c}{P_c}\left(\frac{dP}{dT}\right)_{\vartheta=1} =$$

$$= \frac{1}{T_c}\left[\frac{d \ln p}{d\left(-\frac{1}{T}\right)}\right]_{\vartheta=1} = \frac{T_s}{T_c} K_6^S \cdot f(K_1) = idem_8 \qquad (12)$$

Approved For Release 2009/05/01 : CIA-RDP80T00246A007500340002-0

Approved For Release 2009/05/01 : CIA-RDP80T00246A007500340002-0

Now we shall see that for the same pressure P:

$$K_9 = \frac{1 - \frac{T_s}{T}}{1 - \frac{\pi_s}{\pi_c}} = idem_9 \qquad (13)$$

or

$$\frac{T_s}{T} = idem_9' \qquad (13\text{-a})$$

Since $\frac{T_s}{T} = \frac{T_c}{T}\,\vartheta_s = \frac{K_1}{\vartheta}$

$$\left(\frac{1 - \frac{K_1}{\vartheta}}{1 - K_1}\right)_P = \left(\frac{1 - \frac{K_1}{\vartheta}}{1 - K_1}\right)_\pi \qquad (13\text{-b})$$

Hence it follows that from equation (13-b) $\varphi(\pi, \vartheta) = 0$.

$$p = \pi p_c \quad ; \quad T = \vartheta T_c \quad ; \quad v = \varphi v_c$$

Then

$$K_{10} = \left(\frac{RT}{Pv}\right)_{\pi,\vartheta} = \frac{R T_c}{P_c v_c}\,\frac{\vartheta}{\pi\varphi} = K_{11}\,\frac{\vartheta}{\pi\varphi} \qquad (14)$$

Correspondingly for dry saturated vapour

$$K_{12} = \left(\frac{RT}{Pv}\right)_\vartheta \qquad (15)$$

From the Clapeyron-Clausius equation:

$$\frac{r_s}{AR T_s} = (K_3 - K_{13})\,\frac{K_5}{K_{11}} = \frac{K_6}{\psi} = \frac{idem_6}{idem'}$$

where

$$K_{13} = \varphi_s' = \varphi(K_1) = idem_{13} \qquad (16)$$

Then

$$K_{11} = idem_{11} \qquad (17)$$

$$K_{10} = idem_{10} \quad ; \quad K_{12} = idem_{12} \qquad (18)$$

Approved For Release 2009/05/01 : CIA-RDP80T00246A007500340002-0

Approved For Release 2009/05/01 : CIA-RDP80T00246A007500340002-0

Equation (14) can be written as:

$$K_{10\text{-}a} = \frac{R T_c}{P_c v} \quad \frac{\vartheta}{\pi} = \left(\frac{R T_c}{P_c v}\right)_{\pi, \vartheta} \tag{14-a}$$

In this case for $P = 0$ and $T = 0$:

$$\left(\frac{R T_c}{P_c v_{T=0}}\right)_{\pi=0;\ \vartheta=\infty} = idem_0 \tag{19}$$

Hence taking into account equation (17)

$$K_{14} = \left(\frac{v}{v_c}\right)_{\substack{P=0 \\ T=0}} = \frac{idem_{11}}{idem_0} = idem_{14} \tag{20}$$

Further

$$K_{15} = \frac{0{,}5\left(\frac{1}{\varphi'} + \frac{1}{\varphi''}\right) - 1}{1 - \vartheta} = idem_{15} \tag{21}$$

Finally we examine the dimensionless group

$$K_{16} = \frac{T_B}{T_c} \tag{22},$$

where: T_B - is the temperature corresponding to the Boyle point. It is quite possible to utilize the equation $P v = R T_B$ as the Boyle point exceeds the critical point several fold. Therefore

$$K_{16} = \frac{P v}{R T_c} = \frac{P_c v_c}{R T_c}\, \pi\varphi = \frac{\pi\varphi}{K_{11}} \tag{22-a}$$

Since π and φ are in corresponding states

$$K_{16} = idem_{16} \tag{22-b}$$

Approved For Release 2009/05/01 : CIA-RDP80T00246A007500340002-0

Approved For Release 2009/05/01 : CIA-RDP80T00246A007500340002-0

Hence all the most important criteria $K_{x+1} \ldots K_m$ are actually combined by two: K_1 and K_2. Designating K_1 by the first letters of Guldberg's name and taking into consideration that $K_2 = \pi_5$ we can establish a general criterion consisting of two dimensionless quantities

$$K' = (\pi_5)_{g_u} \tag{23}$$

and therefore

$$f(\pi; \vartheta; \varphi; K') = 0 \tag{24}$$

Since the number of dimensionless quantities should be no less than two and since they are all interchangeable, K' may be replaced, for example, by the following:

$$K' = (K_6)_{g_u} = (\pi_2)_{g_u}\ ;\ K'' = (K_3)_{g_u} = (Ri)_{g_u}\ ;\ K''' = (K_{15})_{g_u} = (Pl)_{g_u}\ ;$$

$$K'''' = (K_{11})_{g_u} = (Wa)_{g_u}\ ;\ K''''' = (K_{16})_{g_u} = (Bo)_{g_u}$$

It should be mentioned that the criterion K' was first suggested in the study /1/. The designation π_2 /Trouton/, Ri /Riedel/, Wa /Van-der-Waals/ we have used in conformity with a suggestion by R. Plank /2/.

Owing to the impossibility of precisely determining Wa (it is impossible to determine the critical volume directly from experiment), its utilization as a criterion is inexpedient. To choose K_1 and K_2 it is the most convenient as the criteria, the more so, that the P-φ-T parameters can be determined from only two experimental values

Approved For Release 2009/05/01 : CIA-RDP80T00246A007500340002-0

Approved For Release 2009/05/01 : CIA-RDP80T00246A007500340002-0

on the vapour pressure curve, viz., at I atmosphere and at the critical point.

The criteria $K_{x+1} \dots K_m$ are determined without the use of any arbitrary assumptions or empirical coefficients. However, owing to the impossibility of complete coincidence between the Guldberg numbers and between the critical pressures, for practical calculations it is necessary to use such criteria of the group $K_{x+1} \dots K_m$ that have the least sensitivity.

On the basis of the above said we take into account that according to equation (9) depending upon the degree of influence of $f\left(\frac{T_s}{T}\right)$ the vapour pressure curve can be divided into a number of elementary or wider linear sections. According to experimental data in general it approaches a straight line over the entire pressure range utilized. Therefore, near the critical point $(\vartheta \to 1)$ and especially for close values of K_1 and K_{1n} with an infinitesimally small error $\frac{f(K_1)}{f(K_{1n})} = 1$ and from equations (8) and (II):

$$\frac{d\left(-\frac{T_s}{T}\right)_{p\to 1}}{d \ln p} = \frac{1}{K_6}, \quad d\left(-\frac{T_s}{T}\right)_{\substack{\vartheta=1 \\ \vartheta\to 1}} = d\left(-\frac{T_s}{T}\right)_{p\to 1} \cdot \frac{1}{f(K_1)}$$

$$\left[\frac{d\left(-\frac{T_s}{T}\right)}{d\left(-\frac{T_{s_n}}{T_n}\right)}\right]_{P\left\{\begin{matrix}\vartheta=1 \\ \vartheta\to 1\end{matrix}\right.} = \dots = \left[\frac{d\left(-\frac{T_s}{P}\right)}{d\left(-\frac{T_{s_n}}{T_n}\right)}\right]_{p=1} \qquad (25)$$

Integrating the right part of equation (25), we obtain:

$$\left[\frac{1-\frac{T_s}{T}}{1-\frac{T_{s_n}}{T_n}}\right]_{p\to 1} = \left[\frac{1-\frac{T_s}{T}}{1-\frac{T_{s_n}}{T_n}}\right]_{p} = \left[\frac{1-\frac{T_s}{T_c}}{1-\frac{T_{s_n}}{T_n}}\right]_{P\left\{\begin{matrix}\vartheta=1 \\ \vartheta_n\to 1\end{matrix}\right.} \qquad (26)$$

Approved For Release 2009/05/01 : CIA-RDP80T00246A007500340002-0

Approved For Release 2009/05/01 : CIA-RDP80T00246A007500340002-0

Consequently for equal p :

$$\frac{1-\frac{T_s}{T}}{1-\frac{T_s}{T_c}} = \frac{1-\frac{T_{sn}}{T_n}}{1-\frac{T_{sn}}{T_n'}} \qquad (27)$$

where T_n' corresponds to the critical pressure of the unknown compound.

If the equation (26) is applicable for $\vartheta = 1;\ \vartheta_n \to 1$, then it must be true also at $\vartheta = 1;\ \vartheta_n = 1$. Then $\rho_c = \rho_{c_n}$ and $T_n' = T_{c_n}$, and the expression (27) fully coincides with the criteria K_9 which is proof of the correctness of the initially made assumptions. This is also confirmed by the fact that for well studied compounds with close K_1 and K_2 deviation in the values of T obtained according to equation (27) lies within the limits of experimental accuracy /3/.

A comparison of compounds with somewhat varying K_1 and K_2 (Freons II, 12, 13, 21, 22) has revealed that in the most well known range $\vartheta \leq 0{,}9$ the maximum deviation of the values from the mean curve $K_{12} = f(\vartheta)$ does not exceed 1%. For the values $\pi \leq 0{,}5$ used in refrigerating engineering (the experimental data are not quite reliable at higher pressures) and for various isotherms up to the critical, the maximum deviation $K_{10} = f(\pi, \vartheta)$ was below 2%.

Coordination of work directed towards the establishment of unity of criteria on an international scale as well as the specification and classification of the properties of standards is of considerable importance to theory and practice.

Approved For Release 2009/05/01 : CIA-RDP80T00246A007500340002-0

Approved For Release 2009/05/01 : CIA-RDP80T00246A007500340002-0

References

I. Badylkes I. Working substances of refrigerating machines. Moscow, Pishcheprom izdat, 1952.

2. Plank R. Report at the meeting of the Scientific Council of VNIKhI, September, 1958.

3. Properties of Commonly Used Refrigerants, ARI, Washington, 1957.

Copyright reserved

Approved For Release 2009/05/01 : CIA-RDP80T00246A007500340002-0

Approved For Release 2009/05/01 : CIA-RDP80T00246A007500340002-0

Un appareil mécano-électrique pour la mesure de la puissance frigorifique

A Mechanic-electric Apparatus for Measuring Refrigerating Capacity

J. CHYTRÁČEK[1] et J. PETRMICHL[2]
Prague, Tchécoslovaquie.

SUMMARY. The refrigeration industry requires an apparatus for measuring refrigerating capacity, capable of recording the amount of cold produced per unit of time. The apparatus makes possible economical operation for given electric power consumption. A mechanic-electric apparatus was developed which may be connected with an ammonia refrigerating system of 25,000-250,000 kcal/hr for evaporation temperatures of -5°, -35°C. and for temperatures of 0°, +25°C. before the regulation valve. The apparatus is made of two parts. The first one includes sensing elements connected to potentiometers for measuring the main characteristic values and for computing final results. Manometers, thermometers and a flowmeter regulate the respective potentiometers.

The other part includes a stabilized low voltage source with specific voltage, a stabilized source of high voltage to supply the electronic coupling, between computor and indicator, giving the results of measurements. The apparatus solves the well-known equation: $Q_o \triangleq G.(i_1 - i_2)$, the result of which is given by a Deprez apparatus.

The temperature of the liquid refrigerant before the regulating valve is measured by means of a thermocouple and the pressure of saturated vapours after the evaporator is measured by means of a spring manometer. The respective values of pressure and temperature proportional to enthalpy values are transformed into electric voltage by potentiometers. The values of voltage being substracted from one another, a voltage proportional to the difference of enthalpy values $i_1 - i_2$ is obtained. In the following section of the apparatus, the difference of enthalpies is multiplied by the weight of circulating refrigerant. This operation is also performed in the potentiometric transmittor, controlled by an orifice plate located in the suction line. In both last sections a correction is made for the charge of the specific weight of superheated vapour, flowing through the orifice. The last section is coupled with a Deprez indicator or with a recording apparatus.

---

[1] Institut de Recherches des Machines Thermiques.

[2] Institut de Recherches des Machines Frigorifiques et Alimentaires.

Approved For Release 2009/05/01 : CIA-RDP80T00246A007500340002-0

Approved For Release 2009/05/01 : CIA-RDP80T00246A007500340002-0

Bien que l'idée du mesurement de la puissance frigorifique soit aussi ancienne que le refroidissement lui-même, il n'existe pas même à présent aucun appareil de service éprouvé qui pourrait indiquer la quantité du froid produite par unité de temps, comme il y en a dans le cas de l'énergie électrique etc. Les appareils mis au point jusqu'à présent ne donnent que des valeurs approximatives ou ils ne fonctionnent avec sécurité que sous conditions spécifiques que l'on ne peut maintenir que très difficilement dans l'exploitation pratique. Nous trouvons donc justifié l'effort de donner à l'industrie du froid un tel appareil qu'indiquera sur l'échelle d'un indicateur avec des moyens simples la puissance frigorifique du système de manière qu'on puisse la contrôler par unité de temps et, la consommation de l'énergie électrique étant connue, apprécier ainsi l'économie de l'exploitation.

Les méthodes principales de mesure de la puissance frigorifique, utilisées jusqu'à présent, sont les suivantes:

La mesure de la puissance frigorifique utile dans l'agent de transmission à l'état liquide ou gazeux p.ex. la saumure, l'eau, l'air. On mesure le débit de l'agent de transmission et l'écart des températures;

la mesure de la puissance frigorifique globale directement dans la section de l'agent par mesurement du débit de l'agent circulant dans la section liquide ou dans la section vapeur du circuit. Le débit du liquide est mesuré généralement avant le détendeur soit à l'aide de bac jaugé, soit par un débitmètre. Un tel équipement demande un régime permanent, c'est à dire dans l'évaporateur il ne doit entrer que la quantité du liquide qui vraiment sera évaporée. Le débit de la vapeur est mesuré par débitmètres soit dans la conduite d'aspiration, soit dans la conduite de refoulement du compresseur. La mesure dans la conduite d'aspiration est plus facile et convenable. La mauvaise homogénéité de la vapeur passante qui contient des traces de l'air et de l'huile peut être remédiée plus facilement et on la trouve aussi plus basse que dans la conduite de refoulement. Cependant, en raison de la compressibilité des vapeurs et de la possible aspiration des gouttes de l'agent liquide de l'évaporateur, si la construction du dernier est inconvenable ou si la conduite est courte, les données de la mesure peuvent être déformées.

Il y a encore plusieurs méthodes indirectes et des méthodes calorimétriques se basant p.ex. sur le chauffage de vapeur d'une certaine valeur en déterminant ainsi le débit de l'agent frigorigène.

A la base des expériences des mesurements accomplis dans quelques entrepôts importants et aussi en considérant la simplicité, il nous semblait la plus convenable méthode du mesurement de la puissance frigorifique exécutée par le mesurement du débit de l'agent frigorifique dans la section vapeur du circuit dans la conduite d'aspiration derrière l'évaporateur et les valeurs d'enthalpie spécifique étaient dérivées de la température de sousrefroidissement avant le détendeur et de la pression dans la sortie de l'évaporateur (Fig. 1 et 2).

L'appareil était construit pour un système (circuit) frigorifique à ammoniac avec une puissance frigorifique entre 25000 et 250000 frig/h, la température d'évaporation étant de -5°C à -35°C et la température avant le détendeur de 0°C à +25°C.

Approved For Release 2009/05/01 : CIA-RDP80T00246A007500340002-0

Approved For Release 2009/05/01 : CIA-RDP80T00246A007500340002-0

L'appareil solve la relation bien connue $Q_o = G.(i_1 - i_3)$ et fonctionne à la base du principe d'un calculateur analogique.

Les valeurs particulière de la relation principale sont exprimées par analogie mécano-électrique, dont on accomplie les calculs donnés par la relation. La valeur résultante Q_o est indiquée sur l'échelle de l'appareil indicateur à l'aiguille ou par l'appareil régistrant.

Le débit G (ou différence des pressions au débitmètre, installé dans la conduite d'aspiration) est indiqué par un débitmètre dont les données sont transformées à l'aide d'un potentiomètre en une valeur électrique. Les valeurs de l'agent frigorigène sont données par les pressions ou températures respectives. La valeur d'enthalpie de l'agent frigorigène liquide avant le détendeur dans la gamme de l'appareil donnée est une fonction linéaire de la température liquide (Fig. 3).

La relation

$$i_3 = A + a.t_3 \qquad (1)$$

peut être exprimée aisément par un potenciomètre linéaire et transformée en tension électrique, la relation (1) étant transcrite ainsi en forme suivante

$$i_3 = k_2.(E_2 + E_2') \qquad (2)$$

Pour simplifier le calcul nous considérons la valeur de l'enthalpie à la sortie de l'évaporateur comme pour la vapeur saturée. Nous y commettons une certaine faute, la vapeur étant en réalité surchauffée (ou même humide), mais cette faute n'est pas de nature décisive. L'enthalpie de la vapeur saturée i_1 peut être donnée soit par la pression, soit par la température dans l'évaporateur

$$i_1 = f(p,x) \qquad i_1 = f(t,x).$$

Nous choisissons la fonction $i_1 = f(p,x)$ parce qu'il est plus facile de mesurer la pression que la température de la vapeur saturée (Fig. 4). La continuité de cette fonction peut être remplacée par une parabole exprimée par la relation

$$i_1 = C + (-\tfrac{1}{2} a \varphi^2 + b.\varphi + c) \text{ (Fig. 5).} \qquad (3)$$

Un potentiomètre non-linéaire exprimant la continuité de cette relation nous donne une tension correspondant à i_1.

Il en résulte la rélation

$$i_1 = K_1.(E_1 + E_1') \qquad (4)$$

Nous obtenons la tension $E_1 + E_1'$ aux résistances $R_1 + R_1'$ arrangées en série. La tension $E_2 + E_2'$ est formée à la série des résistances $R_2 + R_2'$ et R_4, alimentées par la même source comme les premières résistances. Les résistances fixes R_1 et R_2 correspondent aux valeurs fixes de l'enthalpie, pour pouvoir se servir de la gamme entière des potentiomètres

Approved For Release 2009/05/01 : CIA-RDP80T00246A007500340002-0

Approved For Release 2009/05/01 : CIA-RDP80T00246A007500340002-0

R_1' et R_2' pour les valeurs variables de l'enthalpie. Afin que le rapport entre les tensions $(E_1 + E_1')$ et $(E_2 + E_2')$ corresponde au rapport entre les enthalpies i_1 et i_3, on doit arranger la résistance R_2'' en série avec les résistances $(R_2 + R_2')$ (Fig. 6).

A l'aide des deux potentiomètres représentantes les valeurs i_1 et i_3 nous accomplirons la soustraction

$$i_1 - i_3 = k_{12} \cdot E_{12} + (E_1' - E_2') \qquad (5)$$

La constante k_{12} exprime la transformation des tensions en valeurs d'enthalpie.

A l'aide d'un autre potentiomètre R_3' on multiplie la différence entre les valeurs d'enthalpie par la racine carrée de la différence entre les pressions au débitmètre qui correspondra au débit G. La tension résultante (considérée pour le maximum de la valeur du poids spécifique du fluide circulant) doit encore être multipliée par le coefficient du correction de la variation de ce poids spécifique dûe à la surchauffage. Les vapeurs circulantes à travers du débitmètre sont surchauffées et il est nécessaire de déterminer le poids spécifique à base de pression et de température. Dans la gamme choisie de l'appareil et pour une température maximum de la vapeur surchauffée de +20°C (Fig. 7) le poids spécifique peut être exprimé par une relation approximée

$$\gamma = 209 \cdot \frac{p}{T} \qquad (kg/m^3) \qquad (6)$$

Dans ce cas on ne peut pas considérer la vapeur comme saturée parce que l'erreur en résultante serait grave. Une correction correspondante est introduite par les deux autres potentiomètres R_4' et R_5'. Ces résistances expriment la partie variable, les résistances R_4 et R_5 la partie fixe de la gamme du poids spécifique.

Le patron du potentiomètre R_4' a été ajusté pour la variation du coefficient de détente ε en fonction de pression avant le débitmètre (pour une certaine gamme moyenne du débitmètre).

La puissance frigorifique est donc donnée par la relation

$$Q_o = K_c \cdot K_m \cdot \frac{m_3}{n_3} \cdot \frac{m_4}{n_4} \cdot \frac{m_5}{n_5} \cdot k_{12} \cdot k_3 \cdot k_A \, (E_{12} + (E_1' - E_2')) \qquad (7)$$

où $K_c = 0{,}01252 \cdot \alpha \cdot d^2 \cdot \sqrt{\gamma_{Hg}}$ est la constante du débitmètre donnée par les dimensions géométriques de l'élément de mésure (diaphragme) et de la conduite.

$K_m = \sqrt{\Delta p_{max}} \cdot \sqrt{\gamma_{max}} \cdot \varepsilon_{max}$ est une constante pour les valeurs maximum des paramètres variables qui déterminent la quantité du débit du fluide.

$\frac{m_3}{n_3}$, $\frac{m_4}{n_5}$, $\frac{m_5}{n_5}$ sont les rapports entre la résistance du curseur et

Approved For Release 2009/05/01 : CIA-RDP80T00246A007500340002-0

Approved For Release 2009/05/01 : CIA-RDP80T00246A007500340002-0

celle du potentiomètre entier, dont $\frac{m_3}{n_3}$ correspond à l'indication du débitmètre

$$\frac{m_3}{n_3} \sim \sqrt{\Delta p}$$

$\frac{m_4}{n_4}$ au manomètre pour la correction du poids spécifique et du coefficient de détente en fonction de pression et $\frac{m_5}{n_5}$ au thermomètre pour la correction du poids spécifique en fonction de la température de la vapeur dans le point du débitmètre.

$$\frac{m_4}{n_4} \cdot \frac{m_5}{n_5} \sim \Delta \varepsilon \sqrt{\Delta \gamma} = \Delta \varepsilon \sqrt{A\left(\frac{p_o}{T_o} + \frac{p}{T}\right)} = \Delta \varepsilon \sqrt{A_1(p_o + p)} \cdot \sqrt{A_2\left(\frac{1}{T_o} + \frac{1}{T}\right)}$$

Les coefficients k_{12} et k_3 sont les constantes qui expriment les relations des différentes tensions et valeurs thermodynamiques. k_A est un coefficient exprimant le gain des amplificateurs cathodiques qui séparent les étages particuliers de calcul.

Les expressions déterminantes les régimes sur les potentiomètres particuliers et l'expression déterminante la tension peuvent être exprimées par une déflection de l'aiguille sur l'échelle de l'appareil N (divisions). $k_{12} \cdot k_3 \cdot k_A = K$ qui est la constante de l'appareil.

La relation (7) peut être puis formée

$$Q_o = K \cdot K_c \cdot K_m \cdot \frac{N}{n} \qquad (8)$$

Parce que la constante K_m est donnée par les valeurs maximum et l'échelle de l'appareil est divisée en "n" divisions, il est nécessaire d'introduire N/n.

L'appareil propre se compose de deux potentiomètres pour soustraire et de trois potentiomètres pour multiplier; ceux sont commandés par des manomètres, thermomètres et par un débitmètre. La tension de mesure pour les potentiomètres est délivrée par une source d'alimentation stabilisée, dont la valeur précise est reglée par un rhéostat et contrôlée par un voltmètre. Les étages particuliers des opérations de calcul sont separés l'un de l'autre par les amplificateurs cathodiques. Le résultat est indiqué par un milliampèremètre (avec l'échelle en frig/h) ou par un appareil-régistreur. Les tubes des amplificateurs sont alimentées par deux sources stabilisées de tension anodique. La tension de chauffage des tubes est aussi stabilisée. (Fig. 8). Le voltmètre, ampèremètre, le réglage de la tension de mesure et du zéro sur milli-ampèremètre, le commutateur du système et de la tension de mesure et aussi les couplages pour les potentiomètres et pour le régistreur se trouvent sur la plaque en face de l'appareil. (Fig. 9 et 10). Les potentiomètres sont commandés directement par les pick-ups placés au conduites du circuit frigorifique et connectés par les câbles avec l'appareil. (Fig. 11).

Approved For Release 2009/05/01 : CIA-RDP80T00246A007500340002-0

Approved For Release 2009/05/01 : CIA-RDP80T00246A007500340002-0

Les pick-ups pour la mesure de pression sont les manomètres à ressort ou à membrane. Les températures sont mesurées à l'aide des thermomètres bimétalliques au à pression et le débit est mesuré p.ex. par un diaphragme et une balance pendulaire. Tous les pick-ups sont munis des potentiomètres qui transforment les déflections mécanique en valeurs électriques.

On a fait des essais de fonctionnement de l'appareil par vérification de l'influence des quantités diverses (Δp, p_o, t_3, p^c, t^c) pour les différentes valeurs de la gamme de l'appareil. On a comparé les résultats et les valeurs calculées correspondantes aux valeurs ajustées. La limite supérieure de l'erreur était voisine de $\pm$ 2%.

Les essais pratiques étaient effectués dans un entrepôt frigorifique en régime continu et avec un équipement d'essai dans une usine de construction des machines frigorifiques. La puissance frigorifique a été contrôlée simultanément à l'aide des méthodes de mesure classique (manomètre différentiel, pressions et températures). On a trouvé les différences $\pm$ 1% en régime stable et maximum $\pm$ 5% en régime instable.

La limite supérieure de l'erreur totale pendant la détermination de la puissance frigorifique ne dépasse pas $\pm$ 5%, l'erreur dû à l'instabilité de l'appareil $\pm$ 1%. L'instabilité de tension peut être contrôlée pendant la mesure et corrigée d'après un voltmètre et par la rémission à zéro de l'appareil. L'erreur générale dû aux imprécisions des patrons de potentiomètres se monte à 1%. La précision absolue de l'indicateur à aiguille est de 1% et peut-être encore plus élevée.

Approved For Release 2009/05/01 : CIA-RDP80T00246A007500340002-0

Approved For Release 2009/05/01 : CIA-RDP80T00246A007500340002-0

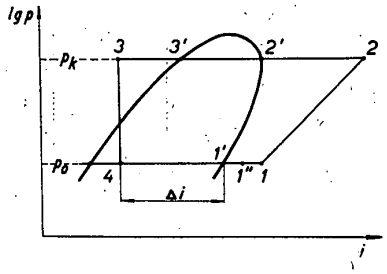

Fig. 1.

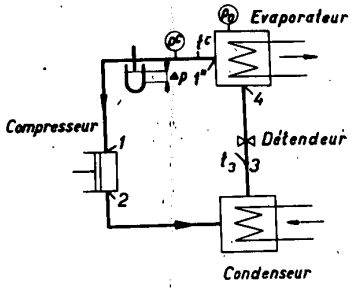

Fig. 2.

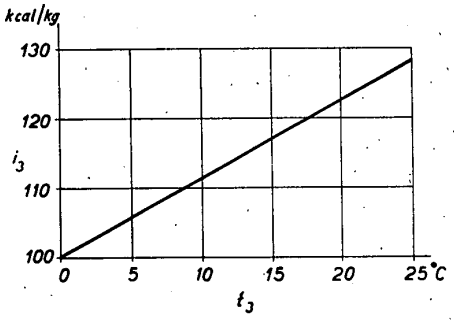

Fig. 3.

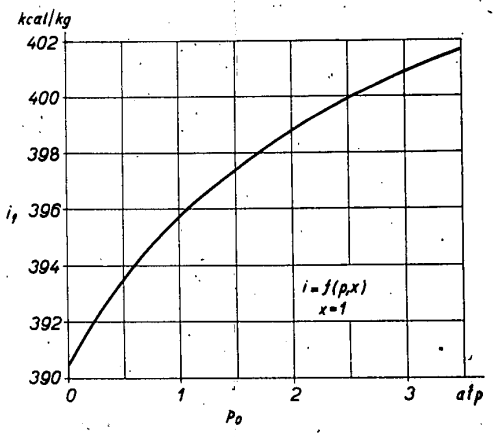

Fig. 4.

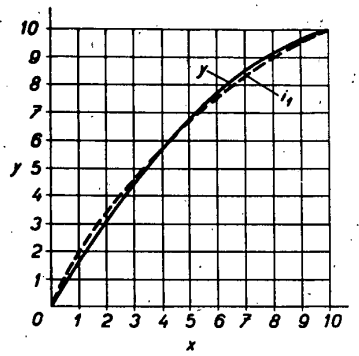

Fig. 5.

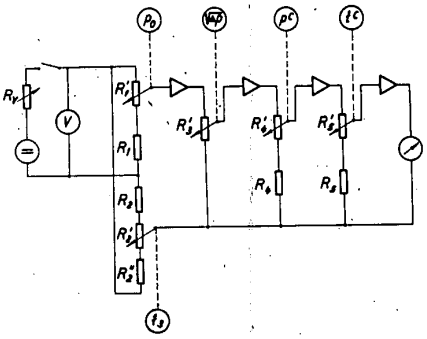

Fig. 6.

Approved For Release 2009/05/01 : CIA-RDP80T00246A007500340002-0

Approved For Release 2009/05/01 : CIA-RDP80T00246A007500340002-0

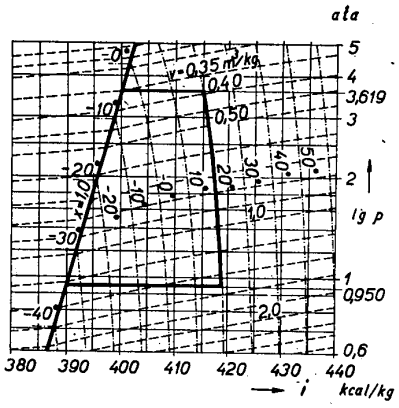

Fig. 7.

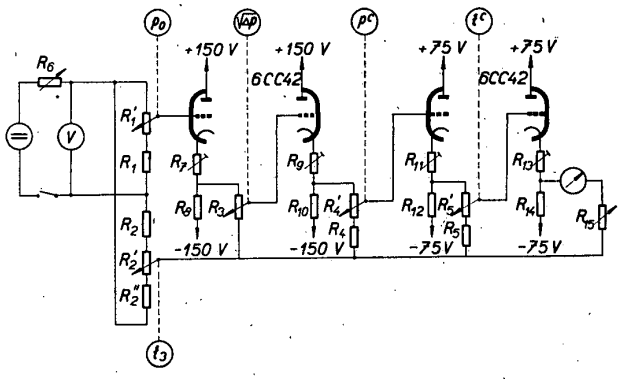

Fig. 8.

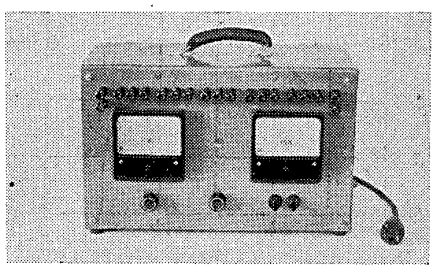

Fig. 9.

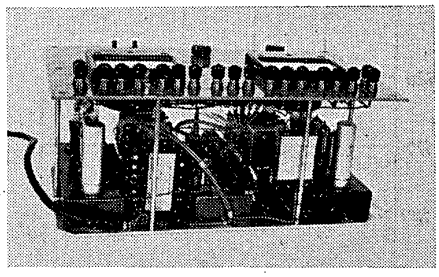

Fig. 10.

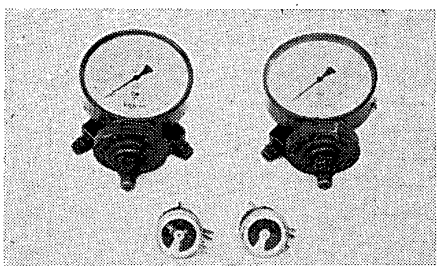

Fig. 11.

Approved For Release 2009/05/01 : CIA-RDP80T00246A007500340002-0

Approved For Release 2009/05/01 : CIA-RDP80T00246A007500340002-0

Simulation Tests of Refrigeration Turbo-Compressors

Essais par simulation de turbo-compresseurs frigorifiques

ING. FRANTIŠEK WERGNER
CKD, Praha, Czechoslovakia.

SOMMAIRE Méthodes d'essai pour un prototype de turbo-compresseur dans un circuit de remplacement. Méthodes d'essais par simulation d'un prototype de turbo-compresseur à l'aide d'un fluide de remplacement; principe des essais par simulation; analogie du phénomène physique, théorie et regles pour le choix des fluides frigorigènes essayés; effet des nombres d'analogie individuels; exemple de méthode d'essai par simulation; description du materiél frigorifique et du circuit de remplacement approprié; technique de mesure et appréciation des resultats.

TEST CIRCUITS OF REFRIGERATION TURBO-COMPRESSORS

Testing refrigeration turbo-compressors for the purpose of establishing their characteristic curves, i e. determining the dependence of compression on the intake quantity of refrigerant and the dependence of compression efficiency on that quantity, is a complicated task. As a rule there are no facilities at the manufacturer's premises for installing complete refrigeration equipment for testing the turbo-compressor, due to the considerable cost and space requirements involved. A simplified, so-called substitute cycle, is therefore used. A diagram of such a cycle for testing a compressor of a two-stage installation with three-stage throttling of liquid is shown in Fig. 1. Cooling-water quantities in the cooler and refrigerant pressures for the tests should be adjusted so as to prevent vapour condensation in the cooler. The conditions in the tirbo-compressor suction and additional suction should be within the range of superheated vapour, so that they may be successfully controlled by measuring the pertaining pressures and temperatures.

Fig. 2 shows test cycle in diagram i-log p.

TURBO-COMPRESSOR TESTS WITH SUBSTITUTE MEDIUM

Refrigerant used in the chemical industry are usually of the explosive type, such as hydrocarbon propane, C_3H_8. Ammonia NH_3 is also used which again exerts unfavourable effects on the surroundings and plant workers. In no case can these refrigerants be used in plant tests, because it is hardly possible to provide such protection and safety measures to safeguard the plant and the workers on the test bench and its surroundings against explosion, fire, poisoning, etc. Turbo-compressors using similar refrigerants are, therefore tested by so-called simulation tests.

In these tests substitute refrigerants or gases are used. The most generally available gas is air. Most suitable refrigerant replacing refrigerants of higher molecular weight, e g. propane, can be one of the freons, which is nonimflammable, nonexplosive and harmless to human health. In our works propane is substituted by refrigerant

Approved For Release 2009/05/01 : CIA-RDP80T00246A007500340002-0

Approved For Release 2009/05/01 : CIA-RDP80T00246A007500340002-0

F12 (CF_2CL_2), being easily available. Air can be used to replace ammonia.

The principle of simulation tests is based on the theory of analogy of physical phenomena, these phenomena being characterized by flow analogy numbers such as Reynolds number and Mach number. It is understood that when changing the working medium one must simultaneously change not only the working parameters, such as pressures and temperatures of the working cycle, but also the machine speed. When determining this change use is made of the fundamental principles of theoretical problem of analogy. Use is also made of the fact that in a certain working sphere it is possible to simulate with satisfactory precision the physical phenomenon of circulation in a machine even when neglecting the change of Reynolds number.

Tests with substitute medium on a finished compressor prototype represents a special case of simulation tests in which the machine serves as its own simulation test model. Therefore, simulation ratio, as concerns geometrical dimensions, equals 1.

As concerns change of speed one must realize that only change to lower speed comes into consideration, for reasons of strength, the impellers of the turbo-compressor are always designed with maximum utilization of material strength at rated working speed.

When choosing the pressure in a working cycle with substitute medium it is necessary to check, besides the conditions of analogy mentioned later, lest the compressor input should exceed the rated output of the driving motor, for reasons of admissible stress of coupling pins, gearing, etc.

THEORY OF SIMULATION TESTS

As already mentioned, the purpose of simulation tests is to determine turbo-compressor characteristics, i e the dependence of compression on the quantity delivered, dependence of compression efficiency on that quantity and dependence of compressor input on the quantity at actual working conditions, i e while working with the genuine refrigerant. It is important to realize that both the compression and the machine input depend firstly on the shape of gas-flow channels and machine dimensions, especially its impellers, secondly on circumferential velocity of these impellers and, thirdly, on compression efficiency. As a result, the foremost fundamental condition for arranging simulation tests is to create such working conditions as to obtain the same compression efficiency of the individual stages when working with substitute refrigerants, as in reality.

From the theory of analogy of physical phenomena in fluid flow we learn that this will be the case if we attain: 1. proportionality of velocities in all respective points of gas-flow channels when working with actual or substitute medium, and 2. equivalence of Reynolds numbers in all corresponding cross-sections of gas-flow channels.

Another condition, that of full geometric analogy of gas-flow channels including the analogy of roughness of surfaces, has naturally in our case been fulfilled, because the machine serves as its own simulation model.

Approved For Release 2009/05/01 : CIA-RDP80T00246A007500340002-0

Approved For Release 2009/05/01 : CIA-RDP80T00246A007500340002-0

Adherence to the first condition, i e. proportionality of velocities, requires that the relative change of specific volume at the end and the beginning of compression be the same,

$$\frac{V_k}{V_o} = \frac{V_k^x}{V_o^x} \qquad (1)$$

where V_k a V_o stands for specific volume when working with actual medium and V_k^x and V_o^x when working with the substitute.

Let us mention the method for determining necessary relationships under assumption of constant values of adiabate exponent k within the working range of the actual and substitute media. Although specific heats C_p and C_v in the sphere of superheated vapours of all refrigerants are variable, their relation

$$k = \frac{C_p}{C_v}$$

is to a certain extent approximately constant or it can be substituted by a certain mean value which can be considered as constant.

Under these assumptions the following equation will apply for the compression of the genuine medium:

$$H = \frac{Hpol}{\eta pol} = \frac{1}{\eta pol} RT_o \frac{m}{m-1} (\varepsilon^{\frac{m-1}{m}} - 1) = B \cdot \lambda 21 \cdot \frac{u_{21}^2}{g} \qquad (2)$$

Nomenclature - equation 2:

R gas constant

T_o initial temperature on compressor suction branch

m polytropic exponent

ε relative compressor compression

$\lambda 21$ input coefficient of 1st stage

u_{21} circumferential velocity of 1st stage impeller

g acceleration due to gravity

B constant

Value $\lambda 21$ is input coefficient depending on impeller shape, number and angle of blades and on value

$$\frac{Cr2}{u_2}$$

i e. on the relation of the radial component of speed to circumferential velocity, which can be determined by the Bussemann or Stodola methods.

For the compressor working with substitute medium, analogous equation 3 will apply:

$$H^x = \frac{1}{\eta pol} R^x T_o{}^x \frac{m^x}{m^x-1} (\varepsilon^{x \frac{m^x-1}{m}} - 1) = B \lambda 21 \frac{u_{21}^{x2}}{g} \qquad (3)$$

Approved For Release 2009/05/01 : CIA-RDP80T00246A007500340002-0

Approved For Release 2009/05/01 : CIA-RDP80T00246A007500340002-0

According to the foregoing values η_{pol} and ξ_{21} remain unchanged. For polytropic exponent the well-known relation is valid:

$$\frac{m}{m-1} = \eta_{pol} \frac{k}{k-1} \quad \frac{m^x}{m^x - 1} = \eta_{pol} \quad \frac{k^x}{k^x - 1} \qquad (4)$$

In equations 2 and 2 one can substitute:

$$a_o^2 = k\ g\ RT_o \qquad a_o^{x2} = k^x g\ R^x T_o^x \qquad (5)$$

where a_o and a_o^x are sonic velocities pertaining to the condition in compressor suction with actual and substitute media. Dividing equations 2 and 3 and substituting relations 4 and 5 we obtain:

$$\frac{\xi \frac{m-1}{m^x} - 1}{\xi \frac{m^x - 1}{m^x} - 1} = \frac{k-1}{k^x - 1} \quad \frac{\frac{u_2^2}{a_o^2}}{\frac{u_2^{x2}}{a_o^{x2}}} \qquad (6)$$

In order to adhere to the first principal condition, i.e. equal relative change of specific volumes with genuine and substitute media it is necessary to replace ξ^x in relation 6 by

$$\xi \frac{1}{m} = \xi^x \frac{1}{m^x} \qquad (7)$$

from the equation of polytropic curve, thus finally obtaining

$$\frac{\xi \frac{m-1}{m} - 1}{\xi \frac{m^x - 1}{m} - 1} = \frac{k-1}{k^x - 1} \quad \frac{\frac{u_2^2}{a_o^2}}{\frac{u_2^{x2}}{a_o^{x2}}} \qquad (8)$$

If we succeeded in finding a substitute medium with which adiabate exponent k^x would remain equal to k, then $m^x = m$ and, according to equation 7, compression would also remain equal, i.e. $\xi^x = \xi$.

From equotation 8 the following would result:

$$\frac{u_2^2}{a_o^2} = \frac{u_2^{x2}}{a_o^{x2}} \qquad (9)$$

The same compression will therefore be attained (at $k^x = k$), if the relation of circumferential velocity of the first wheel to the sonic velocity pertaining to the condition in suction, is the same. The value of sonic velocity depends exclusively on the condition and physical properties of the medium. For its magnitude with most common refrigerants and gases (see Table 1).

Approved For Release 2009/05/01 : CIA-RDP80T00246A007500340002-0

Approved For Release 2009/05/01 : CIA-RDP80T00246A007500340002-0

Table 1

	H_2	NH_3	air	CO_2	C_3H_8	F 12	F 11
m	2,016	17,03	(28,95)	44,01	44,1	120,92	137,4
R	420,6	49,79	29,27	19,25	19,25	7,03	6,17
k	1,407	1,30	1,40	1,30	1,13	1,14	1,13
T_o °C	20	-15	20	20	-15	-15	-15
a_o m/sec	1303	403	341	268	234,2	142,3	133

As may be seen from the above data, refrigerant F 12 will be a suitable substitute for propane, because under maintenance of the same relation

$$\frac{u^2}{a_o} = \frac{u_2^x}{a_o^x},$$

u_2^x of substitute medium will be lower, i e. the test speed will be lower, which will be satisfactory from the viewpoint of stress.

From the pertaining relations one can gather that in case $k = k^x$, there will be at each point of compressor gas-flow channels a constant relation of not only specific volumes and pressures, but also of absolute temperatures.

From the relation for sonic velocity

$$a^2 = k\ g\ R\ T \qquad a^{x2} = k^x\ g\ R^x\ T^x$$

then results that also the relation of sonic velocities $\frac{a^x}{a}$ will be constant, since relation $\frac{a^{x2}}{a^2} = \frac{R^x T^x}{RT}$ will then also be constant.

From this result it follows that while maintaining relation

$$\frac{u_2}{a_o} = \frac{u_2^x}{a_o^x} \qquad (9)$$

Mach number at any point of gas-flow channels will remain unchanged when working with substitute medium. The Mach number being determined by the relation of flow velocity at a given point to sonic velocity pertaining to the conditions at that point, perfectly equivalent conditions are given for possible formation of shock waves, since local speed acceleration owing to various curves in anuloid channels, are ruled by the same relation. This fact is important, especially because the machine efficiency is very sensitive to eventuel formation of shock waves. According to experience with divergent character of gas-flow channels, shock waves in turbo-compressors are followed by turbulence which deteriorates compression efficiency.

Let us point out at this stage that the conditions described above will be very closely approximated if working medium propane is replaced by refrigerant F12 as substitute medium, since for propane $k = 1,13$ and for refrigerant F 12 $k^x = 1,14$. Similarly, when replacing ammonia NH_3 by carbon dioxide CO_2, in both cases $k = k^x = 1,3$.

Approved For Release 2009/05/01 : CIA-RDP80T00246A007500340002-0

Approved For Release 2009/05/01 : CIA-RDP80T00246A007500340002-0

The effect of Reynolds number still remains to be pursued. This analogy number according to the known definition used for radial compressors

$$Re = \frac{u_2 D_2 \gamma}{\eta g} \qquad (10)$$

may be influenced by the choice of pressure level in test circuit with substitute medium, because this will directly influence specific weight γ. The choice of pressure level in the test circuit is ruled by two viewpoints. First of all it is the possibility of medium condensation behind cooler GC according to Fig. 3. Delivery pressure behind the compressor must not be so high as to cause condensation in cooler GC at the given degree of cooling, which would have disturbing effects on the test.

Choice of pressure level is also limited by compressor input, that is, by admissible load of electric motor E. At the same time one must keep in mind that admissible load of driving electric motor at lower speeds used at simulation tests, is lower than would correspond to rated speed.

As concerns the effect of Reynolds number on the efficiency we must say that both according to our tests and according to literature, efficiency does not depend on Re for values higher than $7{,}5 \cdot 10^6$. Dependence on Re exists for lower values only. It is a similar phenomenon as with the rest of blade machines, turbines and axial compressors. This greatly facilitates the task of determining simulation parameters, in particular the choise of suction and delivery pressures.

EXAMPLE OF SIMULATION TESTS

The mentioned methodics of measuring turbo-compressors by substitute medium has been applied for determining characteristics of a propane compressor by means of refrigerant F 12. Sectional drawing of the compressor is given in Fig. 3. As may be seen, the compressor consists of three wheel groups and, therefore, the characteristicks of the individual groups had to be determined separately.

The diagram of measuring may be seen in fig. 1. The compressor works in closed circuit, the discharge gas passing through the circuit cooler. Here the gas is cooled approximately to suction temperature. Before entering the turbo-compressor the valves throttle the refrigerant to the required pressure of suctions 1, 2 and 3. The pressures and temperatures in the course of cooling were chosen and controlled so as to prevent gas condensation. For determining the characteristics it is important to measure temperatures at the points of return channels A and B, before the point of additional suction. These temperatures are needed for determining efficiencies in parts 1 and 2. Since in this part of the machine Mach flow number is higher than 0.5, a special design of thermocouples must be used here. Prior to the measurements these thermocouples are gauged in a channel attached to the compressor discharge and connected with its suction.

At points where flow velocity and the corresponding Mach number are smaller than 0.4, the measurements are taken by standard mercury thermometers or thermocouples.

Approved For Release 2009/05/01 : CIA-RDP80T00246A007500340002-0

Approved For Release 2009/05/01 : CIA-RDP80T00246A007500340002-0

The refrigerant quantity was measured by a diaphragm in the compressor suction piping and checked on the discharge. Calculation and design have been carried out according to VDI Standards. The input was measured on the motor side. Net input on turbo-compressor coupling was computed by subtracting mechanical losses of motor bearings and gear box.

Table 2

Calculated parameters used for simulation tests with refrigerant F 12, in comparison with actual working parameters when using propane

	C_3H_8	CF_2Cl_2
Intake quantity, stage I	19 500 kg/h	17 200 kg/h
Pressure in suction branch, stage I	1,55 at	1 at
Temperature -"-	-26°C	+35°C
Intake quantity, stage II	23 100 kg/h	20 300 kg/h
Pressure in suction piping stage II	2,54 at	1,58 at
Temperature in suction branch, stage II	-15°C	+35°C
Intake quantity, stage III	8 500 kg/h	7 500 kg/h
Pressure in suction branch, stage III	5,8 at	3,5 at
Temperature in suction branch, stage III	+ 7,5°C	37°C
Pressure in delivery branch	13,1 at	7,7 at
Temperature in delivery branch		125°C
Speed, r.p.m.	6 000	3 900
Required input	1917 kW	700 kW
Reynolds number of 1st wheel	$42,6 \cdot 10^6$	$17,5 \cdot 10^6$
Reynolds number of 8th wheel	$150,0 \cdot 10^6$	$74,5 \cdot 10^6$

In this table values are given corresponding to the nominal point. However, the measurements were taken for the whole progress of characteristics. The machine speeds were 3720 rpm and 3900 rpm. Fig. 4 shows propane characteristics of all three compressor parts in a summary diagram, ascertained by freon tests. Points marked by circle were converted from measurements at 3720 rpm and points marked by cross from measurements at 3900 rpm. Overall characteristic of the compressor, under the assumption that both refrigeration stages are proportionately increasing or decreasing the output, is shown in Fig. 5.

The simulation test method used in Czechoslovakia for determining working characteristics of refrigeration turbo-compressors as described in this report offers facilities for taking these measurements in factories even when explosive or otherwise dangerous refrigerants are involved. By observing laws of analogy of physical phenomena it is thus made possible to determine properties of the compressor in

Approved For Release 2009/05/01 : CIA-RDP80T00246A007500340002-0

Approved For Release 2009/05/01 : CIA-RDP80T00246A007500340002-0

actual service. For conversion, values are used of certain properties of refrigerants in the sphere of superheated vapour, known in the form of diagrams or can be derived from vapour-stage equation. Accuracy of the cable will, therefore, depend on reliability of these data. A practical test for the purpose of determining machine characteristics by means of simulation measurements with substitute refrigerant and subsequently with the working refrigerant at the user's premises to enable drawing of comparisons, has not yet been materialized. It is provided for in our plant research programme to carry out these comparisons as soon as an opportunity is offered for using the equipment of a chemical works for taking these measurements.

References:

Ris, V.F. - Centrobežnyje compresornyje mašiny

Eckert, B. - Axialkompressoren und Radialkompressoren

Approved For Release 2009/05/01 : CIA-RDP80T00246A007500340002-0

Approved For Release 2009/05/01 : CIA-RDP80T00246A007500340002-0

The Vortex Refrigerating Unit

Groupe frigorifique à effet vortex

A.P. MERKULOV

The Kuibishev Aviation Institute, Kuibishev, U.S.S.R.

SOMMAIRE. La possibilité d'obtenir un effet frigorifique considérable, pour une grande pamme de détentes ainsi que la simplicité et la sécurité exceptionnelles de la construction du refroidisseur à effet vortex incitent la recherche de moyen d'utiliser en pratique cet effet dans les groupes frigorifiques.

Les principaux moyens permettant d'augmenter le rendement du refroidisseur à vortex sont: Utilisation d'un collecteur de pression dynamique de l'écoulement de froid pour augmenter le degré de détente dans le refroidisseur à vortex; récupération du froid, autrement perdu; utilisation de l'énergie d'un écoulement de chaleur pour augmenter le degré de détente dans le refroidisseur à vortex; et diminution de la longeur de la zone du vortex pour augmenter le rendement du refroidisseur a vortex et abaisser la perte de charge totale dans l'écoulement de chaleur.

Cette utilisation de l'énergie permet une augmentation de l'effet frigorifique de 7o à 1oo % et augmente notablement le rendement du cycle. Tous ces facteurs sont employés dans le groupe frigorifique à vortex conçu par l'A. Les principales parties du groupe sont: le refroidisseur à vortex avec zone de vortex réduite, un diffuseur à détorsion, une chambre froide, un échangeur de chaleur et un éjecteur dirigé.

Les recherches sur le refroidisseur à vortex et une analyse des travaux précédents ont permis d'obtenir des renseignements généraux sur la base desquels on peut calculer un refroidisseur à vortex pour différentes applications. Une méthode a été mise au point pour le calcul d'un groupe frigorifique à vortex. Pendant l'essai de la chambre du refroidisseur son effet frigorifique constituait o,64 de l'effet isentropique, c'est-a-dire était supérieur de près de 5o % à l'effet frigorifique obtenu pour un refroidisseur a vortex seul de mêmes dimensions(d'apres HILSCH pour 17,6 mm de diamètre).

En raison de sa simplicité, de sa sécurité et de sa mobilité, la chambre frigorifique a vortex convient spécialement aux besoins de froid occasionnels dans l'industrie et en laboratoire.

Approved For Release 2009/05/01 : CIA-RDP80T00246A007500340002-0

Approved For Release 2009/05/01 : CIA-RDP80T00246A007500340002-0

The vortex effect for the energy separation of gases has the following outstanding merits: exceptional simplicity and reliability of operation of a vortex refrigerating unit; absence of moving parts, lomgevity of the unit and low operating costs, and increase in temperature efficiency with increase in degree of pxpansion. All these give reason to consider the possibility of utilizing the vortex effect practically for obtaining moderately low temperatures, despite its shortcomings from an energy standpoint.

FLOW DIAGRAM AND DESIGN OF THE VORTEX REFRIGERATING UNIT.

An important property of the vortex plant is its low energy characteristics. The maximum coefficient of performance has been found to be 0.235. In order to raise the efficiency of the unit one must strive to take maximum advantage of the energy outflow from its streams.

The principal ways for doing this are:

Straightening out of the cold stream - utilization of its impact pressure to raise its degree of expansion in the vortex cooler,

Regenerating low temperature heat in the heat exchanger,

Shortening the length of the vortex zone with the objective of increasing the effectiveness of the vortex cooler and lowering the over-all pressure losses in the hot stream,

Utilizing the energy of the hot stream for increasing the degree of expansion in the vortex cooler.

By such means the cooling effect of the unit may be raised by 7o-1oo% and the efficiency of the cycle markedly improved.

All these measures have been carried out in the refrigerating units developed by the Kuibishev Aviation Institute. The schematic diagram of such units is shown in Fig. 1 and the design of one of them (refrigerated chamber KhK-3) in Fig. 2.

Compressed air is supplied through nipple 1 (Fig. 2) to the filter and silicagel dessicant 2 whence via the heat exchanger tubes 3 it enters the cavity 4 and through the nozzle entrance 5 to the vortex tube 6. After separation in the vortex tube the cold stream passing through the orifice in the diaphragm 7 and through the straightening out diffusor to enter the refrigerated chamber 8, cooling its load.

Through the opening 9, the ring cavity lo and the second section of the heat exchange, the spent cold stream is drawn off by ejector 11 operating by means of the hot stream of the vortex tube.

Approved For Release 2009/05/01 : CIA-RDP80T00246A007500340002-0

Approved For Release 2009/05/01 : CIA-RDP80T00246A007500340002-0

The temperature of the cold stream is regulated by changing the cold component with the aid of the adjusting needle 12 of the ejector set with the aid of the lever 13.

During operation of the unit, particularly under conditions of maximum cooling effect, vacuum is set up with the aid of the ejector in the flow circuit of the cold stream (to the refrigerated chamber, ring cavity and second section of the heat exchanger), the cover 14 of the refrigerated chamber being carefully hermetized by means of the rubber gasket 15 and the clamp screw 16.

The refrigerated chamber is insulated from the outer mantle with the aid of two centered rings of foam plastic and mineral wool 18. The hermetic cover of the refrigerated chamber carries a layer of foam plastic insulation 19 and the heat exchanger a layer of asbestos 20.

On the instrument panel of the refrigerated chamber there are mounted a manometer for recording the pressure of the incoming compressed air and a galvanometer with a temperature scale of from 20 to -70°C, giving the temperature of the cold stream entering the chamber.

The temperature pickup of the refrigerated chamber is a chromel-copel thermopile, the working junctions of which are located beneath the chamber bottom and the compensating junctions behind the instrument panel.

There is a hatch at the lower end of the unit for changing the silica gel.

TECHNICAL CHARACTERISTICS OF THE REFRIGERATED CHAMBER.

Depending upon the required cooling temperature the refrigerated chamber may function over a wide range of pressures and temperatures of the feed air. The refrigerated chamber is designed to operate over a range of pressures from 1 to 8 atm.

On Fig. 3 curves are presented depicting the dependence of the temperature in the refrigerated chamber and of the velocity of the compressed air on the pressure of the latter at 15°C. The broken line represents the dependence of the cold stream temperature obtained by R. Hilsch for a vortex tube 17.6 mm diameter(the diameter of the vortex tube used in the present unit was 17 mm). A comparison of the curves showed that the temperature effect of the cooling obtained with the unit was almost 50% greater than for a vortex tube alone.

Approved For Release 2009/05/01 : CIA-RDP80T00246A007500340002-0

Approved For Release 2009/05/01 : CIA-RDP80T00246A007500340002-0

The main technical characteristics of the refrigerated chamber are as follows:

Parameters of the air supply:	
Maximum pressure	8 atg
Temperature	15°C
Minimum chamber temperature	-70°C
Maximum air velocity	2.2 Nm^3/min.

CALCULATION PROCEDURES FOR THE UNIT.

Owing to the absence of analytical expressions for calculating the vortex effect that satisfactorily agree with experiment, the calculation may be made with the aid of empirical correlations. The basis for such a calculation serve the following relations obtained from experimental studies of vortex coolers:

Each value for the weight fraction μ of the cold stream (equal to the ratio between the weight velocities of the cold G_c and the overall G streams) possesses a corresponding optimal diameter D_g of the diaphragm orifice, with respect to optimal cooling effect. For the given diameter D of the vortex tube, D_g may be calculated within the limits $0.2 \leq \mu \leq 0.8$ according to the formula

$$D_g = D(0,350 + 0,313\,\mu) \qquad (1)$$

The optimal cross section of the nozzle orifice F_d with respect to the cooling effect and refrigerating capacity may be presented by the relation

$$F_d = 0,0754 \cdot D^2 \qquad (2)$$

The temperature efficiency η (equal to the ratio of the cooling effect of the cold stream Δt_c to the cooling effect Δt_s on isoentropic expansion from the parameters at the entrance to the pressure of the cold stream) is practically independent of the level of the pressures at the inlet and outlet of the vortex tube and also of the temperature of the entering gas. It depends mainly on the weight fraction μ and the degree of expansion π, i.e. on the ratio of the total pressure of the entering gas to the statical pressure of the cold stream at the diaphragm.

$$\eta = f(\mu, \pi) \qquad (3)$$

The degree of incompleteness of expansion of the hot flow π (ratio of the total pressure of the hot to the statical pressure of the cold streams) for optimal values of the diaphragm orifice does not depend upon μ and for a tube with a vortex zone 9 times as long as its diameter (constricted by a cross piece) may be determined from the expression

$$\pi = 1,59 - 0,27\pi + 0,062\,\pi^2 \qquad (4)$$

Approved For Release 2009/05/01 : CIA-RDP80T00246A007500340002-0

Approved For Release 2009/05/01 : CIA-RDP80T00246A007500340002-0

It should be noted that the expressions have been obtained on studies of vortex tubes with D = 2o to 5o mm over the range $2 \leq \pi \leq 6$.

The sections calculated we designate as shown in Fig. 1. The calculations will be made for the case of steady state conditions the following assumptions being made: Hydraulic losses in the communications of the unit (excepting the heat exchanger) are compensated by the total pressure recovery effect of the straightening-out diffusor. Hence these losses and the diffusor effect are eliminated from the calculation. The isobaric heat capacity is assumed to be constant.

For sufficiently good regeneration the ratio of the absolute temperatures of throttling of the cold stream beyond the heat exchanger and of the hot stream

$$\theta = \frac{T_3}{T_h} \approx 1 \qquad (5)$$

Owing to the low velocities in these sections the calculations are carried out for the overall parameters.

The basic equations for rating the unit are:

The equation for the vortex tube

$$T_c = T_1 \cdot B/^{o}K/ \qquad (6)$$

Here $$B = \left[1 - \eta\left(1 - \frac{1}{\pi^{\frac{k-1}{k}}}\right)\right] = f(\mu, \pi) \qquad (7)$$

K is the isoentropy exponent.

The equation for the heat balance of the heat exchanger

$$T_o - T_1 = \mu (T_3 - T_2) \qquad (8)$$

The heating of the stream in the refrigerated chamber by external heat exchange

$$\Delta t_k = T_2 - T_c = \frac{Q_k}{\mu \cdot G \cdot C_p} \quad [^{o}C] \qquad (9)$$

Here Q_k (kcal/hr) is the hourly quantity of exterior heat inflowing through the chamber insulation.

Losses due to incomplete regeneration

$$t_T = T_o - T_3 \quad [^{o}C] \qquad (10)$$

The energy equation of the vortex tube is

$$T_1 = \mu \cdot T_c + (1 - \mu) \cdot T_h \qquad (11)$$

Approved For Release 2009/05/01 : CIA-RDP80T00246A007500340002-0

Approved For Release 2009/05/01 : CIA-RDP80T00246A007500340002-0

The approximate equation for ejector impulses is

$$P_4 = \frac{\alpha \cdot P_h + P_c}{\alpha + 1} \qquad (12)$$

where

$\alpha = \frac{F_h}{F_c}$ = geometric parameter of the ejector

F_h, F_c = cross section of the orifice of the ejector nozzle

The equation for the velocity in the ejector is

$$n = \frac{P_c \cdot q(\lambda_c)}{P_h \cdot q(\lambda_h)} \quad \frac{1}{\alpha\sqrt{\theta}} \qquad (13)$$

$q(\lambda)$ = the gasodynamic functions.

Combining equations (6), (8), (9) and (10) we obtain the equation for T_c in the form

$$\frac{T_c}{T_o} = \frac{\frac{1}{\pi} + N}{\frac{1}{\pi^B} - 1} \quad \text{here } N = \frac{\Delta t_k + \Delta t_T}{T_o} \qquad (14)$$

From equations (6), (11) and (14) we have

$$\frac{T_h}{T_o} = 1 + \mu \cdot N \qquad (15)$$

Expression (14) contains a function B the value of which for the selected value of μ depends upon the conditions of operation of the ejector (the vacuum it establishes, i.e. the degree of expansion π in the vortex tube).

We shall determine the value for P_c from the equations for the ejector.

Assuming $q(\lambda_{h_p}) = 1$ (tapering nozzle) and $P_c \approx P_3$ we obtain from equation (13)

$$\pi' = \frac{P_h}{P_c} \approx \frac{P_h}{P_3} = \frac{q(\lambda_c)}{n \cdot \alpha} \quad \text{or} \quad \alpha = \frac{(\lambda_c)}{n \cdot \pi}, \qquad (16)$$

Bearing in mind that the stream from the nozzle is ejected into the atmosphere, we assume $P_4 = 1$ and find from equations (12) and (16);

$$\pi = \frac{q(\lambda_c)}{n\left[\left(q(\lambda_c) + 1\right) P_c - 1\right]} \qquad (17)$$

By solving together equations (17) and (4) the value for P_c may be determined for a given value of P_o, assumed in the first approximation equal to P_1, and for chosen values of μ and λ_c.

Approved For Release 2009/05/01 : CIA-RDP80T00246A007500340002-0

Approved For Release 2009/05/01 : CIA-RDP80T00246A007500340002-0

It is feasible to choose $\mu = 0.6$ (which corresponds to maximum cooling capacity of the vortex unit) and $\lambda_c = 0.7$ ($\mathcal{T}(\lambda_c) = 0.894$).

Most often the basis for the calculation may be the selection of a heat exchanger for given values of T_o, T_c, P_o and chosen values of μ and λ_c. For rating the heat exchanger one must know the value of the overall compressed air input G. This may be determined from the conditions for the permissible heating of the cold stream in the refrigerated chamber Δt_k, by external heat exchange in the steady state.

The hourly heat inflow Q_k is calculated for the chosen geometry of the refrigerated chamber, type and thickness of the insulation and minimum required temperature in the chamber and then one obtains from expression (9)

$$G = \frac{Q_k}{\mu \cdot c_p \cdot \Delta t_k} \quad [kg/hr] \qquad (18)$$

The amount of heat transmitted by the heat exchanger

$$Q_T = G \cdot C_p (T_o - T_1) = G \cdot C_p T_o \left(1 - \frac{1}{B} \cdot \frac{T_c}{T_o}\right) [kcal/hr] \qquad (19)$$

The maximum temperature head in the heat exchanger

$$\Delta t_T = T_1 - T_2 = T_c \left(\frac{1}{B} - 1\right) - \Delta t_k \quad [°C] \qquad (20)$$

From the known values for G, Q_T, Δt_T and Δt_T the heat exchanger is calculated as well as the hydraulic losses in the compressed air circuit $\Delta P_1 = P_o - P_1$ and in the circuit of the cold stream

$$\Delta P_c = P_c - P_3$$

With the aid of these values a more precise evaluation is made of the degree of expansion

$$\mathcal{T} = \frac{P_1}{P_c} = \frac{P_o - \Delta P_1}{P_3 + \Delta P_c}$$

and the calculation is repeated.

The cross section of the vortex tube nozzle is determined from the overall input according to the formula

$$F_d = \frac{G \cdot \sqrt{T_1}}{36 \cdot 0{,}4 \cdot d_d \cdot P_1} \quad [mm^2] \qquad (22)$$

Here

d_d is the nozzle discharge coefficient of the vortex cooler.

Approved For Release 2009/05/01 : CIA-RDP80T00246A007500340002-0

Approved For Release 2009/05/01 : CIA-RDP80T00246A007500340002-0

The diameter of the vortex tube is calculated by means of equation (2) and of the diaphragm orifice by means of (1).

The cross section of the ejector nozzle is determined in a manner similar to that for the vortex tube nozzle

$$F_h = \frac{G\,(1- \qquad) \cdot \sqrt{T_h}}{36 \cdot 0{,}4 \cdot d_h \cdot P_h} \qquad (23)$$

Here

is the discharge coefficient of the ejector nozzle.

The other dimensions of the ejector are calculated from the value for α determined from expression (16).

Approved For Release 2009/05/01 : CIA-RDP80T00246A007500340002-0

Approved For Release 2009/05/01 : CIA-RDP80T00246A007500340002-0

Expérimentation d'un grand tube Ranque dans la République Populaire Roumaine.

Testing of a Large Ranque Tube in Rumania.

P. IOANID
Institut Énergétique de l'Académie de la République Populaire Roumaine, Bucarest, Roumanie.

SUMMARY. Scientific and experimental investigations on the Ranque tube have extended over recent years. Thanks to its special features (rapid starting, production of very low temperatures, simplicity of construction, possibility of using the pressure of natural gases before their combustion or chemical change etc.) this device may be used for many purposes in the field of refrigeration. In the Power Institute of Rumania, a Ranque tube of industrial size, operating with methane gas with high flow rate and under high pressure was studied. The report describes the arrangement and presents the theoretical principles of operation of the Ranque tube, as well as the experimental results of the performance of the device (capacity of thermal separation, minimum temperature, output) for different working conditions and with different types of construction. The Ranque tube used is larger than mentioned up to now in literature (diameter : 170 mm) and produces temperatures of - 80°C. The gas velocity and temperature fields in the tube have been determined from which some conclusions on operational process have been drawn (uselessness of supersonic expansion) as well as the elaboration of recommendations useful for the construction of similar devices.

Le refroidisseur toubillonnaire, dénommé en littérature "tube Ranque" représente un appareil qui réalise la séparation continuelle d'un jet gazeux, ayant une certaine surpression initiale en deux jets, l'un chaud et l'autre froid.

L'utilisation de cet appareil dans l'industrie de la République Populaire Roumaine, a nécessité des recherches théoriques et expérimentales à l'Institut de l'Énergétique de l'Académie Roumaine. Ces recherches ont été effectuées dans une station expérimentale située près d'une zone riche en gaz méthane, ce qui assure un débit relativement grand de gaz, ayant une gamme de pression jusqu' à 100 at.

L'appareil expérimental (Fig. 1) représente un refroidisseur tourbillonnaire à contre-courant ayant les particularités suivantes:

- Le diamètre de la chambre de tourbillonnement: D - 17 cm.
- L'ajoutage de l'admission tangentielle exécuté dans les variantes: un ajoutage convergent $\varphi_{aj} = 25$ mm; un ajoutage convergent $\varphi_{aj} = 15$ mm ; un ajoutage convergent-divergent $\varphi_{ajer} = 16$ mm ; $\varphi_{aj_{max}} = 25$ mm.

Approved For Release 2009/05/01 : CIA-RDP80T00246A007500340002-0

Approved For Release 2009/05/01 : CIA-RDP80T00246A007500340002-0

- La chambre de tourbillonnement présente aux deux extrémités des diaphragmes aux diamètres différents qui bornent à droite et à gauche les tubes d'écoulement du gaz chaud et froid. Cette installation permet la variation de la pression initiale, la variation des contre-pressions dans le tube chaud, respectivement froid, des mesures des températures des pressions d'admission et d'évacuation, de même que du champ des pressions dans la chambre de tourbillonnement et dans le tube chaud (en vue de la détermination du champ de vitesse), le calcul du débit à l'admission dans l'appareil et à l'évacuation des deux tubes.

Parmi les buts poursuivis dans nos expériences citons:

- La clarification du mécanisme d'obtention de l'effet frigorifique.

- La détermination des conditions nécessaires pour obtenir la plus grande efficacité frigorifique, en étudiant la pression initiale, la vitesse d'admission, le diamètre de l'ajoutage de l'admission et la contre-pression dans les tubes (chaud et froid).

Le refroidisseur tourbillonnaire est constitué d'un tube central où est pratiqué un orifice tangentiel par lequel entre le gaz sous pression. L'entrée tangentielle du gaz dans la chambre de tourbillonnement provoque un mouvement de rotation. Le champ de vitesse établi dans la section initiale est modifié dans l'intérieur de la chambre à cause des forces de friction des couches concentriques du gaz.

La modification du champ des vitesses produit le transfert de l'énergie cinétique parmi les couches concentriques du gaz.

Si l'on sépare les deux domaines avant l'embrouillement mécanique où avant la transmission de la chaleur (ce qu'on ne peut pas éviter intégralement), on peut obtenir deux jets de gaz: chaud et froid. La séparation peut être réalisée directement, par l'introduction d'un tube central qui prélève le gaz froid, ou bien par voie pneumatique, en créant dans le tube chaud une contre-pression plus forte que dans le tube froid. Ainsi le gaz de la zone centrale de moindre pression est dirigé vers le tube froid, indépendamment de sa position. Cette opération constitue le mode de séparation dans le refroidisseur tourbillonnaire en contre-courant.

Pour analyser le mode de production de l'effet frigorifique, il faut déterminer le champ des vitesses dans le régime initial et final en considérant le mouvement stationnaire pour le fluide visqueux et en appliquant l'équation du moment de la quantité du mouvement.

Les forces extérieures qui actionnent sur un élément annulaire sont représentées par les valeurs de friction.

La tension tangentielle a l'expression suivante:

$$\tau = \mu \left(\frac{1}{r} \frac{\partial V_r}{\partial \Theta} + \frac{\partial V_\Theta}{\partial r} - \frac{V_\Theta}{r} \right)$$

où : τ = tension tangentielle

μ = le coefficient de la viscosité cinématique

ω = la vitesse annulaire de la rotation

Approved For Release 2009/05/01 : CIA-RDP80T00246A007500340002-0

Approved For Release 2009/05/01 : CIA-RDP80T00246A007500340002-0

V_r = La vitesse radiale

V_θ = la vitesse tangentielle

parce que $\frac{\partial V_r}{\partial \theta} = 0$, nous aurons $\varphi = \mu r \frac{d\omega}{dr}$

Le moment des forces de la friction appliquée à un cylindre au rayon "r" a l'expression :

$M_f = 2\pi\mu r^3 \frac{d\omega}{dr}$; pour un élément "dr" nous aurons

$$dM_f = 2\pi r^2 \left(3\frac{d\omega}{dr} + r\frac{d^2\omega}{dr^2}\right) dr \qquad (1)$$

Le moment de la quantité de mouvement du fluide qui pénètre radialement dans le cylindre de rayon "r" et d'une longueur unitaire est exprimée par : $M_c = -r V_\theta m$ ou: m = le débit de la masse

Pour un élément "dr" nous aurons : $dM_c = -m(r^2 d\omega + 2r\omega dr)$ (2)

En équivalent les expressions (1) et (2) et en intégrant l'équation différentielle ainsi obtenue, nous trouverons la solution :

$$V_\theta = C_1 r^{1 - \frac{m}{2\pi\mu}} + \frac{C_2}{r}$$

Pour obtenir la dernière vitesse dans le centre du refroidisseur tourbillonnaire : $C_2 = 0$; donc $V_\theta = C_1 r^{1 - \frac{m}{2\pi\mu}}$ (3)

En analysant la solution (3) on peut observer que dans le régime initial, quand le débit radial "m" est grand (le gaz sorti de l'ajoutage tangentiel tend à occuper toute la section) la vitesse tangentielle est fortement poussée vers le centre du tube.

En régime final, quand le débit radial tend vers zéro, la vitesse tangentielle a tendance à se partager en rapport avec la loi du mouvement des corps solides, donc elle est grandissante vers la périphérie.

Cette analyse schématique explique l'effet frigorifique du refroidisseur tourbillonnaire.

La détermination du champ des pressions dynamiques dans le refroidisseur tourbillonnaire expérimenté indique que l'expliquation présentée ci-dessus est confirmée qualitativement par les résultats expérimentaux (voir Fig. 2 et 3).

A proximité du centre, les déterminations indiquent un courant inverse, qui persiste même dans le tube chaud. Le phénomène de transmission centrifuge de l'énergie cinétique et le phénomène de la séparation thermique ont lieu par conséquent aussi dans ce tube.

Schématiquement, le champ des vitesses axiales et par conséquent la circulation du fluide se réalise de la manière suivante (voir Fig. 4).

Pour mettre en évidence les performances obtenues avec le refroidisseur tourbillonnaire expérimental, on indique dans la Fig. 5 les caractéristiques de fonctionnement dans les conditions suivantes:

- l'ajoutage φ_{aj} = 14,05 mm ;
- le diamètre du diaphragme du tube "froid" : D_r = 40 mm ;
- le diamètre du diaphragme du tube "chaud" : D_c = 110 mm.

Approved For Release 2009/05/01 : CIA-RDP80T00246A007500340002-0

Approved For Release 2009/05/01 : CIA-RDP80T00246A007500340002-0

Les caractéristiques indiquent la variation de la température du gaz froid et chaud en fonction du rapport "n" entre le débit du gaz froid et le débit total pour les différentes pressions d'admission.

On peut constater qu'on a obtenu des températures proches de -70°C, la température du gaz à l'admission étant de 16°C.

En expérimentant différentes variantes, on a conclu:

- L'augmentation de la pression initiale jusqu'à une certaine limite contribue à l'augmentation de l'effet frigorifique. A cette limite, on remarque une réduction de la capacité de séparation (fait mis en évidence par l'intersection des courbes caractéristiques de la Fig. 5). Ce phénomène a lieu lorsque dans le diaphragme du tube chaud ou froid on atteint approximativement la vitesse du son et la détente du gaz dans la chambre de tourbillonnement est limitée.

  Plus le diaphragme du tube froid a un diamètre réduit, autant la température du gaz est moindre, mais le débit du gaz froid diminue.

- La contre-pression dans le tube chaud constitue le paramètre qui assure le fonctionnement et le réglage du refroidisseur à contre-courant. L'augmentation de la contre-pression conduit à l'augmentation du débit du gaz froid.

- L'agrandissement de la vitesse d'admission lors de la vitesse du son diminue l'efficacité frigorifique.

Ce résultat expérimental confirme encore une fois le mécanisme de séparation décrit. Quand la vitesse d'admission est de beaucoup supersonique, on ne peut plus obtenir un gradient de vitesse convenable dans la section initiale (la vitesse est uniforme, proche de la vitesse maximum et occupe seulement la zone périphérique de la chambre de tourbillonnement), donc un transfert radial puissant de l'énergie cinétique ne peut pas se produire.

- L'efficacité frigorifique augmente en même temps que le rapport entre le diamètre de la chambre de tourbillonnement et le diamètre de l'ajoutage tangentiel. (Dans les variantes expérimentées, le rapport maximum a atteint $D/D_{aj} = 11,3$). Ce phénomène s'explique par la réduction de l'effet de la couche limite, par l'agrandissement du rapport et d'autre part par la réduction des vitesses axiales, donc par la réduction des pertes hydrauliques.

Pour les variantes de construction du refroidisseur tourbillonnaire expérimenté on a établi les relations suivantes entre les divers diamètres, pour réaliser le maximum de l'efficacité frigorifique (c'est-à-dire le maximum de frigories).

$$\frac{Dr}{Daj} \cong \sqrt{n \frac{P_o}{P_r}} \qquad \frac{Dc}{Dr} \cong 2,8 \qquad \frac{D}{Dr} = 4,25$$

Approved For Release 2009/05/01 : CIA-RDP80T00246A007500340002-0

Approved For Release 2009/05/01 : CIA-RDP80T00246A007500340002-0

où: D = le diamètre de la chambre de tourbillonnement
D_r= le diamètre du diaphragme du tube froid
D_{aj}=le diamètre de l'ajoutage de l'admission
D_c =le diamètre du diaphragme du tube chaud
P_o =la pression initiale
P_r =la pression moyenne à la sortie du gaz froid
n = le coefficient du débit

COPYRIGHT RESERVED

Approved For Release 2009/05/01 : CIA-RDP80T00246A007500340002-0

Approved For Release 2009/05/01 : CIA-RDP80T00246A007500340002-0

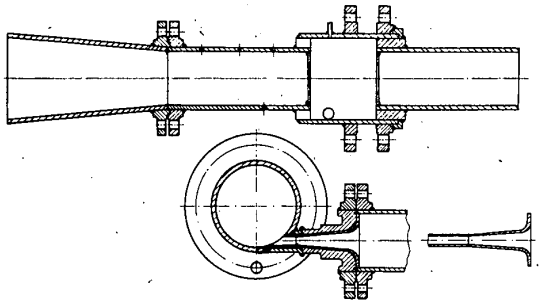

Fig. 1. L'appareil expérimental – un refroidisseur tourbillonnaire à contre-courant.

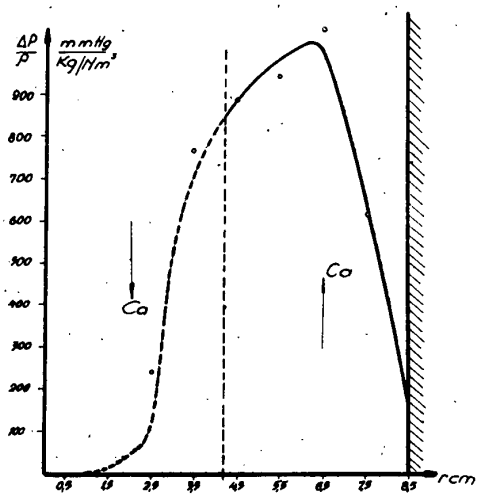

Fig. 2. La répartition des pressions dynamiques dans la chambre de tourbillonnage.

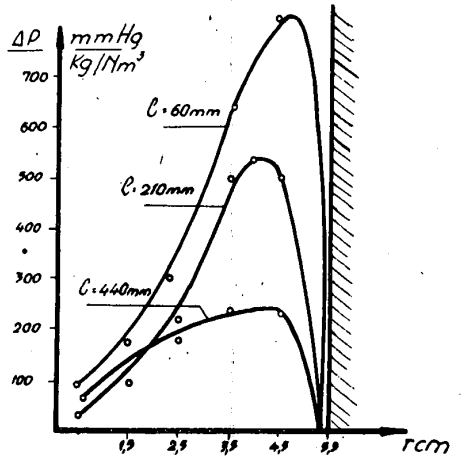

Fig. 3. La répartition des pressions dynamiques dans le tube chand.

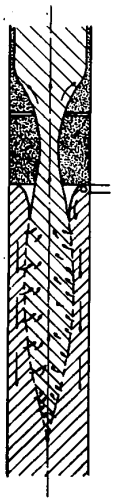

Fig. 4. Circulation du fluide.

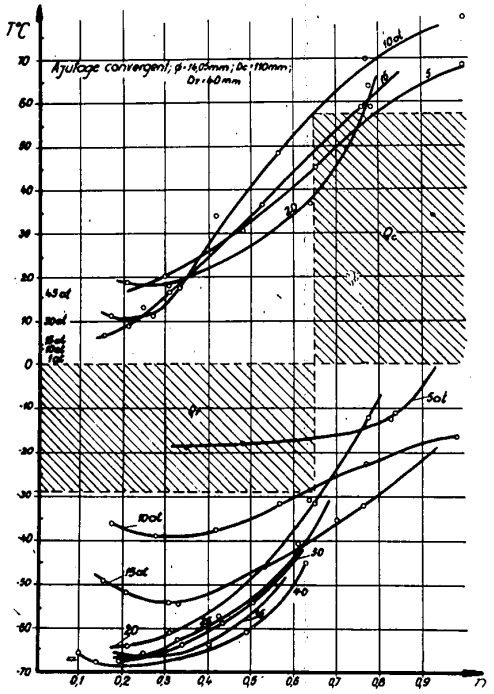

Fig. 5. Caractéristiques de fonctionnement.

Approved For Release 2009/05/01 : CIA-RDP80T00246A007500340002-0

Approved For Release 2009/05/01 : CIA-RDP80T00246A007500340002-0

Carbon Dioxide as a Means of Prolonging the Storage Life of Chilled Fish Products

La prolongation de la durée de conservation des poissons refrigérées par l'emploi du gaz carbonique

A.P. MAKASHEV
Krasnodar Branch of the Central Scientific Research Institute of the Canning and Vegetable Drying Industry, Krasnodar, USSR

SOMMAIRE. Le CO_2, dissous dans les tissus musculaires du poisson, entraîne un certain nombre de changements. Les plus importants sont: la modification de l'équilibre osmotique, l'accroissement de la concentration en ions hydrogène, l'accroissement de l'activité des enzymes protéolytiques, la transformation de l'hémoglobine en méthémoglobine. Le CO_2, dissous dans la denrée lui confère un goût acide qui disparaît quand on aère la denrée. Le CO_2 diminue effectivement l'activité des microorganismes responsables de la putréfaction. Son action préservatrice est renforcée quand il est combiné avec l'utilisation du froid ou un traitement du produit.

L'action préservatrice se manifeste davantage sur le poisson réfrigéré. Quand la température est abaissée en dessous de 15 à 16° C, la croissance des microorganismes qui peuvent se développer en atmosphère carbonique est ralentie. En milieu carbonique, l'altération due à l'oxydation du poisson gras est retardée. Mais les avantages du CO_2 ne se manifestent qu'à certaines conditions: non seulement son action préservatrice, mais aussi son effet sur le produit lui-même, comme par exemple son action sur l'activité enzymatique, doivent être prises en même temps en considération.

L'Auteur a défini les conditions d'utilisation du CO_2 pour la conservation des produits à base de poisson. Le poisson frais qui possède un complexe cathepsine de faible activité (la sandre, la brème, etc...) se garde 1,5 à 1,8 fois plus longtemps dans un milieu contenant de 20 à 70 % de CO_2 que dans l'air. A 5-8° C, du poisson fumé se conserve 5 à 6 fois plus longtemps dans un milieu contenant 70 à 90 % de CO_2 que dans l'air. A 5-8° C, du poisson salé (10-12 % de sel) se conserve 5 à 7 fois plus longtemps en présence de CO_2 qu'en l'absence de CO_2. La maturation du poisson salé est considérablement accélérée dans un milieu contenant du CO_2.

On a montré expérimentalement que le stockage et le transport du poisson fumé et réfrigéré peuvent être effectués non seulement dans des récipients étanches, mais aussi dans des récipients non hermétiques à condition que la perte de CO_2 soit compensée par une lente sublimation de glace carbonique. En USSR, on a projeté d'employer la conservation en atmosphère carbonique dans les entrepôts de distribution et pendant le transport et l'on envisage d'utiliser le CO_2 à l'échelle industrielle pour la conservation et le transport du poisson fumé.

Approved For Release 2009/05/01 : CIA-RDP80T00246A007500340002-0

Approved For Release 2009/05/01 : CIA-RDP80T00246A007500340002-0

Results are presented of experiments carried out in the Don-Kuban Branch of the Scientific Research Institute of Marine Fisheries and Oceanography of the U.S.S.R. aimed at developing procedures and techniques for using carbon dioxide to extend the storage life of fish products.

Experimental determination has been made of the solubility of gaseous carbon dioxide in fish tissue depending upon the composition of the latter (fat, protein, free water and salt contents) and upon the temperature and partial pressure of the gas. For fish of average fattiness the solubility coefficient α is 0.8-1 ml. CO_2/g at 0° C. 1.4 - 1.5 ml CO_2/g at 0° C.

Dissolved in the tissues carbon dioxide causes a number of changes in them, some of which are irreversible.

In a carbon dioxide medium the flesh of fresh fish becomes more supple and elastic and the surface of fish cuts turns somewhat moist owing to the liberation of tissue juice. This bears evidence of an impairment in the osmotic equilibrium of the muscular tissue. Analogous action of carbon dioxide has been observed by V.S. Zagoryansky in plant tissue [1].

The acidity of the muscle increases about two-fold and the pH falls on the average from 7 to 6.2. The buffering capacity of the muscle as determined by potentiometric titration with alkali of aqueous extracts increases by 2 to 2.5 times. The increase in the buffering capacity of the muscle hinders shift of the pH to the alkaline, a necessary condition for activity of putrefying microorganisms. This together with the fall in pH and other changes in the tissue we believe is one of the most important factors hindering the growth of such microorganisms. In a medium insufficient buffering capacity, as a result of microbial activity, the pH quite rapidly goes over to the alkaline.

Shifting the pH in the acid direction carbon dioxide increases the activity of muscular proteinases and hence accelerates the autolysis of fresh fish and the ripening of little and medium salted products [2, 3]. The amino acid content in the muscular tissue of bream, herring and anchovy kept at 0° C. in a carbon dioxide medium increasss considerably faster than when stored in air.

Some of the carbon dioxide is bound by the proteins to form a compound.

The preservative action of carbon dioxide both on the surface and in the bulk of the product is manifested already at low concentrations of the gas and increases with increase in concentration.

The effect is strong at a CO_2 content of 70 % and is maximum for a 100 % gas. The action increases with increase in the CO_2 pressure. However, in a medium with a high CO_2 content at room temperature putrefying micrococci characterized by A.Y. Aldakimova as close to the species Micrococcus candidus, responsible for rapid souring, often develop on fish.

When the temperature is lowered to below 15 - 16° C. growth of these micrococci is depressed and souring of the fish in the carbon dioxide medium does not take place.

The preservative action of carbon dioxide also noticeably increases in the presence of salt in the fish (within the limits of 6 - 14 % NaCl). Salted fish is kept from bacterial spoilage

Approved For Release 2009/05/01 : CIA-RDP80T00246A007500340002-0

Approved For Release 2009/05/01 : CIA-RDP80T00246A007500340002-0

in a carbon dioxide medium about 2 - 3 times longer than the fresh product.

Chilling negatively affects the development of pathogenic bacteria, in particular, botulinus. It has been established by special experiments that carbon dioxide in concentrations of 90 % does not stimulate botulinus growth on smoked fish at temperature of 20, 25 and 30° C. [4].

Carbon dioxide depresses the growth of microorganisms more effectively on cooling ensuring relatively greater storage periods for the products than at room temperature. The results of determining the effect of carbon dioxide on the growth of microflora on smoked fish[1] for different temperature are presented in Table 1.

Table 1. The effect of carbon dioxide on the growth of microflora on smoked fish for different temperatures.

Storage temperature	CO_2 concentration, %	Duration of storage (days)				
		0	4-5(5)[1]	8-10(33)	15 (50)	60
		Log number of cells per g				
23-25	0	3.0	8.1[3]	10.6	9.8	-
	70 - 80	3.2	6.4	9.4	8.9	-
	80 - 90	3.2	5.8	8.3	8.1	-
	100	3.2	5.1	7.1	8.1	-
13-16	0	1.0	6.8	9.3[3]	10.0	-
	80 - 90	1.0	3.2	6.2	7.5	-
	100	1.0	3.6	6.0	6.5	-
5-7	0	1.3-0[2]	3.7-4.4[3]	4.9-6.0	-	-
	90 - 100	1.3-0	1.3-1.4	1.5-2.0	1.8-2.5	1.7-2.6

[1] In parenthesis are shown storage lives for the temperatures 5-7° C.

[2] The first figure is for surface contamination (subcutaneous). The second figure is for the muscular contamination (at the backbone).

[3] Control fish completely covered with mold.

Carbon dioxide is not only a preservative and an activator of cathepsin, but also effectively retards oxidation of fat, a fact observed by many authors [5, 6, 7]. This highly important property is already manifested at low carbon dioxide contents in air (20 - 30 %) and is intensified with increase in concentration.

Dissolving in the blood of fresh fish carbon dioxide converts the hemoglobin to methemoglobin, resulting in a brownish colour of the gills. This, however, is not a sign of deterioration of the fish as in the case of ordinary storage.

It has been found during storage of fresh fish that with species possessing a highly active cathepsin complex (anchovy) quality deterioration sets in within 3 - 4 days owing to autolytic

---

[1] Hot-smoked fish should be understood when the term "smoked fish" is mentioned.

Approved For Release 2009/05/01 : CIA-RDP80T00246A007500340002-0

Approved For Release 2009/05/01 : CIA-RDP80T00246A007500340002-0

softening of the tissues. Carbon dioxide, activating proteolysis, accelerates the softening of tissues and therefore has no beneficial effect on the storage of such fish.

With fish possessing less active proteinases (pike-perch, sprat, bream) loss in quality takes place after 6-11 days as a result of bacterial action. Although carbon dioxide in concentrations of 20-70 % promotes proteolysis, it effectively retards putrefactive processes, prolonging the storage life of these fish in comparison with gas-free storage by 1.3 - 1.8 times. At carbon dioxide concentrations above 70 % proteolysis markedly increases and the muscles soften more rapidly than at lower concentrations. In 100 % CO_2, owing to the accelerated autolytic softening of the muscles, the storage life of these fish increases only insignificantly as compared with that for storage without gas.

It thus follows that carbon dioxide may be employed in concentrations not exceeding 70 % for the storage of only such fish that possess cathepsin complexes of low activity.

Laboratory and field experiments on the storage of smoked fish were carried out on a large variety of species (anchovy, herring, mackerel, saurel bream, etc.).

Carbon dioxide does not change the appearance of smoked fish but lends it an acid flavour, which disappears, however, on holding the product for some time in air (degassation).

Because of the increase it causes in the buffering capacity of muscle, carbon dioxide has a strong stabilizing action on the pH value of smoked (and fresh) fish (Fig. 1) and retards to a certain extent its dehydration, helping to maintain the high quality of the product (the tenderness and succulence of the tissues).

The change in proteins of smoked fish, in particular the increase in non-protein and volatile base nitrogen contents, proceeds much slower in a carbon dioxide medium than under ordinary conditions, especially at diminished temperatures.

In smoked fish cathepsin is practically inactivated during the heat treatment (the fish is heated to a temperature of 80 - 85°) so that this product may be stored in media with a high carbon dioxide content (above 70 %), possessing maximum preservative action and effectively protecting the product from oxidation.

The storage life of smoked fish in a medium containing 70 - 99 CO_2 at 15 - 30° C. increases 2 - 3 fold in comparison with storage in air. However, the development of micrococci causing acid spoilage of the product is excluded only at temperatures below 15 - 16° C. Optimum storage conditions are provided at 2 - 8° C., the storage life increasing 5 - 6 fold. With lower carbon dioxide concentrations (40 - 60 %) at a temperature of 0 - 3° C. the storage life is increased threefold.

The strongest preservative action of carbon dioxide with respect to salted fish falls on 90 - 100 % concentrations of the gas with an 8 - 12 % salt content and at reduced temperatures (Fig. 2).

The ripening of salted fish is accelerated in a carbon dioxide medium, a fact which is confirmed both organoleptically and by the rate of increase in soluble nitrogen, by changes in the pH and by the bound water content of the flesh [2, 3].

Approved For Release 2009/05/01 : CIA-RDP80T00246A007500340002-0

Approved For Release 2009/05/01 : CIA-RDP80T00246A007500340002-0

Alongside the strong preservative action of the carbon dioxide at 5 - 8° C., overripening does not set in for quite a time so that the storage life of salted fish saturated with carbon dioxide increases 4 - 7 fold in comparison with ordinary conditions.

In the field tests of the carbon dioxide method the storage and transport of smoked fish was carried out both in hermetic and non-hermetic containers using gaseous and solid (dry ice) carbon dioxide.

On the gaseous conditions within the hermetic container considerable influence is exerted by the sorption of the carbon dioxide by the product. To ensure optimal conditions for the gas on sufficiently dense packing of the product in the container, the product should preliminarily be flushed with carbon dioxide, which is accomplished by simply exposing the former to a medium containing 90 - 100 % CO_2 for a time sufficient to attain a value of 70 - 80 % complete saturation.

In a non-hermetic (but sufficiently tight) container the loss of carbon dioxide is conveniently replenished by slow sublimation of dry ice placed in a thermally insulated packing. The rate of sublimation depends upon the insulation and may be calculated. In this case saturation of the product by carbon dioxide is accomplished in the container after the packing operation. In a non-hermetic thermally insulated container, not only the required gaseous medium is ensured, but the temperature is by 15 - 17° C. lower than the ambient (in summer), the consumption of dry ice amounting to about 0.02 - 0.03 kg/kg product daily.

We are of the opinion that transportation of chilled smoked saurel in a carbon dioxide medium will preserve its commercial qualities (consistency, succulence and tenderness of the tissues, retardation of fat rancidity) and make for lower operating costs than transportation in the frozen state.

Bacteriological investigations of smoked fish after its transportation and storage carried out by the Institute of Nutrition of the Academy of Medical Sciences of the U.S.S.R. have confirmed the powerful preservative action of carbon dioxide with respect to this product under chill conditions.

The Ministry of Public Health of the U.S.S.R. has approved the carbon dioxide method for the commercial storage of smoked fish.

REFERENCES

1. ZAGORYANSKY, V.S. The Effect of CO_2 on the Storage Life of Fruits. Works of the Central Scientific Research Biochemical Institute of the Food Industry, 111, 141, 1933.

2. MAKASHEV, A.P. The Use of Carbon Dioxide for Preservation of Weakly and Medium Salted Fish. Rybnoe Khozyaistvo, (12), 1954.

3. MAKASHEV, A.P., MINKINA, A.I., and SOKOLOVA, E.V. The Effect of Carbon Dioxide on the Activity of Muscular Cathepsin and on the Keeping Qualities of some Types of Fresh and Salted Fish. Works of the Azovo-Chernomorsk

Approved For Release 2009/05/01 : CIA-RDP80T00246A007500340002-0

Approved For Release 2009/05/01 : CIA-RDP80T00246A007500340002-0

Scientific Research Institute of the Fisheries and Oceanography, Simpheropol, XVI, 1955.

4. KORNITSKAYA, N.V, FIRSOVA, V.I., MAKASHEV, A.P. and ALDAKIMOVA, A.Y. The Action of Carbon Dioxide on the Bac. Botulinus in Smoked Fish. Voprosy Pitaniya, 2, 1956.

5. ALEKSEEV, P.A. The Effect of CO_2 on Perishable Foods Collection 'For Advanced Refrigerating Engineering', [illegible], 1939.

6. GABRIELYANTS, M.A. Carbon Dioxide Storage of Some Fish Products. Collections of Works of the Plekhanov Institute of People's Economy, 8, Gostorgizdat, 1956.

7. TARR, H.L.P. Control of Rancidity in Fish Flesh. J. of R.B. of Can., 7, [illegible], 1936.

Copyright reserved

Approved For Release 2009/05/01 : CIA-RDP80T00246A007500340002-0

Approved For Release 2009/05/01 : CIA-RDP80T00246A007500340002-0

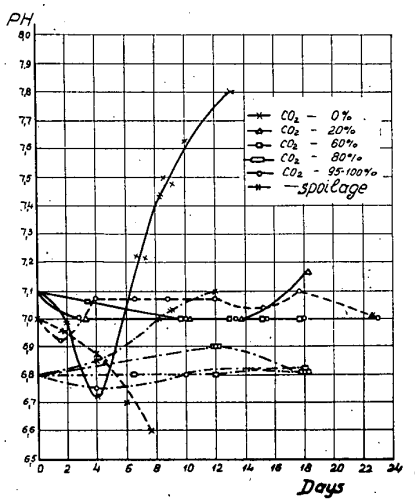

Fig. 1. Changes in the pH of muscular tissue: Chilled sprat (Clupeonella delicatula delicatula) [————]. Cooked roach (Rutilus rutilus heckeli) [– – – – –]. Smooked bream (Abramis brama) [–.–.–.–]. Storage temperature of the cooked and smooked fish 15–25° C.

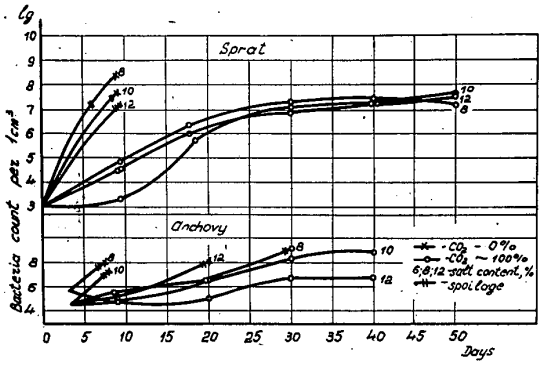

Fig. 2. The effect of carbon dioxide on the growth of bacteria in sprat (*Clupeonella delicatula delicatula*) and anchovy (*Engraulis mordax*) of varying salt content. Storage temperature 18–20° C.

Approved For Release 2009/05/01 : CIA-RDP80T00246A007500340002-0

Approved For Release 2009/05/01 : CIA-RDP80T00246A007500340002-0

Evaporation of Moisture from Products During Freezing in an Air Blast

Déshydratation des produits pendant la congélation en courant d'air forcé

A. B. KHACHATUROV
The Scientific Research Institute of the Refrigerating Industry of the U.S.S.R., Moscow, U.S.S.R.

SOMMAIRE. L'A. a procédé au VNIKhI à des recherches expérimentales sur le mécanisme de l'évaporation d'humidité du poisson au cours de la congélation.

On a déterminé la forme de l'équation entre les groupes sans dimension, exprimant la relation entre l'intensité d'échange de chaleur et le champ de température dans la section transversale du poisson la plus épaisse et à partir de là on a obtenu l'équation réduite à la forme sans dimension pour la température moyenne à la surface du poisson. Il a aussi été etabli une corrélation sous forme de groupe sans dimension entre l'intensité de l'évaporation et les propriétés thermodynamiques du mélange air-vapeur. En transformant cette équation de groupes sans dimension en équation à forme dimensionnelle, en obtient une expression à l'aide de laquelle la perte de poids du poisson au cours de la congélation est déterminée à partir des données initiales sur la congélation pour chaque cas individuel.

On a trouvé que l'augmentation de la vitesse de l'air et de sa température réduisait les pertes de poids du poisson. Ainsi en élevant la vitesse de l'air de 1 à 10 m/s, la perte de poids du poisson au cours de la congélation est divisée par 3,2 fois.

The process of freezing foods in an air blast is accompanied by evaporation of moisture from the product. The weight losses in unpacked products frozen in air are from 1 to 2%.

The determination of the freezing time in the calculation of quick-freezers is accomplished by means of known formula, while the weight losses during the freezing process are defined very roughly.

The evaporation of moisture from the surface of fish being frozen has not yet been sufficiently investigated. Prof. G. B. Tchigeov suggests an approximate solution, with the assumption of proportionality between the amount of heat removed by evaporation and the amount of evaporated moisture irrespective of whether there is evaporation of liquid or sublimation of ice (1).

This paper presents a solution of the problem obtained from experimental investigation of the process of evaporation from fish during freezing.

Approved For Release 2009/05/01 : CIA-RDP80T00246A007500340002-0

Approved For Release 2009/05/01 : CIA-RDP80T00246A007500340002-0

An experimental unit was designed and installed by the author for this purpose at the Scientific Research Institute of the Refrigerating Industry of the U.S.S.R. Continuous determination of the weight of fish in the course of its freezing in air was performed by scales. Measurements were taken during the investigations of the temperature at various points in the fish (in the centre and under the skin), also of the temperature of the air and its rate of flow as well as of the dimension, surface area and volume of the fish. The investigations were carried out on whole fish of the sheat-fish and pike-perch species. The amount of moisture evaporated from the fish during the freezing process Δg is a function of many variables

$$\Delta g = f(\tau, W, t_a, t_s, F, \ldots\ldots)$$

where τ - freezing time, hrs,

W - velocity of air, m/sec,

t_a - temperature of air, ^{o}C,

t_s - temperature on surface of fish, ^{o}C,

F - area of fish surface, m^2.

The experimental data have been, therefore, treated and generalized in similarity criteria and their relations are given in a dimensionless group form. The form of the equation correlating the dimensionless groups, expressing the influence of the heat exchange intensity upon the temperature field in the thickest cross section of the fish, has been determined. Relations have been derived from this equation determining the final temperature at the surface of the fish and the mean final temperature in its thickest section.

The relation has been determined between the mean intensity of moisture evaporation from the surface of the fish and the thermodynamic evaporation criterion including the mean surface temperature of the fish and the air temperature.

The temperature at the fish surface has a decisive influence on the evaporation of moisture from the surface, but no formula for the determination of this temperature is available.

Several curves plotted according to experimental data and characterizing the change in the surface temperature and weight loss in the fish during freezing at various velocities of the air, are given in Fig. 1.

It follows from the curves in Fig. 1 that with a raise of the velocity of the air, the weight losses in the fish are reduced, the air temperature remaining constant at -29 -30°C.

Fig. 2 illustrates the influence of the surface temperature on the intensity of the moisture evaporation from the fish. The curves show that the intensity of moisture evaporation is maximum

Approved For Release 2009/05/01 : CIA-RDP80T00246A007500340002-0

Approved For Release 2009/05/01 : CIA-RDP80T00246A007500340002-0

at the beginning of the process. With a drop of the temperature at the fish surface, i.e. with a decrease in the temperature difference between the surface of the fish and the air, the intensity of moisture evaporation from the surface reduces until at -20° C or lower at the fish surface it becomes negligibly small due to the fact that at -20° C at the surface of the fish and -30° C air temperature the difference of the saturated water vapour pressure becomes insignificant.

Based on data obtained during the experiments, a curve was plotted of the dependence of the parametric criterion $\frac{t_{fs} - t_a}{t_{fm} - t_a}$ upon the Biot number, expressing the influence of the intensity of heat exchange upon the temperature field in the thickest section of the fish at the end of freezing.

The experimental points lie on a straight line corresponding to the following equation

$$\frac{t_{fs} - t_a}{t_{fm} - t_a} = \frac{1}{1 + 0{,}62\ Bi} \qquad (1)$$

where: t_{fs} - final temperature at the fish surface (°C) in its thickest section;

t_{fm} - mean final temperature of the fish in its thickest section °C;

Bi - Biot number $Bi = \frac{\alpha_m\ \delta}{2\lambda_m}$

α_m - mean film coefficient of heat transfer from the fish to the air, kcal/m^{2}hr°C;

δ - thickness of the fish, m;

λ_m - mean thermal conductivity of the fish, kcal/m °C hr.

It has been determined by the author in his previous work (2) that

$$t_{fm} = t_a + \frac{t_{fc} - t_a}{0{,}86 + 0{,}31\frac{\alpha_m \delta}{\lambda_{fc}}} \qquad (2)$$

$$\alpha_m = 4{,}5\ \frac{\lambda_a}{\delta}\left[\frac{w\delta}{\nu}\right]^{0{,}28} \quad \text{kcal/m}^2\text{hr°C} \qquad (3)$$

where additionally:

t_{fc} - final temperature of the fish in the centre of the thickest section; °C.

λ_a - thermal conductivity of the air, kcal/m hr °C;

Approved For Release 2009/05/01 : CIA-RDP80T00246A007500340002-0

Approved For Release 2009/05/01 : CIA-RDP80T00246A007500340002-0

ν - coefficient of kinematic viscosity of the air, m^2/sec;

W - velocity of the air, m/sec.

We derive from equation (1) an expression for the determination of the final temperature at the surface of the thickest section of the fish

$$t_{fs} = t_a \frac{t_{fm} - t_a}{1 + 0{,}62\ Bi} \qquad (4)$$

A comparison of the temperature values, calculated according to the formula (2) and (4), with the experimental data indicates that the deviations are within 10%.

Prof. A. Gukhman was the first to point out the specific role of the thermodynamic criterion of the evaporation in the theory of dehydration and suggested introducing it into the criterional equation as an argument (3).

The criterion of evaporation $\frac{T_{ms} - T_a}{T_a}$ denotes the influence of mass exchange upon heat exchange where:

T_{ms} - mean temperature on surface of fish thick section equal to $\frac{T_i + T_{fs}}{2}$

T_i - initial temperature at fish surface $T_i = 273.16 + t_i$

T_{fs} - final temperature at fish surface $T_{fs} = 273.16 + t_{fs}$

The dependence of the mean intensity of moisture evaporation (b) from the fish during freezing upon the criterion of evaporation has been determined on the basis of experimental data.

Fig. 3 illustrates this dependence showing that all the experimental points obtained at air velocities of from 1.6 to 10.4 m/sec are located on one curve, its equation being:

$$b = \sigma \left[\frac{T_{ms} - T_a}{T_a} \right]^4 \quad kg/m^2hr \qquad (5)$$

σ is here the constant of evaporation; experimental data (Fig. 3) show that it is equal to 14.10^2 kg/m^2hr.

Thus, equation 5 indicates, on the basis of considerable experimental data, the influence of all the factors intensifying the heat exchange upon the moisture evaporation from the fish.

By inserting the value of evaporation mean intensity

$$b = \frac{\Delta g}{\tau F}$$

where: τ - freezing time necessary for lowering the temperature at the surface down to T_{fs} (hrs);

Approved For Release 2009/05/01 : CIA-RDP80T00246A007500340002-0

Approved For Release 2009/05/01 : CIA-RDP80T00246A007500340002-0

into equation (5), the following equation is obtained for determining the weight loss in the fish:

$$\Delta g = 14.10^2 \, F \tau \left[\frac{T_{ms} - T_a}{T_a} \right]^4 \quad kg \qquad (6)$$

or

$$\Delta g' = 14.10^4 \, \frac{F}{g} \tau \left[\frac{T_{ms} - T_a}{T_a} \right]^4 \quad \% \qquad (7)$$

When including the value $g = V\gamma$ (V is the volume, γ - the specific weight of the fish) the equation (7) acquires the following form:

$$\Delta g' = 14.10^4 \, \frac{F}{V\gamma} \tau \left[\frac{T_{ms} - T_a}{T_a} \right]^4 \quad \% \qquad (8)$$

The value $\frac{F}{V\gamma}$ is determined according to the curves of the specific weight variation and the ratio of surface area to the volume of the fish (2).

Besides T_{fs}, determined in accordance with the formula (4), the values of τ, determined from the following dependence suggested by the author (2) are required for determining the weight loss by the formula (6):

$$\tau = 0{,}041 \, \frac{\delta^3}{\alpha_{in}} \, \frac{F}{V} \, \frac{1}{\left[\frac{\alpha_m \delta}{2 \lambda_m} \right]^{0{,}84}} \, \frac{\lambda}{i_i - i_{fm}} \, \frac{t_i - t_a}{t_{fm} - t_a} \quad hr \qquad (9)$$

where: λ - latent heat of ice melting, kcal/kg;

i_i - initial heat capacity of the fish, kcal/kg;

i_{fm} - heat capacity of the fish at the end of the freezing process corresponding to the mean final temperature of the fish, kcal/kg;

In the case when t_{fs} is lower than $-20^\circ C$ calculations are to be made with the assumption of $t_{fs} = -20^\circ$ as with the subsequent drop of the surface temperature of the fish the moisture evaporation practically stops.

The freezing time τ is determined in this case in accordance with the formula (9) with the value t_{fm} derived from the formula (4) inserted in formula (9):

$$t_{fm} = t_a + \left[1 + 0{,}31 \, \frac{\alpha_m \delta}{\lambda_m} \right] \left[t_{fs} - t_a \right] \qquad (10)$$

(t_{fs} is assumed to be -20° C)

Approved For Release 2009/05/01 : CIA-RDP80T00246A007500340002-0

Approved For Release 2009/05/01 : CIA-RDP80T00246A007500340002-0

All the equations are true only within the investigated range of air temperatures from -10° to -45° C and at velocities of the air from 1 to 12 m/sec.

The degree of precision of the formula has been determined to be within approximately 12% by checking the derived formula for the determination of the weight losses in the fish according to the data of industrial tests on quick-freezers (carried out by the Technological Laboratory For Refrigerating Fish and Fish Products at the Scientific Research Institute of the Refrigerating Industry of the U.S.S.R.). This degree of precision is sufficient for technical calculations.

REFERENCES

1. TCHIGEOV, G. B. Problems of the Theory of Freezing Foods. Pishchepromizdat, 1956.

2. KHACHATUROV, A. B. Thermal Processes During Air-Blast Freezing of Fish. Papers from the U.S.S.R. to the Moscow Session of the Comission 4 of the I.I.R. Sept. 1958.

3. LYKOV, A. V. Heat and Mass Exchange at Dehydration. Gosenergoizdat, 1956.

Copyright reserved

Approved For Release 2009/05/01 : CIA-RDP80T00246A007500340002-0

Approved For Release 2009/05/01 : CIA-RDP80T00246A007500340002-0

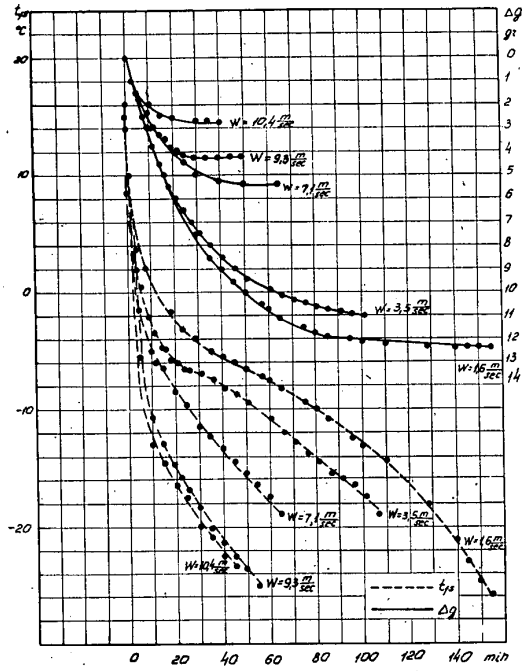

Fig. 1. Curves on change in the surface temperature and weight loss of fish.
t_{fs} °C. – final temperature at fish surface; $\triangle g$ – weight loss of fish; w – velocity of air.

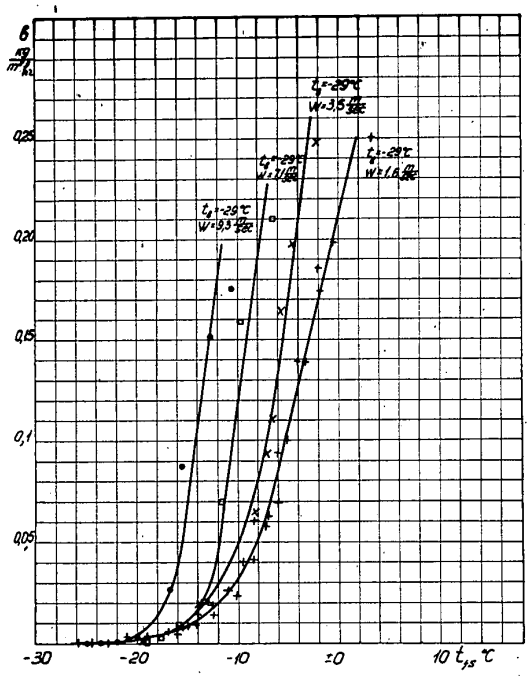

Fig. 2. Influence of temperature at fish surface on intensity of moisture evaporation from the surface.
t_{fs} °C. – final temperature of fish surface; b – evaporation intensity; w – velocity of air.

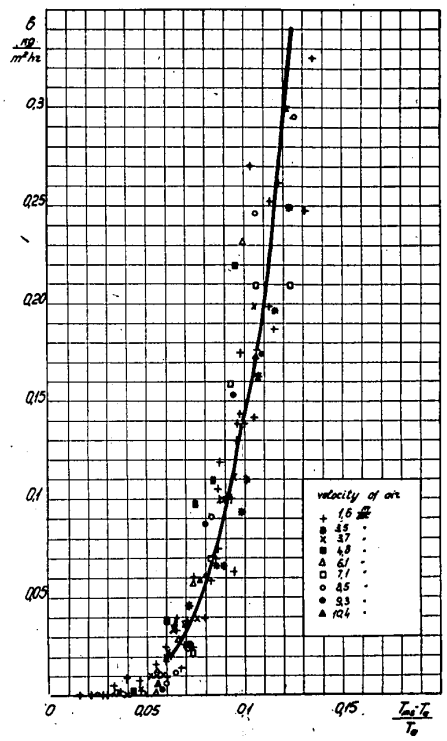

Fig. 3. Dependence of intensity of moisture evaporation from fish (b) upon criterion of evaporation $\frac{T_{ms} - T_a}{T_a}$

Approved For Release 2009/05/01 : CIA-RDP80T00246A007500340002-0

Approved For Release 2009/05/01 : CIA-RDP80T00246A007500340002-0

Bacterial Index of the State of Freshness of Cooled Products

Les numérations bactériennes, directes et indirectes, comme indice possible de l'altération des protéines des produits alimentaires réfrigérés

G.L. NOSKOVA and G.J. PECK

The Scientific Research Institute of the Refrigerating Industry of the U.S.S.R., Moscow, U.S.S.R.

SOMMAIRE. Aucune méthode de numération objective, en vue de déterminer l'altération initiale des protéines alimentaires n'a été largement appliquée. L'altération des denrées réfrigérés provient de microorganismes psychrophiles et, d'après de nombreux chercheurs et d'après nos expériences, elle se manifeste lorsque le nombre des bactéries produisant l'altération atteint une certaine valeur, à savoir 107 à 108 bactéries par gramme. On peut donc s'attendre à ce que la numération des bactéries donne un indice valable de la naissance de l'altération.

Dans cette communication, on passe en revue les méthodes directes et indirectes de numérations bactériennes, et l'on en tire les conclusions suivantes:

a) Les numérations directes de bactéries, à partir d'un nombre de colonies dans un milieu nutritif, sont un procédé trop lent si le développement des bactéries psychrophiles est prédominant, alors que, dans les autres cas, ces numérations ne sont pas assez spécifiques.

b) Le comptage indirect des bactéries, en fonction de la mesure d'un paramètre variant avec le nombre de microorganismes, est une méthode plus riche d'avenir pour la détermination de la naissance de l'altération.

L'emploi de comptage indirect de bactéries peut éliminer un des inconvénients majeurs des méthodes existant pour déterminer l'altération microbienne, notamment la variation de la composition des denrées alimentaires.

Approved For Release 2009/05/01 : CIA-RDP80T00246A007500340002-0

Approved For Release 2009/05/01 : CIA-RDP80T00246A007500340002-0

Although considerable success has been achieved in recent years in studies of biochemical changes taking place in foodstuffs during storage, there is still no reliable, objective method for determining food quality. This also refers to chill storage when the activity of the tissue enzymes is considerably reduced and quality deterioration is caused predominantly by psychrophilic bacteria.

Undoubtedly the biochemical activity of a bacterial culture is a function of the number of individual cells, although the relationship should be expected to be quite involved, since with growth in the bacterial number, the culture becomes older, and with age, as is well known, changes take place in the activities of the bacterial enzymes. The enzymatic activity, moreover, changes, depending upon the changes in the medium caused by bacterial action.

However, experiments very often reveal a definite relationship between the number of bacteria and the content of this or that substance (or group of substances) serving as index of quality change.

Such a correlation may be seen for example on the curves obtained by Shewan (1) for changes in dogfish and in the number of bacteria during storage on ice (Fig. 1) and obtained by us (2) for the changes at 0° C. in cooked meat substrate inoculated with Achromobacter and Pseudomonas (Fig. 2).

A comparison of the changes in the substrate with the bacterial numbers shows that the lower, flat part of the S-shaped curves representing the chemical changes continues until a given amount of bacteria, 10^{7} - 10^{8} cells/g in our experiments and 10^{6} cells/g in the experiments of Shewan has accumulated, following which an abrupt, nearly linear rise takes place in the chemical

Approved For Release 2009/05/01 : CIA-RDP80T00246A007500340002-0

Approved For Release 2009/05/01 : CIA-RDP80T00246A007500340002-0

curves, whereas the curves for bacterial growth begin to round off, gradually assuming a horizontal position (maximum stationary growth phase). The beginning of the sharp rise in the chemical index usually coincides with the beginning of noticeable spoilage.

A relationship between the bacterial number and incipient spoilage has been established by many investigators on a variety of protein foods (3,4,5,6,7).

On Fig. 3 are represented curves we obtained with pure cultures of bacteria in cooked meat juice and cooked ground meat and of a mixed bacterial flora in raw ground meat obtained from retail stores. The sign x on the growth curves designates the beginning of spoilage of the product.

When the initial bacterial count was relatively low (19×10^4 and 34×10^3 per gram medium curves 2 and 3) spoilage of the medium at 0° C. took place just as soon as the number of bacteria rose to 10^8 - 10^7 per gram.

At the same time a number of cases was observed, when the initial bacterial content in the product exceeded 10^7 per gram and yet no spoilage was apparent while the bacteria were in the lag phase of growth (curves 1,4 and 5). Change in the substrate was observed only when the bacteria began to multiply. The advent of spoilage is, therefore, determined not only by the number of bacteria but also by their condition.

This was confirmed to a certain extent by experiments we carried out on meat juice strongly inoculated with various strains of Pseudomonas and Achromobacter (from 74×10^7 to 462×10^7 per gram). When kept under vaseline oil at 6° C. i.e. under conditions retarding bacterial growth the juice remained for long without noticeable change. In the presence of air the bacteria multiplied actively and the juice quickly spoiled (8).

Approved For Release 2009/05/01 : CIA-RDP80T00246A007500340002-0

Approved For Release 2009/05/01 : CIA-RDP80T00246A007500340002-0

Thus from all the above said it may be seen that of all the characteristics the most sensitive under conditions of cooled storage of protein foods is the number of actively growing psychrophilic bacteria.

Since after the initial lag phase the growth rate of bacteria on food products is more or less constant for a given temperature, from the number of bacteria one may estimate the length of further storage life of the products at the given temperature.

In order to avail oneself of this possibility in practice, one must possess a quick method for the evaluation of psychrophilic bacteria in the product.

The methods of determining the number of bacteria known at present may be divided into direct: counting of cells under the microscope or plating methods, and indirect: from physical characteristics or from reactions of bacteria with some substance, serving as indicator.

Direct microscopic counts are inaccurate, particularly when the bacterial content is below 10^7 per gram, when determination of the state of freshness of the product and of its stability in storage is of the greatest interest. Direct microscopic count is unsuitable also because not only living but dead cells and not only psychrophilic but also mesophilic bacteria are included in the count.

Determination of bacteria by counting the colonies is more accurate, but lengthy. If accelerated, undoubtedly this method would be of interest.

We believe that for the exact determination of the content in the products of bacteria responsible for spoilage they should be transferred to a medium of standard composition, containing a

Approved For Release 2009/05/01 : CIA-RDP80T00246A007500340002-0

Approved For Release 2009/05/01 : CIA-RDP80T00246A007500340002-0

substance easily attacked by the bacteria on the one hand and easy to determine on the other. The concentration of this substance should be maximal but not great enough to cause undesirable effects on the bacterial activity.

The content of bacteria per unit volume of indicator medium should also be maximum, since only then do they cause quick reaction. Concentration of bacteria in the product itself in the case of liquids and of washes of the product in the case of solids prior to introducing the bacteria into the indicator medium may be carried out by centrifugation or filtration.

As indicator of the number of psychrophilic bacteria in the medium one may utilize one of the nitrogen extractives, which, as is known are easily attacked by bacteria (9).

However, in this case quantitative determination of the indicator would entail certain inconveniences. A more simple way would be to utilize such indicators as would change colour under the action of bacteria.

Indicators, chiefly of the redox type such as methylene blue and resazurin are extensively used in practice, in particular for determining the state of freshness of milk and some other dairy products. However, attempts to utilize these indicators for fish were unsuccessful owing to the "poising" action of trimethylamine oxide.

In recent years one may meet more and more often with investigations devoted to the use of tetrazolium salts as indicators of the content of active, growing bacteria.

Mallmann et al used tetrazolium salts for determining the storage life of poultry (5), Mustakallio for milk (10), Laxminarayan and Iya (11) showed their use for a number of purposes.

Approved For Release 2009/05/01 : CIA-RDP80T00246A007500340002-0

Approved For Release 2009/05/01 : CIA-RDP80T00246A007500340002-0

Shewan and Liston reported promising results on the use of 2-p-iodophenyl-3-p-nitrophenyl-5-phenyl tetrazolium chloride for the case of fish (12). Here, according to the authors, in the reduction of the tetrazolium salt to coloured formazans only actively growing bacteria took part, i.e. just such as would cause fish spoilage under conditions of storage on ice. The authors indicated that significant amounts of formazan are formed only when the bacterial count $\geqslant 10^6$ cm^2.

Moorjani et al (13) also pointed out that the indicator is the most successful for large numbers of bacteria.

Using triphenyltetrazolium chloride we observed a correlation between the bacterial growth in meat juice inoculated with Pseudomonas.sp. no. 99 and the time for a tetrazolium-containing medium of the type used by Mallmann to give a red colour after the addition of a aliquot of the juice. The relation, very much like that obtained by Mallmann, points out to the existence of an inverse linear function between the time required for the appearance of the colour and the logarithm of the bacterial number. In addition we determined the number of bacteria in the indicator medium at the time of the colour change. As can be seen from the figure, this also falls within the zone of incipient spoilage, being in all cases near 10^8 cells/ml. That the external manifestation of bacterial activity should here also take place at about the same bacterial content as in foodstuffs is of considerable interest.

The time t necessary for bacteria of initial number B/g to reach a value of 10^8/g in the logarithmic growth phase is given by the expression: $t = \frac{-g\log B + g\log 10^8}{\log 2}$, where g is the generation time.

It follows from this that the above observed inverse linear relation is just what is to be expected.

Approved For Release 2009/05/01 : CIA-RDP80T00246A007500340002-0

Approved For Release 2009/05/01 : CIA-RDP80T00246A007500340002-0

Tetrazolium salts may be used for accelerating the plating method. The formazans produced as a result of bacterial action colour the living cells, allowing the colonies to be counted under the microscope 4-6 hours after inoculation (11).

Thus from the above data and the discussion, it follows that whatever its shortcomings the most universal, reliable and objective method of determining the freshness of cooled food products is the count of active psychrophilic bacteria. For the present the determination may be made by plating methods or by the more rapid indirect procedures, i.e. by changes in standard media-indicator systems inoculated with concentrated bacterial suspensions obtained by centrifugation of liquid foods or of washes of solid products.

REFERENCES

1. Biochemical Society Symposium, (6), 28, 1951
2. Kholod. Tekhn., (5), 44-48, 1958
3. World Health Organization. Monog. Ser., 33, part IV, Geneva, 1957
4. Appl. Micr., 4, (6), 345-349, 1956
5. Food Tech., 12, (3), 122-126, 1958
6. Food Tech., 12, (8), 385-386, 1958
7. Appl. Microb., 2, (2), 110-117, 1954
8. Report VNIKhI, 1958
9. Adv. Food Res., (9), 42-82, 1956
10. Science, 122, (3177), 971-972, 1955
11. Current Sci., 21, (5), 124-125, 1952
12. Intern. Inst. Refrig. Comm. 4, Suppl. 1956, 137-147; J. Sci. Food Agric., 8, (4), 222-231, 1957
13. Food Sci., 6, (12), 275-276, 281, 1957

Copyright reserved

Approved For Release 2009/05/01 : CIA-RDP80T00246A007500340002-0

Approved For Release 2009/05/01 : CIA-RDP80T00246A007500340002-0

L'Influence du paraffinage et de la préréfrigération rapide des oeufs conservés par réfrigération.

The Effect of Waxing and Quick Cooling on the Storage of Eggs.

CIOBANU A., CRISTEA S., Racovita A.
Institut de Recherches Alimentaires,
Bucarest, République Populaire, Roumanie.

SUMMARY. The effect of waxing on eggs has been studied, taking account of their freshness and their storage conditions, as well as the effect of quick cooling on unwaxed eggs. After 3 months' storage the best results were obtained for waxed eggs stored at subcooling temperatures ranging between -1.5° and -2.5°C. After 4 months' storage there was observed on the inner surface of the shell of certain waxed eggs the occurrence of mucilaginous granules due to the following moulds: Fusarium, Penicillium, Sporotrichum and Sclerotium. After 6 months' and especially after 8 months' storage, the occurrence of similar granules was observed on most waxed eggs. The quality of these eggs (flavour, odour, colour) was however normal in most cases. It was, moreover, observed that waxing resulted in a marked decrease in the resistance of the vitelline membrane, after longer storage. After long storage, the best results were obtained with quickcooled unwaxed eggs. This observation does not confirm the opinion of some authors recommending the gradual cooling of eggs.

Les récentes recherches ayant rapport à la conservation des oeufs par réfrigération ont été dirigées dans deux directions principales, à savoir: l'abaissement de la température de conservation et la découverte de moyens auxiliaires afin de compléter l'action du froid artificiel, tel que le paraffinage, la pasteurisation, la désinfection, etc.

La plupart des auteurs recommandent d'effectuer le paraffinage immédiatement ou dans un intervalle de 24 heures après la ponte. Toutefois, il peut se produire des altérations. On cite ainsi le cas d'un transport d'oeufs paraffinés expédiés du Canada en Angleterre, qui a dû être jeté à cause des taches de moisissures dans la chambre à air des œufs (1).

Fesq et Pan (2) ont constaté l'apparition de petites taches noires autour de la chambre à air des oeufs paraffinés, ainsi que quelques phénomènes de nature physique comme l'augmentation de la résistance de la membrane du vitellus et la formation de dépôts gommeux sur la coquille; la viscosité du blanc d'oeuf n'a pas changé pendant la conservation.

Approved For Release 2009/05/01 : CIA-RDP80T00246A007500340002-0

Approved For Release 2009/05/01 : CIA-RDP80T00246A007500340002-0

Salton, Scott et Vickery (3) ont observé une altération des oeufs paraffinés due à l'apparition de granulations sèches ou molles à la face externe de la coquille. Les auteurs expliquent l'apparition de ces granulations par la diminution de l'oxygène disponible, qui détermine la modification des processus métaboliques et l'activité des bactéries qui se trouvent à l'intérieur de l'oeuf. De tels oeufs doivent être considérés altérés, quoiqu'il n'y ait aucun signe apparent d'altération.

De même, il faut mentionner encore un facteur dont l'influence est encore assez controversée dans la littérature spécialisée, soit: la technique de la préréfrigération. Tuschneid (4) mentionne que les oeufs ne doivent pas être introduits directement dans une chambre frigorifique à basses températures, parce qu'il peut se produire des condensations de vapeurs d'eau à la face interne de la coquille et un scindement des albumines. La préréfrigération graduée est également recommandée par Dräger (5) ainsi que par les normes espagnoles (6). Par contre, Golovkin (7) montre que la préréfrigération peut être effectuée pendant un temps plus court, en utilisant des chambres à températures de 0° à +2°C et une circulation de l'air ayant une vitesse de 0.3 à 0.5 m/sec.

EXPERIENCES EFFECTUEES.

Dans nos expériences, nous avons étudié l'influence des facteurs suivants:

1.- le paraffinage;

2.- la conservation aux températures de sous-réfrigération (-2°C ±0.5°C) et à un dégré hygrométrique de 87 ±2% des oeufs paraffinés et non paraffinés. Les échantillons de comparaison ont été conservés au même degré hygrométrique, mais à une température de 0°C ±0.5°C;

3.- la préréfrigération rapide;

On a utilisé simultanément des oeufs de deux catégories de fraîcheur, soit:

a.- des oeufs de ferme ayant une ancienneté de 24 heures et une hauteur de la chambre à air de 3 mm, une résistance de la membrane du vitellus de 100% et un indice du jaune d'oeuf de 0.525;

b.- des oeufs de diverses provenances ayant une hauteur de la chambre à air de 5 à 7 mm, une résistance de la membrane du vitellus de 84% et un indice du jaune d'oeuf de 0.455;

Pour l'étude de l'influence de la préréfrigération rapide on a utilisé seulement des oeufs de ferme très frais, ayant une hauteur de la chambre à air de 3 mm au maximum. La préréfrigération a été effectuée à l'air, à une température de 0 à -2°C

Approved For Release 2009/05/01 : CIA-RDP80T00246A007500340002-0

Approved For Release 2009/05/01 : CIA-RDP80T00246A007500340002-0

et une vitesse de 1.2 m/sec. La durée de l'abaissement de la température intérieure de l'oeuf, à +2°C, a été obtenue après 6 heures. Les échantillons de comparaison ont été lentement préréfrigérés, la température de l'air diminuant de 1°C toutes les 2-3 heures. La durée de préréfrigération a été de 48 heures.

Les oeufs ont été emballés en caisses avec de la sciure de bois. Pour le paraffinage on a utilisé de l'huile de vaseline médicinale d'une densité de 0.88 et d'une viscosité de 3°E à 50°C. Au moment du paraffinage, la température de l'huile a été de 21 à 25°C.

La résistance de la membrane du vitellus a été déterminée en cassant les oeufs à une hauteur de 10 cm au-dessus d'une plaque de verre. Les résultat ont été exprimés par rapport au total en pourcentage d'exemplaires dont le jaune ne s'est pas étalé sur le verre.

Pour le calcul de la moyenne de l'indice du jaune d'oeuf, on a pris uniquement en considération les valeurs des oeufs dont la membrane du vitellus a résisté à l'épreuve décrite ci-dessus.

Les altérations indiquées dans le tableau ci-joint, se rapportent aux oeufs attaqués par les moisissures (attaques massives ou taches peu visibles) ainsi qu'à d'autres formes d'altération, mais non les cas dans lesquels on a constaté les granulations mucilagineuses et adhérentes, décrites plus bas.

RESULTATS.

Nous présentons le tableau des resultats après 6 mois de conservation, parce que nous considérons que c'est le plus intéressant. Après les premiers trois mois de conservation, on constate une différence en fonction de la variante, uniquement pour les oeufs moins frais (hauteur de la chambre à air plus grande que 5 mm). Les oeufs paraffinés de cette catégorie (moins frais) ont donné de meilleurs résultats, que dans les variantes non paraffinées de la même catégorie. On a constaté après 3 et 6 mois de conservation, que la majorité des altérations sont dues aux moisissures.

Après 6 mois de conservation, on constate que les oeufs paraffinés indépendamment du degré de la fraîcheur initiale, enregistrent moins de pertes par altérations que les oeufs non paraffinés. Toutefois, dans beaucoup d'oeufs paraffinés, on a constaté l'existence de granulations mucilagineuses incolores, adhérentes à la face interne de la coquille. De telles granulations paraissent dans un petit nombre d'oeufs à partir du 4ème mois de conservation. Leur fréquence augmente à partir du 6ème mois et se trouve dans la majorité des oeufs paraffinés après

Approved For Release 2009/05/01 : CIA-RDP80T00246A007500340002-0

Approved For Release 2009/05/01 : CIA-RDP80T00246A007500340002-0

8 mois. Ce phénomène n'a pas été constaté dans les oeufs non paraffinés, fait qui nous autorise à supposer qu'il s'est produit à la suite des conditions spéciales dues à l'imperméabilisation de la coquille par la paraffinage.

D'après le contrôle microbiologique, il ressort que ces granulations sont dues au mycélium des moisissures suivantes: Fusarium, Penicillium, Sporotrichum, Sclerotium, et pas aux bactéries comme dans l'expériences de Salton (3). Une autre particularité dans notre cas est la formation des granulations décrites plus haut, à la face interne de la coquille, et non à la face externe.

Quoique, au point de vue organoleptique, les oeufs ayant de telles granulations étaient normaux, nous les considérons altérés. Si l'on admet ce point de vue, le paraffinage a donné, dans les conditions de notre expérience, de meilleurs résultats que dans les échantillons de comparaison, mais seulement au cours des premiers 3 mois de conservation.

Dans le cas des oeufs paraffinés, le pourcentage des oeufs altérés non identifiés à l'ovoscope est d'environ 2 fois plus grand que dans les oeufs non paraffinés et ceci sans tenir compte des granulations mucilagineuses adhérentes à la face interne de la coquille, qui elles aussi n'ont pas été identifiées à l'ovoscope.

En ce qui concerne la résistance à la fêlure de la coquille due à la congélation, dans la variante de conservation par sous-réfrigération, on a constaté que le nombre des oeufs paraffinés fêlés a été de 3 à 5 fois moindre que dans ceux non paraffinés.

La fluidité du blanc d'oeuf a été beaucoup plus grande dans les oeufs paraffinés que dans les échantillons de comparaison.

Après 8 mois de conservation, la seule variante qui n'a pas subit d'altération a été celle avec préréfrigération rapide.

CONCLUSIONS.

1.- Le paraffinage a donné de meilleurs résultats, par rapport aux échantillons de comparaison, dans l'intervale des premiers 3 mois de conservation, indépendamment du degré de la fraîcheur initiale.

Pour une période de conservation supérieure à 4 mois, le paraffinage a donné des résultats moins satisfaisants en ce qui concerne la résistance à l'altération. De même, la résistance de la membrane du vitellus a été moindre et le blanc d'oeuf plus fluide que dans les oeufs non paraffinés.

2.- La préréfrigération rapide expérimentée avec des oeufs

Approved For Release 2009/05/01 : CIA-RDP80T00246A007500340002-0

Approved For Release 2009/05/01 : CIA-RDP80T00246A007500340002-0

de première fraîcheur a donné les meilleurs résultats parmi toutes les variantes, n'enregistrant dans ce cas, aucune perte due aux altérations après un laps de temps de 8 mois.

TABLEAU RECAPITULATIF AYANT TRAIT AUX MODIFICATIONS DES OEUFS APRES 6 MOIS DE CONSERVATION.

Indices		Oeufs non paraffinés t = -2°C φ = 87%		Oeufs non paraffinés t = 0°C φ = 87%		Oeufs paraffinés t = -2°C φ = 87%		Oeufs paraffinés t = 0°C φ = 87%
		Hauteur de la chambre à air (mm)						
		3	5-7	3	3 2)	3	5-7	3
Altérations %	1) A l'enlèvement de la chambre frigorifique	2	19,34	12,5	-	-	2.2	-
	Après 14 jours de l'enlèvement	-	8,00	-	-	-	-	-
	Total	2	27,34	12,5	-	-	2,2	-
Pertes en poids %		1,71	1,61	3,52	2,91	0,72	0,59	0,91
Indice du jaune d'oeuf		0,46	0,44	0,47	0,43	0,49	0,51	0,47
Résistance de la membrane de vitellus %		60	50	71	70	56	32	42
pH du jaune d'oeuf		6,83	6,41	6,86	6,52	5,96	6,26	6,76

1) Les oeuf avec des granulations mucilagineuses adhérentes à la face interne de la coquille n'y sont pas compris.

2) Préréfrigération rapide.

Approved For Release 2009/05/01 : CIA-RDP80T00246A007500340002-0

Approved For Release 2009/05/01 : CIA-RDP80T00246A007500340002-0

BIBLIOGRAPHIE.

1. Moississures dans la chambre à air d'oeufs huilés. Bulletin de l'Institut International du Froid (6) 1954.

2. FESQ et PAN, J. Méthode pratique de huilage des oeufs en coquille destinés à l'entreposage frigorifique. Rapport 5.38, Congrès IX, Institut International du Froid, 1955.

3. SALTON, M.R.J., SCOTT, W.J. and VICKERY, J.R. Studies in the Preservation of Shell Eggs. VI, The Effect of Pasteurization on Bacterial Rotting. Australian Journal of Applied Science, 2 (1), 205-221, 1951.

4. TUSCHNEID, M.W. Die kältetechnologische Verarbeitung schnellverderblicher Lebensmittel Brücke. Verlag Kurt Schmeisow-Kirchain N.L., 1936, pag. 346.

5. DRAGER, H. Die Kältekonservierung unserer tierischer Lebensmittel. Fachbuchverlag, Leipzig, 1955, pag. 131.

6. Norma spaniola. Rev.Frio. N° 34.500, 1957, pag. 162.

7. GOLOVKIN, N.A., CIJOV, J. et SCHOLNIKOVA, E.F. Holodilnaia tehnologia piscevih productov. Moskva 1955, pag. 187.

Approved For Release 2009/05/01 : CIA-RDP80T00246A007500340002-0

Approved For Release 2009/05/01 : CIA-RDP80T00246A007500340002-0

L'Expérience de l'entreprise d'état ANTREFRIG concernant la conservation par le froid des produits alimentaires

The Experience of the State Plant ANTREFRIG for the Cold Storage of Foodstuffs.

FICIU, S., MURARIU, M., et NACEA, E.
Institut de Recherches des Produits Alimentaires, Bucarest, Roumanie.

SUMMARY. A cold storage plant for storage of cooled or frozen foodstuffs, quick-freezing of fruit, vegetables and prepackaged meat cuts, of precooked or half-processed food is described. The technilogical processes used for each product and the principal devices are described. Some observations are also reported related to physico-chemical and bactériological changes in fruit, vegetables, meat and precooled meat food, from raw material to the finished product.

L'entreprise spécialisée "Antrefrig" répond aux objectifs suivants:

Entreposage de certains produits alimentaires réfrigérés et congelés.

Congélation de la viande portionnée et pré-emballée.

Production de plats cuisinés et de demi-produits culinaires.

Production de la glace hydrique.

Dans ce qui suit, nous allons présenter quelques aspects des principales activités de l'"Antrefrig".

A. ENTREPOSAGE DES PRODUITS ALIMENTAIRES REGRIGERES ET CONGELES.

Les unités frigorifiques ont été construites dans la période 1923-1942 et ont été modernisées et agrandies pendant les dernières dix années.

Chaque entrepôt est pourvu de chambres d'entreposage à une température de -16 à -20°C pour des produits alimentaires congelés et de chambres pour les aliments réfrigérés.

La plupart des frigorifiques appliquent le refrodissement à saumure, en utilisant des appareils du type sec, humide, ou bien des éléments de chambre.

Approved For Release 2009/05/01 : CIA-RDP80T00246A007500340002-0

Approved For Release 2009/05/01 : CIA-RDP80T00246A007500340002-0

La majorité des entrepôts ont des installations de télétransmission pour les importants paramètres, comme la température et l'humidité de l'air des chambres frigorifiques.

Chaque unité est dotée de tunnels à congélation rapide d'une capacité moyenne de 10 tonnes/24 h et de chambres de préréfrigération ou de réchauffage.

On n'admet pour entreposage que les produits de qualité supérieure qui réunissent toutes les conditions prévues dans les standards uniformes pour tout le pays.

Durant la réception, on effectue les examens organoleptiques et le contrôle au laboratoire conformément aux méthodes unitaires. A la suite de ces examens, on donne des indications concernant le mode d'entreposage et sa durée.

Les produits sont déposés par lots; pour chaque lot on effectue un contrôle périodique en laboratoire, afin de déterminer les modifications physico-chimiques et microbiologiques.

A la livraison après l'entreposage, les produits alimentaires sont soumis de nouveau à des examens organoleptiques et au contrôle de laboratoire, après quoi on émet le certificat de qualité.

B. PRODUCTION DES FRUITS ET DES LEGUMES CONGELES.

Cette production a été commencée à l'échelle industrielle en 1955, et en 1958 on était déjà arrivé à un accroissement de 15 fois par comparaison avec la première année. En 1958 a été mise en exploitation une nouvelle section, dotée d'un outillage moderne.

Les principaux produits sont: fraises, framboises, griottes myrtilles, prunes, raisins en moût, petits pois, haricots-verts, courgettes, gombo, mais en épi et tomates.

On envisage l'utilisation de la nouvelle section de la manière suivante:

- octobre-mars: viande portionnée, pré-emballée pour usage individuel et viande désossée pour l'industrie;

- mars-avril: oeufs congelés;

- mai-septembre: fruits et légumes congelés.

L'indice d'utilisation de la section peut atteindre ainsi 92-95%, les outillages technologiques étant adaptables ou bien pouvant être changés facilement. On a prévu une période de

Approved For Release 2009/05/01 : CIA-RDP80T00246A007500340002-0

Approved For Release 2009/05/01 : CIA-RDP80T00246A007500340002-0

réparations de 20 jours en mai et de 10 jours en octobre.

Le mode de distribution de l'espace résulte de la figure ci-jointe.

L'installation frigorifique assure la température de -35° dans les tunnels à congélation rapide, de -40° dans les appareils congélateurs à plaques, de -18° dans les dépôts-tampon des produits congelés et de 0°C dans les chambres de conservation de la matière première réfrigérée.

Le transport, en commençant par le déchargement de la matière première jusqu'à la fabrication, est réalisé à l'aide de bandes de transport. Le lavage, le triage et l'emballage sont mécanisée à l'aide d'outillages construits en Roumanie, parmi lesquels on peut citer:

- machine à laver à action continuelle avec barbotage et douches;

- bande de triage triple à vitesse variable;

- blanchisseur à vapeurs, à action continue, pour utilisation universelle;

- refroidisseur à douches et séchoir.

L'emballage utilisé varie selon les produits.

Pour les fruits sucrée, on utilise des boîtes en carton paraffiné, dont la capacité unitaire est de 250 et de 400 g. Les fruits sans sucre, de même que la plupart des légumes sont emballés dans des sacs doublés de papier parcheminé, scellés et pesés.

A partir de 1958, on a employé les emballages en matière plastique (Polychlorure de vynile, polyethylène), surtout pour les fruits.

Comme emballage de transport, on emploie des boîtes en carton gaufré, dont les dimensions sont de 530 x 265 x 265 mm.

Les dépôts-tampon de la section sont utilisés pour l'entreposage des produits congelés seulement durant quelques jours. L'entreposage de longue durée est réalisé dans un frigorifique situé près de la section des produits congelés rapidement.

C. PRODUCTION DE LA VIANDE PORTIONNEE, PRE-EMBALLEE ET CONGELEE.

L'"ANTREFRIG" a commencé cette production en 1958.

La viande de boeuf ou de porc est tranchée auparavant en portions anatomiques, ensuite portionnée et emballée dans le

Approved For Release 2009/05/01 : CIA-RDP80T00246A007500340002-0

Approved For Release 2009/05/01 : CIA-RDP80T00246A007500340002-0

cellophane et congelée dans des appareils à plaques. La durée de la congélation est de 120 - 150 minutes. On produit les assortiments suivants:

- spécialités de porc et de boeuf en paquets de 0.200 kg (côtelettes de porc - carré -, filet, colet, entrecôte, faux-filet);

- viande pour rôti dans de paquets de 1 kg (escalope, fricandeau etc.);

- viande de cuisine en paquets de 1 kg et de 0.500 kg;

- viande de boeuf hachée en paquets de 1 kg et de 0.500 kg.

Les paquets de 1 kg et de 0.500 kg sont congelés dans des chassis parallélépipédiques en aluminium à l'aide desquels on obtient une forme régulière des paquets.

Ce système de congélation de la viande permet de réaliser une économie considérable d'espace frigorifique destiné à l'entreposage. C'est ainsi qu'en 1958 on a pu augmenter le chargement spécifique d'une chambre frigorifique jusqu'à 58.2% en appliquant le nouveau système de congélation.

On produit aussi de la viande désossée, qui est congelée pour l'industrie de la charcuterie, en blocs de 7 et de 20 kg, ainsi que la viande tranchée par spécialités, qui est livrée réfrigérée aux grandes unités consommatrices (restaurants, cantines, etc.).

D. PRODUCTION DE PLATS CUISINES ET DE DEMI-PRODUITS CULINAIRES CONGELES.

A partir de 1958, on a mis au point la production des produits culinaires suivants: boulettes de viande en feuilles de vigne ou de chou (sarmale), poivrons farcis et autres mets nationaux spécifiques.

Ces produits sont présentés dans des boîtes en carton paraffiné ou bien dans des sacs de polyéthylène, ayant un contenu de 0.500 kg. On peut les consommer après un simple réchauffement, ou bien en ajoutant des ingrédients d'après le goût de chacun.

La ligne technologique a fonctionné en 1958 à titre d'expérience et elle sera définitive en 1959.

On prévoit pour l'avenir une production de l'ordre de centaines de tonnes, comme résultat du sondage effectué parmi les consommateurs qui ont apprécié favorablement les nouveaux produits.

Approved For Release 2009/05/01 : CIA-RDP80T00246A007500340002-0

Approved For Release 2009/05/01 : CIA-RDP80T00246A007500340002-0

QUELQUES OBSERVATIONS CONCERNANT LES MODIFICATIONS PHYSICO-CHIMIQUES ET MICROBIOLOGIQUES QUI ONT LIEU DANS CERTAINS PRODUITS CONGELES.

1.- Modifications du contenu en vitamine C par phases du processus technologique (la matière première, la congélation, l'entreposage).

On a fait des recherches sur trois lots de fruits spécifiques pour les conditions de culture en Roumanie. Les resultats de ces recherches sont donnés dans le tableau 1.

Tous ces fruits ont été congelés sucrés. Pour determiner le contenu en vitamine C on a employé la méthode de titrage avec diclofenolindofenol.

TABLEAU 1. CONTENU EN VITAMINE C.

Dénomination des produits	Contenu en vitamine C, mg % g								
	Matière première	Après la congélation		Après 1 mois		Après 3 mois		Après 4 mois	
			pertes %		pertes %		pertes %		pertes %
Fraises	56,8	55,6	5,2	54,8	5,8	54,2	7,5	53,6	13,6
Framboises	40,62	30,8	2,03	39	4	38,6	4,9	36	11
Griottes	22,3	21,8	2,2	21	5,7	20,2	9,4	19	14,7

2.- Modifications microbiologiques observées dans la viande portionnée pré-emballée (viande de boeuf).

On a déterminé la variation du nombre des germes par phases du processus technologique. Les resultats de ces déterminations sont donnés dans le tableau n° 2.

TABLEAU 2. DETERMINATIONS DE LA VARIATION DU NOMBRE DES GERMES PAR PHASE DU PROCESSUS TECHNOLOGIQUE.

Phases du processus technologique	Nombre total des germes par gramme de produit
La matière première avant d'être tranchée	250.000
" " " après avoir été "	480.000
Le produit fini après la congélation	18.000
" " " après 3 mois d'entreposage	10.000

Approved For Release 2009/05/01 : CIA-RDP80T00246A007500340002-0

Approved For Release 2009/05/01 : CIA-RDP80T00246A007500340002-0

On constate que grâce à la congélation, le nombre total des germes se réduit considérablement, c'est-à-dire de 480.000 à 18.000 germes/g. Pendant l'entreposage, on constate une nouvelle réduction du nombre qui représente 10.000 germes/g.

Bien que cette réduction du nombre de germes représente un effet favorable de la conservation par la congélation, on ne doit pas accorder une moindre attention aux conditions sanitaires et hygéniques. It ne faut pas oublier que certains germes pathogènes résistent assez bien à l'action des températures basses et que pendant la décongélation le nombre total des germes augmente de nouveau à un rythme accéléré.

Approved For Release 2009/05/01 : CIA-RDP80T00246A007500340002-0

Approved For Release 2009/05/01 : CIA-RDP80T00246A007500340002-0

The Investigation of new Cold Store Cooling Systems.

Recherches sur les nouveaux systèmes frigorifiques des entrepôts

S.G. CHUKLIN, D.G. NIKULSHINA and V.P. CHEPURNENKO

The Odessa Technological Institute of the Food and Refrigerating Industry, Odessa, U.S.S.R.

SOMMAIRE. Le rapport examine un nouveau système, proposé et étudié par les AA., de "refroidissement par panneaux longitudinaux de serpentins" pour équiper les chambres froides à doubles-parois sans modifier de la construction et pour réduire la différence de température entre l'air de la chambre et la fluide frigorigène. Le même système permet de produire un refroidissement intense, quand les aliments sont en cours de chargement dans la chambre froide en transformant les serpentins à ailettes longitudinales en système bilatéral. Les relations entre la transmission de chaleur au système, les besoins de froid du serpentin, la répartition de la température à la surface d'échange dans la chambre et entre les parois ont été établies pour les deux utilisations courantes, ainsi que les variations des pertes de poids des aliments au cours de l'entreposage.

On donne les résultats des recherches expérimentales sur le système frigorifique proposé, qui montrent l'accord entre les données théoriques et expérimentales.

La seconde partie du rapport présente les résultats des recherches expérimentales sur un système frigorifique de faible puissance avec tube lisse et serpentins à ailettes en cascade, effectuées en laboratoire et dans les entrepôts frigorifiques de l'industrie de transformation de la viande. Les caractéristiques thermiques et hydrauliques de ce système ont été déterminées et l'on donne des recommandations pour sa modernisation future par transformation des serpentins en système à cascade partiellement noyé. L'efficacité de cette mesure a été confirmée par les essais comparatifs supplémentaires pour un système à faible puissance dans une chambre expérimentale polyvalent ainsi que dans les entrepôts frigorifiques de deux installations de transformation de la viande.

Le rapport présente la relation pour la transmission de chaleur d'un tube lisse en cascade et de serpentins à ailettes dans les conditions de l'échange de chaleur sèche ou humide. Les relations ont été établies pour le temps de formation de givre à des températures inférieures à 0^{o} C. Les résultats de l'essai d'un refroidisseur d'air à ailettes pour le refroidissement, l'entreposage et la congélation sont donnés à la fin du rapport.

COPYRIGHT RESERVED.

Approved For Release 2009/05/01 : CIA-RDP80T00246A007500340002-0

Approved For Release 2009/05/01 : CIA-RDP80T00246A007500340002-0

The strive to improve the conditions of food storage in cold stores and to decrease weight losses led to the development of jacketed cold stores. A model of a jacket with panel cooling by means of longitudinal coils has been designed and tested by the authors for experimental purposes.

An experimental room (3.15 x 3.05 x 2.88 m) equipped with such refrigerating elements is shown in Fig. 1. Finned "cascade" type coils have also been installed and tested in the cold room. The specific feature of these coils is that the liquid ammonia is supplied into the upper pipes and flows down these pipes to the lower ones in a stream occupying only a part of the pipe section.

The vapour is drawn off a header connected with all the pipes of the coil.

Fig. 2 gives a schematic diagram of the experimental cold room, its equipment, auxiliaries and measuring instruments used for the experiments.

TESTS AND CALCULATIONS OF A PANEL COOLING SYSTEM

The main element of the tested panel cooling system given in Fig. 1 and 2 is a 16.6 m^2 single-row "cascade" type wall coil. The 57 x 3.5 mm pipes of the coil have a 270 mm pitch. A 1.5 mm thick steel plate is welded to the pipes on the side of the cold room. By this plate a part of the space is fenced off the room and thus a protective jacket is formed. The external heat gain is absorbed by the plate and the coil pipes. Additional external heat gains were created during the tests by means of screened electric heaters (7) located inside the jacket.

For determining the total heat load of the coil electric heaters 10 were mounted on the line removing vapour from the coil. Electric heaters (9, Fig. 1) were applied to reproduce an internal heat gain from fresh goods charged into the room.

Approved For Release 2009/05/01 : CIA-RDP80T00246A007500340002-0

Approved For Release 2009/05/01 : CIA-RDP80T00246A007500340002-0

The removable longitudinal coil fins, arranged in the upper and lower parts of the coils were opened when switching in the heaters 9 and thus the circulation of air at the coils was intensified.

An overflow pipe was connected to the header from which the vapour generated in the coil was drawn off. By opening valve a and shutting off the valve b it was possible to fill 2/3 of the coil pipe with liquid ammonia thereby providing a reliable removal of heat at an insignificant hydrostatic liquid column in the coil. The upper pipes of the coil remained partially full whereby the main advantage of the "cascade" system was provided, namely, reliable operation and simplicity of the refrigerating installation.

Copper-constantan thermocouples, shown in Figs. 1 and 2, were used for temperature measurements at the surface of the coil as well as of the ammonia and of the air both in the cold room and in the jacket.

The following analytical relationships were obtained for calculating the heat exchange of the flooded part of the longitudinal fin coil; these relationships were then checked experimentally.

a) <u>In case of an absence of internal heat gain in the cold room</u>. The temperature changed along the height of the fin

$$\theta_x = \frac{\theta_0 - b_1}{2ch(\sqrt{a_1}h)}\left[\left(\frac{e^x}{e^h}\right)^{\sqrt{a_1}} + \left(\frac{e^h}{e^x}\right)^{\sqrt{a_1}}\right] + b_1 \qquad (1)$$

where: θ_0 - temperature difference between the fin base and the air in the room, °C;

$$a_1 = \frac{\alpha_2 + \alpha_3}{\lambda_1 \delta_1} \qquad b_1 = \frac{t_2 - t_3}{1 + \frac{\alpha_3}{\alpha_2}}$$

Approved For Release 2009/05/01 : CIA-RDP80T00246A007500340002-0

Approved For Release 2009/05/01 : CIA-RDP80T00246A007500340002-0

α_2 - film coefficient of heat transfer at the external surface of coil facing cold room, kcal/m^2 hr $^\circ$C;

α_3 - ditto of the surface facing jacket, kcal/m^2 hr $^\circ$C;

t_2 - temperature of air in cold room, $^\circ$C;

t_3 - temperature of air in jacket, $^\circ$C;

λ_1 - thermal conductivity of plate material, kcal/m hr $^\circ$C;

δ_1 - fin thickness, m;

h - fin height, m.

The amount of heat transferred by the plate to the pipe

$$Q_1 = \frac{b_2 - b_1}{c_2 - c_1} \quad \text{kcal/m hr}$$

where: $a_2 = \frac{\alpha_1 \cdot K_1 + \alpha_4 \cdot K_2}{\lambda_2 \delta_2}$; $b_2 = \frac{t_1 - t_3}{1 + \frac{d_2}{d_1} \cdot \frac{\alpha_4}{\alpha_1}}$; $c_1 = \frac{1}{\lambda_1 \delta_1 \sqrt{a_1} \cdot th(\sqrt{a_1} h)}$ (2)

$$c_2 = \frac{1}{\lambda_2 \delta_2 \sqrt{a_2}\, th(\sqrt{a_2}\, l_1)} ; \quad K_1 = \frac{d_1}{d_m} ; \quad K_2 = \frac{d_2}{d_m} ; \quad l = \frac{\pi d_m}{2}$$

α_1 - film coefficient of heat transfer to evaporating ammonia, kcal/m^2 hr $^\circ$C;

α_4 - ditto from air to pipe, kcal/m^2 hr $^\circ$C;

t_1 - evaporating temperature, $^\circ$C;

λ_2 - thermal conductivity of pipe, kcal/m hr $^\circ$C;

δ_2 - pipe wall thickness, m.

The amount of heat transferred from the air through the external surface of the pipe

$$Q_2 = \frac{\alpha_4 \pi d_2 b_2}{2} - \frac{Q_1}{1 + \frac{d_1}{d_2} \cdot \frac{\alpha_1}{\alpha_4}} \quad \text{kcal/m hr} \qquad (3)$$

Approved For Release 2009/05/01 : CIA-RDP80T00246A007500340002-0

Approved For Release 2009/05/01 : CIA-RDP80T00246A007500340002-0

The heat leakage into the cold room from the jacket through a fin

$$Q_3 = \alpha_2 \left[(t_1 - t_2) h + \frac{\theta_0 - t_1}{\sqrt{a_1}} th\,(\sqrt{a_1}\, h) \right] \quad \text{kcal/m hr} \qquad (4)$$

b) In the case of an internal heat gain in the cold room. The temperature of the air in the jacket and in the room may be considered in this case equal and the film coefficients of heat transfer to the surface of the coil from the air in the jacket and in the cold room are equal likewise.

Then

$$Q_1 = \frac{t_1 - t_2}{\left(1 + \frac{d_2}{d_1} \cdot \frac{\alpha_4}{\alpha_1}\right)(C_3 + C_4)} \quad \text{kcal/m hr} \qquad (5)$$

where

$$C_3 = \frac{1}{\sqrt{2 \alpha_4 \lambda_1 \delta_1}} \cdot th \left(\sqrt{\frac{2 \alpha_4}{\lambda_1 \delta_1}} \cdot h \right)$$

and

$$Q_2 = \frac{\alpha_4 \pi d_2 b_2}{2} - \frac{Q_1}{1 + \frac{d_1}{d_2} \cdot \frac{\alpha_1}{\alpha_4}} \quad \text{kcal/m hr} \qquad (6)$$

A comparison of the calculated and experimental values of the heat flows and of the temperature distribution along the heat exchange surface of the coils illustrates their good coincidence.

The following conclusions have been drawn.

a) The longitudinal fin coil panel cooling made it possible to intercept a considerable part of external heat gains and to decrease the temperature difference between the air in the room and the ammonia at an absence of internal heat gains.

b) In the case of products being cooled in the cold room, the jacket principle is upset. However, in this case the shrinkage is still lower as compared with conventional refrigerating systems (without a cooling jacket). Thermal calculation of the

Approved For Release 2009/05/01 : CIA-RDP80T00246A007500340002-0

Approved For Release 2009/05/01 : CIA-RDP80T00246A007500340002-0

coil may be made in this case with the help of the expressions (5,6).

c) A decrease of the shrinkage depends upon the design of the coil and is determined by the coefficient

$$\xi = \frac{Q_3}{Q_1 + Q_2}$$

A drawback of the suggested system is the penetration of some external heat into the room through the panel coil fins, also a certain complexity of construction of the cooling coils with longitudinal fins. Further work is required in this connection in order to improve this system.

EXPERIMENTAL INVESTIGATIONS OF TYPICAL DESIGNS OF WALL AND OVERHEAD "CASCADE" TYPE FINNED COILS MOUNTED IN THE EXPERIMENTAL COLD ROOM

The coils were made of 57 x 3.5 mm pipes with 46 x 1 mm steel band 35.6 mm pitch helical fins. The 13-row high spiral wall coil with a 220 mm horizontal pitch and 180 mm vertical pitch had 31.5 m^2 external heat transfer surface and a 7.85 fin to bare pipe surface ratio.

The finned surface of the 3-row high 6-row wide overhead coil with a 185 x 185 mm pipe pitch was 47.3 m^2.

Both coils were tested under both operating conditions - partially and completely filled. The wall coil was tested under a third routine, with only the lower pipes completely flooded. The latter routine was attained by means of an overflow pipe of the vapour header and valves „c" and „d" (Figs. 1, 2).

The flooded part of the coil in this case constituted 46% of the entire heat transfer surface.

The thermal characteristics of the coil were determined at a temperature in the room and the entire building structure equal

Approved For Release 2009/05/01 : CIA-RDP80T00246A007500340002-0

Approved For Release 2009/05/01 : CIA-RDP80T00246A007500340002-0

to the ambient air temperature. The heat evolved by screened electric heaters installed in the room was completely removed by the tested coil and its heat load was determined by the electric power consumption of the heaters.

The temperature of the cooling surface as well as of the air and refrigerant at the points shown in Figs. 1 and 2 was measured by means of copper-constantan thermocouples. Besides, the described method of determining the thermal characteristics of the coils, their film coefficients of heat transfer were compared by confronting the distribution of temperature on the finned surfaces.

The change of the film coefficient of heat transfer of the tested coils depending upon their filling with liquid ammonia and method of refrigerant supply is given in Fig. 3.

The data have been obtained when testing the wall coil at -4.3° - -9.1°C evaporating temperature and 10.5° - 13.9°C difference between the evaporating temperature and the temperature of the air. The film coefficient of heat transfer from the air to the finned surface amounted to 4.75 - 5.33 kcal/m^2 hr $^{\circ}$C.

The overhead coil was tested at a -6.0° - -9.0°C evaporating temperature and a 10.5 - 12.0°C temperature difference. The film coefficient of heat transfer was 4.0 to 4.5 kcal/m^2 hr $^{\circ}$C on the air side.

Lower values of K in completely filled coils may be explained by the negative influence of the liquid head amounting to 3.2 m liquid ammonia in the wall finned coil, and to 1.65 m in the overhead finned coil.

A smaller overall coefficient of heat transfer in the coils with all the pipes partially filled as compared with the coils in which the lower pipes are flooded, should be explained by an increase of the temperature in the upper part of the pipes in contact with the vapour flow.

Approved For Release 2009/05/01 : CIA-RDP80T00246A007500340002-0

Approved For Release 2009/05/01 : CIA-RDP80T00246A007500340002-0

The tests have shown that with partially filled upper pipes and completely flooded lower ones, the coil, retaining the advantages of the "cascade" type coil is destinguished by the following additional advantages as compared with the latter: smaller (by 30 to 50%) circulation receiver capacity requirements; less sensitivity to stoppages in the liquid ammonia feed to the coil.

Copyright reserved

Approved For Release 2009/05/01 : CIA-RDP80T00246A007500340002-0

Approved For Release 2009/05/01 : CIA-RDP80T00246A007500340002-0

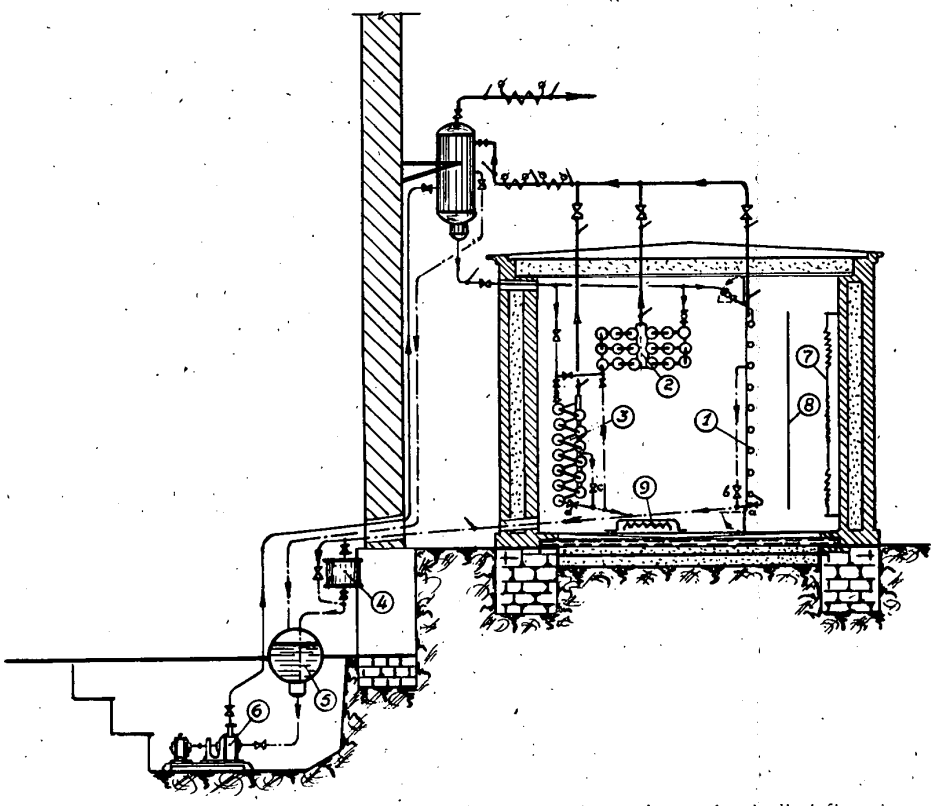

Fig. 1. Experimental cold room and its cooling system. 1) cascade type longitudinal fin wall coil; 2) overhead 3-row cascade type finned coil; 3) wall 2-row cascade type finned coil; 4) measuring vessel; 5) receiver; 6) ammonia pump; 7) electric heater in the room jacket; 8) screen; 9) electric heater in room.

Approved For Release 2009/05/01 : CIA-RDP80T00246A007500340002-0

Approved For Release 2009/05/01 : CIA-RDP80T00246A007500340002-0

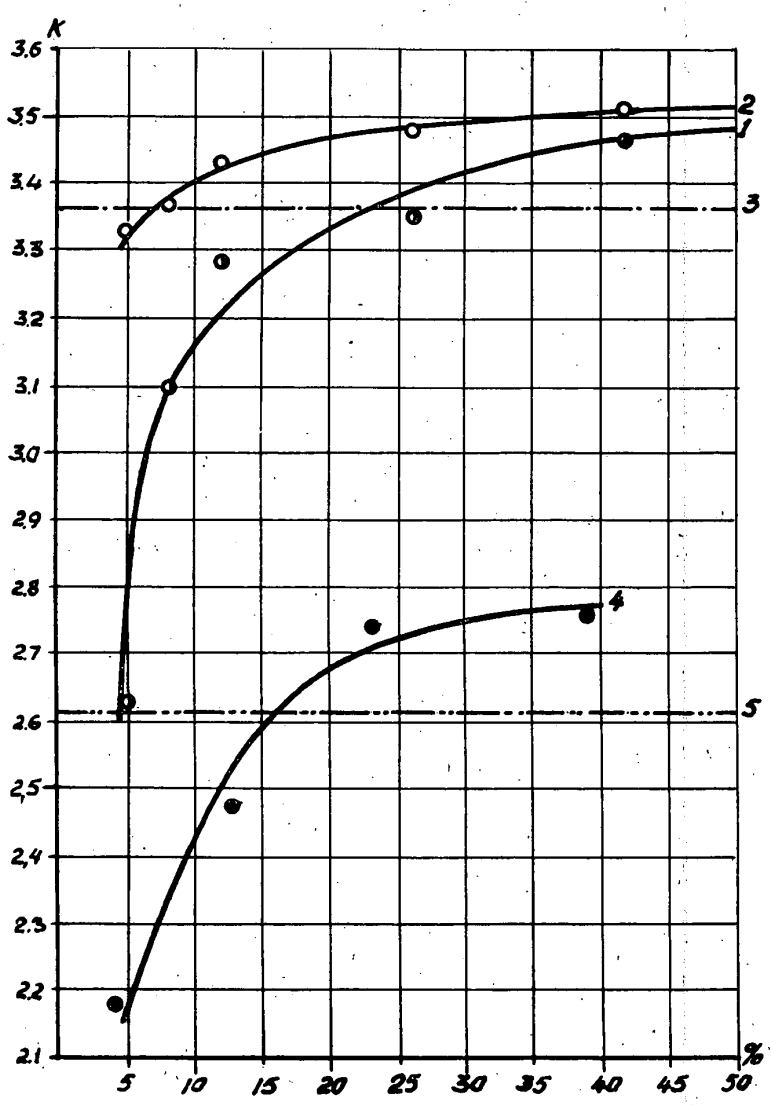

Fig. 3. Overall coefficient of heat transfer of finned coils depending upon their filling with liquid ammonia.
Wall coil. 1) partial filling of all the pipes (cascade type coil); 2) partial filling of the upper and complete filling of the lower pipes; 3) complete filling of all the pipes.
Overhead coil. 4) cascade operation; 5) flooded operation.

Approved For Release 2009/05/01 : CIA-RDP80T00246A007500340002-0

Approved For Release 2009/05/01 : CIA-RDP80T00246A007500340002-0

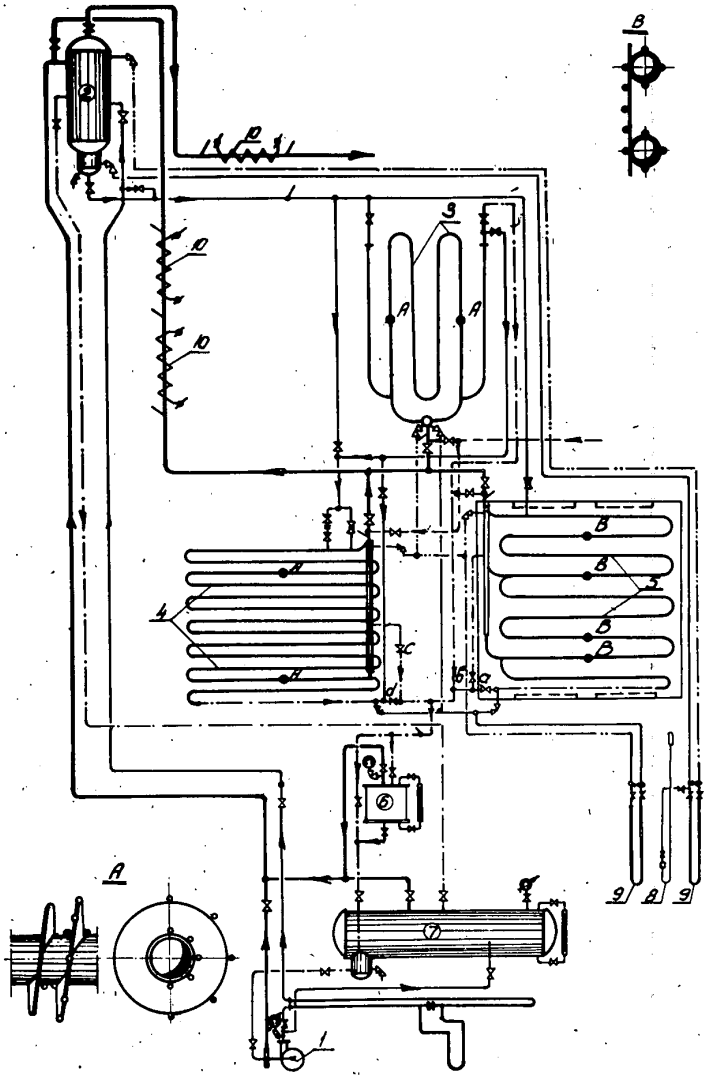

Fig. 2. Schematics of experimental room cooling system. 1) ammonia pump; 2) distributing vessel; 3) overhead 3-row cascade type coil; 4) wall 2-row cascade type coil; 5) wall cascade type coil with longitudinal fins; 6) measuring vessel; 7) receiver; 8) mercury pressure gauge; 9) differential pressure gauge; 10) electric heaters A. Location of thermocouples on surface of finned coils. B. Location of thermocouples on coil with longitudinal fins.

Approved For Release 2009/05/01 : CIA-RDP80T00246A007500340002-0

Approved For Release 2009/05/01 : CIA-RDP80T00246A007500340002-0

Recherches sur la cryodessication de quelques produits enzymatiques utilisés dans l'industrie alimentaire

Investigations in the Freeze-drying of Some Enzymatic Products used in the Food Industry

A. SAVU, A. CIOBANU and G. ADAM.
Institut de recherches alimentaires
Bucarest, R.P.Roumaine

SUMMARY. Freeze-drying of pepsin and rennet were studied. Interesting results were obtained by using a medical lyophilizing plant. Pepsin and rennet were quick-frozen in films on the walls of flasks plunged in ethyl alcohol at - 37° C, then these materials were lyophilized to a moisture content of 3.27 % for pepsin and 1.72 % for rennet. Coagulating ability determined immediately after drying was 1:400,000 for pepsin and 1:88,000 for rennet. It was concluded that freeze-drying has no negative effect on the original coagulating power. Subsequent storage was in flasks closed at ordinary temperature in three different ways : sealed, under vacuum, and in carbon dioxide atmosphere. The coagulating ability of pepsin did not vary during 3 months under all methods; however, after 8 months storage, only flasks under vacuum retained their original ability. As for rennet, its coagulating ability did not vary during 4 months under all methods. These good results show the future industrial possibilities for the storage of these enzymatic products.

Appliquée d'abord en medicine pour la conservation du plasma sanguin et des produits antibiotiques pendant la seconde guerre mondiale, la cryodessication (dénommée aussi lyophilisation) a été ensuite utilisée pour d'autres produits pharmaceutiques. Les expériences effectuées en U.R.S.S., U.S.A. et ailleurs ont démontré que cette méthode peut être appliquée aussi à certains produits alimentaires. Licov [1], Neumann [2] et Flosdorf [3] affirment qu'on a réalise avec succès la cryodessication des fruits et des légumes, de la viande et du poisson, des jus de fruits et des solutions aqueuses de ferments.

Les principaux avantages de la déshydratation par sublimation sous vide sont :

Approved For Release 2009/05/01 : CIA-RDP80T00246A007500340002-0

Approved For Release 2009/05/01 : CIA-RDP80T00246A007500340002-0

1.- Température basse durant le processus, ce qui inhibe les modifications biochimiques.

2.- Dispersion uniforme et constante du solvant sans augmenter la concentration à mesure que se produit la déshydratation. C'est ainsi qu'on atteindre une humidité très réduite, sans que le produit subisse des modifications chimiques ou colloïdales.

3.- Le manque d'oxygène empêche l'oxydation des composants pendant la cryodessication.

4.- Réhydratation rapide au moment de l'utilisation.

Dans le processus technologique de lyophilisation interviennent les phases principales suivantes: congélation, sublimation et le complément de la déshydratation par la vaporisation à des températures positives.

Le résultat final de la cryodessication est conditionné par la manière de congélation ; les meilleures résultats sont obtenus par l'autocongélation, car cette méthode assure la décroissance plus rapide de la température du produit.

Ainsi, on réalise aussi une réversibilité plus avancée et, en même temps, une plus grande surface d'évaporisation grâce aux petits cristaux de glace formés.

Cependant on peut agrandir la vitesse de congélation en employant aussi la méthode de congélation en couche fine, pour les liquides.

Durant la sublimation, les transferts de chaleur et de masse sont déterminés par la vitesse de déplacement de l'humidité de l'interieur du produit vers la surface, par la température à laquelle se produit la sublimation et par la différence de pression en rapport à la pression ambiante.

L'intensité de la vaporisation (et par conséquent du séchage) doit être égale à celle de l'élimination des vapeurs et doit correspondre à la faculté de condenser ces vapeurs. L'intensité de vaporisation pendant la sublimation dépend du flux de chaleur que reçoit le matériel en cours de lyophilisation. Ce flux est déterminé en proportion de 40-45 % par la radiation et 60-65 % par la convection.

Approved For Release 2009/05/01 : CIA-RDP80T00246A007500340002-0

Approved For Release 2009/05/01 : CIA-RDP80T00246A007500340002-0

Pratiquement on peut considérer la pression des vapeurs à la surface du produit comme représentant 60 % de la pression des vapeurs d'eau à la surface de la glace, pour la même temperature [illegible].

Seule la sublimation ne peut pas réaliser la déshydratation du produit jusqu'aux limites nécessaires et c'est pour cela que dans le processus technologique de séchage intervient une troisième phase, celle de l'élimination de l'humidité rémanente, jusqu'à une teneur d'humidité finale d'environ 1 %. Durant cette phase, la vaporisation se produit à des températurss supérieures à celle de 0° C.

Après la cryodessication, le produit obtenu doit être introduit dans des emballages hermétiques, de préférence dans l'absence d'oxygène, puisque la surface en contact avec le milieu ambiant est très grande, ayant une structure extrémement poreuse.

La longue durabilité du produit lyophilisé est une propriété importente qui a suscité l'attention des chercheurs et qui a été vérifiée dans diverses conditions.

Sous l'aspect économique, le prix de revient de la lyophilisation n'est pas très élevé du point de vue des frais spécifiques d'énergie, mais les dépenses d'investissements sont trop importantes par rapport à la productivité de telles installations. C'est pour cela qu'à l'Institut de recherches alimentaires de Bucarest les recherches effectuées ont été dirigées particulièrement dans la direction de conservation de certains produits microbiologiques ou enzymatiques utilisés dans l'industrie alimentaire. Ces produits se préparent en quantités relativement petites, mais ils ont un prix de revient élevé et sont indispensables pour de nombreux processus technologiques, par exemple dans l'industrue laitière.

RECHERCHES EFFECTUÉES

Pendant l'année 1958, on a expérimenté la lyophilisation de la présure et de la pepsine.

Les recherches ont été effectuées dans une installation pou lyophilisation du plasma sanguin système "Usifroid", ayant des plateaux pour les fioles ou les flacons qui contiennent le produit, disposés dans une cuve hermétiquement fermée.

Approved For Release 2009/05/01 : CIA-RDP80T00246A007500340002-0

Approved For Release 2009/05/01 : CIA-RDP80T00246A007500340002-0

Cette cuve circulaire, isolée du point de vue thermique, est à l'intérieur refroidie par les tubes qui constituent l'évaporateur d'une installation de froid. Le vide à l'intérieur de la cuve est d'environ 10^{-2} mm Hg, tandis que la température du condenseur est de -40 à -50° C.

Il y a aussi un appareil indépendant pour la congélation du produit par l'immersion et la rotation des flacons dans un bain à alcool refroidi jusqu'à -40° C.

LA CRYODESSICATION DE LA PEPSINE

On a employé une solution de pepsine obtenue par le procédé Tiperovitsch [4] , ayant une teneur d'humidité de 89,58 % et l'activité coagulante de 1 : 46.000 (qui peut etre considérée normale). Pour l'expérience furent utilisés 700 cm^3 de pepsine répartie dans 14 flacons.

La congélation a été réalisée dans un appareil de congélation par immersion, à la température de - 35° C, durant 5 minutes; ensuite les flacons dont le contenu a été congelé en une couche extrêmement fine, ont été conservés pendant 2 heures à la température de - 16° C, après quoi ils ont été introduits dans l'appareil de lyophilisation.

Le plateau de l'appareil fut préalablement refroidi à - 20° C. Le processus de séchage s'est prolonge 9 heures 3o minutes. Les variations de la température du produit dans les flacons, du plateau et de la surface du condenseur ont été mesurées à intervalles réguliers, à l'aide des thermomètres à résistance.

A la fin du processus de séchage, la température du produit s'elevait jusqu'à + 21° C.

Après le séchage, la teneur en humidité de la pepsine a été de 3,27 % et son activité coagulante de 1 : 400.000. Tout en considérent la proportion dans laquelle a été réduite l'humidité, il en résulte que par lyophilisation, la pepsine a conservé son activité de coagulation initiale.

Pour déterminer le comportement de la pepsine après la lyophilisation pendant quelques mois de conservation, om a expérimenté les variantes suivantes:

Approved For Release 2009/05/01 : CIA-RDP80T00246A007500340002-0

Approved For Release 2009/05/01 : CIA-RDP80T00246A007500340002-0

a. la conservation dans des fioles en verre, fermées par flambage, de la manière habituelle;

b. la conservation dans des fioles en verre, fermées sous vide de 50 mm Hg;

c. la conservation dans des récipients en atmosphère de bioxyde de carbone.

Avant d'être introduit dans les fioles, le produit a été broyé, afin de réduire sa porosité.

Le comportement des échantillons de pepsine par rapport à la durée et aux conditions de conservations ressort du tableau 1.

Tout les échantillons ont été conservés à la température ambiante (+ 16 ÷ 20° C).

Tableau 1. COMPORTEMENT DES ÉCHANTILLONS DE PEPSINE LYOPHILISÉE

Nr. crt.	Manière de fermer les flacons	Activité coagulante		
		Initiale	Après 90 jours	Après 230 jours
1.	Habituelle (flambage)	1 : 400,000	1 : 400.000	1 : 160,000
2.	Sous vide	1 : 400.000	1 : 400.000	1 : 400.000
3.	Dans l'atmosphère de bioxyde de carbone	1 : 400.000	1 : 400.000	On n'a pu determiner

De l'examen du Tableau 1, il résulte que la pepsine a conservé son activité initiale durant 90 jours, dans toutes les 3 variantes expérimentales. Durant la conservation de 230 jours, l'activité coagulante s'est maintenue sans modifications, uniquement dans les flacons fermés sous vide.

Pour déterminer ce qu'on appelle "l'activité coagulante" on a pris en considération le moment de l'apparition du caillot.

Approved For Release 2009/05/01 : CIA-RDP80T00246A007500340002-0

Approved For Release 2009/05/01 : CIA-RDP80T00246A007500340002-0

LA CRYODESSICATION DE LA PRÉSURE

On a employé une solution de présure obtenue de même à l'Institut, à partir d'estomacs de veaux, par le procédé Berridge [5] .

Pour l'expérience, on a introduit une quantité de 300 cm^3 de solution de présure ayant une teneur en humidité initiale de 88,93 % et une activité coagulante de 1 : 9,900 (qui est considérée normale).

La congélation a été effectuée rapidement dans les flacons, dans les mêmes conditions que pour la pepsine. Après la congélation, les flacons contenant la présure furent déposés sur le plateau de l'appareil de cryodessication, refroidi au préalable à - 20° C. Le processus dura 8 heures 3o minutes et la température finale du produit fut de 23° C.

Après le séchage, on a déterminé une teneur en humidité de la présure de 1,72 % et une activité coagulante de 1 : 88,000.

En vue d'observer le comportement de la présure après la lyophilisation et pendant la conservation, on a expérimenté les mêmes variantes que pour la pepsine.

Les résultats sont indiqués dans le tableau 2.

Tableau 2. COMPORTEMENT DES ÉCHANTILLONS DE PRÉSURE LYOPHILISÉE.

Nr. crt.	Manière de fermer les flacons	Activité coagulante		
		Initiale	Après 75 jours	Après 120 jours
1.	Habituelle	1 : 88.000	1 : 88.000	1 : 80.000
2.	Sous vide	1 : 88.000	1 : 88.000	1 : 80.000
3.	Dans l'atmosphère de bioxyde de carbone	1 : 88.000	1 : 88.000	1 : 73.000

Il résulte du tableau 2 qu'après une conservation de 75 jours, l'activité de coagulation s'est maintenue inchangée, tandis qu'après 120 jours la diminution de qualité peut être considérée comme insensible.

Approved For Release 2009/05/01 : CIA-RDP80T00246A007500340002-0

Approved For Release 2009/05/01 : CIA-RDP80T00246A007500340002-0

Pourtant, pour l'échantillon conservé dans l'atmosphère de bioxyde de carbone les résultats sont moins satisfaisants après 120 jours de conservation. À motre avis c'est une conséquence des vapeurs d'eau contenues dans le bioxyde de carbone utilisé.

Pour illustrer le développement du processus de lyophilisation, nous reproduisons dans la figure ci-jointe, pour la présure, la variation des températures du produit, du plateau et du condenseur.

Le diagramme correspondant pour la pepsine a la même allure.

CONCLUSIONS

À la suite de la lyophilisation, l'activité coagulante de la pepsine et de la présure reste inchangée.

La résistance à la conservation à la longue, après sechage, dépend de la méthode utilisée pour fermer les flacons. L'emballage sous vide confère aux produits étudiés une stabilité suffisante durant la conservation, à la longue même aux températures d'ambiance

BIBLIOGRAPHIE

1. LICOV, A.V. et GRIAZNOV, A.A. Moleculiarnaia susca. Pișcepromizdat, Moscou, 1956

2. NEUMANN, K. Grundrisse der gefriertrocknung, Wiss Verlag, Gottingen, 1954.

3. FLOSDORF, E.W. Freeze-Drying by Sublimation. Reinhold Publishing Corp., New York, 1949.

4. Tiperovitsch, A.S. Rev. de biochimie de l'Ucraïne, 19(1), 1958.

5. BERRIDGE, N.J. et WOODWARD, C. The Journal af Dairy Research, s/1953, p.255-257.

Approved For Release 2009/05/01 : CIA-RDP80T00246A007500340002-0

Approved For Release 2009/05/01 : CIA-RDP80T00246A007500340002-0

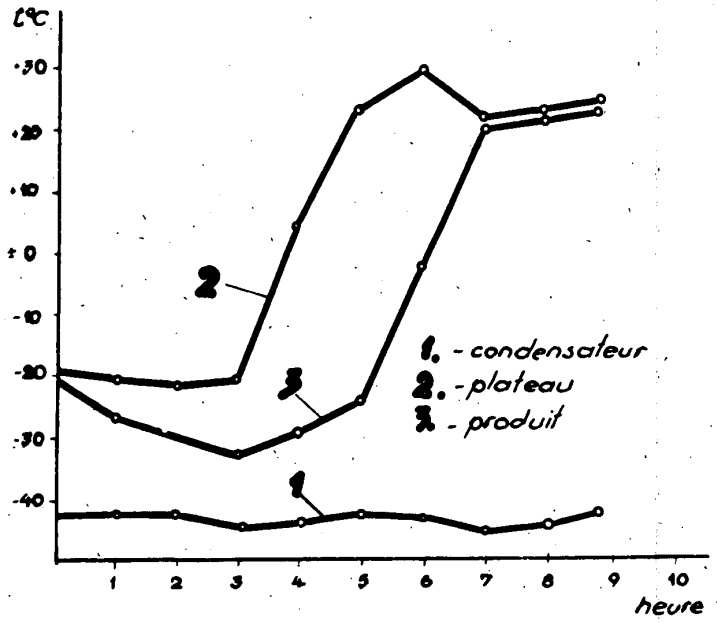

Fig. 1. Variation des températures pendant le processus (présure).

Approved For Release 2009/05/01 : CIA-RDP80T00246A007500340002-0

Approved For Release 2009/05/01 : CIA-RDP80T00246A007500340002-0

The Application of Refrigeration for Prolonged Preservation of Blood

Application du froid à la conservation prolongée du sang

F.R. VINOGRAD-FINKEL, F.G. GINSBURG, L.I. FYODOROVA
The Central Lenin Order Institute of Hematology and Blood Transfusion

E.L. KAUKHCHESHVILI
The Moscow Technological Institute of the Meat-Packing and Dairy Industry

Moscow, U.S.S.R.

SOMMAIRE. La méthode de conservation du sang à des températures inférieures à 0°C. entraînant la suppression presque complète du métabolisme des cellules a une grande importance du fait qu'elle permet de prolonger nettement la durée de conservation du sang.

On a obtenu récemment à cet égard quelques résultats nets après que l'influence nocive de la congélation sur les cellules vivantes a été décelée fondamentalement.

Le problème de la conservation du sang à des températures inférieures à 0°C. se résout de deux façons:

a) la conservations du sang liguide de sous-refroidi (méthode pratiquement la plus séduisante) et b) la conservation du sang à l'état solide (congelé) pour permettre l'inhibition totale de l'activité des enzymes et une plus longue conservation du sang.

On a mis au point une solution protectrice pour protéger les globules rouges de l'effet nocif des basses températures. Tous les éléments de cette solution peuvent être admis pour la transfusion. De cette façon, la quantité totale du sang peut être utilisée pour la transfusion sans pertes contrairement à ce qui a lieu avec la conservation du sang avec de la glycérine, citée dans la littérature. Cette dernière méthode implique une opération compliquée pour l'élimination de la glycérine du sang, ce qui provoque une perte de plasma considérable.

La solution permet de conserver le sang pendant une longue durée à l'état liguide, non congelé, entre -8° et -10°C., les globules rouges gardant toute leur valeur et restant aptes à la transfusion pendant 100 jours.

La même solution protège les globules rouges contre la destruction quand le sang est congelé entre -12° et -16°C et conservé à des températures pendant une longue durée.

On a élaboré des méthodes de refroidissement, de congélation et de décongélation avec l'application de la solution ci-dessus.

Approved For Release 2009/05/01 : CIA-RDP80T00246A007500340002-0

Approved For Release 2009/05/01 : CIA-RDP80T00246A007500340002-0

The problems of prolonged preservation of blood are highly important for practical medicine.

The period (from 30 to 40 days) during which blood can now be preserved at reduced temperatures (i.e. from 4 to 5°C) does not meet the growing requirements of medicine.

The method of preserving blood at sub-zero C. temperatures, resulting in a practically complete cessation of methabolism in the cells, is of great importance as it provides the possibility of considerably prolonging the preservation period.

Efforts have been made in various countries for many years to obtain erythrocytes undamaged after freezing and thawing. Recently some definite results in this respect were attained as the general nature of the injurious effect of freezing has been disclosed.(1,2,3,4,5,6)

It has been proved that the deterioration of erythrocytes at sub-zero temperatures is caused by the simultaneous influence of two factors: the injury caused by ice crystals and the effect of concentrated electrolyte solutions.

Theoretically, the most perfect method for the preserving the integrity of the erythrocytes is freezing without crystallization, i.e. vitreous solidification. This can be obtained by instantaneously cooling to very low temperatures (-195°C.).

At present the elaboration of such a method is being attempted. However, rather complicated equipment is needed for this type of work, and consequently the joint co-operation of specialists in various fields is required. For this reason the problem of preserving blood at more easily available low temperatures has been studied simultaneously.

THE APPLICATION OF MODERATE LOW TEMPERATURES.

Investigations have armed at developing preserving solutions which would protect the erythrocytes from the injurious effect of crystallization of intra- and extracellular water.

The substances to be tested should fulfill the following requirements: 1) lower the freezing point of the blood with the solution added; 2) retard the crystallization of water; 3) prevent the growth of crystals and 4) hamper increasing concentrations of electrolytes.

According to data available in the literature, glycerol meets all these requirements as it allows the preservation of blood up to 12 months at -20°C. or -70°C. and still lower temperatures with only a small percentage of erythrocytes being destroyed. However, this method has not gained practical application due to the complicated procedure of removing the large amount of glycerol.

Considering this disadvantage of the glycerol method the protective action of some non-electrolytes has been tested. These investigations proved that the rate of the protective action depends upon the ability of the substance to penetrate into the erythrocytes.

A colloidal suspension of carbohydrates in alcohol was developed. This solution contained a high concentration of glucose, and this and ethyl alcohol are substances characterised by a high rate of penetration into the erythrocytes. In addition ethyl alcohol is known to lower the freezing point. Another constituent of great importance in this solution is saccharose (or mannite) which has the property of reducing the water content of the cell. Particularly important are also colloidal substances such as polyglukin (a Soviet preparation of dextran) or albumin.

Approved For Release 2009/05/01 : CIA-RDP80T00246A007500340002-0

Approved For Release 2009/05/01 : CIA-RDP80T00246A007500340002-0

The joint action of the substances included in the above solution in preventing the formation of large ice crystals during the freezing of blood is almost analogous to the action of the Mollison glycerol solution.

This is proved by the X-ray analysis of the frozen blood structure. The X-ray diffraction patterns (Figs. 1 and 2) illustrate in both blood samples only small crystals and zones of unfrozen matter (halo).

Blood, mixed with the solution mentioned above in a proportion of 1:1 and cured for 24 hours at 4°C. for better action of its constituents can be preserved for a long time in a cold room at -13° to -15°C. in a solid frozen state without any considerable destruction of the erythrocytes.

The blood should be thawed by a rapid transfer of the vessels holding it into a water bath at 30°C.

Tests of a very large number of blood samples have shown that blood drawn from different donors varies with respect to the injurious effect of freezing and thawing.

The blood proved to be stable in more than 70 % of the cases. Observations have shown that in most cases no hemolysis occurs after thawing blood which was stored for 2-3 days in the frozen state. When the time at which blood is kept in the solid frozen state is further increased, there is an insignificant increase of hemolysis: e.g. thawing after one month results in a loss of erythrocytes varying from 1 to 3-5 %. In a number of cases the rate of hemolysis remains nearly constant insignificantly increasing during 75 days of storage at -13 to -15°C. These losses do not exceed those cited in the literature for the glycerol method.

The morphology of the thawed erythrocytes does not differ markedly from that of untreated ones. Thawed erythrocytes are discoid, and thorn-like (Fig. 3) due to the action of the preserving solution.

The full physiological value of the restored erythrocytes is proved by the reversibility of their thorn-like shape into a discoid shape when transferred to fresh plasma. At the same time they stick together showing rouleaux formation. (Fig. 4). The addition of fresh plasma, represents to some extent an experimental model of transfusion.

The functional value of the erythrocytes is proved by the fact that up to 85 % of their glycolytic activity is preserved.

Unlike the method of freezing blood with glycerol, the method described allows use of the blood for transfusion without any losses of the plasma as the substances contained in the solution may be used in intravenous injections.

It is highly important to note that blood prepared according to this new method does not freeze and remains fluid at -8°C., i.e. at a temperature somewhat below its freezing point (-5,2°C.). At -8°C. it may be stored without hemolysis on an average up to a hundred days. During this period the erythrocytes retain their thorn-like shape. Approximately 64 % of the glycolytic activity preserved even on the 120th day of storage.

Approved For Release 2009/05/01 : CIA-RDP80T00246A007500340002-0

Approved For Release 2009/05/01 : CIA-RDP80T00246A007500340002-0

The biological transference and therapeutic effectiveness of the blood stored both in the solid and the liquid state at the moderately low temperatures mentioned have been proved by means of experimental transfusions to animals and subsequently to patients.

The practical importance of the methods discussed is quite obvious. A better preservation of blood is achieved, and in addition transportation of it in winter is much simplified due to the fact that the danger of deteriorating the blood by freezing is eliminated and especially insulated containers are unnecessary.

THE USE OF ULTRA-LOW TEMPERATURES (-195°C).

The use of very low temperatures to achieve vitreous solidification of the blood has been attempted. The promising results obtained are given below.

It is known that when water containing material freezes, the water is crystallized, thus evolving the latent heat of solidification.

It is also known that the size of the crystals depends upon the rate of freezing, and that quick-freezing produces smaller crystals. With a rate of temperature drop of 100°C. per second it is possible to obtain an amorphous structure, (the isotropic state), i.e. a complete absence of crystals.

The vitrification of blood was attained some time ago in thin layers (smears on glass slides in foil packages) by submersion in liquid nitrogen. (7, 8).

The present experiments have shown that the best way to obtain vitrification of large volumes of blood is to spray the blood into liquid nitrogen. This is in full agreement with data cited in the literature. (9).

It is necessary to solve two problems when applying the vitrification method: 1) the preservation of integrity of the structure of the erythrocytes as well as their biological functions during the process of vitrification and devitrification and 2) the development of a method for prolonged preservation of blood in the vitrous state.

Only the first of these problems is discussed in this paper. Protective solutions containing sugar, colloids and other substances which reinforce the membrane of the erythrocytes have been developed so that blood can be obtained in the vitrous state. Dispersion by means of spraying is one of the main stages in obtaining vitrified blood.

The degree of dispersion is also important: the smaller the drop, the quicker the heat will be removed by the cooling medium.

A detailed investigation of a number of various nozzles enabled the design of a special nozzle which is the main constituent of our special spraying equipment (Fig. 5). This pneumatic nozzle is made of plastic and its special feature is that it allows the blood to flow through peripheral holes while the gas (in this case nitrogen gas) passes through a central hole. Control of gas pressure in the nozzle and above the blood surface is provided with sufficient precision by means of two pressure gauges and a system of valves.

Approved For Release 2009/05/01 : CIA-RDP80T00246A007500340002-0

Approved For Release 2009/05/01 : CIA-RDP80T00246A007500340002-0

Investigations of the influence of the gas pressure (Fig. 6) have made it possible to determine the optimum value to 0.1 - 0.16 atm.

Liquid nitrogen was chosen as a refrigerant due to its low temperature (-195°C.) and comparative safety in handling.

However, irrespective of the serious attention payed to the two highly important factors promoting vitrification (small size of the spray drops and low temperature), a certain insignificant part of the blood may undergo crystallization due to the low coefficient of heat transfer of the gas layer formed around the blood drop when it enters the liquid nitrogen.

The determination of the structure of the solidified blood corpuscles sprayed into liquid nitrogen, i.e. the corroboration of the state of vitrification is of considerable interest.

A direct investigation of the structure of the blood powder in liquid nitrogen is quite difficult. The possibility of applying X-ray examinations of the structure is strongly impeded by the low temperature of the object.

Consequently a simple method for determining the structure of the solidified blood, has been developed. This method is based on the investigation of the thermal and material balance of the process.

We proceeded from the assumption that the amount of heat to be removed during freezing of any material containing moisture (in this case blood) is determined according to the well-known equation (10):

$$Q_x = G \left[C_1 (t_1 - t_2) + W_w R + C_2 (t_2 - t_3) \right] \quad (1)$$

where: G = weight of blood sample, kg;

C_1 = specific heat capacity of non-frozen blood, kcal/kg°C;

C_2 = specific heat capacity of frozen blood, kcal/kg°C;

t_1 = initial temperature of blood, °C;

t_2 = freezing point of blood, °C;

t_3 = final temperature of frozen blood, °C;

W_w = weight of ice in 1 kg of frozen blood, kg/kg;

R = latent heat of water freezing, kcal/kg.

We can now, as a first approximation for determining the amount of heat to be removed during vitrification of blood, use the following equation:

$$Q_v = G \cdot C (t_1 - t_2) \quad (2)$$

where G = weight of the blood sample, in kgs;

C = mean integral heat capacity of the liquid and vitrified blood (approximate); kcal/kg°C.;

t_1 = initial temperature, °C.;

t_2 = final temperature, °C.;

Approved For Release 2009/05/01 : CIA-RDP80T00246A007500340002-0

Approved For Release 2009/05/01 : CIA-RDP80T00246A007500340002-0

We are discussing a case in which no crystallization occurs. Thus the necessity of removing the latent heat of solidification of water is eliminated. This is the main distinction of vitrification from normal freezing with crystallization.

It is evident from a comparison of equations (1) and (2) that the amount of heat to be removed at vitrification is less than in the case of freezing. Hence, by comparing the heat removed when spraying the blood with that removed at an ordinary freezing of the same amount of blood in liquid nitrogen, it is possible to obtain an approximate estimation of the structure of the solidified sprayed blood.

Aliquots of blood were frozen by submersion in liquid nitrogen and sprayed for vitrification in the same medium.

A Dewar flask with liquid nitrogen put on a balance made it possible to determine with sufficient precision the heat removed in each case expressed as the amount of nitrogen evaporated during the experiment.

For example, approximately 2.6 g of nitrogen was evaporated in freezing 1 ml of blood; while in spraying 1 ml of blood, approximately 1,6 g of nitrogen was evaporated. The average experimental and calculated amounts of heat removed are tabulated below.

TABLE 1. HEAT REMOVED AT VARIOUS CONDITIONS OF BLOOD SOLIDIFICATION.

Symbol	Condition	Heat removed (cal per ml)	
		Calculated	Experimental
Q_f	At freezing	152	122
Q_v	At vitrification	92	75.2
$\frac{Q_f}{Q_v}$		1.65	1.62

It should be noted that the actual values obtained are of no special importance. They are approximate only due to the fact that a number of physical data are lacking. Of significance, however, is a comparison of the calculated and experimental values of the ratio:

$$\frac{Q_f}{Q_v}$$

If we obtained, for example, $\frac{Q_f}{Q_v} = 1$, it would be possible to consider that $Q_f = Q_v$, i.e. there would be no vitrification. On the other hand if it were found to be =1.65, which is the theoretically calculated value, it would mean that the entire blood volume was vitrified.

From this the assumption may be made that the difference 1.65 - 1 = 0.65 corresponds to a hundred per cent vitrification of the blood.

A comparison of the experimental+) value of this difference with the theoretically calculated value would determine the percentage of blood vitrified in each experiment.

$$\left[\left(\frac{Q_f^+}{Q_v^+} - 1\right) : \left(\frac{Q_f}{Q_v} - 1\right)\right] \cdot 100 = v$$

+) Experimental values are marked with a cross (+).

Approved For Release 2009/05/01 : CIA-RDP80T00246A007500340002-0

Approved For Release 2009/05/01 : CIA-RDP80T00246A007500340002-0

For the case cited above (see Table)

$$v = \frac{0.62}{0.65} \cdot 100 = 95\%.$$

It has been established that in our experiments on the average up to 95% of the blood was vitrified.

In order to obtain undamaged blood from the -195°C. "blood powder" it is necessary to provide complete reversibility of vitrification, i.e. to perform devitrification without the formation of ice crystals.

This was carried out by a rapid transfer and submersion of the blood powder into a vessel containing a preserving solution of the type mentioned earlier (physiological solution, plasma, 10% saccharose, etc.). This solution is preheated to 40-50°C. depending upon the composition of the medium applied.

The quantity of erythrocytes remaining intact after devitrification amounted to 85 - 90%.

The utilization of the described experimental calculation method of determining the degree of blood vitrification allows establishing at which of the two stages (spraying into nitrogen or devitrification) the damage of the blood corpuscles occurs and thus taking measures for preventing the resulting losses of blood.

The results obtained so far indicate that the major damage occurs during the devitrification process. An improvement in the technique of applying ultra-low temperatures, and especially, in the method of thawing blood should reduce the losses of blood to a minimum.

CONCLUSIONS.

1. To achieve prolonged preservation of blood in a state full physiological value, methods have been developed which permit the storage of blood at sub-zero temperatures. The investigations have been carried out along two lines:

a) the use of moderate low temperatures (down to -15°C.);
b) the use of ultra-low temperatures (-195°C.) - vitrification.

2. A preserving solution has been developed to protect the erythrocytes from the injurious effect of low temperatures.

All the components of the solution are admissible for intravenous injection. Thus, the entire amount of blood may be used for transfusion without any losses which is different from the glycerol method cited in the literature.

3. The solution allows the storage of blood for long periods in a fluid non-frozen state at -8 to -10°C. The erythrocytes remain morphologically unaltered and the blood is fit for transfusion during a period of a hundred days.

The same solution protects the erythrocytes from destruction when the blood is frozen at -12 to -15°C. and stored at these temperatures.

4. X-ray diffraction patterns of the frozen blood have shown that the preserving solution prevents the formation of large ice crystals, which explains its protective action.

Approved For Release 2009/05/01 : CIA-RDP80T00246A007500340002-0

Approved For Release 2009/05/01 : CIA-RDP80T00246A007500340002-0

5. A spraying device providing sufficient fine dispersion atomization and a minimum injure of blood being sprayed into liquid nitrogen has been developed for obtaining blood in the vitrous state (at -195°C.).

6. A method is described for indirect determination of the structure of the solidified blood sprayed in liquid nitrogen. It has been proved that there is a sufficiently complete vitrification of the blood (95%) if it is cooled instantaneously.

7. The results obtained are promising enough to justify the development of a special device designed to provide sterility of the blood, during all the stages of treatment, for clinical applications.

REFERENCES.

1.	Belyakov, A.D.	Problems of hematology and blood transfusion. (1) 35-39, 1956.
2.	Vinograd-Finkel, F.R.; Ginsburg, F.G.; Fyodorova, L.I.; and Kaukhcheshvili, E.I.	Problems of hematology and blood transfusion. (1) 27-34, 1958.
3.	Smith, A.U.	Lancet, 259, 910-911, 1950.
4.	Lovelock, I.E.	Biochim. et Biophys. Acta. 1953, 10, pp. 414-426.
5.	Chaplin, H. and Mollison, P.	Lancet, 24, 852-858, 1954.
6.	Sloviter, H.A.	Amer. I.Med.Sci. 231, 4, 437-440, 1956.
7.	Luyet, B. and Gehenio, P.	The Sixth Congress of the Blood Transfusion. Basel-NY, p.330-333, 1958.
8.	Pokrovsky, P.I.	Modern problems of hematology and blood transfusion. issue 28, pp.75-81, 1953.
9.	Meryman, H. and Kafig, E.	Proc. Soc. Exptl. Biol. and Med. 90, (3), pp.587-589, 1955.
10.	Golovkin, N.A. and Tchigeov, G.B.	Refrigerating technology of foods. Pishchepromizdat, Moscow, 1951.

Approved For Release 2009/05/01 : CIA-RDP80T00246A007500340002-0

Approved For Release 2009/05/01 : CIA-RDP80T00246A007500340002-0

Heat Exchange at the Refrigeration of the Concrete Masony of Dams

Recherches sur la conductibilite thermique dans les barrages refroidis par serpentins

A.G. TKACHEV, G.N. DANILOVA

The Leningrad Technological Institute of the Refrigerating Industry, Leningrad, U.S.S.R.

SOMMAIRE. On discute des résultats de recherches entreprises sur le refroidissement du béton de grands barrages à l'aide de serpentins.

La conductibilité thermique au sein d'un massif de béton, avec ou sans source de chaleur interne, a fait l'objet de recherches théoriques et experimentales. Les essais eurent lieu en laboratoire sur des blocs prismatiques de 300 mm de coté ou cylindriques de 360 mm et 545 mm de diamètre. Chaque bloc était refroidi par une circulation d'eau à travers des tubes de 6 ou 10 mm placés au centre de l'eprouvette. Pendant toute la durée de l'expérience, l'eau de refroidissement entrait a température constante. Les essais conduisirent à des formules approchées reliant la température moyenne du bloc de béton à un certain nombre de paramètres: température moyenne de l'eau température initiale, caractéristiques thermiques, source de chaleur, dimensions des blocs de béton et des canalisations de refroidissement, durée de l'essai.

L'expérience acquise en matière de refroidissement de barrages montre que l'évacuation de la chaleur du béton par l'eau de refroidissement commence, soit aussitot après la pose du reseau de circulation d'eau soit quelque temps après (1 mois a 1 mois 1/2). l'analyse des différents procédés de réfrigération, en fonction des résultats obtenus, montre la supériorité de la première solution. Dans ce cas, la température maxima du béton consécutive aux réactions exothermiques qui s'y développent, est plus basse et la durée du refroidissement un peu plus brève.

The following nomenclature is used in the paper:

a - thermal diffusivity, m^2/hr;

c - specific heat, kcal/kg ^{o}C;

Approved For Release 2009/05/01 : CIA-RDP80T00246A007500340002-0

Approved For Release 2009/05/01 : CIA-RDP80T00246A007500340002-0

J_o, J_1 - Bessel's functions of the first class of zero and first orders;

$k = \frac{R}{r_o}$ - ratio of external and internal radiuses;

l - distance between pipes in block in vertical direction, m (Fig. 1);

q_v - exothermal heat, kcal/m^3 hr;

r_o - internal radius of pipe, m (Fig. 2);

R - external radius of cylindrical block, m (Fig. 2);

r - radius of point being considered, m (Fig. 2);

t_f - temperature of cooling medium, °C;

t_i - initial temperature of concrete, °C;

t - temperature of concrete at point being considered, °C;

u - over temperature, °C;

$$V_o\left(\frac{r}{r_o}, x_i\right) = J\left(\frac{r}{r_o}, x_i\right) \cdot Y_o(x_i) - J(x_i) Y_o\left(\frac{r}{r_o}, x_i\right) \quad (1)$$

x_i - roots of transcendental equation

$$J_o(x_i) Y_1(k x_i) - J_1(k x_i) Y_o(x_i) = 0 \quad (2)$$

Y_o, Y_1 - Bessel's functions of the second class of zero and first orders;

γ - specific weight, kg/m^3;

ϑ - relative temperature;

λ - thermal conductivity of material, kcal/m °C, hr;

τ - time, hr;

$Fo = \frac{a\tau}{r_o^2}$ - Fourier's number;

$K_1 = \frac{q\, r_o^2}{\lambda (t_i - t_o)}$ - dimensionless number characteristic of the relation between the internal heat generation and the thermal conductivity of the cylinder.

Refrigeration of concrete is used in the construction of high dams in order to avoid cracking at the evolution of exothermal heat and subsequent cooling. The problem is solved either by cooling the components of the concrete prior to and during its preparation, or by cooling the concrete masonry by means of built-in pipes. Works published on piping refrigeration of concrete present some theoretical and experimental data (1,2,3,4).

Approved For Release 2009/05/01 : CIA-RDP80T00246A007500340002-0

Approved For Release 2009/05/01 : CIA-RDP80T00246A007500340002-0

THEORETICAL SOLUTION OF THE PROBLEM OF PIPING REFRIGERATION OF CONCRETE MASONRY

A schematic diagram of a concrete construction with built-in cooling water pipes is shown in Fig. 1. The pipes and surrounding mass of concrete remote from the surface are under more difficult conditions than that part at the surface. Therefore, the first case will be discussed in the present paper. The entire bulk of the concrete may be considered as being composed of elements comprising a concrete block in the form of a rectangular or hexahedron prism and a cooling pipe passing through its centre (Fig. 1a and 1b).

The determination of the temperature field in the concrete may be reduced with certain approximation to the definition of the distribution of temperatures in a single hollow cylinder of infinite length with an adiabatic external surface and the heat removed through the internal surface. The radius R of the cylinder under consideration is found from the condition of equality of the cross-section of the prism and cylinder.

It was also assumed that the temperature t_o at the external surface of the pipe was equal to the mean temperature t_f of the cooling water in the pipe and was constant in time. This allowance is possible due to the fact that with 1" and 2" dia. pipes being used at present, l = 1,5 - 3 m and the water flow having a speed of 0.6 to 1 m/sec, the thermal resistance of the heat transfer to the water and of the pipe walls amounts to 1 - 2% of the thermal resistance of the concrete. The internal heat generated by the concrete (exothermal heat) is assumed to be constant in time.

Under these assumptions, the differential equation and the boundary conditions, characterizing the process of heat diffusion in the cylinder, is as follows

at $r_o \leq r \leq R$

$$\frac{\delta t}{\delta \tau} = a \left(\frac{\delta^2 t}{\delta r^2} + \frac{1}{r} \frac{\delta t}{\delta r} \right) + \frac{q_v}{c\gamma} \qquad \text{I}$$

Approved For Release 2009/05/01 : CIA-RDP80T00246A007500340002-0

Approved For Release 2009/05/01 : CIA-RDP80T00246A007500340002-0

The boundary conditions

$$\text{at } \tau > 0 \qquad r = R \qquad \frac{\delta t}{\delta r} = 0$$

$$\text{at } \tau > 0 \qquad r = r_o \qquad t = t_o \qquad \text{II}$$

$$\text{at } \tau = 0 \qquad t = t_i \text{ for } r_o \leqslant r \leqslant R$$

When no exothermal heat is evolved, the differential equation characterizing the cooling process is simplified ($r_o \leqslant r \leqslant R$):

$$\frac{\delta t}{\delta \tau} = a\left(\frac{\delta^2 t}{\delta r^2} + \frac{1}{r}\frac{\delta t}{\delta r}\right) \qquad \text{III}$$

with the boundary conditions remaining in the form of system II. The second problem was solved first (equations III and II).

The solution obtained has the form:

$$U = t - t_o = -\pi \sum_{i=1}^{\infty} \frac{(t_i - t_o) J_1^2(kx_i)}{J_o^2(x_i) - J_1^2(kx_i)} \cdot V_o\left(\frac{r}{r_o} x_i\right) 1^{-Fox_i^2} \qquad (3)$$

At sufficiently large values of Fo the mean value of the relative over temperature throughout the volume required for calculating the heat losses is determined according to the formula:

$$\bar{\Theta} = \frac{\bar{t} - t_o}{t_i - t_o} = \frac{4}{k^2 - 1} \cdot \frac{J_1^2(kx_1)}{J_o^2(x_1) - J_1^2(kx_1)} \cdot \frac{1}{x_1^2} 1^{-Fox_1^2} \qquad (4)$$

The solution of equation (I) at the boundary conditions (II) has the form

$$t = \frac{q_v R^2}{2\lambda} \ln \frac{r}{r_o} - \frac{q_v}{4\lambda}(r^2 - r_o^2) + t_o +$$

$$+\pi \sum_{i=1}^{\infty} \frac{J_1^2(kx_i)}{J_o^2(x_i) - J_1^2(kx_i)} \left[\frac{q_v R^2}{\lambda x_1^2 k^2} - (t_i - t_o)\right] V_o\left(\frac{r}{r_o} x_i\right) 1^{-Fox_i^2} \qquad (5)$$

Approved For Release 2009/05/01 : CIA-RDP80T00246A007500340002-0

Approved For Release 2009/05/01 : CIA-RDP80T00246A007500340002-0

At sufficiently large values of Fo and k, we obtain the following expression of the mean relative temperature:

$$\bar{\Theta} \approx \frac{K_1}{k^2-1}\left[k^2\left(\ln k - \frac{3}{4}\right)+1\right] + \frac{4}{k^2-1}\cdot\frac{J_1^2(kx_1)}{J_0^2(x_1)-J_1^2(kx_1)}\cdot\frac{1}{x_1^2}\,1^{-Fox_1^2}\left(1-\frac{K_1}{x_1^2}\right) \qquad (6)$$

Formula (6) at $K_1 = 0$ results in the expression (4).

An examination of the solutions obtained indicates that when exothermal heat is present $\bar{\Theta} = f(Fo, K_1, k)$ and in the absence of such heat $\bar{\Theta} = f(Fo, k)$.

EXPERIMENTAL INVESTIGATION OF PIPING REFRIGERATION OF CONCRETE BY WATER AT AN EVOLUTION OF EXOTHERMAL HEAT

A special experimental installation has been designed for checking the theoretical formulae allowing investigation of the process of non-stationary thermal conductivity of a concrete block refrigerated by means of water circulated through a pipe embedded in the block. The experiments were carried out on models of cylindrical and prismatic cross-section.

The experimental installation (Fig. 3) consisted of a condensing unit 1, and evaporator 2, centrifugal pumps 3 and 5, a thermostat 4, a concrete block 11 with a pipe 10 run along the axis of the block, and a differential gauge 12.

The following devices were installed for maintaining the temperature of the water in the thermostat constant at the required level: an agitator 6, electric heater 8, cooling coil 9 and contact thermometer 7.

After the concrete has been timbered, the concrete block was insulated by a 300 mm thick layer of Iporka.

The experiment was carried out as follows.

First of all the initial temperature of the concrete was measured by means of thermocouples. Then the centrifugal pump was started and 5° C, water was run from the thermostat through the cooling pipe; the time of the beginning of the experiment

Approved For Release 2009/05/01 : CIA-RDP80T00246A007500340002-0

Approved For Release 2009/05/01 : CIA-RDP80T00246A007500340002-0

was recorded. Thereafter in definite time intervals (more often at the beginning of the experiment) measurements were made of the temperatures in the central section of the sample, og the water on entering and leaving the pipe, and corresponding time of the measurements was recorded. Besides, the ambient air temperature was periodically measured as well as the temperature on the surface of the insulation. The experiments were run until the temperature difference between the mean temperature in the pipe and the concrete block surface temperature reached 4 to 5° C. The average duration of an experiment was about 3 days.

The results of the experiments were treated in the form of a dependence of the mean relative temperature and the Fourier number Fo at various conctant values of the dimensionless number K_1.

Fig. 4 illustrates a comparison of the results of one of the experiments on cooling concrete with the data of the theoretical curve. At the beginning of the process, when the temperature in the block was close to the ambient temperature, there was a good coincidence of the experimental and theoretical data.

With the drop of the temperature of the concrete, due to the inflow of external heat, the cooling rate in the experiment gets slower.

CONCLUSION

The theoretical solutions obtained may be used for calculating the processes of piping refrigeration of concrete in designing various dams.

REFERENCES

1. CARSLOW H., and JAEGER, I. Conduction of heat in solids. Oxford, 1948.

2. CHAPELLE, J. Le froid dans la construction des barrages. La Revue Generale du Froid, Janvier 1957.

Approved For Release 2009/05/01 : CIA-RDP80T00246A007500340002-0

Approved For Release 2009/05/01 : CIA-RDP80T00246A007500340002-0

3. CHU-BE-FANG. Calculation of Temperatures in Mass Concrete with Internal Source of Heat. Journal of Hydraulic Engineering Society of China, 1957, No. 4.

4. LAMKIN, M.S. On the Calculation of Piping Refrigeration of Concrete Structures. Leningrad Polytechnical Institut. Scientific-Technical Information Bulletin, 1958, No.8.

Approved For Release 2009/05/01 : CIA-RDP80T00246A007500340002-0

Approved For Release 2009/05/01 : CIA-RDP80T00246A007500340002-0

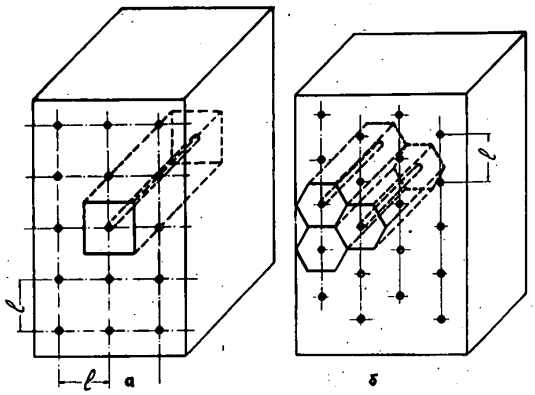

Fig. 1. Schematics of problem.

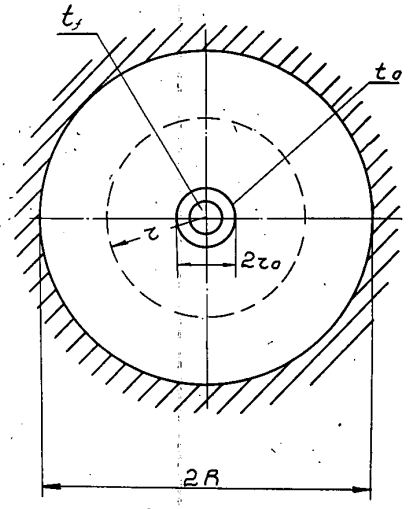

Fig. 2. Cylinder being cooled.

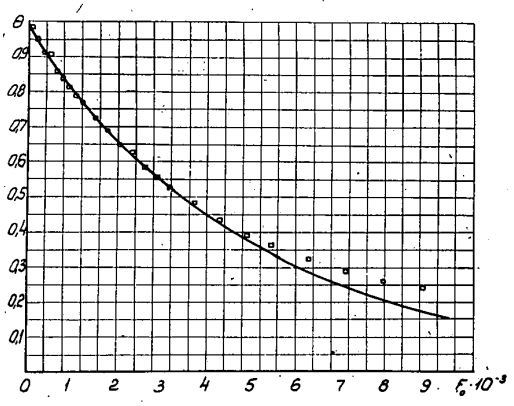

Fig. 3. Diagram of installation for investigating piping refrigeration of concrete by water.

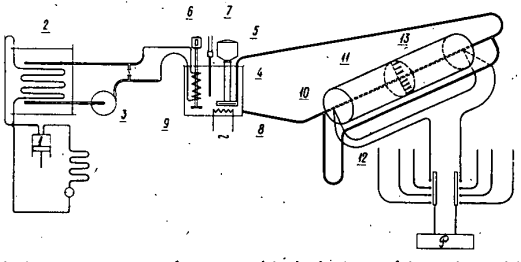

Fig. 4. Mean relative temperature of concrete block during refrigeration with an evolution of exothermal heat. ⊡ – experimental cooling from 21.0° C. to 9.1° C. at $q_v = 31.6$ kcal/m³hr and $K = 54.5$ — theoretical curve.

Approved For Release 2009/05/01 : CIA-RDP80T00246A007500340002-0

Approved For Release 2009/05/01 : CIA-RDP80T00246A007500340002-0

Preservation of Haematopoietic Tissues for the Therapy of Radiation Disease.

Conservation des tissus hématopoïétiques pour le traitement des maladies dûes aux radiations

ALENA LENGEROVA

Department of Experimental Biology and Genetics, Biological Institute of the Czechoslovak Academy of Sciences, Prague, Czechoslovakia

SOMMAIRE. La possibilité de la conservation à long terme de tissus viables est un facteur important du traitement des maladies dûes aux radiations. La possibilité d'application pratique des résultats expérimentaux couronnés de succès pour le traitement par moelle osseuse dépend principalement de deux conditions: 1, la possibilité d'utiliser des tissus hématopoïétiques homoloques sans retard nocifs (par exemple du tissu homoloque dont l'efficacité therapeutique serait semblable à celle d'une substance isologue dont on ne disposerait que dans des conditions expérimentales), et 2, la possibilité d'une conservation à long terme de cette substance à l'état viable pour en disposer toutes les fois où c'est nécessaire (accidents imprévus là où des êtres humains sont exposés à des doses mortelles de radiations ionisantes).

La première de ces conditions est remplie lorsqu'on utilise un tissu embryonnaire homologue, dont l'application permet d'éviter les effets lents défavorables du traitement par moelle osseuse homologue d'adulte. La seconde condition semble remplie grâce à la méthode de conservation des tissus à la température de CO_2 solide, en utilisant l'action protectrice du glycérol. Des expériences sont en cours pour apprécier les différentes conditions de congélation et décongélation agissant sur l'efficacité thérapeutique de cellules hépatiques embryonnaires de souris injectées dans des souris d'une autre espèce ayant subi des doses mortelles d'irradiation.

The death of a lethally irradiated organism may be prevented by a single injection of bone marrow cells taken from a nonirradiated donor and administered shortly after exposure. At present, this procedure is the only effective way of treating radiation disease accessible not only under laboratory conditions, but also in the case of human emergency. From the practical point of view, two

Approved For Release 2009/05/01 : CIA-RDP80T00246A007500340002-0

Approved For Release 2009/05/01 : CIA-RDP80T00246A007500340002-0

important conditions need to be fulfilled: 1) the possibility of using homologous material, the effectiveness of which would be comparable with effectiveness of isologous material available only in experiments on inbred animals; 2) the possibility of long-term storage of suitable material in a viable state, available, whenever necessary.

There is a great deal of experimental evidence that the therapeutic effect displayed by the nonirradiated blood-forming cells in the irradiated recipient is based on their multiplication and their replacing the host haematopoietic tissues destroyed by radiation, in other words on the transplantation mechanism. By the homo- or heterotransplantation of haematopoietic cells from adult donors, however, a secondary disease develops; this is due to the simultaneously grafted immunological competent cells of the donor reacting against the recipient of a different genetic constitution. This secondary disease, which can be fatal, may be eliminated by using homologous haematopoietic tissue (e.g. liver) from embryonic donors. Under these conditions, the problem of long-term preservation of viable embryonic blood-forming cells seems to be even more important than the preservation of adult bone marrow, since the latter could most probably be obtained in a fresh state from volunteer donors in an emergency. The method most suitable for this purpose seems to be preservation at low temperatures using the protective effect of glycerol as discovered by Polge et al. (1). With regard to this problem the suitability of various freezing methods, effective for other tissues needs to be investigated. This paper is confined to several technical details of freezing and thawing as well as testing the viability of haematopoietic mouse tissue subjected to these procedures.

Apparatus. The apparatus used for freezing was constructed on the principle of Polge and Lovelock (2), but supplemented by the regulation of the freezing rate. Barnes and Loutit (3) using the same principle did not with their apparatus obtain the exact

Approved For Release 2009/05/01 : CIA-RDP80T00246A007500340002-0

Approved For Release 2009/05/01 : CIA-RDP80T00246A007500340002-0

physical characteristics required. They found it necessary to balance the freezing rate by a heating coil. In the experiments presented here another modification was used (Fig.1). The freezing bath is placed into a 2000 ml. Dewar flask filled with methanol which is cooled in advance to -70°C. This temperature is kept constant by means of a ribbed duralumin vessel filled with solid CO_2, which is inserted into the wood alcohol. The advantage of this arrangement is that during the experiment the level of the freezing bath does not change due to evaporation of CO_2 as when solid CO_2 is mixed directly with the alcohol. This is important with regard to the principle of regulation used in this apparatus. The test-tube with the sample is placed into a wire holder, the stem of which contains one connection of the thermocouple (Constantan - Cu). The other connection is kept under constant temperature at 20°C. The rate of temperature fall measured at the surface of the frozen sample is carefully followed with a stop watch and galvanometer and regulated at will, simply by raising or lowering the duralumin vessel in the freezing bath. The duralumin vessel contains the specimen immersed in glycerol. This simple arrangement was found to work quite satisfactorily. The basic scheme of freezing rate used was that of Barnes and Loutit (1° per minute down to -15°C and then not more than 10° per minute). In addition the effect of some variations was tested. When the temperature reached -70°C, the sample was quickly transferred to a refrigerator for prolonged storage in solid CO_2.

The preparation of specimens. Mice used in the present experiments were derived from a random bred strain H. Embryonic liver (from 18-19-day old embryoes) or adult spleen was excised under sterile conditions and minced into small fragments. One volume of the tissue was mixed with 10 volumes of 15% glycerol in homologous serum. The mixture was incubated from 5 minutes to 2 hours at 4°C and then frozen according to the scheme being tested. To render the frozen material ready for use the specimen was thawed rapidly in a water-bath at 41°C, the tissue transferred into a glass homogenizer and a suspension of the desired cell concentration was prepared for intravenous injection. In some experiments glycerol was removed according to the Sloviter method (4) in the modification of Ferrebee et al. (5).

Approved For Release 2009/05/01 : CIA-RDP80T00246A007500340002-0

Approved For Release 2009/05/01 : CIA-RDP80T00246A007500340002-0

Testing the viability of frozen cells. The effectiveness of healthy haematopoietic cells to prevent death in a lethally irradiated recipient depends on their proliferation and repopulation of marrow spaces destroyed by radiation. Since it is expensive and time consuming to test the viability of frozen haematopoietic cells directly by their therapeutic effectiveness in irradiated animals, the possibilities of an indirect test, the results of which would be comparable with those obtained by the direct method, were studied. Experiments were carried out with different types of in vitro cultivation of mice embryonic liver cells without satisfactory results. Rey (6) found that cultures of frozen fibroblasts grew just as well as untreated controls. In contrast to this the growth of frozen embryonic liver cells in our experiments started with a considerable delay and displayed various abnormalities. This agrees rather well with the findings of Ferrebee et al. (5) that freezing of mouse marrow cells results in considerable loss of these cells' ability to synthesize DNA in vitro in spite of the fact that their ability to proliferate in vivo is retained. The freezing and thawing procedure thus seems to represent a certain damage for the mouse haematopoietic cells, which may be reversible only under in vivo conditions. The results of another in vivo test presented here fit in well with this hypothesis. Its principle is based on the ability of viable adult spleen cells to induce a significant spleen enlargement if injected into a newborn recipient of a different genetic constitution. Simonsen (7) demonstrated that this enlargement of the host spleen is due to its colonization by donor cells stimulated to multiplication and antibody formation by antigens of the newborn recipient. The splenomegaly index, therefore, gives a good picture of the reproductive capacity of the cells injected. As such it could be a suitable indicator of whether the freezing and thawing procedure or occasional changes in temperature during storage (to which the spleen cells were submitted simultaneously with the liver cells for radiation disease therapy) did not harm their proliferative capacity on which both the effects of splenomegaly and radiation disease therapy are based. Homologous spleen cell suspensions to be tested were injected intraperitoneally into newborn recipients (0.1 ml. per mouse) which were killed ten days later. The relative

Approved For Release 2009/05/01 : CIA-RDP80T00246A007500340002-0

Approved For Release 2009/05/01 : CIA-RDP80T00246A007500340002-0

enlargement of their spleen, as compared with that of the saline injected controls of the same age, was expressed as the splenomegaly index. This testing-system proved to be suitable; some of the results are presented in Table 1.

The spleen enlargement induced by spleen cells frozen to -79°C with 15% glycerol compares well with the effect of fresh cells. The only difference between groups 3 and 4 was a different incubation time with glycerol before freezing (5 minutes and 2 hours respectively). There is no statistically significant difference between the splenomegaly index in the two groups in spite of a considerable difference found when the vital staining test with eosin was applied to the injected spleen cells. From approximately 2000 cells counted in each of the groups 3 and 4, 99% and 9% of the cells, respectively, were viable according to this test. The discrepancy between the results obtained by these two different tests may yield alternative explanations. Firstly, the sensitivity of glycerolized cells (regardless of whether fresh or frozen) to osmotic damage may be different under in vivo and in vitro conditions. An alternative explanation may be that even the lower amount of viable spleen cells injected in group 4 (order 10^6) is sufficient to induce a similar degree of splenomegaly as that produced by the suspension in group 3 containing 10^7 of viable cells per mouse. This explanation is in agreement with the relationship between the degree of splenomegaly and the amount of fresh spleen cells injected (Fig.2). From this curve it may be seen that if a certain threshold amount of cells is reached, the degree of splenomegaly remains constant in certain limits of increasing spleen cell concentration. The fact that a similar situation exists with regard to the effectiveness of embryonic liver cells in inducing survival of lethally irradiated recipients, justifies the use of the test described.

Conclusions. On the basis of the experiments carried out the following conclusions may be drawn: The storage of mouse embryonic liver cells frozen with 15% glycerol in homologous serum preserves their full ability to induce recovery in lethally irradiated mice. The time of storage does not seem to play a decisive role. The damage is apparently connected in the first instance with the freez-

Approved For Release 2009/05/01 : CIA-RDP80T00246A007500340002-0

Approved For Release 2009/05/01 : CIA-RDP80T00246A007500340002-0

ing, thawing and glycerolization procedures. A lower freezing rate (less than 1° per minute) down to -15°C does not seem to influence the effectiveness of the frozen cells, whereas more rapid freezing in this range may result in considerable cell damage. The glycerol concentration may vary within relatively wide limits (5 - 20%) without considerable effect on the viability of the frozen cells. The prolongation of incubation with glycerol affects the cell viability favourably as judged by vital staining. The ability of adult spleen cells to induce splenomegaly in newborn mice was found to be a good test of different modifications of the freezing and thawing scheme and of their effect on the reproductive capacity of the cells from haematopoietic tissues; freezing procedures retaining the ability of adult mouse spleen cells to induce splenomegaly in newborn hosts, would apparently also be suitable for retaining the therapeutic effectiveness of embryonic liver cells in preventing death in lethally irradiated recipients.

References:

1. Polge, C., Smith, A.U. and Parkes, A.S. Revival of Spermatozoa after Nitrification and Dehydratation. Nature, 164; 666, 1949.

2. Polge, C. and Lovelock, J.E. Preservation of Bull Semen at -79°C. Vet.Rec., 64; 396, 1952.

3. Barnes, D.W.H. and Loutit, J.F. The Radiation Recovery Factor: Preservation by the Polge-Smith-Parkes Technique. J.Nat. Canc.Inst., 15; 901, 1955.

4. Sloviter, H.A., Tietze, R.M. A Method for Preparing Thawed Erythrocyte-glycerol Mixtures for Transfusion. Am.J.Med. Sci., 231; 437, 1956.

5. Ferrebee, J.W., Billen, D., Urso, J.M., Wan Ching Lu, Thomas, E.D. and Congdon, Ch.C. Preservation of Radiation Recovery Factor in Frozen Marrow. Blood, 12; 1096, 1957.

6. Rey, L. Studies on the Action of Liquid Nitrogen on Cultures in vitro of Fibroblasts. Proc.Roy.Soc., B, 147; 460, 1957.

7. Simonsen, M. The impact on the developing embryo and newborn animal of adult homologous cells. Acta pathol. et microbiol. Scandin., 40; 480, 1957.

COPYRIGHT RESERVED

Approved For Release 2009/05/01 : CIA-RDP80T00246A007500340002-0

Approved For Release 2009/05/01 : CIA-RDP80T00246A007500340002-0

Table 1. Comparison of the effectiveness of fresh and frozen mouse spleen cells to induce splenomegaly in newborn recipients.

Group No.	Material injected	Mean spleen weight mg.	Standard deviation of the mean	Splenomegaly index	Statistical significance of the differences between the means of the groups No.:
1	Tyrode solution	21.9	$\pm$ 1.3	1	
2	$1.2 \cdot 10^7$ fresh spleen cells	59.8	$\pm$ 4.0	2.73	1 : $P < 0.001$
3	$1.2 \cdot 10^7$ frozen spleen cells (viability 99%)	58.1	$\pm$ 2.3	2.65	2 : $P \gg 0.05$ 1 : $P < 0.001$
4	$1.1 \cdot 10^7$ frozen spleen cells (viability 9%)	58.6	$\pm$ 3.6	2.67	2 : $P \gg 0.05$ 1 : $P < 0.001$

Approved For Release 2009/05/01 : CIA-RDP80T00246A007500340002-0

Approved For Release 2009/05/01 : CIA-RDP80T00246A007500340002-0

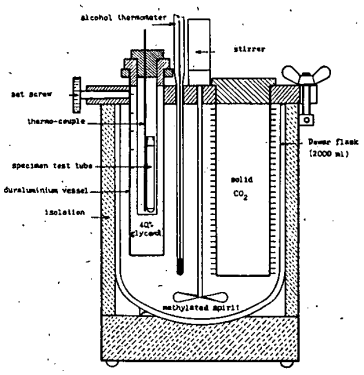

Fig. 1. Diagram of apparatus used.

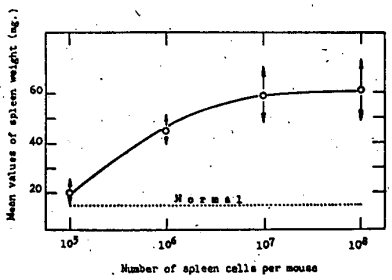

Fig. 2. The relationship between the degree of splenomegaly and the amount of fresh spleen cells injected.

Approved For Release 2009/05/01 : CIA-RDP80T00246A007500340002-0

Approved For Release 2009/05/01 : CIA-RDP80T00246A007500340002-0

Velocity of Sound at Different Temperatures in H_2, N_2, Air, O_2, and CO_2

La vitesse du son à différentes températures dans l'H_2, N_2, air, O_2 et CO_2

VÄINÖ HOVI
Wihuri Physical Laboratory, University of Turku, Turku, Finland

SOMMAIRE. Un appareil pour des mesures précises de la vitesse du son dans des gaz réels a été construit. Cet appareil fut calibré en employant comme gaz standard de l'air sec à des conditions connues. Il fut trouvé que la correspondance entre les valeurs standard antérieures et les données actuelles est très bonne. Il fut aussi possible de mesurer la vitesse du son dans des gaz réels au moyen de cet appareil avec une précision de $\pm$ 0,1 %.

La vitesse du son dans de l'H_2, N_2, air, O_2 et CO_2 fut mesurée à de différentes températures entre + 190° C et -69° C pour des fréquences allant de 1000 à 3000 cycles. La correspondance entre les valeurs obtenues et mesurées préalablement par des méthodes électroniques modernes fut quantitative. Presque dans tous les cas une légère augmentation de la vitesse du son pour des fréquences croissantes fut trouvée. Cette dispersion de la fréquence était pourtant beaucoup plus petite que pour les hautes fréquences.

Les valeurs déterminées sont un supplément pour les valeurs ultérieures. L'usage possible des nouvelles données pour la détermination empirique de second coefficient de viriel, B, est discuté.

INTRODUCTION

During the last ten years only a few measurements of the velocity of sound in some real gases have been carried out at different temperatures by means of modern electronic techniques at the frequency region of 750 - 3000 c/s [1, 2, 3]. Even though the accuracy of the data appearing in these publications is extremely high, the number of values is too small for any systematic investigation of the velocity of sound in a real gas as a function of temperature and frequency. In order to supplement the experimental data found in the available literature, the velocity of sound was measured accurately in H_2, N_2, Air, O_2 and CO_2 at different temperatures and frequencies.[2] The object was also to obtain a larger experimental basis for the verification of the theoretical values which can be calculated from the quantum mechanical expressions of the second virial coefficient. Since the quantum effects do not occur at high temperatures, the contribution to the second virial coefficient arising from the interactions between the gas particles should be dominant.

Approved For Release 2009/05/01 : CIA-RDP80T00246A007500340002-0

Approved For Release 2009/05/01 : CIA-RDP80T00246A007500340002-0

Analysis, Experimental Method and Results

The velocity of sound in a gas, c, can be represented by the formula

$$c = \sqrt{\frac{RT}{M}\left(\varphi + \frac{\gamma R}{\chi C_V \infty}\right)}, \qquad (1)$$

where R is the gas constant, M the molecular weight, T the absolute temperature, and

$$\left.\begin{aligned} \varphi &= 1 + \frac{2B}{V} + \frac{3C}{V^2} + \cdots, \\ \gamma &= \left(\frac{V}{R}\frac{\partial p}{\partial T}\right)^2_V = \left(1 + \frac{B + T\frac{\partial B}{\partial T}}{V} + \frac{C + T\frac{\partial C}{\partial T}}{V^2} + \cdots\right)^2, \\ \chi &= 1 - \frac{RT}{VC_V\infty}\left(2\frac{\partial B}{\partial T} + \frac{1}{V}\frac{\partial C}{\partial T} + T\frac{\partial^2 B}{\partial T^2} + \frac{T}{2V}\frac{\partial^2 C}{\partial T^2} + \cdots\right) \end{aligned}\right\} \qquad (2)$$

B and C stand for the second and third virial coefficient, respectively.

These equations differ slightly from those represented by Hardy et al. [4]. One can easily see from our equations the dependence of the quantities φ, γ, and χ on the virial coefficients and their derivatives. By substituting expressions (2) into (1) it is possible to represent the velocity of sound, c, as a function of the virial coefficients and their derivatives.

The experimental arrangement is given in Fig. 1. The method is the common tube method. By using the calibrated Muirhead Wigan Decade Oscillator, the maximum error of the frequency was less than $\pm$ 0.2 % at all frequencies.

In order to control the temperature of the gas inside the tube A, three copper-constantan thermocouples were installed on the tube, at both ends and the middle point. Thus, it was possible to measure the temperature in A with an accuracy of $\pm$ 0.02°.

For the constancy of the temperature inside the tube A, a larger brass tube (diameter 10 centimeters) M was installed coaxially with the tube A. Around the tube A a long brass plate was soldered for the guidance of the circulating cooled alcohol. This alcohol was cooled by ice or solid carbon dioxide and circulated around A by the pumping system N.

Usually dried air under standard conditions is accepted as the reference gas in measurements of the velocity of sound. In fact, this gas has been investigated thoroughly near room temperature. After the temperature in the gas tube and its surroundings had reached a constant value, the sound waves were sent from the oscillator to the gas. When the microphone was moved, the knotpoints of the standing waves in the gas were observed accurately as the maxima of the curves on the screen of the oscilloscope. In this way it was possible to read the points corresponding to the maxima within 0.5 millimeters on the scale F. As can be seen from Fig. 3, at the frequency range of 1000 - 2000 cycles our results for air are in excellent

Approved For Release 2009/05/01 : CIA-RDP80T00246A007500340002-0

Approved For Release 2009/05/01 : CIA-RDP80T00246A007500340002-0

agreement with the standard data. Outside this range, however, the disturbances were higher, and no good agreement was obtainable. This is caused, in the first place, by the geometry of the tube A and by some new resonance effects connected with the tube material. Therefore in Table 1 and Fig. 2, 3, and 4 we have collected from quite large experimental material only that which was measured at the frequency range of 1000 - 3000 cycles. In all our measurements the pressure of the gas to be investigated was very near one atmosphere.

If we examine the results appearing in Table 1 and Fig. 2, 3, and 4, we can draw the following conclusions:

1. The values obtained for the velocity of sound in air in the present investigation are in good agreement with the best previous data. Apart from hydrogen, the agreement between ours and others values with regard to nitrogen, oxygen, and carbon dioxide is also good. For a comparison in more detail the lack of sufficient previous modern data will, however, cause difficulties. Nevertheless, we believe that our values can offer a considerable supplement to the experimental material dealing with the velocity of sound in the gases just mentioned. The greater dispersion found for H_2 is probably caused by the three following factors: First, it was very difficult to prevent this gas diffusing slowly out of the tube during measurements. Thus, the points in Fig. 2 corresponding to the frequency of 3000 cycles are less reliable because of small air impurities. Secondly, common hydrogen is a mixture of ortho- and parahydrogen. It is known, that the ortho-para composition varies considerably as a function of temperature. At lower temperatures the relative amount of parahydrogen will increase. Therefore, hydrogen gas cooled to the temperature of $-67.5^{\circ}C$ will contain more parahydrogen than at higher temperatures. Thirdly, the dimensions of our tube were not suitable for light hydrogen as for heavier gases.

2. A slight increase in the velocity of sound with increasing frequency can be found almost in all cases. This is in agreement with the data observed previously for air in a few points and O_2 at $+1.9^{\circ}C$ (cp Fig. 3). It is interesting that at lower frequencies also one can verify an effect of that kind. Usually the frequency dispersion has been found at higher frequencies.

3. In order to clear up the accuracy of our measurements, the mean error of one observation (that is the error of the difference between the maximum of amplitude) and the same quantity of the mean value were calculated for O_2 and air at room temperature and the frequency of 2000 cycles. For both these gases the mean error of one observation turned out to be less than 0.2 % while the mean error of the mean value was smaller than 0.05 %. Furthermore, after having compared our results with the standard data of air we can state that <u>it is possible to measure the velocity of sound in real gases by means of our apparatus with an accuracy of about 0.1 %</u>. This means that the variations of temperature in the gas can be observed clearly if they are larger than $\pm$ 0.75 $^{\circ}$.

The oxygen used for our measurements contains impurities of about 0.3 %. On the other hand, the nitrogen, carbon dioxide, and hydrogen were practically free of impurities.

Approved For Release 2009/05/01 : CIA-RDP80T00246A007500340002-0

Approved For Release 2009/05/01 : CIA-RDP80T00246A007500340002-0

By using equations (1) and (2) and neglecting the third virial coefficient and all the derivatives except $\frac{\partial B}{\partial T}$, it may be possible to calculate approximate values for the quantity B of real gases on the basis of the data obtained for the velocity og sound. This has been examined in paper [5].

REFERENCES

1. SMITH, P.W., Jr. J.Acoust.Soc.Amer., 23, 715, 1951; 25, 81, 1953.

2. BANCROFT, D. Amer.J.Phys. 24 (5), 1956.

3. BERANEK, L.L. Acoustic Measurements. 1st ed. John Wiley & Sons, Inc., New York, 1949; Chapman & Hall, Ltd, London, 1950.

4. HARDY, H.C. Telfair, D, and Pielemeier, W.H., J.Acoust.Soc.Amer., 13, 226, 1942.

5. HOVI, V. and NÄSÄNEN, R. Unpublished work.

Copyright reserved

Approved For Release 2009/05/01 : CIA-RDP80T00246A007500340002-0

Approved For Release 2009/05/01 : CIA-RDP80T00246A007500340002-0

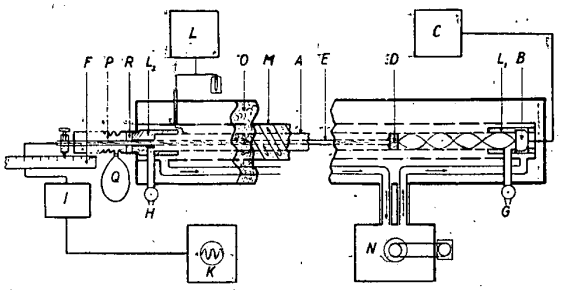

Fig. 1. Principle of the measuring apparatus.

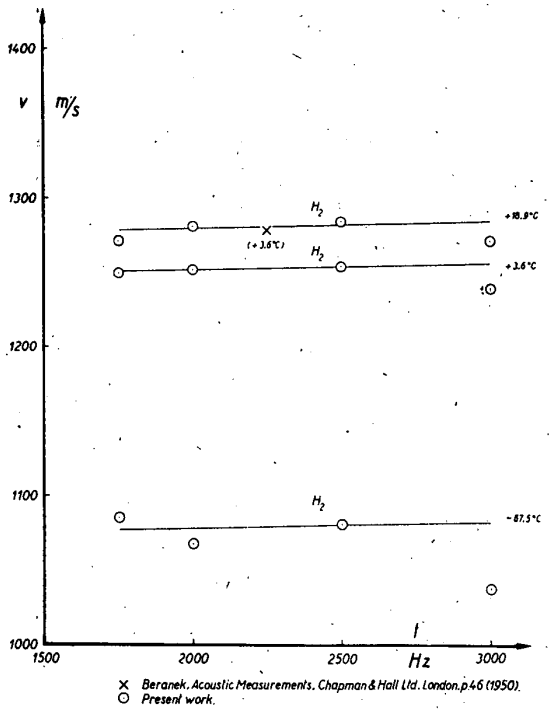

Fig. 2. Velocity of sound in H_2 at different temperatures and frequencies.

Approved For Release 2009/05/01 : CIA-RDP80T00246A007500340002-0

Approved For Release 2009/05/01 : CIA-RDP80T00246A007500340002-0

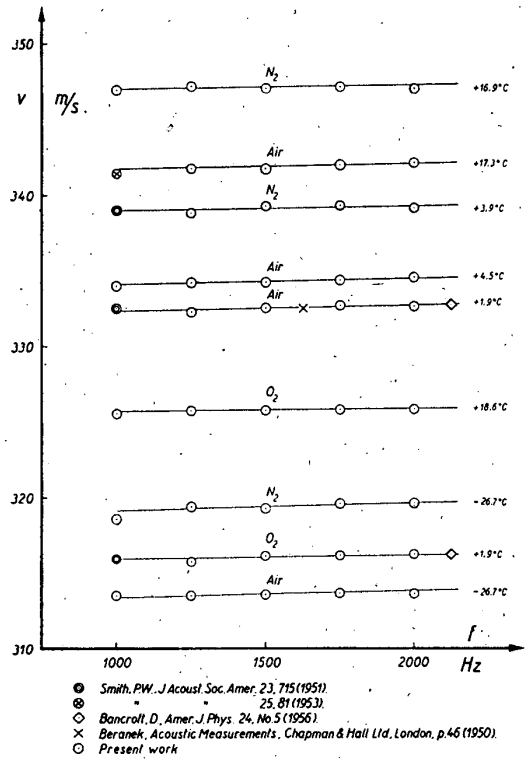

Fig. 3. Velocity of sound in N_2, Air, and O_2 at different temperatures and frequencies.

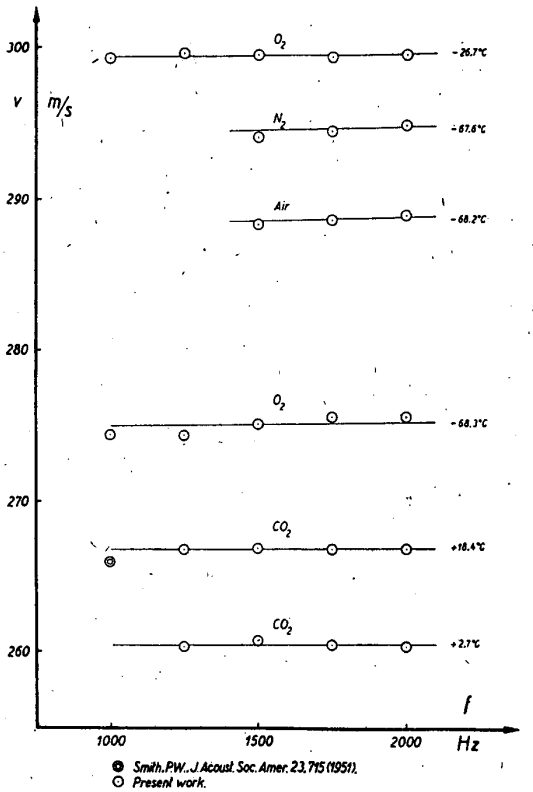

Fig. 4. Velocity of sound in N_2, Air, O_2, and CO_2 at different temperatures and frequencies.

Approved For Release 2009/05/01 : CIA-RDP80T00246A007500340002-0

Approved For Release 2009/05/01 : CIA-RDP80T00246A007500340002-0

Ultrasonic Investigation of the Elastic Constants of Solid Carbon Dioxide

Etude aux moyen d'ultrasons des constantes élastiques de l'anhydride carbonique solide

VÄINÖ HOVI and ESA MÄNTSALO
Wihuri Physical Laboratory, University of Turku,
Turku, Finland

SOMMAIRE. Un appareil à ultrasons pour faire des mesures sur les constantes élastiques des solides a été construit. En employant cet appareil les constantes élastiques de l'anhydride carbonique solide ont été mesurées à la température de sublimation de $-78,5^{\circ}$ C et à des fréquences d'environ 2 Mc. L'anhydride carbonique solide est considéré comme un cristal isotropique. La compressibilité cubique adiabatique fut calculé à partir des vitesse ultrasoniques. Les résultats obtenus sont du même ordre de grandeur que ceux mesurés antérieurement pour l'argon solide.

INTRODUCTION

It was not possible to find from the available literature any report on the elastic properties of crystalline CO_2. However, experimental knowledge of the elastic constants of this typical van der Waals crystal would be very important for the theory of its potential energy. In the present work we used a simple modified ultrasonic resonance method for the study of the elastic constants of solid carbon dioxide.

PREPARATION OF THE CARBON DIOXIDE CRYSTALS

The crystals to be investigated were prepared by liquefying first the pure CO_2 gas under 55 atmospheres at temperature below -10° C. and then by crystallizing the liquid CO_2 by means of liquid oxygen. In order to prepare larger transparent CO_2 crystals, it was necessary to perform the cooling of the liquid CO_2 slowly enough. It was possible to grow transparent and quite large CO_2 crystals (length 5-10 mm and thickness 5-7 mm).

PERFORMANCE OF MEASUREMENTS AND RESULTS

We constructed an ultrasonic apparatus for measurements of the elastic constants of solids (Figs. 1 and 2). The ultrasonic frequency was about 2 Mc during measurements. The carbon dioxide crystals were put between the quartz crystals for the measurements at the sublimation temperature of $-78,5^{\circ}$ C. The crystal holders and the quartz crystals were, however, at a little higher temperature than the CO_2 crystal. Thus, during the sublimation process the length of the CO_2 crystal decreased continously. At the same time, the quartz transducers were hold by a spring in good contact with the CO_2 crystal. Because the knotpoints of the standing waves correspond to the maximum value of the ultrasonic intensity, the ultrasonic wavelength in the CO_2 crystal can be calculated from the number of knotpoints corresponding to the sublimated part of the crystal. We used a photographic method for the reading of the output voltage. During the observations

Approved For Release 2009/05/01 : CIA-RDP80T00246A007500340002-0

Approved For Release 2009/05/01 : CIA-RDP80T00246A007500340002-0

the temperature of the crystal to be investigated remained constant since the energy coming off was exhausted in the sublimation.

3. - we have the relations of the classical theory which have been used as a basis of calculations.

It is well-known that the velocity of propagation of longitudinal waves can be expressed by the equation

$$v_l = (c^o_{11}/\varrho)^{\frac{1}{2}}, \qquad (1)$$

where c^o_{11} stands for the adiabatic elastic constant in the direction of a certain crystal axis, and ϱ for the density of the crystal. Correspondingly, for the transverse waves we have

$$v_t = (c^o_{44}/\varrho)^{\frac{1}{2}}. \qquad (2)$$

Here c^o_{44} is the adiabatic elastic constant in the direction perpendicular to that mentioned above. According to the classical theory, the quantities c^o_{11} and c^o_{44} are independent of each other. However, the third elastic constant c^o_{12} is connected with c^o_{11} and c^o_{44} by the relation

$$c^o_{12} = c^o_{11} - 2c^o_{44}. \qquad (3)$$

The adiabatic cubic compressibility of the cubic crystals is given by the formula

$$\chi = \frac{3}{c^o_{11} + 2c^o_{12}}. \qquad (4)$$

From the ultrasonic measurements we obtained for the velocities the following values:

$$\begin{cases} v_l = 1960 \text{ m/s, and} \\ v_t = 975 \text{ m/s.} \end{cases}$$

If we substitute for v_l, v_t, and ϱ in equations (1) and (2) the values 1960 m/s, 975 m/s, and 1.563 g/cm^3 at -78.5° C, [illegible] we get for the independent elastic constants the values

$$c^o_{11} = 6.03 \cdot 10^{10} \text{ dyne/cm}^2, \text{ and}$$
$$c^o_{44} = 1.48 \cdot 10^{10} \text{ dyne/cm}^2.$$

By taking into account the isotropy condition (3) we have

$$c^o_{12} = 3.06 \cdot 10^{10} \text{ dyne/cm}^2.$$

From equation (4) we find for the adiabatic cubic compressibility the value

$$\chi = 3.3 \cdot 10^{-11} \text{ cm}^2/\text{dyne}.$$

It also shows the results of this work. We found for the adiabatic cubic compossibility of solid carbon dioxide at the temperature of -78.5° C the value

$$\chi = 3.3 \cdot 10^{-11} \text{ cm}^2/\text{dyne}.$$

Approved For Release 2009/05/01 : CIA-RDP80T00246A007500340002-0

Approved For Release 2009/05/01 : CIA-RDP80T00246A007500340002-0

DISCUSSION

We have compiled in Table 1 some data measured previously by means of ultrasonic methods for the elastic constants of alkali halides [1] and solid argon [2]. Inspecting the values of the elastic constants appearing in Table 1, we find a considerable decrease of c'_{11} and c'_{44} in moving from typical ionic crystals towards van der Waals crystals. The weaker the cohesive forces, the smaller are the elastic constants.

TABLE 1 - VALUES OF THE ELESTIC CONSTANTS

Crystal	Measuring temperature and reference	$c'_{11} \cdot 10^{-11}$ dyne/cm^2	$c'_{44} \cdot 10^{-11}$ dyne/cm^2
LiF	Room temperature	9,74	5,54
NaCl	" "	4,85	1,26
KCl	" "	3,98	0,625
KBr	" "	3,45	0,508
KI	" "	2,69	0,362
CO_2	194,7°K This work	0,603	0,148
A	80°K	0,27	0,082

This work has been reported in more details in paper [3].

REFERENCES

1. Bergmann L. Der Ultraschall, S.Hirzel Verlag, Stuttgart, 6th ed., p.609, 1954.
2. Barker, J.R. and Dobbs, E.R. Phil. Mag. 46, 1069, 1955.
3. Hovi, V. and Mäntysalo, E., Ann. Acad. Sci. Fenn. A VI 24, 1959.

Copyright reserved

Approved For Release 2009/05/01 : CIA-RDP80T00246A007500340002-0

Approved For Release 2009/05/01 : CIA-RDP80T00246A007500340002-0

Electronic Specific Heat of α and β-Brasses at Low Temperatures

La chaleur spécifique électronique de laitons α et β aux basses températures

VÄINÖ HOVI and KAUKO MANSIKKA
Wihuri Physical Laboratory, University of Turku, Turku, Finland

SOMMAIRE. Les chaleurs spécifiques électroniques de laitons α et β ont été étudiées en fonction de la composition en appliquant la formule de Sommerfeld et en faisant une hypothèse concernant les électrons libres. Il est démontré que les valeurs théoriques sont en bon accord avec les données expérimentales de Rayne dans le cas du laiton α. Pourtant pour le laiton β une comparaison similaire ne peut être faite à cause du fait que des données expérimentales convenables semblent toujours manquer.

INTRODUCTION

According to Sommerfeld's theory [1] the electronic specific heat is given by the equation

$$C_e = 0.136\, V_m^{2/3}\, n_a^{1/3}\, T = \gamma T \text{ millijoules/mole.degree}, \tag{1}$$

where V_m is the molar volume in cm^3, n_a the number of free electrons per atom, T the absolute temperature, and γ is a constant. For the validity of equation (1), one has to assume that the electrons have a rest mass m_o, and that they move in a constant potential field. In the case of monovalent simple metals formula (1) gives a quite good approximation of theoretical electronic specific heat.

Although this model can be regarded as an over-simplified one, we may take into account, to some extent, the fact that the electrons are moving in a periodic potential field due to the lattice by giving them an "effective" mass m^+. Thus, instead of equation (1) we have

$$C_e = \frac{m^+}{m_o}\, \gamma T. \tag{2}$$

If we compare equation (2) with the experimental linear term of the specific heat, we obtain

$$m^+/m_o = \gamma_{exp}/\gamma_{theor}. \tag{3}$$

By means of equations (1), (2), and (3) it is immediately possible to carry out numerical calculations for the value of the electronic specific heats of different metals.

It is clear that one can improve the theory by including the effect of the periodic potential $V(r)$ due to the lattice in the wave equation

$$\nabla^2 \psi + (2m/\hbar^2)\,[E - V(r)]\,\psi = 0. \tag{4}$$

According to Bloch's well-known theorem the solutions of this equation are of the form

Approved For Release 2009/05/01 : CIA-RDP80T00246A007500340002-0

Approved For Release 2009/05/01 : CIA-RDP80T00246A007500340002-0

$$\psi = U_k(r)\, e^{ik \cdot r}, \qquad (5)$$

where $U_k(r)$ has the periodicity corresponding to $V(r)$. We see that the special case, $U_k(r)$ = constant, represents Sommerfeld's model.

Furthermore, in the exact mathematical treatment of the electronic energy of metals we should take into account the perturbation caused by electron-electron interactions. One might also expect that the degree of order in alloys would have some experimentally observable influence on the electronic specific heat at very low temperature. In fact, the recent measurements by Rayne [2] show that the electronic specific heats of an $AuCu_3$-alloy corresponding to the ordered and disordered states differ slightly from each other.

In this work, we have determined, by means of Sommerfeld's theory, values for the electronic specific heat of α and β-brasses as functions of compostion. In the case of α-brass we have compared our theoretical results with the experimental data of Rayne [3]. However, for β-brasses we have not found from the available literature experimental values of heat capacity measured at very low temperatures.

RESULTS AND DISCUSSION

By assuming that each copper atom will give one, and each zinc atom two, free electrons to the system of free electrons, the average number of free electrons per atom in a copper-zinc alloy can be represented by the formula

$$n_{av} = 1 + 10^{-2}\, p, \qquad (6)$$

where p stand for the atomic percentage of zinc. If our assumption is true, equation (6) is valid only for zinc concentrations of 0-50 atomic percentages. This is because, as we know from experimental investigations of the electronic specific heat of zinc, the number of free electrons per atom in pure zinc is not equal to two (cp [4]). At zinc concentrations larger than 50 %, we may suppose that only those of the zinc atoms corresponding to the same number of copper atoms will behave according to equation (6). The excess of zinc atoms would behave like the atoms in pure zinc as regards the number of free electrons per atom. On the basis of equations (1) and (6), it is highly probable that the values of γ will have a maximum at about equal concentration of components.

In order to calculate values for V_m in equation (1), we should know the average atomic weight of the alloy. This can be obtained from the formula

$$M_{av} = \frac{pZ_{Zn} + qZ_{Cu}}{100}, \qquad (7)$$

Here p and q are the atomic percentage of zinc and copper, respectively, and Z_{Zn} and Z_{Cu} are the corresponding atomic weights. Then

$$V_m = \frac{M_{av}}{\rho_{alloy}}, \qquad (8)$$

where ρ_{alloy} denotes the density in g/cm^3. For our calculations we used the measured values of density appearing in paper [5].

Approved For Release 2009/05/01 : CIA-RDP80T00246A007500340002-0

Approved For Release 2009/05/01 : CIA-RDP80T00246A007500340002-0

The theoretical data calculated for the quantity γ of α and β -brasses are given in Table 1. Table 2 shows the "effective" mass ratio of α-brass as function of composition. The theoretical and experimental values of γ are represented graphically in Fig. 1.

Table 1

Theoretical values of γ obtained for α and β at different compositions

p (%)	n_{av}	V_m (cm^3)	γ (millijoules/mole·degree^2)
0.00	1.000	7.065	0.501
1.49	1.015	7.167	0.508
3.15	1.031	7.198	0.513
5.98	1.060	7.243	0.519
7.80	1.078	7.271	0.523
8.18	1.082	7.277	0.524
9.76	1.098	7.304	0.529
15.07	1.151	7.378	0.540
19.97	1.200	7.446	0.551
24.50	1.245	7.507	0.561
29.19	1.292	7.573	0.571
32.98	1.330	7.618	0.579
40.00	1.400	7.707	0.593
42.00	1.420	7.732	0.598
44.00	1.440	7.759	0.602
46.00	1.460	7.784	0.606
48.00	1.480	7.808	0.610
50.00	1.500	7.832	0.614

Table 2

The "effective" mass ratio of α-brass as a function of composition

p (%)	γ_{exp} (millijoules/mole·degree^2)	γ_{theor} (millijoules/mole·degree^2)	m^+/m_0
0.00	0.687	0.501	1.37
1.49	0.708	0.508	1.39
3.15	0.725	0.513	1.41
5.98	0.737	0.519	1.42
7.80	0.740	0.523	1.41
8.18	0.741	0.524	1.41
9.76	0.742	0.529	1.40
15.07	0.744	0.540	1.38
19.97	0.746	0.551	1.36
24.50	0.748	0.561	1.33
29.19	0.749	0.571	1.31
32.98	0.751	0.579	1.30

In this investigation we have resmoothed the experimental values of γ measured by Rayne [3] for α-brass. Because the experimental point corresponding to the highest zinc concentration deviates considerably from the general course of the other points,

Approved For Release 2009/05/01 : CIA-RDP80T00246A007500340002-0

Approved For Release 2009/05/01 : CIA-RDP80T00246A007500340002-0

we have neglected it. In this way, our smoothed curve representing γ will have no maximum.

Inspecting the values appearing in Tables 1 and 2 we find that the theoretical values of γ for α-brass are systemically smaller than the experimental ones. However, the "effective" mass ratio seems to remain approximately constant. The mean value of the "effective" mass ratio is 1.37, which equals that of pure copper. If our basic assumption made in equation (6) is valid, it is clear that Sommerfeld's theory can give quite good approximations of the electronic specific heat of α-brass. Regarding β-brass, we cannot at present say anything about the agreement between theoretical and experimental data because of lack of suitable observed values. A consequence of our basic assumption is also that there is no discontinuity in the values of γ at zinc concentrations of 0-50 %. Moreover, the quantity γ^{-1} will show a maximum at about equal concentration of copper and zinc.

This work has been reported in more detail in [6].

REFERENCES

1. SOMMERFELD, A. Z.Physik 47, 1, 1928.

2. RAYNE, J.A. Phys.Rev. 108, 650, 1957.

3. RAYNE, J.A. Phys.Rev. 108, 22, 1957.

4. PARKINSON, D.H. Reports on Progress in Physics, Vol. XXI, p.249, 1958.

5. MELLOR, J.W. Inorganic and Theoretical Chemistry, Longmans, Green and Co., London, 1946, Vol. IV, p. 674.

6. HOVI, V. and MANSIKKA, K. Ann.Acad. Sci.Fenn. A VI, (25), 1959.

Copyright reserved

Approved For Release 2009/05/01 : CIA-RDP80T00246A007500340002-0

Approved For Release 2009/05/01 : CIA-RDP80T00246A007500340002-0

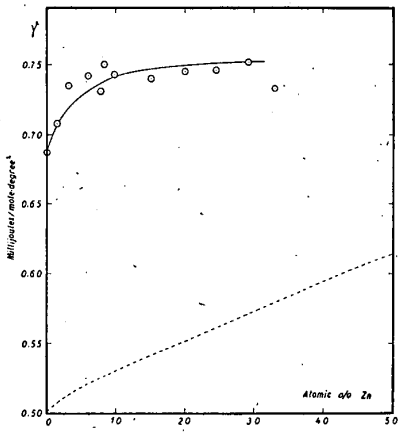

Fig. 1. Theoretical and experimental values of γ in the cases of α and β-brass with different compositions. The dashed curve represents theoretical, and the solid curve experimental, data. Experimental data are measured for α-brass.

Approved For Release 2009/05/01 : CIA-RDP80T00246A007500340002-0

Approved For Release 2009/05/01 : CIA-RDP80T00246A007500340002-0

The Specific Heat C_v of Liquid Helium Near the λ-point at Various Densities

La chaleur spécifique C_v de l'hélium liquide près du point λ pour de divers densités.

E. KOJO and O.V. LOUNASMAA
Wihuri Physical Laboratory, University of Turku, Turku, Finland

SOMMAIRE. La chaleur spécifique C_v de l'hélium liquide a été mesurée entre les lignes d'équilibre liquide et liquide-vapeur. Le résultat démontre que la hauteur du maximum λ diminue quand la densité augmente, quoique le maximum est toujours très prononcé le long de la ligne d'équilibre liquide-solide. Les mesures sont employées afin d'analyser la dépendance de la transformation λ de la pression et d'obtenir l'augmentation d'entropie associée à cette transformation. De même que les mesures directes de p et de Δp qui sont en cours, les résultats seront employés afin de calculer les fonctions thermodynamiques de l'hélium liquide dans les régions de température et de densité mentionnées ci-dessus.

INTRODUCTION

The specific heat C_v of liquid helium has been measured from 1.5 to 2.8°K at various densities between the liquid-vapour and liquid-solid equilibrium lines. The earlier specific heat measurements in this temperature region are almost entirely confined to the liquid under its saturation vapour pressure. Little is known about the exact behaviour of the λ-peak at higher densities. The only older experiments showing the λ-anomaly under pressure are those of Keesom and Keesom [1]; two runs with rather scattered points at about 19 and 25 atm. The measurements of Hercus and Wilks [2] do not extend to the λ-point. Furthermore, their specific heat values are somewhat doubtful as their results under the saturation vapour pressure are 10 % higher than the presently accepted values of Kramers, Wasscher, and Gorter [3] (see also Hill and Lounasmaa [4].

The thermodynamics of liquid helium is poorly known in the temperature region mentionned above. This is particularly true if one wishes to make exact calculations - the scale of the best existing entropy diagram is very small indeed. Of course, the C_v measurements alone are not sufficient for computing the thermodynamic functions of helium as they do not extend to temperatures low enough. However, when they are combined with the measurements of $(\partial p/\partial T)_v$, which are in progress, the whole thermodynamics can be calculated by starting from the known values of entropy and internal energy along the liquid-vapour equilibrium line. The present work thus extends the entropy diagram of Hill and Lounasmaa [5] from 3 to 1.5°K.

APPARATUS AND EXPERIMENTAL PROCEDURE

The calorimeter is shown in Fig. 1. It had two compartments, the sample space and the pot, the latter acting as a container for liquid helium used for cooling purposes and for thermometer

Approved For Release 2009/05/01 : CIA-RDP80T00246A007500340002-0

Approved For Release 2009/05/01 : CIA-RDP80T00246A007500340002-0

calibrations. The calorimeter was made of copper and the sample space packed with thin copper wire. Similarly, a number of copper rods were soldered to the bottom of the pot. These precautions ensured almost instant equilibrium even above the λ-point. The volume left for helium in the sample space was 19.53 cm^3. This was measured by filling the calorimeter at 4.0°K to a known pressure and by using the corresponding densities of Hill and Lounasmaa [5]. The vacuum case around the calorimeter was surrounded by liquid helium.

The calorimeter was first cooled by exchange gas in the vacuum space down to about 10°K. Exchange gas was then removed and the cooling completed by condensing liquid helium to the pot. Evaporation of this helium under reduced pressure cooled the calorimeter below the bath temperature, and by a combination of pumping and heating a suitable starting temperature (1.4 -1.5°K) could be achieved. Since exchange gas had only been used at temperatures where its removal was easy, a good vacuum was secured and the heat leaks were small. The method employed for the specific heat measurements was the usual one in non-adiabatic calorimetry. The heating periods were 30 seconds and measured with a calibrated and current-switch controlled stop-watch.

Before each experiment the carbon resistance thermometer was calibrated with the greatest possible care against the vapour pressure of liquid helium condensed to the calorimeter pot. The temperature scale used was T_{58}, proposed by Brickwedde [6].

RESULTS AND DISCUSSION

Experiments were made at the following densities: 0.1439, 0.1505, 0.1571, 0.1627, 0.1635, 0.1690, 0.1745, 0.1778, and 0.1834 g/cm^3. The lowest density corresponds to liquid under its saturation vapour pressure and the two highest ones follow partly the liquid-solid equilibrium line. The points from seven runs are plotted in Fig. 2 on a logarithmic scale in C_v. The gradual shift of the λ-peak to lower temperatures when density is increased is very evident. At the same time the height of the peak is diminishing although it is still pronounced at the liquid-solid equilibrium line. Below the λ-point high density corresponds to high specific heat, above the λ-point the situation is reversed.

When the specific heat data are plotted as a function of density at different temperatures the scatter from smooth curves is only about 1 %. The values corresponding to the liquid under its saturation vapour pressure join easily to these curves below 1.9°K, where the $C_p - C_v$ correction is small. This indicates good internal consistency of the data and suggests, together with a closer analysis of the experiments, an accuracy of about 2 % for the present results.

Some comparisons can be made with earlier measurements. Under the saturation vapour pressure our results agree well with those of Kramers, Wasscher, and Gorter at 1.6 and 2.0°K, but are about 4 % higher at 1.8°K. The discrepancy is within the experimental errors of both measurements. Above the λ-point very good agreement exists with the values of Hill and Lounasmaa [4]. Our results under pressure can be compared with the data of Hercus and Wilks from 1.5 to 1.8°K. It is observed that the latter are about 10 % higher in agreement with the similar

Approved For Release 2009/05/01 : CIA-RDP80T00246A007500340002-0

Approved For Release 2009/05/01 : CIA-RDP80T00246A007500340002-0

situation under the saturation vapour pressure. It might thus be possible, by suitably correcting the values of Hercus and Wilks, to use them together with the present measurements for extending the entropy diagram down to 1.2°K. At 2.8°K good agreement is found with the data of Hill and Lounasmaa [5].

The λ-transition in liquid helium is studied at present very extensively. An analysis of our results from this point of view has to be postponed until the $(\partial p/\partial T)_v$ experiments are completed. A full account of our work will be published in Annales Academiae Scientiarum Fennicae.

REFERENCES

1. KEESOM, W.H., and KEESOM, A.P. Physica, 2, 557, 1935.
2. HERCUS, G.R., and WILKS, J. Phil.Mag., 45, 1163, 1954.
3. KRAMERS, H.C., WASSCHER, J.D., and GORTER, C.J. Physica, 18, 329, 1952.
4. HILL, R.W., and LOUNASMAA, O.V. Phil. Mag., 2, 143, 1957.
5. HILL, R.W., and LOUNASMAA, O.V. Proc. 5th Intern. Conf. on Low Temp. Phys. and Chem., p. 48, 1958. A full account in: Lounasmaa, O.V., Thesis, Oxford, 1958.
6. BRICKWEDDE, F.G., Physica, 24, 128, 1958.

Copyright reserved

Approved For Release 2009/05/01 : CIA-RDP80T00246A007500340002-0

Approved For Release 2009/05/01 : CIA-RDP80T00246A007500340002-0

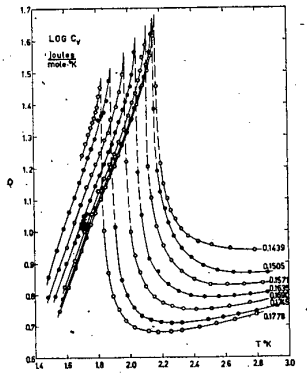

Fig. 1. The calorimeter. A = sample tube 0.3 mm I.D., B = vapour pressure tube, C = pumping tube, D = pot, E = sample space, F = carbon thermometer.

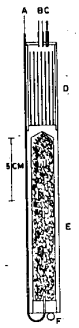

Fig. 2. Experimental C_v points. The density of sample corresponding to each run is given in the figure. For the run at 0.1778 g/cm^3 only the single phase region is shown. The results at 0.1439 g/cm^3 are uncorrected for the vapour present in the calorimeter.

Approved For Release 2009/05/01 : CIA-RDP80T00246A007500340002-0

Approved For Release 2009/05/01 : CIA-RDP80T00246A007500340002-0

Thermoelectric Cooling.

Evaluation du refroidissement thermoélectrique.

IOFFE, A.F., Academician,
The Institute of Semiconductors,
Academy of Sciences of the USSR,
Leningrad, USSR.

SOMMAIRE. On sait depuis plus de cent ans que suivant le sens du courant une couche limite entre deux conducteurs différents peut être refroidie ou chauffée. Cependant tant qu'on utilisait des métaux, l'abaissement de température ne dépassait pas 6°C. Les semi-conducteurs arrivent déjà à 70°C et iront sans doute encore plus loin.

La situation actuelle et les perspectives pour un avenir proche sont les suivantes: Les thermocouples dont on dispose actuellement peuvent consommer 1,5 à 2 w pour transformer chaque watt à 0°C si la différence de température entre la branche chaude et la branche froide d'un thermocouple atteint 40°C. A 30°C il ne faut que 1 à 1,2 watt. Le coût d'une batterie est proportionnel au rendement de celle-ci et peut être évalué à 30-50 roubles pour 100 w. Les dispositifs dont on dispose pour éliminer la chaleur du côté chaud de la batterie ont la plus grande importance. Il faut utiliser du courant continu. En considérant la situation dans son ensemble, on peut dire que le refroidissement thermoélectrique devient utilisable actuellement pour les petites installations, mais est trop onéreux pour les grandes. Par suite de leur amélioration, les thermoéléments rivaliseront avec de plus en plus de succès avec les installations à compression.

Thermoelectricity was discovered by Seebeck in 1821. In 1834 Peltier published his observations about phenomena accompanying a passage of electric current across a boundary between two conductors. It is an interesting historical fact that neither of them understood what they had discovered. Seebeck insisted that he had found magnetization and Peltier tried to disprove Ohms law. Four years later, in 1838, Academician Lenz demonstrated that a drop of water placed on the contact of two metals froze or melted depending upon the direction of the current going through. Thus, thermoelectric cooling was well established 120 years ago but was never used practically.

In 1909-1911 Altenkirch developed the theory of thermoelectric cooling and of generation of electric energy. He came to the conclusion that thermoelectric phenomena were too weak to be applied technically. He was right as metals were used and no other conductors had been known at that time. Semiconductors changed the situation.

Approved For Release 2009/05/01 : CIA-RDP80T00246A007500340002-0

Approved For Release 2009/05/01 : CIA-RDP80T00246A007500340002-0

The essential feature of any cooling device is the ratio η of the heat Q withdrawn at a low temperature T to the electric energy E spent. If the temperature of the system receiving heat is T_o then η may be expressed as:

$$\eta = \frac{Q}{E} = \frac{T}{T_o - T} \cdot \frac{\sqrt{1 + Z\frac{T + T_o}{2}} - \frac{T_o}{T}}{\sqrt{1 + Z\frac{T + T_o}{2}} + 1} \qquad (1)$$

The first multiplicand $\frac{T}{T_o - T}$ is the ideal thermodynamic ratio, while the second represents the irreversible process involved.

The only magnitude depending upon the properties of the materials is Z - an abbreviation for

$$Z = \alpha^2 \cdot \frac{\sigma}{\varkappa} \qquad (2)$$

where:

α = the thermoelectric power per 1°C

σ = the specific electric conductivity

$\varkappa$ = the specific thermal conductivity.

The higher the value of Z the higher the efficiency η. Therefore we define Z as the figure of merit of the material.

The highest temperature difference achieved by a thermocouple with a figure of merit Z is given by the formula

$$\Delta T_{max} = \frac{1}{2} Z T^2 \qquad (3)$$

For metals $Z < 2.10^{-4}$ and ΔT max about (5-7)°C, while semiconductor thermoelements have $Z > 2.10^{-3}$ and accordingly ΔT max rises to (70-100)°C.

Applying all our knowledge about the behaviour of semiconductors we now reach

$$Z \cong 3.3.10^{-3} \frac{1}{°C}.$$

It means that a thermoelement with $Z = 3.0.10^{-3}$ cools down from 300°K to 225°K by 75°C or from 110°C to 0°C by 110°C.

Approved For Release 2009/05/01 : CIA-RDP80T00246A007500340002-0

Approved For Release 2009/05/01 : CIA-RDP80T00246A007500340002-0

The cooling coefficient $\eta = \frac{Q}{E}$ becomes equal to 1.0 for a temperature difference of 30°C and to $\eta = 0.6$ for $T_o - T = 40°C$.

The formulae 1 and 3 are derived under a simplifying assumption of a uniform temperature gradient along the thermocouple; the actual temperature difference is a little smaller.

As a thermocouple consists of two different wings, the definition of Z must be changed

$$Z = \frac{(\alpha_1 + \alpha_2)^2}{\left(\sqrt{\rho_1 \varkappa_1} + \sqrt{\rho_2 \varkappa_2}\right)^2} \quad ; \qquad (2a)$$

where ρ_1 and ρ_2 denote the specific resistivity of the two materials.

The value of η could be improved by connecting two thermoelements in series. For instance η becomes $\eta = 0.7$ instead of 0.6 for $Z = 3.10^{-3}$ and $T_o - T = 40°C$.

The efficiency of a thermoelectric device is highly dependent on the temperature difference on the ends of the thermobattery. While the cold end has to draw the heat Q we have to take from the hot end both the heat Q and the electric energy E. It is most important to improve the conditions for the dissipation of heat at the hot end. If water of 15°C is available, the cooling coefficient of a refrigerator may reach a value of (1.5 - 2.0) while the use of air at a temperature of 25°C leads to η = (0.7 - 0.8).

The amount of materials M necessary for a thermoelectric battery is directly proportional to the square of the thickness L of the battery.

$$M = cL^2 \quad \ldots\ldots\ldots\ldots \qquad (4)$$

Thermoelements could be applied for heating purposes. For a thermocouple with $Z = 3.0 \cdot 10^{-3} \frac{1}{°C}$ we find

$$\eta = \frac{Q}{E} = 2.15 \text{ for } T - T_o = 30°C.$$

We have developed the following small scale apparatus with the aid of semiconductor thermoelements.

1. Several apparatuses destined to adjust the temperature on a microtom for biological experiments; on a microscope to observe an object between -30° and +60°C.

Approved For Release 2009/05/01 : CIA-RDP80T00246A007500340002-0

Approved For Release 2009/05/01 : CIA-RDP80T00246A007500340002-0

2. Thermostats for radio devices especially for quarz stabilizers.

3. Hygrometers for temperatures below 0°C.

4. Vessels for transport at low temperatures in an autocar.

5. Vacuum apparatus cooled to -50°C, especially a device to cool oil vapours in a vacuum gauge.

6. Refrigerators with water or air cooling.

The efficiency of devices for thermoelectric cooling is lower than achieved by compression refrigerating machines but is somewhat higher than for absorption installations. We must, however, remember that refrigerating compressors already have a long history while thermoelements are at the very dawn of their development. The figure of merit of our first thermoelements about 20 years ago did not exceed $0.5 \cdot 10^{-3}$; it grew steadily and increased by a factor of 7. We may expect a further favorable development.

The work on thermoelements is now going on in many laboratories in the USA, England, France, China, etc.

It seems to be too early to discuss large scale energy problems. Thermoelements are still unable to compete with compression machines. However, the simplicity and the cheapness of a thermoelectric battery represent a significant preference everywhere if the expenses for electric energy play a secondary role. Thermoelements represent the only possible solution for cases where small dimension installations are required.

In accordance with the rise of the figure of merit of thermocouples the boundary between the practical and the unpractical applications will certainly move towards semiconductor thermoelements.

- copyright reserved.

Approved For Release 2009/05/01 : CIA-RDP80T00246A007500340002-0

Approved For Release 2009/05/01 : CIA-RDP80T00246A007500340002-0

Page Denied

25X1

Approved For Release 2009/05/01 : CIA-RDP80T00246A007500340002-0

Approved For Release 2009/05/01 : CIA-RDP80T00246A007500340002-0

The Two-storied Cold Store with Direct NH_3 Evaporation

Les entrepôts frigorifiques à deux étages à détente directe d'ammoniac:

E. GRÖSCHNER
Forschungsinstitut für die Kühl- und Gefrierwirtschaft,
Magdeburg, Germany

SOMMAIRE. Les chambres frigorifiques en sous-sol sont destinées à des températures de 0° à 2° C. Celles du rez-de-chaussée servent à différentes utilisations entre 0° et –20° C. La protection coûteuse contre la congélation du sol est rendue rentable par l'utilisation de chambres frigorifiques au sous-sol. Le matériel fournit un refroisissement avec ou sous circulation d'air ou avec combination des deux systèmes. Au rez de chaussée deux tunnels de congélation d'une capacité de congélation de 15 tonnes chacun, augmentent les possibilités d'entreposage. Au lieu de saumure, il est simplement prévu une évaporation directe de NH_3 avec circulation par pompes du fluide frigorigène. Pour l'évaporation directe, il a été prévu:

2 compresseurs en V avec 165.000 kcal/h à t_0 –12° C.
(dont un functionnant en booster) à t_0 –28° C.
2 compresseurs en V de 65.000 kcal/h à t_0 –28° C.
2 compresseurs de 58.000 kcal/h chacun à –35° C. pour les tunnels de congélation.

Des tayaux ordinaires avec ventilateurs centrifuges servent de refroidisseurs d'air pour les principales chambres du sous-sol. Le rez-de-chaussée a été muni en outre systèmes de tuyaux muraux et plafonniers ordinaires. Les chambres annexes ont des refroidisseurs d'air muraux normaux et servent au dégivrage. A tous les refroidisseurs d'air il a été adjoint des conditionneurs fonctionnant à l'électricité. Des installations de conditionnement d'air ont été adaptées aux couloirs de service. Toute l'installation de commande électrique est automatique. De plus, il a été prévu un dispositif de pré-refroidissement pour les wagons de chemin de fer.

A two-storied cold store, consisting of basement and groundfloor, must be considered as more advantageous according to our economical conditions, when it is projected as a multi-purpose cold store. In the German Democratic Republic, such a cold store with a cooling surface of about 8000 m^2 is being erected just now; another will be begun shortly. The basement rooms will be operated at a temperature of ±0° C. The air temperature of the ground floor rooms can be set at either ±0° C. or –18° C. In the cold store being built, cooling is by 2 brine circuits. For the other, a direct NH_3 evaporation and a NH^3 circulation by means of NH^3 circulation pumps are provided. Both will be vastly automated.

In the scheme of the NH_3 circuit, the connection of the two NH_3 circuits are shown. The NH_3 circuits of the 2 tunnel freezers and of the ice-making equipment have not been drawn up. These have separate compressors and show no peculiarities.

The whole NH_3 and electric connection are subdivided into the following main groups: 1) NH_3 refrigerating compressors; 2) NH_3 liquid coolers, NH_3 circulation pumps and defrosting equipment; 3) NH_3 air cooler with direct evaporation.

NH_3 REFRIGERATING COMPRESSORS

For each of the 2 NH_3 circuits 2 compressors of the same type and size are provided. The compressors for evaporating at –28° C. work in two stages. Of

Approved For Release 2009/05/01 : CIA-RDP80T00246A007500340002-0

Approved For Release 2009/05/01 : CIA-RDP80T00246A007500340002-0

the 2 compressors for –10° C. evaporation it is possible to switch one either on one stage or on 2 stages. This compressor acts as a booster for the two NH_3 circuits. The change-over of the booster compressor takes place by hand. In normal operations, a pressure-operating control link (a) inserts or uncouples the first compressor of a NH_3 circuit. For this, it is possible to use a pressure control or a gauge with electric minimum and maximum contact.

An equal control link (b) additionally inserts the second compressor automatically only when, as a result of increased heat in the cold storage rooms, the NH_3 pressure rises above an adjustable desired value. The uncoupling takes place in reverse order. An electric locking with the control links of all the cold storage rooms of the NH_3 circuit concerned hinders a starting of the compressors, when all the control links (room thermostats) of the cold storage rooms are cut off.

At the insertion, the compressors are started pressure-relieved. This is done by electric motor stop-valves by means of time-limit connection.

In the NH_3 circuit for –28° C. evaporation there is still a signaller (1). The control links c and d belonging to it have the same function as the control links a and b of the circuit of –10° C. evaporation. When in spite of the additional insertion of the 2nd compressor, it is not possible to keep the NH_3 pressure on the level desired, the signaller uncouples an acoustical or optical signal. Such is the case, if, at this moment, the capacity of the 2 running compressors is not sufficient. Through this signal it is additionally possible to insert the booster compressor. Besides, in the 2 NH_3 circuits there are the necessary low-pressure safety switches, gauges, NH_3 check valves, oil-separators, condenser, and receiver. This receiver is furnished with inserted subcooling coils or additional NH_3 subcooler.

NH_3 LIQUID COOLERS, CIRCULATION PUMPS AND DEFROSTING EQUIPMENT

Each of the 2 NH_3 circuits has 2 NH_3 circulation pumps for the NH_3 transfer to the air coolers. Temperature, or pressure control links additionally insert or cut off the NH_3 circulation pumps electrically. The structure of the two-storied multi-purpose cold store with about 8000 m^2 of cooling surface is that of a flat cold store. An automatic NH_3 circuit practicable in cold stores having a superstructure, is not practicable in a one floor cold store because of the smaller statical differences of level. Details of the automtic control of the NH_3 circulation pumps, described as follows, accordingly are valid for the 2 NH_3 circuits.

The NH_3 circulation pump (G), the so-called fundamental pump, is switched on by a contactor. Its commanding-impulses for switching on or cutting off are given by the contactors of the air coolers by means of a control sliding-lead. Consequently all the switching appliances of the air coolers are to be furnished with an additional working contact. Going into operation, the cold storage room will switch on the primary pump (G) by a switching impulse from the control-lead mentioned above, if it has not already been started from a cold storage room already in operation. The fundamental pump (G) cuts off only when the last working cold storage room of this NH_3 circuits has reached its lower temperature limit and cuts off.

The additional NH_3 circulation pump (Z) switches on or cuts off depending on the capacity desired of the NH_3 circuit. The commanding-impulses necessary for this are given by a pressure control or a gauge with maximum, or minimum switching contact. These control appliances must be constructed in the form of pressure difference appliances. If the pressure difference between the NH_3 progressive movement and the NH_3 return-movement decreases, that is a sign that other NH_3 air coolers have switched on additionally. If this pressure difference decreases under a certain level, the additional NH_3 circulation pump (Z) switches on. By cutting out the air-coolers again and again the pressure difference between the NH_3 progressive liquid line and the NH_3 return line increases, and the maximum difference pressure will be reached and the additional NH_3 circulation pump will be switched off again.

Approved For Release 2009/05/01 : CIA-RDP80T00246A007500340002-0

Approved For Release 2009/05/01 : CIA-RDP80T00246A007500340002-0

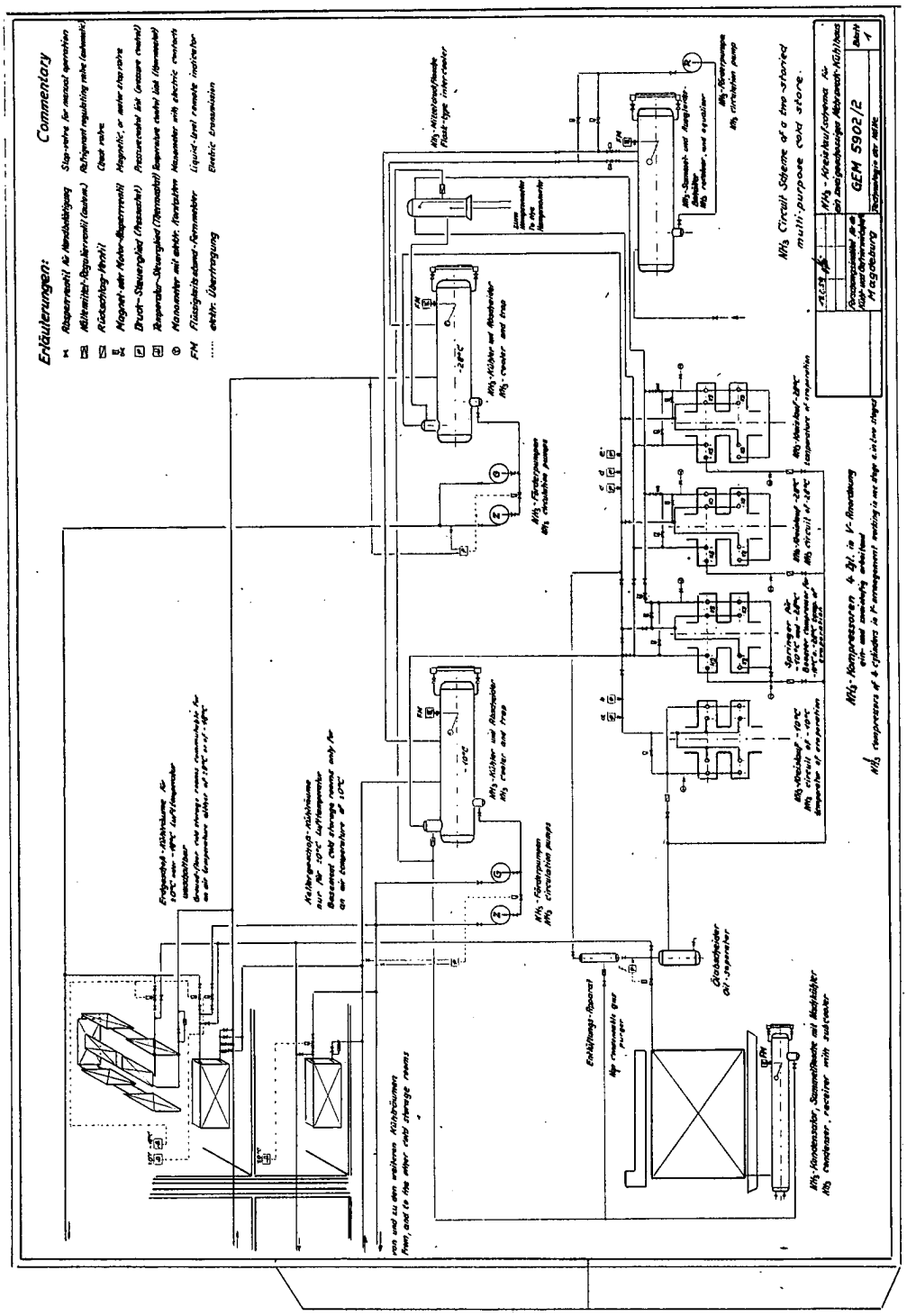

Fig. 1. NH_3 circuit scheme of a two-storied multi-purpose cold store.

Approved For Release 2009/05/01 : CIA-RDP80T00246A007500340002-0

Approved For Release 2009/05/01 : CIA-RDP80T00246A007500340002-0

In case of an extraordinarily high load (heating) of one or several cold storage rooms, it is possible that the ammonia being in the air coolers will wander off to the cold NH_3 liquid coolers. It is possible that an undesirable liquid level is reached and that is troublesome for normal operating. Therefore we have provided a NH_3 receiver and equalizer, to which the liquid NH_3 is drained off from the NH_3 liquid coolers by means of overflow lines.

A NH_3 return circulation pump (R) always enables the supply of the NH_3 lacking in the circuit at the beginning of the normal state. This return of NH_3 to that liquid cooler in which NH_3 is desired occurs by means of the overflow lines described above. For the change-over of the NH_3 return circulation pump to the corresponding overflow line (in this case "return transport line") there are 4 motor stop-valves or 2 three-way motor stop-valves. The return circulation pump and the change-over of the motor stop-valves are switched on by commanding impulses of the NH_3 liquid level indicators; they are at each NH_3 liquid cooler. As NH_3 liquid level indicators, may be used indicators with hydraulic-electro-inductive measuring and switching instruments or NH_3 liquid level indicators. These work by the application of the radioactive isotope Co 60.

The NH_3 air coolers are defrosted by means of the hot NH_3 vapors from the pressure sides of the compressors. Consequently, the condensation heat set free of the ammonia hot vapor is used to get the necessary melting heat for the frosted air coolers. As, according to the operating condition of the refrigerating equipment one or several compressors are running, it is necessary to regulate the volume of the NH_3 hot vapor. When only one compressor is running, it is necessary to lead nearly the whole volume of NH_3 vapor into the line for defrosting. When 4 compressors are running, this would cause an undesired increase of pressure. In order to lead just the quantity of hot vapor each time necessary into the line for defrosting and not to let the NH_3 pressure increase above the normal, we have provided a motor regulating-valve in the main pressure vapor line to the condenser. A pressure control or gauge with electric maximum and minimum switching contact (f) gives the regulating impulses for this motor valve. If the pressure increases, regulation ensues by opening and if the pressure decreases, by closing.

The NH_3 condensing by the defrosting process is again lead to the NH_3 circuit by means of a throttle-valve.

NH_3 AIR COOLER WITH DIRECT EVAPORATION

Each of the basement cold storage rooms contains a separate air cooler with low-pressure centrifugal fan. Some rooms in the basement are furnished with few wall air coolers, each with 2 propeller fans. Motor stop-valves couple the air coolers to the NH_3 progressive liquid movement of the circuit of –10° C. evaporation. The coupling impulses for this are given by the temperature control link being in the cold storage room (room thermostat). Outside of each cold storage room, there is an electric wall switch for that room. This appliance contains the necessary contactors and switching relays for the automatic switching-on of the fans and for the control of the motor stop-valves.

Besides the air coolers already described in the basement, the ground-floor cold rooms still additionally have ceiling, and wall coils for still air cooling at low temperatures. Whereas the air cooler of the ground-floor cold storage rooms may be coupled to the progressive movement of the circuits either of –10° C. or of –28° C. temperature of evaporation at choice, the ceiling, and wall coils are connected only with the NH_3 circuit of –28° C. Because each cold storage room may be connected with 2 temperature circuits at choice, 2 temperature control links with different switching-ranges are necessary for the automatic operation of these rooms. As the switching appliances are outside of the cold storage rooms, when a change in the desired room-temperature range and consequently the necessary control range of the corresponding motor stop-valve may be made easily by a hand-change-over. When the temperature control link for the air-temperature range of –18° C. is switched on it is possible additionally to switch on or to cut

Approved For Release 2009/05/01 : CIA-RDP80T00246A007500340002-0

Approved For Release 2009/05/01 : CIA-RDP80T00246A007500340002-0

off either the motor stop-valve for the air cooler or the motor stop-valve for the wall, and ceiling coils or both at the same time. For the fans and the NH_3 circulation pumps, the same is true as for the basement.

The additional switching-on of the NH_3 hot vapor line at the air cooler in order to begin the defrosting process is caused by a hand-stop-valve, because the air cooler must be under manual control during the defrosting process.

The fresh air cooler necessary for the cold store is connected with the NH_3 circuits, either the –10° C. or the –28° C., by a motor stop-valve. A push-button switch gives the control impulses from the engine-room.

Instead of remotely controlled motor stop-valves, magnetic stop valves may also be used. The motor, or magnetic stop valves in the cold NH_3 circuits are furnished with a heating-appliance to prevent freezing of the control organs of the stop-valves.

Behrndt bogtryk, Denmark

Copyright reserved

Approved For Release 2009/05/01 : CIA-RDP80T00246A007500340002-0

Approved For Release 2009/05/01 : CIA-RDP80T00246A007500340002-0

L'examen d'une machine frigorifique du type »Platen-Munters«

Study of a Refrigerating Machine of the Platen-Munters Type

Dr. Ing. STAFAN GAJCZAK
l'Institut pour la Technique Thermique de Haute Ecole Polytechnique de Varsovie, rue Nowowiejska 25, Varsovie, Pologne

SUMMARY. The study of thermodynamic cycle in diffusion refrigerating machines made by means of the enthalpy-concentration diagram of a NH_3–H_2O solution and of NH_3–H_2 gas-vapour mixtures shows that the low output of these machines is due theoretically to incomplete rectification and to the unsuitable rate of circulation of the gas-vapour mixture. To obtain a quantitative table of losses from these causes tests of an absorption and diffusion refrigerating machine designed for a 45 dm^3 refrigerator were made at the laboratory of the Thermal Technical Institute of the High Polytechnic School of Warsaw.

Measurement of heat, rectification, condensation, diffusion and absorption were given as a function of the average temperature of the evaporator, as desorption heat being taken as a parameter.

On the whole, 40 measurements at evaporating temporatures between – 28°–0° C. and of desorption heat between 52–103 kcal/hr were taken. Measurement of the circulation rate of the solution and of the gas-vapour mixture was made by replacing natural circuits by artificial ones.

Piston electromagnetic metering pumps were also used for measuring circulation.

The data provided by the study of the composition of the solution and of the gas-vapour mixture allowed the definition of mass transfer coefficient and of the average difference between partial absorption and diffusion pressures. Test of a refrigerating machine with column, fed with a rich solution, gave for an average diffusion temperature of –10° C., output coefficients 30 % higher than those obtained by the use of a rectifier alone. The measurements of the concentration of the gas-vapour mixture, of absorption heat and of temperature, gave the following results: only one part of the refrigeration condensed diffuses in the gas-vapour mixture in the evaporator, and the remainder flows uselessly in the absorber. This process occured in a refrigerating machine already at a diffusion temperature of about –5° C. and increased as temperature decreased.

La démonstration des processus qui ont lieu dans les machines frigorifiques à absorption et diffusion, par des diagrammes entalpi-concentration, de la solution H_2O–NH_3 et du mélange gazo-vaporique H_2–NH_3 permet de comprendre facilement les causes principales de la basse valeur du coefficient du rendement frigorifique de ces machines.

Les définitions des états, acceptées dans le schéma fonctionnel des machines frigorifiques d'un type plus ancien, démontré dans la Fig. 1, ont été répétées pendant la disposition des points relatifs du circuit sur les diagrammes i–ξ de la solution H_2O–NH_3, ainsi que du mélange H_2–NH_3 Fig. 2 et 3.

Comme causes principales de pertes de chaleur dans la partie absorbante, peuvent être mentionnées: – la rectification, l'échange de la chaleur des solution et les pertes à l'entourage.

La rectification des vapeurs d'après le schéma fonctionnel dans la Fig. 1, constitute un processus non-réversible à cause de l'emploi du déflegmateur seulement. Le rapprochement du processus de rectification t secondairement aussi de la désorption à la réversibilité peut être atteinte, en complétant le déflegmateur par une colonne de rectification, alimentée d'une riche solution.

Approved For Release 2009/05/01 : CIA-RDP80T00246A007500340002-0

Approved For Release 2009/05/01 : CIA-RDP80T00246A007500340002-0

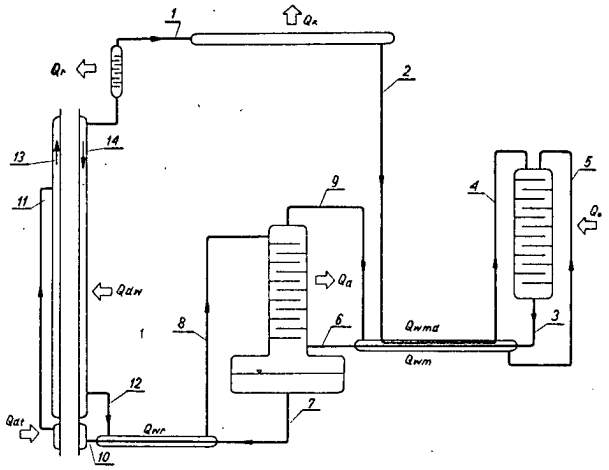

Fig. 1. Schéma fonctionnel d'une machine frigorifique à absorption et diffusion.

Le processús de l'échange de chaleur entre les solutions est non-réversible, à cause de la différence de capacité de chaleur des deux courants, et cela même, comme l'a prouvé Bosnjakovic, dans le cas d'une surface d'échange et d'une circulation réitérée des solutions, infiniment grandes.

Le rapprochement de ce processus à la réversibilité peut être atteint par l'égalisation des capacités de chaleur des deux courants, en divisant le riche dans une partie passant par l'échangeur de chaleur des solutions, et en employant le reste pour le refroidissement du déflegmateur.

La température de la désorption, comparativement assez élevée, fait que la quantité de chaleur rendue à la convection et au rayonnement du désorbeur et de l'échangeur de chaleur, constitute un facteur considérable dans le bilan de chaleur de la machine frigorifique.

Les pertes subies dans la partie d'absorption et diffusion sont causées pour la plupart par la réitération de la circulation des mélanges inappropriée et par la non-réversibilité du processus de l'echange de chaleur, entre les mélanges.

Le point q de la Fig. 3 correspondant à l'état du mélange pauvre, écoulant de l'absorbeur, est exprimé par:

– sa température t_{MU} dite égale à t_D à la température de NH_3 liquéfiée, sortant du condensateur, et

– la concentration ξ_{MU}, qui dépend de la pression partielle du NH_3 au-dessus du miroir de la solution pauvre, entrant dans l'absorbeur.

Point 5 répond à l'état du mélange pauvre refroidi à la température t_0 après l'échangeur de chaleur des mélanges, d'une surface infiniment grande.

Point 3 correspondant à l'état de la solution riche à la sortie de l'évaporateur est marqué par la température t_0 dans laquelle cesse l'arrivée de la chaleur au mélange. La concentration du mélange riche dépend de la réitération de la circulation des mélanges. En rapport avec cette grandeur, le point 3 se déplace le long de l'isotherme t_0 de l'étendue des vapeurs surchauffées, traverse la courbe de la rosée, pour dépasser ensuite l'isotherme t_0 de l'étendue du brouillard.

Dans le cas où la grandeur de la réitération du circuit est infinie, et étant donné que les points 3 = 5 sont identiques, la température du processus de diffusion dans l'appareil – qui, traditionellement quoique injustement est nommé "evaporateur" – est constante, la chaleur échangée entre les mélanges infiniment grande, la puissance frigorifique est définie et est égale à q_0. La diminution de la réitération du circuit jusqu'à position du point 3 sur la ligne de la rosée donne à une invariable puissance frigorifique q_0 une réduction de la chaleur échangée

Approved For Release 2009/05/01 : CIA-RDP80T00246A007500340002-0

Approved For Release 2009/05/01 : CIA-RDP80T00246A007500340002-0

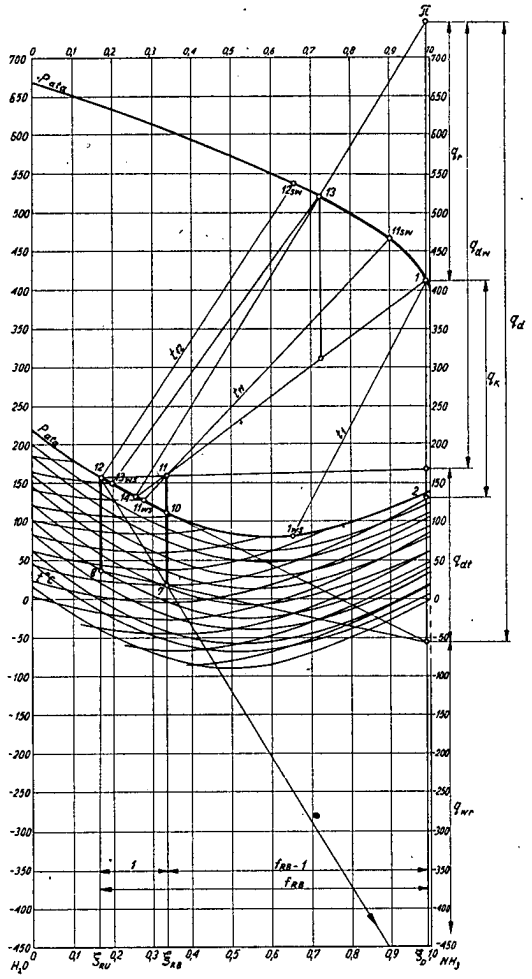

Fig. 2. Circuit de la machine frigorifique à absorption et diffusion en diagramme i – ξ (i kcal/kg; $\xi = \left(\frac{G_{NH_3}}{G_{NH_3} + G_{H_2O}}\right)$ de solution H_2O–NH_3).

entre les mélanges jusqué à q_{wm} qui est fixée sur le dessin Fig. 3. La température du mélangement adiabatique diminue pendant ce temps de t_0 jusqu'à une température correspondant à la température du point de croissement de la ligne du mélangement adiabatique 45, avec la courbe de la rosée, et ensuite augmente jusqu'au t_0 min.

Une diminution ultérieure de la réitération de la circulation a pour conséquence le dépérissement de la puissance frigorifique, de l'évaporateur sort un mélange "mouillé", la quantité de chaleur échangée entre les mélanges diminue, la température du mélangement adiabatique augmente. Au moment où le point 3 se trouve au point du croissement de l'isotherme t_0 de l'étendue du brouillard avec la ligne 45, le rendement est égal à zéro. En diminuant encore plus la réitération de la circulation, il faudrait pour obtenir la diffusion NH_3 reconduire la chaleur de l'évaporateur – ce cas a donc un sens purement théorique.

Il est évident, d'aprés ce qui a été dit ci-dessus, que pour éviter de fournir inutilement du NH_3 liquide à l'évaporateur, la réitération du circuit des mélanges

Approved For Release 2009/05/01 : CIA-RDP80T00246A007500340002-0

Approved For Release 2009/05/01 : CIA-RDP80T00246A007500340002-0

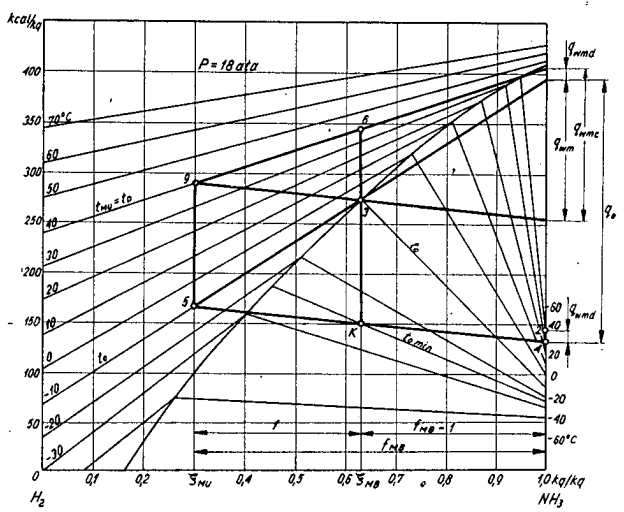

Fig. 3. Circuit de la machine frigorifique à absorption et diffusion en diagramme i – ξ (*i* kcal/kg; $\xi = \left(\frac{G_{NH_3}}{G_{NH_3} + G_{H_2O}}\right)$ du mélange H_2–NH_3).

doit être assez élevée. Cette exigence évoque la nécessité d'une augmentation de la surface de l'échangeur de la chaleur des mélanges.

La non-réversibilité du processus d'échange de la chaleur entre les mélanges, par l'analogie avec l'échangeur de chaleur des solutions, peut être diminuée par l'égalisation de la capacité de chaleur des deux courants des mélanges. Le superflu de la capacité de chaleur du courant du mélange riche, sert à refroidir les condensats du NH_3 avant de les introduire dans l'évaporateur. Sur le dessin Fig. 3, le point 6 répond à l'état du mélange riche, après le passage par l'appareil appelé par abréviation l'échangeur-refroideur. Dans ce même dessin sont désignées par diagramme, la chaleur q_{wm} rendue par le mélange pauvre, q_{wmd} rendue par les condensats, et q_{wmc} pris par le mélange riche.

Pour donner aux considérations, ci-aprés, au moins à un certain degré, l'image quantitative réelle, on a fait des études sur une machine frigorifique à absorption et diffusion, destinée à une armoire frigorifique, d'une capacité de 40 ltr.

Le programme des mesurages a embrassé: a) le bilan thermique complet, b) les températures et pressions entières, c) la tension de l'écoulement des solutions et mélanges, et d) la concentration des solutions et mélanges.

DEDUCTIONS RESULTANT DES MESURAGES DE LA MACHINE FRIGORIFIQUE EXAMINEE

A. La trace de la courbe du puissance frigorifique Q_0 démontre que la chute de cette grandeur est d'autant plus rapide, qu' augmente la chaleur de le désorption Q_d. Ce fait est causé par une diffusion incomplète du NH_3 dans le mélange H_2–NH_3, étant donné une haute valeur Q_d comme conséquence, dans ce cas d'une trop petite réitération de la circulation des mélanges.

B. Le bilan de chaleur de la machine frigorifique ne peut être fermé bien que le désorbeur et l'échangeur de chaleur des solutions aient été isolés additionellment.

Etant donné que l'isolation de ces appareils restait normale, les pertes de chaleur montaient jusqu'à 30 kcal/h.

C. De la relation de la grandeur de la chaleur de la déflegmation Q_r et de la condensation Q_k, il résulte que les vapeurs à leur sortie du désorbeur ont une

Approved For Release 2009/05/01 : CIA-RDP80T00246A007500340002-0

Approved For Release 2009/05/01 : CIA-RDP80T00246A007500340002-0

concentration proche de l'état de l'équilibre avec la solution pauvre, et le processus de déflegmation est proche du processus du contrecourant.

D. Le complèment du déflegmateur par une colonne de rectification a donné une augmentation du coefficient du rendement du refroidissement de 30%, étant donné que la température des parois du vaporateur est de –10° C.

E. Les moyennes logarythmiques des différences des pressions partielles, calculées à la base des mesurages de concentration des solutions et des mélanges, prennent dans l'évaporateur les grandeurs 1 ÷ 1,5 ata et dans l'absorbeur 0,9 ÷ 1,2 ata.

F. Puisque la quantité du NH_3 qui sort du condensateur est connue, on a fixé les moyennes du coefficient de l'échangement de la masse qui sont:

– pour l'évaporateur 40 kg/m²h ata,
– pour l'absorbeur 30 kg/m²h ata, – environ.

Les données susdites concernent les appareils d'une construction en planeaux et elles ont été obtenues à la température de diffusion du rang 0° C.

BIBLIOGRAPHIE

1. BÄCKSTRÖM, M. The Theory of the Evaporator Working with Diffusion. *Kylteknisk Tidskrift,* (30) 1954.

2. BOSNJAKOVIC, F. Irreversibilität im Temperaturwechsler einer Absorptionskältemaschine. *Kältetechnik,* (5), 1953.

3. CRESTA, A. A New Electrical Absorbtion Refrigerator. IXe Congrès International du Froid.

4. LICHARIEWA, N. Isledowanie absorpcjonno-diffuzionnogo cholodilnogo apparata. *Cholodilnaja Tiechnika,* (2), 1957.

5. NESSELMANN, K. Ein Übersichtsdiagram für das Verhalten von Absorptionsmaschinen mit druckausgleichen dem Gas. *Zeitschrift für die gesamte Kälte-Industrie,* (8), 1933.

6. NIEBERGALL, W. Der Vorgang der Austriebung und Lösungsförderung bei Absorptions-Kältemaschinen mit Thermosyphonpumpe. *Kältetechnik,* (8, 9), 1956.

7. SCHOLTZ, F. et FUCHS, R. Absorptionskühlschränke. Kältetechnik Nr 10/1952.

8. WATTS, F. et GULLARD, C. The Behaviour and Performance of a Triple-fluid Vapor Absorption Refrigerator. *Modern Refrigeration,* (704 et 705), 1956; (706), 1957.

Behrndt bogtryk, Denmark

Copyright reserved

Approved For Release 2009/05/01 : CIA-RDP80T00246A007500340002-0

Approved For Release 2009/05/01 : CIA-RDP80T00246A007500340002-0

Limits of Air Humidity Regulation in Storage Rooms of ca. 0° C.

Installation des batteries frigorifiques dans les chambres aux environs de 0° C. pour obtenir de meilleures conditions de l'air

LAJOS GÁNCS
I. Vérmezö – u. 4, Budapest, Hungary

SOMMAIRE. Avec les batteries frigorifiques classiques, l'hygrométrie nécessaire ne peut être atteinte que lorsque les denrées ont été refroidies, c-est-à-dire pendant l'entreposage. Si les besoins de froid sont plus élevés, l'hygrométrie s'abaisse au cours du refroidissement rendant ainsi inévitable une perte de poids. Les pertes de poids peuvent bien entendu être réduites si l'on injecte de la vapeur dans la chambre de conservation.

Il est inutile de faire circuler toute la quantité d'air et les ventilateurs doivent donc être construits de façon à permettre la circulation d'une quantité moins importante. Comme il est expliqué, si les denrées entreposées ont plus de valeur, l'utilisation de batteries frigorifiques de grandes dimensions peut se révéler économique.

As a rule, no regulation of air conditions is expected in storage rooms of 0° C., provided the temperature specified is maintained. Cooling is intermittent so that while it is being done, tÆhe humidity of the air is lower than while it is stopped.

Humidity and temperature can be regulated by:
1) changing the cooling surface; 2) changing the quantity of air driven through the cooling battery; 3) using by pass ducts; 4) drying the air by cooling, followed by reheating; and 5) injecting water.

Let us see to what degree humidity will change if the following are changed: a) cooling power; b) air quantity; and c) cooling surface.

Let us consider the following case in respect to the interrelation of the above factors:
Surface area of storage room: 300 m².
Weight of stored goods: 120 t., occupying 67% of the room space.
Monthly loss of weight: 1%.
Cooling surface of battery: 400 m².
Heat transfer coefficient: k = 8 kcal/m²h°C.
Minimum evaporation temperature in the evaporator: –10° C.
Average room temperature: +1° C.
Suction temperature in the compressor suction line: –10° C. (const.).

The calculations are made as follows:
1. Monthly loss of weight = 1%, in the case of 120 tons of goods = 1200 kg/month, corresponding to an hourly loss of 1200/30 · 24 = 1,67 kg/h
2. Heat quantity to be absorbed: Q = 8000 kcal/h
3. Directional tangent of change in air condition, in diagram i–x

$$\frac{di}{dx} = \frac{8000}{1{,}67} = 4800$$

4. If an air quantity of 24000 m³ – corresponding to a sixteenfold change – that is: 24000 · 1,29 = 31000 kg is being circulated, calories absorbed by an air-cooling system with the evaporation heat of the water vapour amounts to a cooling power demand of 8000 kcal/h
$8000 = 31000 \cdot \Delta\tau \cdot 0{,}24 + 1{,}67 \cdot 600$ whence $\Delta\tau \cdot 1°$ C.

Approved For Release 2009/05/01 : CIA-RDP80T00246A007500340002-0

Approved For Release 2009/05/01 : CIA-RDP80T00246A007500340002-0

5. Temperature difference by heat transfer

$$Q = k \cdot F \cdot \Delta t_k \qquad k = 8 \text{ kcal/}h, \text{ m}^2, \text{C}^0$$
$$F = 400 \text{ m}^2$$

$$\Delta t_k = \frac{8000}{8 \cdot 400} = 2{,}5^0\text{C}$$

6. Temperature of the wall is – for the sake of simplicity – calculated by taking the arithmetic mean value of the temperature change. Average air temperature:

$$t_k = 1^0\text{C}$$
$$t_{vall} = +1 - 2{,}5 = -1{,}5^0\text{C}$$

Relative humidity according to diagram i–x (*see* Fig. 1) $\varphi = 0{,}85$.

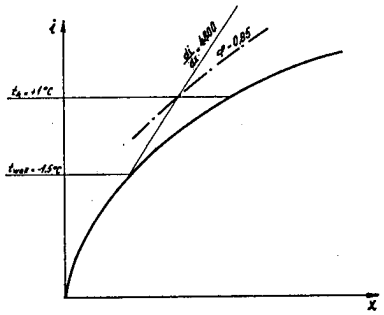

Fig. 1. Relative humidity in a storage room at 0° C.

In this way values of φ have been calculated for different cooling powers and air quantities (Fig. 2).

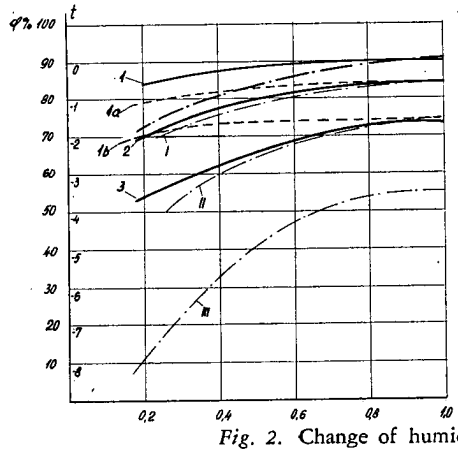

1 Cooling power 5000 kcal/h
2 – – 8000 kcal/h
3 – – 12000 kcal/h
1a – – 5000 kcal/h
1b – – 5000 kcal/h
– – 100 m²
I Temperature of battery in case 1
II Temperature of battery in case 2
III Temperature of battery in case 3
Battery surface 400 m²
– – 400 m²
– – 400 m²
– – 200 m²
– – 100 m²

Fig. 2. Change of humidity during storage.

The three unbroken curves correspond to cooling powers of 5000, 8000 and 12000 kcal/h respectively, desirable when goods are stored at very different outside temperatures.

Conditions to be expected when goods are being cooled will be dealt with separ-

Approved For Release 2009/05/01 : CIA-RDP80T00246A007500340002-0

Approved For Release 2009/05/01 : CIA-RDP80T00246A007500340002-0

ately, as well as the case where outside temperature is lower than that of the storage room, i. e. where the rooms must be heated in order to avoid freezing.

Curve 1 refers to a cooling power of 5000 kcal/h.

If a total of 24000 m³/h air is being circulated, an air humidity of 90% can be reached. By reducing the air quantity, this value is also reduced slightly. If air quantity is 0,2 times the original, relative air humidity of 84% can still be achieved.

In case lower air humidity is wanted, heating of the interior is necessary. However, this would be uneconomical, as cooling power demand is greater. It is more economical to reduce the heating surface and reset the battery surface temperature to a lower value. Curve 1a shows the relation between air quantity and relative humidity when an hourly 5000 kcal heating power is produced by half the cooling surface. In this case, relative air humidity of max. 84% and that of 79% can be achieved, provided air quantity is reduced to 0,2 fold of the previous.

According to curves 1 and 1a respectively, cooling batteries should be connected so that they may be used for a reduced surface as well, considering a slight effect of a cold outside temperature.

By curve 1b (¼ of original surface) relative humidity is shown as a function of air quantity. As shown: reduction of air quantity scarcely reduces the value of relative humidity i. e. smaller air quantity should be used in order to reduce the fan's power demand.

Reduction of power manifests itself in a smaller amount of current consumption, consequently its heat equivalent, therefore cooling power is also reduced.

Air quantity can, of course, be reduced only to a limit securing uniform airing of the goods.

Curves 2 and 3 illustrate the dependance of cooling power of 8000 kcal/h and 12000 kcal/h respectively on the relative air humidity wanted. As is shown, as cooling power increases, relative air humidity is reduced. The less the air quantity the greater the degree of reduction.

As a rule the yearly allround cooling power is scarcely more than 8000 kcal/h, i. e. an air humidity of 80%, satisfactory for most goods can still be achieved. Air quantity can be reduced to about 50% of the original.

The above relates more strictly to curve 1, i. e. if goods are stored without new ones added, circulation of the total air quantity is superfluous.

If less air is forced through the room, relative air humidity is essentially reduced.

In case of 12000 kcal/h, shown by curve 3, air will become harmfully dry and loss of weight will also become greater.

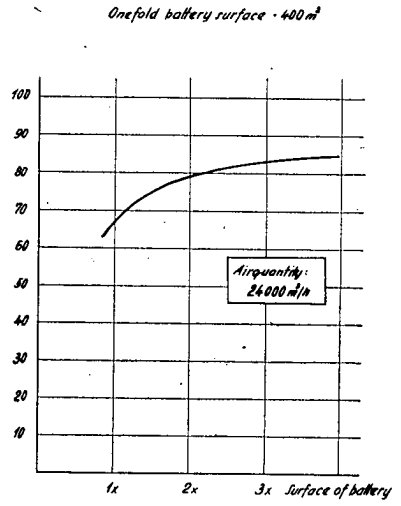

Fig. 3. Change of humidity during cooling.

Approved For Release 2009/05/01 : CIA-RDP80T00246A007500340002-0

Approved For Release 2009/05/01 : CIA-RDP80T00246A007500340002-0

No matter what the cooling power, reduction of air quantity will cause a reduction of temperature of the cooling batteries.

The broken lines I, II and III illustrate the change of temperature of the cooling batteries, as a function of air quantity. The temperature falls more if the cooling power is larger.

The curves of Fig. 2 refer to cooling powers needed to maintain the temperature of goods already cooled.

In Fig. 3, conditions which arise when goods are being cooled are shown. In this case the maximal cooling power is wanted; it was calculated to be:
$Q_{max} = F.k.\Delta t_{max} = 400 \cdot 8 \cdot 9 \cong$ kcal/h.

As already shown, reduction of cooling surface effects air humidity rather unfavourably, if large cooling powers are needed. A cooling surface less than 400 m² had not been dealt with. A circulated air quantity of 24000 m³/h was chosen in all cases.

According to the diagram, while goods are being cooled, – battery surface onefold –, a relative air humidity of 66% can be achieved. With a twofold surface, relative humidity of 79% is secured. From this point onward the increase is slowed down, so with a threefold surface, relative humidity will be 83%, with a fourfold one: 85%.

As revealed by the curve, it would prove useful to investigate the advantages of a twofold cooling surface when loss of weight of goods must be met with a larger battery, and growing air resistance with a larger ventilation power.

Calculations have not been made since they are complicated, and the possible saving in the value of goods depends on shorts of goods, wrapping etc.

We have been dealing with cases where cooling was wanted because of outside temperature. There are periods however when outside temperature is equal to the inside one, and also such, that not cooling, but heating, is wanted, because the colder outside air is streaming into the storehouse.

To stop cooling and let the fans alone do the airing, will not do, because of the high relative humidity. In cases like that heating is wanted to secure cooling there by reducing relative air humidity.

Thus for instance, if humidity as indicated by curve 1 of Fig. 2 is wanted, corresponding heating and cooling must be done. Heating involves the ventilation work and the heat equivalent of the motor loss, possibly the heat produced by the goods as well.

In reality this is not exactly as described, because a monthly loss of weight of 1% had been taken, which is not a constant value, not even during storage, nor had the fact been considered that loss of weight is dependent on infiltration of heat.

If heat is oozing out of the storage room, more heating must be done than in case of temperature balance, however cooling is also wanted at the same time, in order to maintain the desired relative air humidity.

In the above cases we assumed that the calculated temperature of the cooling surfaces is maintained. If the cooling surface is given, a certain cooling power is characterized by a certain temperature. The larger the cooling power, the lower the temperature. Curves drawn in broken lines indicate wall-temperature of the cooling batteries or more exactly: average temperature of outside layer of hoar upon the walls.

Suction pressure of the cooling compressor cannot maintain a certain wall temperature, if several batteries are connected to a single compressor. In order to reach a certain wall temperature, suction valves of individual batteries must be correspondingly choked.

Behrndt bogtryk, Denmark

Copyright reserved

Approved For Release 2009/05/01 : CIA-RDP80T00246A007500340002-0

Approved For Release 2009/05/01 : CIA-RDP80T00246A007500340002-0

The Investigation of a Lithium Bromide Absorption Refrigerating and Heat-pump Machine

Recherches sur la machine frigorifique à absorption à bromure de lithium et la pompe à chaleur.

L. M. ROSENFELD and M. S. KARNAUKH
The Leningrad Technological Institute of the Refrigerating Industry, Leningrad, U.S.S.R.

SOMMAIRE. On utilise depuis peu la solution aqueuse de bromure de lithium comme substance frigorigène dans les machines frigorifiques à absorption. L'objet des travaux étudiés dans ce rapport est de montrer que la chaleur résiduaire (par exemple, sous forme d'eau résiduaire industrielle chaude à une température de 60° à 75° C.) pouvait être utilisée par une machine à absorption à bromure de lithium tout le long de l'année, en été pour le refroidissement et en hiver pour le chauffage.

Un système mis au point par les auteurs est utilisé comme machine à absorption ordinaire en été, tandis que sa marche est inversée en hiver. La température de la chaleur résiduaire est élevée dans la machine inversée en raison de la chaleur de l'eau résiduaire et de la basse température hivernale. Ces facteurs permettent d'utiliser la machine à absorption pour le chauffage, comme transformateur élévateur de chaleur.

Le rapport étudie l'influence de la recirculation de la solution de bromure de lithium sur le rendement de la machine à absorption et indique la relation entre les caractéristiques des calculs de chaleur à l'aide d'un diagramme concentration-enthalpie établi par les auteurs, en tenant compte de l'influence de la recirculation indiquée ci-dessus.

On donne la description d'une machine expérimentale essayée au laboratoire de machines frigorifiques de l'Institut Technologique de l'Industrie Frigorifique de Léningrad, ainsi que le diagramme de cette machine. On indique les résultats de l'essai de la machine fonctionnant suivant le cycle frigorifique et le cycle de la pompe à chaleur – les valeurs du facteur de rendement, le coefficient de transformation de chaleur, les coefficients de transmission de chaleur de l'appareil, la vitesse de circulation et la recirculation de la solution à travers l'absorbeur. Ces données ont été obtenues expérimentalement pour diverses températures.

INTRODUCTION

In many large enterprises a considerable amount of waste water at 60 to 70° C. is available throughout the year. At the same time fuel and electric power are spent in these enterprises in summer to obtain cold water for technological needs or air conditioning, and in winter for heating purposes.

The utilization of the heat of waste water for cooling purposes in summer and heating in the winter time presents certain interests as it allows a considerable economy in fuel.

The authors suggest using a lithium bromide absorption machine which, utilizing the heat of waste water, could be operated as a refrigerating machine in summer and as a heat pump in winter [1].

The results of an experimental investigation of such a system are discussed in the paper.

OPERATING PRINCIPLE

The system operates in summer as an ordinary absorption refrigerating machine [2]. The waste hot water is supplied in this case into the generator where

Approved For Release 2009/05/01 : CIA-RDP80T00246A007500340002-0

Approved For Release 2009/05/01 : CIA-RDP80T00246A007500340002-0

its heat is used for evaporating the water out of the lithium bromide solution. The cooling water (river water or water from a cooling tower) is run successively into the absorber and condenser of the refrigerating machine to remove the heat of absorption and condensation. The evaporator provides cooled water which may be supplied to air conditioners or used for technological purposes at the enterprise.

In winter the absorption machine is operated on the reversed cycle, i. e. it is used as a step-up heat transformer in which the temperature level of the heat being utilized is raised on account of the heat of the waste water and the low ambient temperature during the cold season [3]. The cooling water (river water or recirculated +1 to +5° C. water) is supplied into the condenser for removing the heat of condensation. The waste water is passed into the generator and the evaporator in parallel or in series.

At a relatively high pressure of the water vapour formed in the evaporator the temperature level of the absorption heat increases likewise. The water, serving to remove the heat of absorption, is used for heating purposes.

The processes taking place in the various apparatus of the lithium bromide absorption machine operated on the summer or winter cycles are analogous. No changes are required, therefore, in the design of the apparatus, when shifting from one cycle to another (Fig. 1).

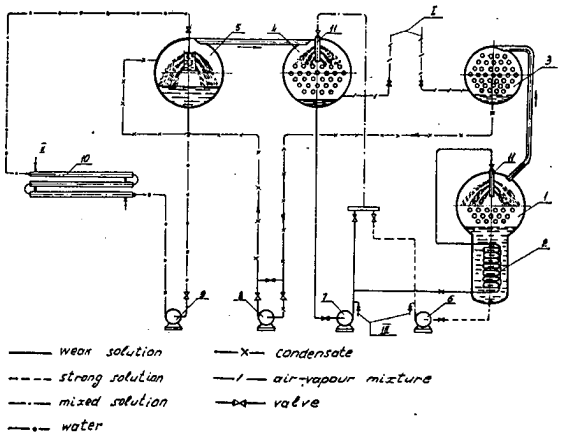

Fig. 1. Diagram of experimental lithium bromide absorption machine: 1 – generator; 2 – solution heat-exchanger; 3 – condenser; 4 – absorber; 5 – evaporator; 6 – strong solution pump; 7 – weak solution pump; 8 – condensation water pump; 9 – water pump; 10 – water heat-exchanger; 11 – nozzle.

A higher pressure is maintained in the generator and in the condenser than in the absorber and the evaporator when the machine is operated on the refrigerating cycle. However when the machine is operated as a heat-pump a higher pressure is maintained in the absorber and in the evaporator than in the generator and the condenser. This is why forced feeding of the condensation water from the condenser into the evaporator is required in the heat pump, while in the refrigerating machine the flow of the condensation water from the condenser into the evaporator through a hydraulic seal is caused by the difference of pressures in these apparatus. A pump is provided for the forced supply of the condensation water. When the system is operated as a refrigeration machine the condensation water is drained through a by-pass missing the pump.

The absolute value of the difference between the high and low pressure in a lithium bromide machine is small. It amounts to 30–40 mm Hg in the refrigerating

Approved For Release 2009/05/01 : CIA-RDP80T00246A007500340002-0

Approved For Release 2009/05/01 : CIA-RDP80T00246A007500340002-0

machine, and to 100–150 mm Hg in the heat pump. To provide a fine atomization of the solution in spray type apparatus two solution pumps are installed which ensure the operation on the refrigerating and the heat pump cycles.

EXPERIMENTAL MACHINE

An experimental lithium bromide absorption refrigerating machine, operating on the refrigerating and heat pump cycles, has been tested in the Refrigerating Machine Laboratory of the Leningrad Technological Institute of the Refrigerating Industry.

The generator (1) of the experimental machine is of the horizontal shell-and-tube type with a 12 m^2 heat transfer surface. The generator can operate either flooded or as spray type apparatus. The condenser (3) is also of the shell-and-tube type with a 15 m^2 heat transfer surface. The horizontal shell-and-tube absorber (4), having a 13.9 m^2 heat transfer surface, is of the spray type. The coil type heat-exchanger (2) with a 4.5 m^2 surface, is an integral part of the generator. The evaporator (5) is a hollow drum with a water spraying device inside. All the apparatus of the experimental machine are mounted separately so as to provide the necessary conditions for carrying out complete tests of the machine.

RESULTS OF INVESTIGATIONS

a) Refrigerating machine. Fig. 2 illustrates the relations of the temperature of the cooled water and the refrigerating capacity of the machine. The curves were drawn on the basis of the data obtained by testing the experimental machine. Line A corresponds to a 70° C. heating water temperature, and line B relates to 60° C. heating water. Consumption of the 22° C. cooling water is, in both cases,

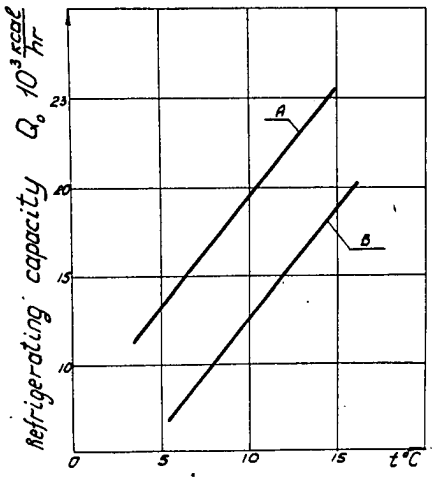

Fig. 2. Dependence of cooled water temperature upon refrigerating capacity: A – 70° C. heating water temperature; B – 60° C. heating water temperature.

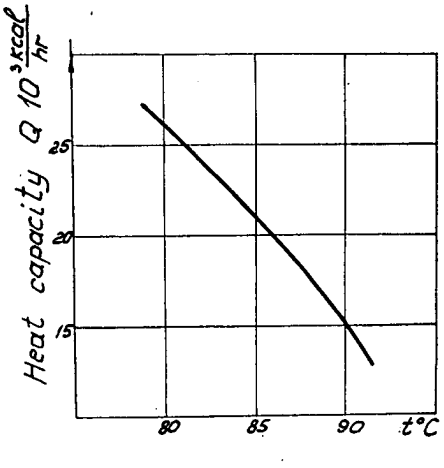

Fig. 3. Dependence of hot water temperature on the heat capacity of the machine.

7.0 m^3/hr, that of the heating water being 7.5 m^3/hr. The results of one test are given in Table 1.

The rate of absorption of the lithium bromide water solution is lower than in

Approved For Release 2009/05/01 : CIA-RDP80T00246A007500340002-0

Approved For Release 2009/05/01 : CIA-RDP80T00246A007500340002-0

TABLE 1. RESULTS OF TESTING A LITHIUM BROMIDE REFRIGERATING AND HEAT PUMP MACHINE

Nos	Value being measured	Refrigerating machine	Heat pump
1	Temperature of heating water, °C.	70	60
2	Temperature of cooling water, ° C.	22	1.4
3	Temperature of cooled water, ° C.	10.6	–
4	Temperature of hot water, ° C.	-	90
5	Concentration of strong solution, %	55.5	61.5
6	Concentration of weak solution, %	51.0	57.5
7	Rate of circulation, kg/kg	12.4	15.4
8	Recirculation ratio, kg/kg	60	40
9	Consumption of heating water, m^3/hr	7.4	12.0
10	Consumption of cooling water, m^3/hr	7.15	5.1
11	Refrigerating capacity, kcal/hr	20000	–
12	Thermal capacity, kcal/hr	–	15000
13	Coefficient of performance factor	0.7	–
14	Coefficient of transformation	–	0.38

the case of aqua ammonia. An efficient means of intensifying the absorption process is the recirculation of the weak solution through the absorber, whereby there is a considerable increase of the time the solution is in contact with the water vapour coming from the evaporator. The required recirculation ratio (the relation of the rate of flow of the recirculated solution to that of water vapour passing the condenser and evaporator) depends upon the overall dimensions of the apparatus, the capacity of the machine and the design of the spraying device. In the tested machine this value amounted to 50–70 kg/kg.

By the recirculation the highest temperature of the solution in the absorber is lowered. The state of the mixed solution is determined by means of a chart [4] by the intersection of the straight line connecting the states of the weak solution ξ_w and of the strong one ξ_s before mixing with the line of concentration of the mixture ξ_m. The latter value is derived from the material balance:

$$\xi_m = \frac{(f-1)\xi_s + \alpha\xi_w}{f+\alpha-1}$$

where f and α are the rates of the circulation and recirculation of the solution.

The experimental data indicate that the concentration of the solution is less than its theoretical value by 1.5 to 2 % in the absorber and by 1 % in the generator.

The static head of the liquid has considerable influence upon the evaporation process in the generator due to the small absolute value of the vapour pressure. This is the reason for the evaporation of the refrigerant out of the solution being the most complete in spray type generators.

b) Heat pump. The dependence of the hot water temperature obtained in the heat pump upon the thermal capacity is given in Fig. 3. The relation is based on the experimental data obtained in the case of the generator as well as the evaporator being heated by means of 60° C. water, while the condenser is supplied with 2° cooling water. The consumption of heating water is 12 m^3/hr, that of cooling water being 5 m^3/hr. The results of one test are given in Table 1.

Due to the fact that water is passed through the absorber without recirculation, it is possible to obtain in the experimental machine water having a temperature up to 100° C. Water, having a temperature up to 110° C., may be obtained in a reversed absorption machine with a closed system of water circulation through

Approved For Release 2009/05/01 : CIA-RDP80T00246A007500340002-0

Approved For Release 2009/05/01 : CIA-RDP80T00246A007500340002-0

the absorber, and 70° C. water for heating the generator and the evaporator. A drop of the highest temperature of the solution in the absorber, due to recirculation of the solution, is highly undesirable in a heat pump as it impairs the operation data of the machine. A 30–50 kg/kg ratio of recirculation proves to be sufficient in such a case. The difference of concentration between a strong and weak solution did not exceed 5.5–6 % in the tests cited.

CONCLUSION

The investigations have determined the technical characteristics of a lithium bromide absorption machine for cooling and heating purposes with an all-year utilization of the heat of waste water having temperatures ranging from 60° to 70° C. The expediency of using the suggested system is to be determined in each particular case on the basis of technical and economical analysis.

REFERENCES

1. ROSENFELD, L. M. and KARNAUKH, M. S. *Kholodilnaya Tekhnika,* (5), 1958.
2. PLANK, R. Kältetechnik, (10), 1956.
3. ROSENFELD, L. M. *Papers of USSR Academy of Sciences.* **82,** (3), 1952.
4. ROSENFELD, L. M. and KARNAUKH, M. S. *Kholodilnaya Tekhnika,* (1), 1958.

Behrndt bogtryk, Danmark

Copyright reserved

Approved For Release 2009/05/01 : CIA-RDP80T00246A007500340002-0

Approved For Release 2009/05/01 : CIA-RDP80T00246A007500340002-0

Sur l'étude de l'influence de la mobilité des porteurs libres du courant et de leur concentration au rendement de la jonction Peltier

Investigation into the Effect of the Mobility of Free Carriers on the Efficiency of Peltier Junction

L. STOURAC, Ingénieur, C. Sc.
Institut de Physique appliquée de l'Académie des Sciences de Tchécoslovaquie, Prague, Tchécoslovaquie.

SUMMARY. The variation of efficiency of direct conversion of electric power in Peltier junctions with the concentration and the mobility of free charge-carriers is discussed. Some welldefined semi-conducting compounds of N and P junction were investigated in the range 80–400° K. The properties and characteristics obtained are discussed. The possible use of these materials for the construction of Peltier junctions suitable for refrigeration is studied.

INTRODUCTION

Ces dernières années, de nouvelles substances, à base de composés semi-conducteurs d'éléments lourds, en particulier de tellurures et de séléniures de plomb, de bismuth et d'antimoine ou encore de leurs solutions solides [1–11] ont été étudiées et mises au point en vue de l'exploitation de l'effet Peltier dans le domaine des techniques du froid.

Notre Institut s'est également occupé, dans la période de 1954 à 1958 [12–16] de l'étude de ces composés semi-conducteurs. Grâce à ces recherches, il a été possible d'obtenir sur les systèmes Bi-Te-Se, employés comme substances de type n et sur les systèmes Bi-Te-Sb de type p, les paramètres suivants:

	Type	δ [Ω^{-1} cm^{-1}]	α [μV/°C]	$\alpha^2\delta$ [VA/°C^{2}cm]	$\varkappa$ [W/°C cm]	z [1/°C]
Bi-Te-Se	n	$(1{,}0—1{,}4)\cdot 10^3$	$(1{,}4—1{,}6)\cdot 10^2$	$(2{,}2—3{,}0)\cdot 10^{-5}$	$1{,}25\cdot 10^{-2}$	$(1{,}8—2{,}25)\cdot 10^{-3}$
Bi-Te-Sb	p	$(1{,}6—2{,}5)\cdot 10^3$	$(1{,}4—1{,}8)\cdot 10^2$	$(4{,}3—6{,}0)\cdot 10^{-5}$	$1{,}70\cdot 10^{-2}$	$(2{,}6—3{,}00)\cdot 10^{-3}$

En partant, au cours de l'étude de leurs paramètres, de la constante

$$Z = \frac{\alpha^2\sigma}{\varkappa} \tag{1}$$

où α est la force thermoélectrique, σ la conductibilité électrique, $\varkappa$ la conductibilité thermique, il est possible, comme le montre relation

$$\Delta T = \tfrac{1}{2} Z T^2 \tag{2}$$

d'obtenir des différences de température de l'ordre de $\Delta T = 70°$ C., pour une valeur de $z = 2{,}5.10^{-3}$ 1/°C. et pour la température de l'extrémité froide de la jonction $T = 230°$ K.

En liaison avec l'exploitation pratique de ces propriétés, la question de la stabilité des substances préparées, qui forment des systèmes relativement compliqués, est du plus haut intérêt. Les systèmes Bi-Te-Sb polycristallins (de type p) sont relativement stables; par contre les systèmes Bi-Te-Se (de type n) montrent les processus de vieillissement.

Approved For Release 2009/05/01 : CIA-RDP80T00246A007500340002-0

Approved For Release 2009/05/01 : CIA-RDP80T00246A007500340002-0

OBSERVATIONS TIREES DES EXPERIENCES EFFECTUEES SUR LES SUBSTANCES DE TYPE N

Des changements de propriétés électriques ont été observés au cours des expériences (acroissement de la force thermoélectrique α, diminution de la conductibilité electrique σ, d'où découle une variation de la conductibilité thermique

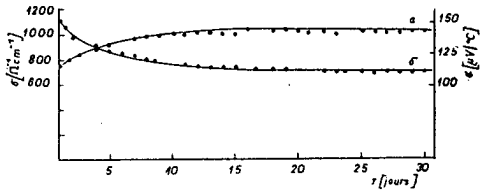

Fig. 1. Les changements de la conductibilité électrique σ et de la force thermoélectrique α sur les substances de type n.

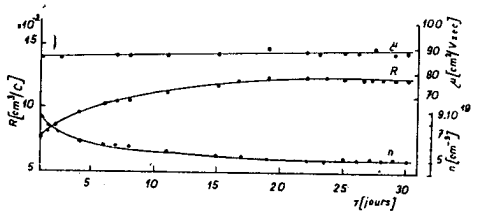

Fig. 2. Les changements de la constante de Hall R, de la mobilité μ des porteurs libres du courant et de leur concentration n.

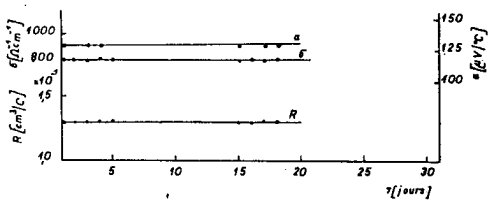

Fig. 3. Les mesures des grandeurs α, σ et R après le traitement thermique.

totale des substances) sur des échantillons de substances polycristallines de type n, préparées par synthèse dans une atmosphère d'azote, à une température de 720° C. et ensuite par refroidissement spontané à la température du laboratoire.

Les changements de la conductibilité électrique σ et de la force thermoélectrique α mesurés[1] sur ces substances se sont manifestés au cours des expériences qui ont duré environ 30 jours à la température du laboratoire. Ces deux grandeurs se sont relativement stabilisées au cours des 30 jours des expériences (fig. 1).

Paralèllement à la mesure de la conductibilité électrique des substances, il a été procédé à la mesure de la constante de Hall R, dont l'allure est donnée à la fig. 2.

Il ressort de l'allure des trois grandeurs observées que la variation indiquée est la plus intense au début des mesures, immédiatement après la préparation des substances.

Par contre, lorsque la substance était soumise au traitement thermique à 400° C., pendant 24 heures, dans un tube scellé, nous n'avons pas observé, au cours des mesures des grandeurs α, σ et R, de variations (fig. 3).

[1] La force thermoélectrique a été mesurée contre la platine, la conductibilité électrique et la constante de Hall ont été établies en courant alternatif de 20 c/sec.

Approved For Release 2009/05/01 : CIA-RDP80T00246A007500340002-0

Approved For Release 2009/05/01 : CIA-RDP80T00246A007500340002-0

DISCUSSION DES RESULTATS OBTENUS

1° La question qui se pose est de connaître les causes responsables des variations des grandeurs σ et α. La mobilité des porteurs du courant μ étant égale au produit de la constante de Hall R par la conductibilité électrique σ.

$$\mu = R \cdot \sigma \tag{3}$$

nous en tirons la conclusion que la grandeur $\mu \sim 90$ cm²/V sec ne varie presque pas au cours du processus de vieillissement (fig. 2). Son accroissement n'est que de l'ordre de 5 %. Par contre, la concentration des porteurs libres du courant n, donnée par la relation

$$n = 6{,}25 \cdot 10^{18} \frac{1}{R} \tag{4}$$

diminue de sa valeur initiale n = $8{,}5.10^{19}$ cm^{-3} pour atteindre la valeur n = $5{,}0.10^{19}$ cm^{-3} à l'état final. Il ressort donc de nos observations que la diminution de la conductibilité électrique par vieillissement n'est pas due à la modification de la mobilité des porteurs du courant, mais à une diminution de la concentration des porteurs libres du courant.

Cette conclusion est en accord avec le fait que la valeur de la force thermoélectrique α augmente au cours du processus de vieillissement.

Prenons alors l'équation

$$\alpha = \pm \frac{k}{e}\left(A + \ln 2\left[\frac{2\pi m^* kT}{h^2}\right]^{3/2} - \ln n\right) \tag{5}$$

où k est la constante de Boltzmann,
e la charge élémentaire,
A la constante dépendante de la forme de la dispersion des porteurs libres n,
m^*leur masse effective,
h la constante de Planck.

En substituant dans cette équation à n (4), les valeurs mesurées et en supposant que A = 2, $\frac{m^*}{m} = 1{,}3$ on arrive à un accord satisfaisant avec les expériences.

Dans le cas de substances soumises au traitement thermique la concentration des porteurs libres du courant ainsi que leur mobilité restent inchangées (fig. 3).

2° Une conclusion concernant l'appréciation de l'influence de ces processus au rendement de la conversion de l'énergie dans les jonctions Peltier peut être tirée des résultats signalés plus haut. Le rendement de cette transformation dépend de la grandeur z (1).

En nous rapportant à la courbe figurative du produit $\alpha^2\sigma$ au numérateur de cette constante (fig. 4), nous observons une diminution partielle de cette constante,

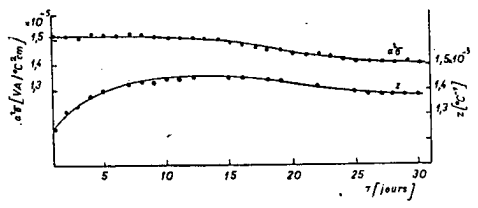

Fig. 4. Les changements du produit $\alpha^2\sigma$ et de la constante z.

Approved For Release 2009/05/01 : CIA-RDP80T00246A007500340002-0

Approved For Release 2009/05/01 : CIA-RDP80T00246A007500340002-0

circonstance avantageuse pour le rendement de la conversion. De son côté, la conductibilité thermique dans le dénominateur de (1) diminue aussi, car sa composante électronique $\varkappa_{el}$ tirée de la relation [1]

$$\varkappa = \varkappa_{el} + \varkappa_f \tag{6}$$

où $\varkappa_f$ est la conductibilité thermique du réseau,
est liée à la conductibilité électrique σ, en vertu de la loi Wiedemann-Franz par la relation

$$\varkappa_{el} = (1{,}0 - 1{,}5) \cdot 10^{-6} \sigma \tag{7}$$

Etant donné que σ décroît, $\varkappa_{el}$ décroît également ainsi que $\varkappa$ [16]. De ce fait nous observons une augmentation partielle de la constante z (fig. 4).

Ioffe et Stilbans [1] ont déduit la relation suivante existant entre la constante z, la mobilité μ et la conductibilité thermique du réseau

$$z \sim \frac{\mu}{\varkappa_f} \tag{8}$$

Après substitution, $\frac{\mu}{\varkappa_f}$ restant pratiquement inchangé au cours du processus indiqué, il semble que les processus qui ont lieu au cours du vieillissement des substances étudiées, n'ont pas une influence directe sur la diminution du rendement de la transformation de l'énergie dans les jonctions Peltier. Bien au contraire, ces processus ne peuvent qu'avoir une influence favorable sur leur rendement.

3° Il nous reste encore à traiter la question de savoir quelles sont les causes qui pourraient influencer de façon défavorable le processus de vieillissement déjà décrit. Etant donné que la grandeur σ des substances varie au cours de ce processus, car elle décroît, les paramètres de construction des piles de réfrigération varient également. Il est alors nécessaire d'adapter réciproquement les sections S_n et S_p d'après la relation

$$M = \sqrt{\frac{\sigma_p \varkappa_p}{\sigma_n \varkappa_n}} \tag{9}$$

$$\text{où } M = \frac{S_n}{S_p}$$

de manière que ces piles soient traversées par le courant optima, nécessaire à l'obtention de la différence de température exigée et à la réalisation de la puissance de réfrigération. Les indexes n et p dans la relation (9) sont rapportées aux substances de type n et p.

Lorsque la diminution de σ au cours du processus de vieillissement est même de l'ordre de 35 %, une telle diminution est déjà substantielle pour le fonctionnement d'une pile construite. Mais comme il ressort de nos résultats, il est possible d'éliminer cette difficulté par le traitement thermique des substances préparées.

CONCLUSIONS

L'étude du processus de vieillissement des solutions solides de type n de composés semi-conducteurs de systèmes Bi-Te-Se montre, que pour l'utilisation des propriétés thermoélectriques de ces composés, qui forment des systèmes relativement compliqués, il est nécessaire de faire attention à leur vieillissement. En construisant des jonctions Peltier pour la réfrigération avec les paramètres optima, il faut tenir compte de ce processus.

Approved For Release 2009/05/01 : CIA-RDP80T00246A007500340002-0

Approved For Release 2009/05/01 : CIA-RDP80T00246A007500340002-0

Je tiens également à remercier M. l'ingénieur Smirous qui a bien voulu préparer les substances nécessaires aux expériences.

BIBLIOGRAPHIE

1. IOFFE, A. F., STILBANS, L. S., JORDANISHVILI, JE. K., STAVICKAJA T. S. La Réfrigération thermoélectrique. Moscou 1956. En russe.
2. STILBANS, L. S., JORDANISHVILI, JE. K., STAVICKAJA T. S. *Izv. Akad. Nauk* (USSR), série phys. **26**, (5), 945, 1956. En russe.
3. JORDANISHVILI, JE. K., STILBANS, L. S. *Journ. Techn. Phys.* **26**, (2), 945, 1956. En russe.
4. GOLDSMID, H. J., DOUGLAS, R. W. *Brit. Journ. Appl. Phys.* **5**, (11), 386, 1954.
5. VLASOVA, R. M., STILBANS, L. S. *Journ. Techn. Phys.*, 25, (4), 569, 1955. En russe.
6. SINANI, S. S., GORDJAKOVA, G. H. *Ibid.*, **26**, (10), 2399, 1956.
7. VASENIN, F. I. *Ibid.* **25** (7), 1190, 1955.
8. CHMELEV, I. C. Dissertation, Leningrad, 1949. En russe.
9. VASENIN, F. I. *Rapport,* Inst. Semicond. Acad. Sci. USSR, Leningrad, 1955. En russe
10. AIRAPETJANE, S. V., JEFIMOVA, B. A., STAVICKAJA, T. S., STILBANS, L. S. *Journ. Techn. Phys.* **27**, (9), 2167. En russe.
11. AIRAPETJANE, S. V., JEFIMOVA, B. Å. *Ibid.*, **28**, (8), 1768.
12. SMIROUS, K., STOURAC, L. *Rapport* No. 418, Inst. Phys. Appl. Prague, 1957.
13. STOURAC, L. *Rapport* No. 426, Inst. Phys. Appl. Prague, 1957.
14. SMIROUS K., STOURAC, L. *Rapport* No. 427, Inst. Phys. Appl., Prague, 1957.
15. –. *El. Obzor,* 1959 (à l'impr.).
16. –. *Ibid.* 1959 (à l'impr.).

Behrndt bogtryk, Denmark

Copyright reserved

Approved For Release 2009/05/01 : CIA-RDP80T00246A007500340002-0

Approved For Release 2009/05/01 : CIA-RDP80T00246A007500340002-0

Operation of Mechanically Refrigerated Railway Trains in the U.S.S.R.

Expérience soviétique en matière d'exploitation des trains frigorifiques.

SH. N. KOBULASHVILI,[1] M. S. MARTINOV,[2] and M. M. SHAPOVALENKO[3]
U.S.S.R.

SOMMAIRE. Le transport des denrées périssables en U.R.S.S. est caractérisé par les longues distances à parcourir. En autonne et en hiver une grande quantité d'aliments est transportée dans des voitures chauffées.

Au cours des dernières années le refroidissement mécanique et le chauffage électrique des voitures isolées thermiquement sont devenus de plus en plus importants. Depuis 1953, les chemins de fer soviétiques ont mis en service des trains frigorifiques composés de 23 voitures chacun. La capacité de chargement totale d'un train est de 600 t. L'équipement est destiné au transport des aliments à des températures de –10° à 6° C. pour des températures ambiantes de 30° C. à –45° C.

Depuis 1957, des sections frigorifiques, composées de 3, 5 ou 12 voitures chacune, ont été utilisées pour le transport de petits chargements. La longueur de la caissée des véhicules a été portée à 17 m; l'isolation thermique a été améliorée et le matériel fonctionne automatiquement. Les sections de train sont destinées au transport des aliments pour les températures suivantes: sections de 12 voitures: jusqu'à –15° C.; sections de 5 voitures: jusqu'à –18° C.; sections de 3 voitures: jusqu'à –20° C. (température ambiante de 35° C.).

Les trains et les sections de trains conviennent à toutes les sortes d'aliments sauf aux carcasses de viande. L'entretien mécanique des voitures est effectué dans des chantiers spécialisés et des ateliers de réparation. Le prix de revient net du fret ne dépasse pas celui des wagons à refroidissement par glace ordinaires. Dans les scetions de trains, il est un peu plus élevé mais il est encore avantageux du point de vue économique si l'on considère que les aliments sont mieux conservés et livrés plus rapidement.

Pour la période de 1959 à 1965, on projette une augmentation considérable du parc de wagons frigorifiques.

The transportation of perishables in the U.S.S.R. with its vast territory is characterized by long distance deliveries.

The average distance of transporting perishables in the 3rd quarter of 1958 was: fresh fish – 2974 km, salted fish – 3096 km, meat and meat products – 1370 km, fresh vegetables – 1126 km, apples – 1471 km, other fruits and berries – 1477 km.

Large lots of fresh fish are transported from the Far East to the Urals and the central regions of the European part of the country over a distance of 7 to 10 thousand kilometres, while fruits are delivered 3 to 6 thousand kilometres from Central Asia, Transcaucasia and other regions.

Railway deliveries are made in the U.S.S.R. under quite various climatic conditions. For instance, in the northern part of the country the mean monthly temperature of the air does not exceed, as a rule, from 17 to 20° C. while in Central Asia and in the South it reaches 30° C. and even on some days a maximum of 45° C. A considerable amount of perishables strongly affected by low tem-

[1] The Scientific Research Institute of the Refrigerating Industry of the U.S.S.R.
[2] Ministry of Railways of the U.S.S.R.
[3] The U.S.S.R. Scientific Research Institute of the Railway Transportation, Moscow, U.S.S.R.

Approved For Release 2009/05/01 : CIA-RDP80T00246A007500340002-0

Approved For Release 2009/05/01 : CIA-RDP80T00246A007500340002-0

ratures are transported at an outisde temperature of –45 – –50° C. in heated insulated cars. The long distances and the hard climatic conditions set high requirements to the refrigerated railway transport as concerns the system of delivery on the whole as well as the technical means, and first and foremost the rolling stock.

Refrigerated trains consisting of 23 four-axle cars each have operated widely on the railways of the U.S.S.R. since 1953. These trains were built in the German Democratic Republic on order and in accordance with technical specifications of the Ministry of Railways of the U.S.S.R. Each train consists of 20 refrigerated cars, refrigerating machinery car, a car housing a diesel electric station and a car for the servicing personnel. The trucks of the cars are of the passenger car type that provide reliable conditions for operating the equipment.

The equipment of the train is designed to maintain temperatures from –10° C. to 6° C. inside the cars at outside temperatures of 30° to –45° C. The cars are cooled by a brine system with two ammonia refrigerating units installed in the machinery car. The condensers of the refrigerating units are air-cooled and equipped with a 40.000 m^3/hr fan each. The shell-and-tube evaporators have a 35 m^2 surface. The goods' compartments of the refrigerated cars are equipped with electric heaters having a capacity of 8 kw to a car.

The electric motors of the refrigerating units as well as the electric heaters are powered from three diesel-generator units installed in the diesel electric station car.

The refrigerated cars are equipped with devices for forced air circulation, plenum and exhaust ventilation and remote temperature control.

The specifications of the train and of its main equipment are given in Table 1 which also provides characteristics of the refrigerated sections to be discussed further.

TABLE 1. SPECIFICATIONS OF REFRIGERATED TRAINS AND SECTIONS

Nos.	Specification	Unit	23-car train	section		
				12 cars	5 cars	3 cars
1.	External length of refrigerated car body	m	15.0	17.0	17.0	17.0
2.	Total length of train or section	m	373.0	214.0	91.0	54.6
3.	Total tare weight of train or section	t	1035.0	544.3	221.0	128.7
4.	Total load-carrying capacity of train or section	t	600.0	399.0	179.0	113.0
5.	Total gross weight of train or section	t	1635.0	943.0	400.0	241.7
6.	Loading volume of refrigerated car	m^3	64.8	78.5	65.8	75.0
7.	Overall coefficient of heat transfer of refrigerated car body	kcal/ m^2hr°C.	0.32	0.27	0.27	0.35
8.	Number of refrigerating units in train or section	– stand.	2	2	10	6
9.	Refrigerating capacity of one refrigerating unit (at $t_0 = -15$; $t_e = 25$; $t_c = 30$° C.)	kcal/hr	88000	58400	8800	12000
10.	Total power of diesel engines in train or sections	hp.	260	270	180	160

The train is serviced by a team of 7 men: train chief, two diesel engine operators, two refrigeration mechanics, an electrician, and a conductor of the servicing personnel car.

Specialized depots are in charge of the technical servicing of the refrigerated trains, current repairs and annual overhauls, the supply of the trains with ammonia, fuel, water, brine, lubrication and spare parts, as well as the education and manning of the teams. Periodic inspection and small repairs during the run are performed by the crew.

Approved For Release 2009/05/01 : CIA-RDP80T00246A007500340002-0

Approved For Release 2009/05/01 : CIA-RDP80T00246A007500340002-0

The trains are supplied with fuel and lubricant during the run at special equipping stations, located at a 4 to 5 days' distance from each other, and at large stations where the perishables are either loaded or unloaded.

There is a special car-repairing plant for medium and general overhauling of the refrigerated trains.

Over six years of experience in operating refrigerated trains has shown the stability and reliability of the power refrigerating and heating equipment, and illustrated the advantages of transporting foods in such trains as compared with iced cars. The most important advantages of refrigerated trains are their independence of stationary icing installations and the feasibility of running as a self-contained unit. The time necessary for delivering perishables was cut nearly in half as compared with the delivery in iced cars. This is mainly due to the elimination of stops at icing stations which is performed every 24–36 hours, and the running of the trains according to a special schedule. The maintenance of the more favourable temperatures in the goods' compartments of the refrigerated cars independent of the outside air temperature, allowed delivery from the Far East, Central Asia and other distant regions of the country of products which could not always be preserved in iced cars.

Refrigerated trains are used mainly for delivering large lots of perishables (train lots), as a rule over large distances.

In order to reduce the empty run, the refrigerated trains on their way to the loading station are used for carrying packaged goods or empty tare which do not damage the inner equipment or affect sanitary conditions in the cars.

The teams are replaced if necessary en route without waiting for the arrival of the train in its depot.

The prime cost of delivering goods in refrigerated trains does not exceed the cost of transporting in iced cars, but the servicing and refrigeration costs are 41% lower.

Proceeding from actually obtained data of a complete and loaded run, turnover percentage of empty run and speed of the run – the prime cost of delivering perishables in refrigerated trains is characterized by the following data as compared with iced cars.

TABLE 2. THE PRIME COST OF DELIVERING PERISHABLES IN REFRIGERATED TRAINS AS COMPARED WITH ICED CARS

Specification	Unit	Refrigerated train	Iced car
Total prime cost of delivery	kopek/t km	9.2	9.2
Including:			
Servicing and refrigeration costs	kopek/t km	1.11	1.89
	%	12.0	20.5

The prime cost of delivering goods in winter with heating in the refrigerated trains is nearly one half that of iced cars as there is no necessity for special conductors, and the utilization of the load-carrying capacity improves by approximately 20%.

In calculating the prime cost of transporting goods in refrigerated trains, the merits of speedy delivery and better preservation of the foods have not been taken into account. These advantages, that cannot be determined in currency, undoubtedly provide an additional economic effect. The prime cost of the deliveries will be reduced with a further improvement of the operating properties of refrigerated trains and wider automation of their equipment.

Since 1957 refrigerated sections, consisting of 3, 5 and 12 four-axle cars each,

Approved For Release 2009/05/01 : CIA-RDP80T00246A007500340002-0

Approved For Release 2009/05/01 : CIA-RDP80T00246A007500340002-0

are used for transporting minor shipments. Tests have been completed on cars with individual mechanical refrigeration and electric heating.

The car bodies have been lengthened to 17 m and the thermal insulation improved as well as the refrigerating equipment automated in order improve the technical and economic properties of the cars.

Five and twelve car sections are built in the German Democratic Republic according to the technical orders of the Ministry of Railways of the U.S.S.R. and three car sections are built in the U.S.S.R.

The following air temperatures are maintained in the cars during the run at an outside temperature of 35° C.; down to –15° C. in a 12 car section, –18° C. in a 5 car section and –20° C. in a 3 car section. The equipment of the section allows also to cool fruits and vegetables in the car compartments from 25° C. down to 4° C. in the course of 2–3 days after being loaded into the car.

The specifications of the refrigerated sections and of their main equipment are given in Table 1.

The refrigerated cars are heated by electric heaters that are switched on and off automatically depending upon the rated range of air temperture variations in the car. The capacity of the electric heaters is rated to maintain the temperature in the car above 12° C. at an ambient temperature of –45° C.

The 12 car section consists of 10 refrigerated cars, a refrigerating machinery car, and a car holding the diesel electric station. The latter car also includes a compartment for the team. The section is serviced by a 5 man team.

The section cars are cooled by 2 two-stage ammonia refrigerating units. The first and second stages are individual units. The refrigerating units are automatically controlled by diaphragm and float valves. The refrigerated cars are equipped with brine coils. The brine is automatically fed to the coil of each car depending upon the required temperature of the air in the goods' compartment.

The goods' compartments of 3 and 5 car sections are refrigerated by means of Freon–12 machines – two to a car. The refrigerating capacity of each Freon unit amounts to 75% of the maximum consumption of refrigeration per car. The goods' compartment is refrigerated by a direct expansion air cooler. The refrigerating units are started and stopped either automatically depending upon the air temperature variations in the compartment, or by hand (remotely) from the diesel electric station compartment located at the end of the middle car of the section.

An additional air supply to the air cooled condensers is provided to facilitate operation of the refrigerating equipment in regions of high outside temperatures.

The goods' compartments of the cars of all the refrigerated sections are equipped with plenum and exhaust ventilation, forced air circulation and remote control of the temperature of the air and goods.

The 5 car sections are serviced by a team of 3 operators and 3 car sections are manned by 2 operators. A compartment for the team is located at the end of the car adjacent to the diesel electric station.

Technical maintenance and repairs of the refrigerated sections are carried out by the same specialized depot and plant which take care of the refrigerated trains.

The prime cost of the deliveries with cooling in the sections increases with a reduction in the number of cars. Preliminary data indicate that it increases by 10 to 20% as compared with the delivery in refrigerated trains. However, this additional cost of delivery of goods in the refrigerated sections is compensated by the better preservation of quality as compared with transportation in refrigerated trains.

Experimental samples of refrigerated rolling stock are subjected to thorough tests on the railways of the U.S.S.R. in order to determine their features with respect to operation and design. The thermal properties of the cars, data on the operation of the power and refrigerating equipment, the automatic controls as well as the design of separate units are all checked during the tests carried out by the U.S.S.R. Scientific Research Institute of the Railway Transportation. Manufacturers are informed of the results of the tests and of definite suggestions before starting serial production of mechanically refrigerated cars.

Approved For Release 2009/05/01 : CIA-RDP80T00246A007500340002-0

Approved For Release 2009/05/01 : CIA-RDP80T00246A007500340002-0

In 1959–1965 many refrigerated railway cars will be added to the rolling stock of the U.S.S.R. railroads. Twenty-one car trains, with 17 m long cars, will be built rated for the delivery of perishables at an outside air temperature up to 40° C.

Behrndt bogtryk, Denmark

Copyright reserved

Approved For Release 2009/05/01 : CIA-RDP80T00246A007500340002-0

Approved For Release 2009/05/01 : CIA-RDP80T00246A007500340002-0

A New Iced Car with Overhead Cooling Equipment

Un nouveau wagon réfrigérant avec bacs refroidisseurs au plafond.

M. S. MARTYNOV[1] and S. O. GOOSSEV[2]
Moscow, U.S.S.R.

SOMMAIRE. L'U.R.S.S. a entrepris en 1958 la construction en série de nouveaux wagons réfrigérants d'un type amélioré, de grande capacité, avec bacs refroidisseurs au plafond. Ces wagons mesurent 17 m de long; leur volume brut est de 117 m^3 et leur volume utile de 82 m^3. Les parois extérieures, la toiture ainsi qu'une partie du chassis sont en acier spécial; le revêtement intérieur et le plancher sont en feuilles d'aluminium. L'isolation est réalisée en panneaux "Mipore" emballés dans une enveloppe de "Perfoil". Le coefficient global de transmission de chaleur de l'enceinte calorifugée est de 0,31 cal/h/m^2°C.

L'équipement frigorifique comprend six bacs refroidisseurs en acier inoxydable; leur surface totale réfrigérante est de 74,6 m^2 et leur capacité de 5,5 tonnes de glace concassée. L'évacuation de la saumure hors des bacs est assurée par 4 dispositifs spéciaux qui maintiennent constamment son niveau aux $^2/_3$ de la hauteur du bac. La température moyenne à l'intérieur des wagons est maintenue à –7° C. par une température extérieure de +30° C., en utilisant un mélange de glace et de sel à une concentration de 30%. Dans de telles conditions, la charge du mélange glace-sel doit être complétée tous les trois jours.

Le poids à vide d'un wagon est de 38,6 tonnes, et sa contenance de 45 tonnes.

Par comparaison avec les meilleurs types de wagons réfrigérants, le coût du transport est abaissé de 5 à 8% et la qualité des denrées périssables est bien mieux préservée.

The manufacture of iced cars with wall ice bunkers has been discontinued in the U.S.S.R. since the second half of 1954 and the production of four-axle 13.6 m long cars with overhead refrigerating equipment was commenced.

In 1957-58 iced cars of the same type, with a longer body (17 m long) and an increased thickness of the walls and roof were manufactured serially by the railway car building plants.

Due to the use of low-alloy steel and bent profiled metal in the construction of the 17 m long cars the tare weight of the cars was somewhat reduced with simultaneous improvement of the thermal insulation as compared with the cars manufactured earlier.

A new car was built and tested in 1958 with a view to further improving the specifications of iced cars with overhead refrigerating equipment. The inner wooden sheathing of the walls was replaced by corrugated aluminium sheets and the design of the thermal insulation was improved.

The new improved type railway car is being built at present on a serial basis. The specifications of the car are tabulated below.

A general view of the car is given in Fig. 1.

The car frame is of welded low-alloy steel with a center sill channel. The body with the supporting outer metal corrugated coating of the walls is reinforced by means of vertical posts of bent profiled metal. The sheathing of the longitudinal walls and roof as well as the longitudinal joints of the roof are made of 2 mm

[1] Ministry of Railways of the U.S.S.R.
[2] All-Union Scientific Research Institute of the Railway Transportation.

Approved For Release 2009/05/01 : CIA-RDP80T00246A007500340002-0

Approved For Release 2009/05/01 : CIA-RDP80T00246A007500340002-0

TABLE 1. SPECIFICATIONS OF THE 1958 ICED CAR

1	External length of body	17.0 m
2	External width of body	3.03 m
3	Thickness:	
	of roof	250 mm
	of walls	200 mm
	of floor	178 mm
4	Floor space:	
	complete	43.6 m^2
	piling	41.3 m^2
5	Internal volume:	
	complete	117.0 m^3
	piling	82.0 m^3
6	Tare weight without ice	31.6 tons
7	Net carrying capacity	45.0 tons
8	Number of overhead ice tanks	6
9	Weight of ice in tanks	5.5 tons
10	Body enclosure heat transfer coefficient	0.31 kcal/m^2hr°C.

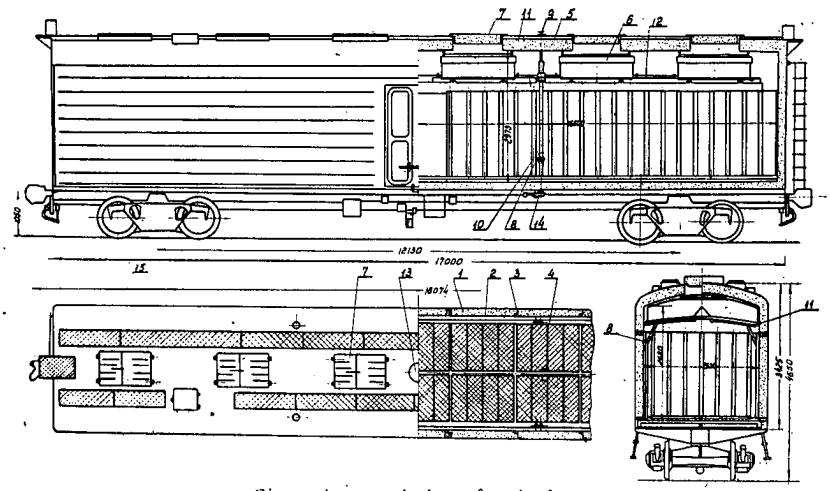

Fig. 1. A general view of an iced car.

thick low-alloy steel, while the supports and the frame are of the same metal 4 mm thick. The face walls are covered on the outside with 3 mm thick steel sheets.

The internal wall coating is made of corrugated (40 mm high vertical corrugation) sheet aluminium 2 mm thick. The sheathing of the ceiling is 16 mm boards. The aluminium sheathing is composed of separate sections fixed to the body frame so as to prevent continuous heat bridges.

Perfoil packets containing Iporka boards, 134 and 230 mm thick respectively, are set between the sheathing of the walls and roof. Asphalted paper is set between the internal sheathing and the insulation packets.

The car floor consists of an external 22 mm thick wooden sheathing coated with goudron and asphalted paper, a 12 mm thick middle and 45 mm thick upper flooring also painted with goudron. Perfoil packets with 96 mm thick Iporka boards are arranged between the external sheathing and the middle flooring. The upper flooring is coated with welded 2 mm sheet aluminium.

The refrigerating equipment of the car consists of six stainless steel tanks located under the ceiling along the car. A longitudinal connection of the tanks by means

Approved For Release 2009/05/01 : CIA-RDP80T00246A007500340002-0

Approved For Release 2009/05/01 : CIA-RDP80T00246A007500340002-0

of pipes is provided for draining the brine into a drain device. The tank bottom and walls are made of 3 mm thick sheets, the cover being 2 mm thick. The total volume of the tanks is 10.5 m^3, the area of the cooling surface amounts to 74.6 m^2.

Baffles of 4 mm thick pressed wood fibre boards are suspended under the tanks to remove the condensate from the external surface of the tanks and to direct the circulated air. Two hundred mm wide air circulation slots are provided between the screens along the longitudinal axis of the car and 80 mm wide ones between the screens and the longitudinal walls of the car.

Metal drain pans are arranged under the lower ends of the screens to drain the condensate into vertical pipes engaged in drain pipes run through the floor into a hydraulic seal.

A 1100 × 700 mm hatch for ice and salt with a two-fold cover and lever lock is located on the roof of the car over each tank. The covers are stamped aluminium boxes filled with Iporka and coated from below with zinc-plated metal. Thus the weight of each fold was reduced to 16 kg.

Four overflow devices are provided for automatically draining the surplus brine and maintaining the level in the tanks not over $^2/_3$ of their height. For a complete drainage of brine and rinse water out of the tanks a valve is opened by hand.

The height of the door opening is increased to 2000 mm. The angles of the door folds and the door frame are rounded for better tightness. The joints of the folds and the door frame are equipped with a double seal of rubber pipe and band rubber along the entire perimeter.

The 100 mm high floor grids are made of metal. Two hatches are provided in the roof of the car for ventilating the loading space.

The car is equipped with automatic coupling and double duty automatic brakes. The trucks are of the freight type but with softer spring suspension and roller axle boxes.

The mean air temperature in the car during the tests is given in Fig. 2.

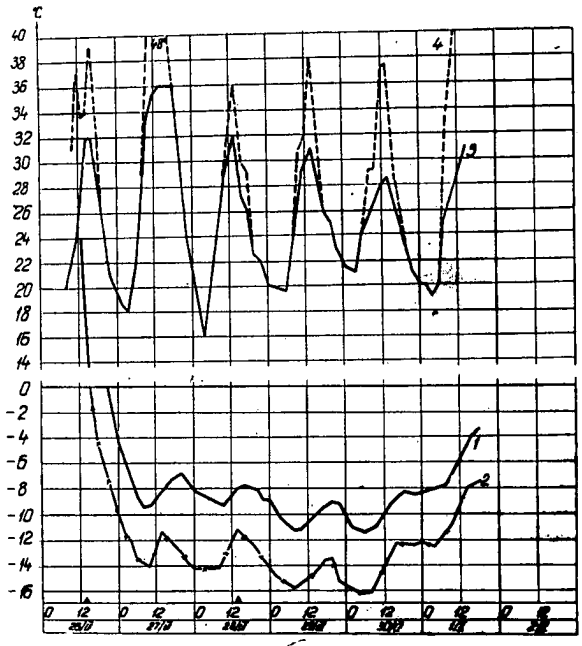

Fig. 2. Temperatures recorded during the tests of the iced car. 1. Mean temperature of air in the car. 2. Mean temperature of the cooling surface of the tanks. 3. Temperature of ambient air in the shade. 4. Temperature of ambient air on the sunny side.

Approved For Release 2009/05/01 : CIA-RDP80T00246A007500340002-0

Approved For Release 2009/05/01 : CIA-RDP80T00246A007500340002-0

The new iced car has the following advantages as compared with the 13.6 m long car of the same type: the loading volume is increased by 25%, the tare-weight is reduced by 3%, the heat transfer coefficient of the body enclosure is decreased by 41%. The temperature in the loading space has been reduced by 1° C. with the geometrical dimensions of the refrigerating equipment unchanged.

The prime cost of transportation of perishable goods is reduced by 5 to 8% in the new car due to improved loading and thermal characteristics.

Behrndt bogtryk, Denmark

Copyright reserved

Approved For Release 2009/05/01 : CIA-RDP80T00246A007500340002-0

Approved For Release 2009/05/01 : CIA-RDP80T00246A007500340002-0

Refrigerating Equipment on the Vessels of the U.S.S.R. Fisheries Industry

Matériel frigorifique à bord des bateaux de l'industrie de la pêche en U.R.S.S.

E. G. PAVLOV[1] and R. V. PAVLOV[2]
Moscow, U.S.S.R.

SOMMAIRE. Le rapport traite des problèmes frigorifiques à bord des batteaux de l'industrie de la pêche de l'U.R.S.S., y compris les bateaux en armement, en projet ou en cours de construction. Il étudie les caractéristiques des principaux types de navires allant en mer munis de systèmes frigorifiques: bateaux de pêche (cordiers, chalutiers moyens); bateaux de pêche et de traitement du poisson (chalutiers, etc); usines flottantes (à auto-propulsion ou non); navires de transport (transport de réception, transport frigorifique). On indique les besoins technologiques fondamentaux des systèmes frigorifiques des navires: refroidissement des cales et installations de congélation, alimentation en glace. On donne le niveau de température désirée et la puissance frigorifique des installations d'après la classe du navire et ses dimensions. Dans la discussion des principes généraux présidant au choix des machines frigorifiques, on veille particulièrement à la désignation appropriée d'un fluide frigorigène, d'un niveau de température convenable et des systèmes frigorifiques des différents types de navires ainsi que du matériel et du plan des installations frigorifiques. On décrit les éléments des machines frigorifiques (compresseurs, installations de congélation et matériel annexe). On donne des exemples de systèmes frigorifiques et de dispositifs automatiques adoptés en se basant sur ceux choisis pour différents navires du type "Pushkin", "Mayakovsky", "Aktyobinsk" et autres, en armement, en construction ou en projet.

GENERAL INTRODUCTION

Over 30% of the fishing vessels of the U.S.S.R. are equipped with refrigerating equipment. The installations for provision chambers are not included in this figure. A considerable increase in refrigerated fishing vessels is planned.

Depending upon the regions and conditions of operation, the fishing vessels of the U.S.S.R. may be divided into four groups according to the use of refrigerating equipment.

1. *Vessels with machinery to maintain the holds at –1° to –2° C. for storing fish, usually in ice.* Included in this group are medium sized trawlers with a 300 hp main engine (SRT–300), trawlers with a 800–2000 hp main engine (RT and BRT), and floating base vessels. The capacity of the refrigerating equipment is from 5.0 to 40.0 thousand normal kcal/hr depending upon the size of the holds. Freon 12 is used; the holds are cooled by direct expansion though sometimes brine cooling is applied. An example of a vessel in this group is a transport having a 80 hp main engine.

2. *Vessels equipped with installations to maintain the temperature in the holds at –1° to –2° C. and for cooling fish.* The group includes RB–150 fishing boats having a 150 hp main engine, medium sized fishing trawlers having a 600 hp

[1] State Planning Commission of the U.S.S.R.
[2] Central Refrigerating Machinery Designing Bureau.

Approved For Release 2009/05/01 : CIA-RDP80T00246A007500340002-0

Approved For Release 2009/05/01 : CIA-RDP80T00246A007500340002-0

(SRT–600) or 400 hp. (SRT–400) main engine, herring base and other vessels. The refrigerating capacity of the machines on these vessels varies from 40.0 to 550.0 thousand normal kcal/hr. The holds are cooled by a brine system (RB–150, SRT–400, floating base vessels) or by a ductless air system (SRT–600). Freon–12 or ammonia are used, the selection of the refrigerant being determined by the particular operating conditions. Characteristic of this group are the fishing boat (RB–150), and the herring base vessel, having a 5000 hp main engine, built in the Polish People's Republic.

3. *Vessels equipped with installations for freezing fish and other sea products as well as for maintaining the temperature in the holds at –10° to –25° C.* Included in this group are large refrigerating fishing trawlers (BMRT) with a 1900–2000 hp main engine, freezing fishing trawlers with a 1300 hp main engine (RTM), freezing fishing vessels with a 600 hp main engine (RMS) and other fishing vessels, refrigerator ships (self-propelled and tugged) and whale base vessels equipped with freezing units. The capacity of the refrigerating installations is up to 1400 thousand normal kcal/hr in the case of single-stage compression and from 500 to 600 thousand kcal/hr at $t_0 = -40°$ C. with two-stage compression. Representative of this group is the large refrigerating fishing trawler *Mayakovsky.*

4. *Vessels equipped with refrigerating units destined only for the maintenance of low temperatures (–10° to –18° C.) in the holds.* This group includes refrigerated transport vessels and barges equipped with various refrigerating installations and hold cooling systems. The refrigerating capacity of the installations reaches 400 thousand normal kcal/hr when operated on single-stage compression and 450 thousand kcal/hr in the case of two-stage compression at $t_0 = -30°$ C. Of particular interest among the vessels of this group are refrigerated diesel-electric ships of the *Aktyubinsk* type, built in the U.S.S.R.

In this paper we shall confine the discussion to a few topics of the above problem.

SELECTION OF THE REFRIGERANT

The use of Freon–12 on board vessels is certainly preferable to ammonia for safety considerations. However, the higher cost of the equipment and the more costly and complex operations are a serious obstacle for greater utilization of large Freon refrigerating machines aboard. Direct expansion is applied only in relatively small refrigerating capacity installations. It should be kept in mind that both ammonia and Freon refrigerating machines are installed in special compartments, isolated from the rest of the vessel, which considerably reduces the possible danger for the crew and the vessel, in the case of a breakdown of the ammonia installation.

Ammonia refrigerating machines are more advantageous as compared with Freon machines from the point of view of the volumetric refrigerating capacity.

The metal requirements of Freon machines exceed those of ammonia machines by approximately 130 to 150%. The specific refrigerating effect of ammonia is somewhat greater than of Freon machines.

Exclusively two-stage ammonia refrigerating machines are used at present for obtaining low temperatures.

Many hopes were set on Freon–22. The possibility of substituting ammonia by this refrigerant in single-stage cycles promised considerable simplification of the entire installation and a higher safety of operation. However, tests of one of the models of a Freon–22 refrigerating machine have shown the following results (*see* the journal *Kholodilnaya Tekhnika,* (5), 24, 1958): at an evaporating temperature below –30° C. the specific refrigerating effect of a single stage Freon–22 compressor proved to be 25–35% lower and the power consumption 25 to 35% higher than those of a two-stage ammonia compressor. The specific

Approved For Release 2009/05/01 : CIA-RDP80T00246A007500340002-0

Approved For Release 2009/05/01 : CIA-RDP80T00246A007500340002-0

metal requirements of an ammonia compressor are from 30 to 40% less than in the case of a Freon–22 compressor.

REFRIGERATING EQUIPMENT

Small Freon refrigerating machines of a 4000 to 25000 standard kcal/hr capacity manufactured in the Soviet Union comprise automatic condensing units, finned or bare-pipe cooling elements, or shell-and-tube evaporators. The operation of such machines on vessels has shown quite satisfactory results.

High capacity marine refrigerating compressors should have a sufficiently deep crankcase and a submerged oil pump providing reliable lubrication of the compressor at sea rolling, and moderately sized pistons to facilitate repairs, that the compressor should have no more than four cylinders, and should be connected directly to the motor through a clutch. A series of refrigerating compressors has been developed by the Central Refrigerating Machinery Designing Bureau, meeting, on the whole, the above requirements and are being used on board vessels.

The monoblock compressors are manufactured in various designs: vertical cylinder machines, the maximum cylinder bore being 200 mm, V-type four-cylinder machines and uniflow with a double crankshaft supported by two bearings. The compressors are driven by electric motors directly through a clutch.

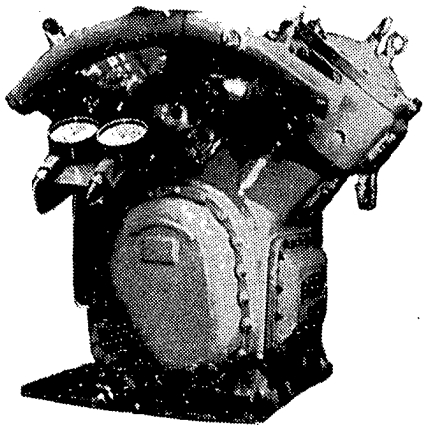

Fig. 1. A 200,000 standard kcal/hr single-stage ammonia compressor.

Fig. 1 shows the AU–200 compressor manufactured at the "Compressor" Plant.

A new two-stage compressor (model DAU–80) having a refrigerating capacity of 80.000 kcal/hr at $t_0 = -40°$ C. and $t_c = +30°$ C. manufactured at the "Compressor" Plant according to drawings of the Central Refrigerating Machinery Designing Bureau is shown in Fig. 2.

Other two-stage ammonia refrigerating machines are also planned.

Shell-and-tube evaporators are manufactured with one or two high vapour domes with built-in coils providing the superheating of the ammonia vapour. Such a design of the domes is aimed at decreasing the danger of liquid refrigerant getting into the compressor suction line.

Condensers installed on board vessels are equipped with a deep liquid receiver thereby providing a hydraulic lock in the case of rolling and listing.

Approved For Release 2009/05/01 : CIA-RDP80T00246A007500340002-0

Approved For Release 2009/05/01 : CIA-RDP80T00246A007500340002-0

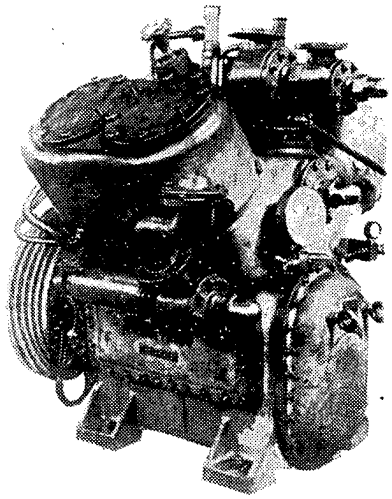

Fig. 2. A two-stage ammonia compressor having a capacity of 80,000 kcal/hr at –40° C. evaporating temperature and +30° C. condensing temperature.

LAYOUT OF REFRIGERATING INSTALLATIONS

When designing a marine refrigerating installation the specific features of sea operations have to be kept in mind, *e. g.*, a possibly small amount of apparatus with a free level of the liquid; the necessity of locating the equipment so that rolling has a minimum influence upon its operation; protection of the compressors from hydraulic impacts, etc. All these requirements are met by the proper selection of the dimensions, shape and design of apparatus, the application of special controls, appropriate location of the machines and apparatus on board vessel, etc. To provide the most uniform refrigeration supply a marine refrigerating installation should comprise three or four machines.

The layouts of ammonia refrigerating installations allow parallel operation of compressors with one or several evaporators and condensers as well as an application of smaller diameter pipes, as compared with Freon systems. In Freon refrigerating machines each compressor operates with a separate system of apparatus.

Layouts of the refrigerated transport vessel *Aktyubinsk* are illustrated below as examples of existing installations. The vessels of this series are designed for transporting frozen fish at –18 to –20° C. in the hold. The displacement of the *Aktyubinsk* is 10,000 tons. There are 10 cargo compartments (holds and 'tween-decks) with a total volume of 8628 m_3. The cargo compartments are cooled by bare-pipe single-row and double-row wall and overhead coils. The total refrigerating capacity of the installation is 480,000 kcal/hr at –30° C. evaporating temperature and 30° C. condensing temperature. One of these machines is mainly a stand-by. The intercooling of gas is accomplished in a heat exchanger with water as a cooling medium. The advantage of the installation is in the simplicity of control and in the absence of inter-coolers with a free level.

A refrigerating installation with intercooling by means of water may be efficiently operated at an evaporating temperature as low as –40° C. However, the refrigerating capacity considerably drops in this case while the power consumption is increased. It is most expedient, therefore, to use this system for an evaporating temperature of –25 to –30° C.

For refrigerated vessels, designed also for fish freezing, two-stage refrigerating installations operating at an evaporating temperature of –40° C. and lower are required. Two-stage installations with complete intercooling are to be used in

Approved For Release 2009/05/01 : CIA-RDP80T00246A007500340002-0

Approved For Release 2009/05/01 : CIA-RDP80T00246A007500340002-0

such cases. The design of refrigerating installations of large refrigerated fishing trawlers of the *Mayakovsky* class is based on the above principle. The refrigerating installation of the vessel is designated to maintain –18° C. in three holds having a total volume of 1800 m³, and to freeze fish in two 15 tons per day freezing apparatus. The holds are cooled by wall and overhead brine coils, while the freezer coils are of the direct expansion type.

The refrigerating installation (Fig. 3) consists of three two-stage DAU–80 compressors with a total refrigerating capacity of 240,000 kcal/hr. This installation operates with single-stage throttling and cooling of the entire amount of liquid ammonia in the intercooler coil. The liquid is supplied into the body of the intercooler by a thermostatic expansion valve.

A freezer ship is being designed at present with larger holds having a 3600 m³ total capacity and two 25 tons per day freezing apparatus.

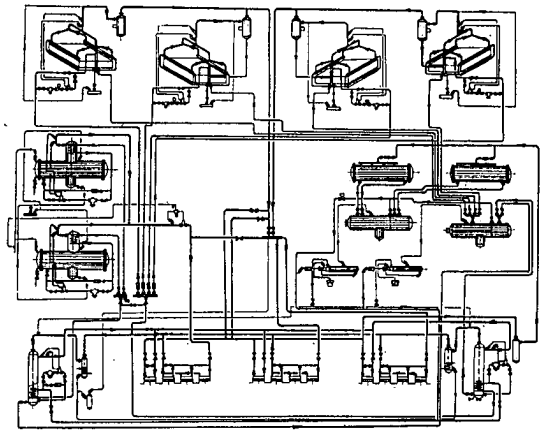

Fig. 3. The loyout of the ammonia system on board large refrigerated fishing trawler Mayakovsky.

AUTOMATIC CONTROL

The problem of controlling the feed of refrigerant to the evaporator was most important. The choice had to be made from three types of automatic expansion valves: a low pressure float, a high pressure float, and a thermostatic. The thermostatic valve was preferred. Tests carried out under operating conditions and on experimental stands confirmed the correctness of the selection. The thermostatic expansion valve, adjusted for a moderate superheat, provided automatic control of the feed of liquid ammonia to the evaporator under all operating conditions within a wide range of refrigerating capacities.

CONCLUSIONS

1 The following types of refrigerating installations are most widespread for use on board ships: a) Small refrigerating capacity Freon installations providing a temperature in the holds –1° to –2° C.; b) ammonia and Freon high capacity installations for large vessels with high temperatures in the holds (–1° to –2° C.); c) two-stage low temperature ammonia installations, providing –18° to –20° C. in the holds, using brine refrigeration; d) two-stage ammonia installations for vessels equipped with freezers, are manufactured for a –40° C. evaporating temperature with brine cooling of the holds and direct expansion for the freezing apparatus.

Approved For Release 2009/05/01 : CIA-RDP80T00246A007500340002-0

Approved For Release 2009/05/01 : CIA-RDP80T00246A007500340002-0

2. The advantage of the Freon–12 refrigerant is greatly reduced due to the more complex operation and higher cost of the equipment.

3. The expediency and necessity of substituting two-stage ammonia machines by single-stage Freon machines has not been confirmed as yet and requires some serious experimental investigation.

4. Intercooling by means of water is successfully used in two-stage refrigerating installations with evaporating temperatures from –30° to –33° C., while for lower evaporating temperatures intercoolers with ammonia subcooling coils are more suitable.

5. Thermostatic expansion valves are successfully used for controlling the feed of refrigerant to the evaporator.

Behrndt bogtryk, Denmark

Copyright reserved

Approved For Release 2009/05/01 : CIA-RDP80T00246A007500340002-0

Approved For Release 2009/05/01 : CIA-RDP80T00246A007500340002-0

The Use of Semi-conductor Thermometers for Measuring Low Temperatures

Utilisation de thermistors pour la mesure des basses températures

I. A. PAVLOVA
The Scientific Research Institute of the Refrigerating Industry of the U.S.S.R., Moscow, U.S.S.R.

SOMMAIRE. Les thermomètres à résistance de semi-conducteur (thermistors) présentent un certain nombre d'avantages essentiels par rapport aux thermomètres à résistance de métal : faibles dimensions, grande sensibilité, faible inertie. La courbe des résistance termiques des thermistors descend le plus brusquement par de basses températures de 0° à –20° C. Des études poussées des thermistors effectuées par le VNIKhI pour des températures de +60° à –200° C. ont montré cette grande stabilité.

L'utilisation de thermistors s'est révélée très utile pour la mesure de la température superficielle ainsi que de celle des tissus internes des divers aliments. Un instrument de ce type a été mis au point au VNIKhI en 1957 et il est très répandu actuellement dans les entrepôts frigorifiques comme dans les laboratoires de recherche. Des instruments comprenant des thermistors, mis au point par l'Institut de Recherches Scientifiques de Léningrad pour la Mécanisation de l'Industrie de la Pêche sont utilisés pour la mesure de la température des produits de la pêche.

Semi-conductor thermometers are volumetric non-linear semi-conductor resistances. The value of the electric resistance of these instruments is subject to a sharp drop at an increase of temperature.

The main advantages of semi-conductor thermometers are in their high temperature sensivity, small dimensions and, consequently, a low thermal inertia of the temperature pickup, and a high stability of the characteristics in time. Semi-conductor thermometers are usually manufactured of oxide semi-crystalline semi-conductors with a large negative temperature coefficient. The following materials are used for the manufacture of semi-conductor thermometers: cobalt oxide (Co_2O_3), titanium dioxide (TiO_2), carborundum (SiC), etc. [1].

Required values of the specific resistance as well as of the temperature coefficient may be obtained by changing the relation of the components included in the semi-conductor thermometer.

Over thirty types of semi-conductor thermometers are manufactured in the Soviet Union.

Various types of semi-conductor thermometers are designated for operation in diverse conditions, *e. g.*, MMT-1 and KMT-1 are intended for use in enclosed dry rooms, MMT-4, KMT-4, EMT-1 – for use in conditions of high humidity and in liquids.

The following parameters are of importance in semi-conductor thermometers:

a) the value of resistance at 20°C termed "cold resistance":

b) the overall dimensions;

c) the value of the temperature coefficient of resistance in per cent per 1° .C. This coefficient α is usually given for the same temperature as in the case of "cold resistance", *i.e.* for 20° C.

The value of the temperature sensivity B, determining the sensitivity of a semi-conductor thermometer in the entire range of its operating temperatures, is also given quite often.

Approved For Release 2009/05/01 : CIA-RDP80T00246A007500340002-0

Approved For Release 2009/05/01 : CIA-RDP80T00246A007500340002-0

d) the maximum permissible temperature up to which the characteristics of the semi-conductor thermometer remain stable;

e) the maximum permissible power of dissipation, in watts, not causing destruction of the semi-conductor thermometer;

f) the time constant τ, characterizing the thermal inertia. – It is the time expressed in seconds required for the temperature of the semi-conductor thermometer to change by 63% of the difference between its own temperature and that of the surrounding medium. This difference is most often accepted as being equal to 100° C.

g) the specific heat "C", in joules per 1° C.

The characteristics of the semi-conductor thermometers, testifying to the clearly expressed dependence of the resistance upon the temperature, make them convenient for use as temperature pickups. The temperature coefficient, reaching $-2\frac{\delta}{\zeta}-6\%$ with some semi-conductor thermometers, exceeds by more than 10 times the temperature coefficient of metals.

The deviation of the actual value of the electric resistance from the nominal of the given type of semi-conductor thermometer by $\pm 20\%$ should be pointed out as a disadvantage of these instruments.

The problem of using semi-conductor thermometers for measuring temperatures is highly influenced by the selection of operating conditions.

An incorrect selection of operating conditions of the semi-conductor thermometer is followed by failures which are erroneously regarded by researchers as a property of the semi-conductor thermometers.

This, in particular, concerns the problem of selecting such a current strength that would not cause noticeable heating of the semi-conductor thermometer. All types of semi-conductor thermometers manufactured in the U.S.S.R. are provided with static volt-ampere characteristics.

The characteristic is linear in its initial part as there is no heating of the semi-conductor thermometer at a low current strength.

With the strength of the current increasing, the temperature of the semi-conductor thermometer is raised above that of the surroundings and its resistance drops.

The temperature-resistance curve is required for calculating the operating conditions of the temperature device.

The dependence of the specific resistance of the semi-conductor ϱ upon the temperature may be expressed within a not very wide range by an exponential equation (1):

$$\varrho = A_\varrho \cdot e^{\frac{B}{T}} \tag{1}$$

where A_θ and B are constant values characterizing the properties of the material of the semi-conductor thermometer, T – the absolute temperature (in °K). It thus follows that the values of the electric resistance of the semi-conductor thermometer R_T (in ohms) at the temperature T will be:

$$R_T = A \cdot e^{\frac{B}{T}} \tag{2}$$

where the constant A is equal to:

$$A = A_p \frac{l}{S} \tag{3}$$

l – is the distance between terminals (cm)

S – the cross section of the semi-conductor thermometer (cm^2).

The values of the constants A and B are given in the certificates of the semi-conductor thermometers.

Approved For Release 2009/05/01 : CIA-RDP80T00246A007500340002-0

Approved For Release 2009/05/01 : CIA-RDP80T00246A007500340002-0

To determine the expediency of using semi-conductor thermometers for measuring temperatures below 0° C., investigations have been carried out at the Scientific Research Institute of the Refrigerating Industry of the U.S.S.R. of EMT-1 bead-type semi-conductor thermometers. The temperature resistance curve as well as the stability of the characteristics of these instruments were formerly determined only for above zero centigrade temperatures. The temperature curve of the EMT-1 semi-conductor thermometer resistance was investigated in the temperature range of from –78° C. to 20° C.

All the measurements were performed by means of a five-decade high-ohmic precision potentiometer. A platinum resistance thermometer was used as a model. The temperature of the medium holding the semi-conductor thermometer being investigated was measured precisely within 0.005° C.

A temperature curve was obtained of the resistance dependence for the EMT-1 bead-type semi-conductor thermometer in the temperature range from –78° C. to 20° C.

This curve, illustrated in Fig. 1, indicates the most expedient utilization of semi-conductor thermometers at subzero temperatures: its most steep part is within the range of –30 to –40° C.

The stability of the characteristics of the EMT-1 semi-conductor thermometer was checked during 1958 every month. The semi-conductor thermometers being investigated were treated in the period between measurements with liquid nitrogen at –196° C. They were also periodically heated up to 100–120° C. in a dessicator and by means of electric current.

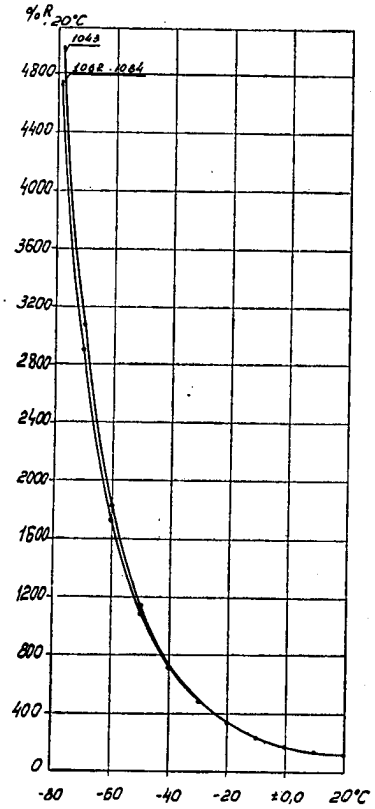

Fig. 1. The curves of the temperature dependence of the resistance for the EMT-1 semi-conductor thermometer (specimens Nos. 1943, 1062, 1084).

Approved For Release 2009/05/01 : CIA-RDP80T00246A007500340002-0

Approved For Release 2009/05/01 : CIA-RDP80T00246A007500340002-0

All the investigations have shown that the characteristics of semi-conductor thermometers remain constant wihtin 0.1° C.

A semi-conductor device for rapid measurements of temperature in one or two points has been developed by the Scientific Research Institute of the Refrigerating Industry of the U.S.S.R. This instrument was designated, in particular, for measuring the temperature on the surface and in the thickness of frozen and cooled foods: meat, butter, cottage cheese, sour cream and even eggs.

The semi-conductor temperature meter consists of pickups of the EMT-1 semi-conductor thermometer connected to an unbalanced Wheatstone bridge with a microammeter.

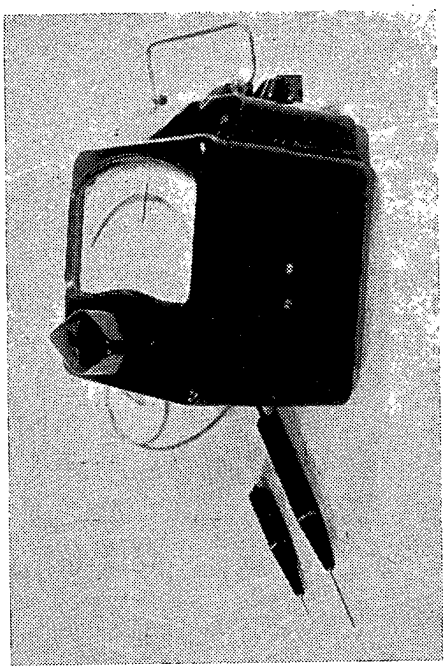

Fig. 2. A general view of the semi-conductor temperature meter.

A general view of the instrument is given in Fig. 2 which illustrates that the semi-conductor thermometers are inside special handles provided with contact plugs. The latter are connected on one side with platinum terminals of the semi-conductor thermometer, and on the other side with the connecting wires leading to the bridge. There are two types of temperature pickups:

a) a pickup for measuring the temperature in the bulk of the food. The bead-type semi-conductor thermometer is inside a special 1.5 to 2.0 mm dia. steel needle 40 to 80 mm long.

b) a pickup for measuring the temperature on the surface of food or some other substance.

The semi-conductor thermometer is set in this case inside a special 1.5 to 2 mm dia. steel tube so that its head is outside the tube while the platinum terminals are inside.

The temperature meter – a 50 microampres microammeter graduated in degrees of the temperature scale, the Wheatstone bridge and the supplying battery are mounted in a plastic box. All the regulating and switching devices are mounted on the side walls of the box.

Approved For Release 2009/05/01 : CIA-RDP80T00246A007500340002-0

Approved For Release 2009/05/01 : CIA-RDP80T00246A007500340002-0

The operating principle of the instrument may be explained by way of an examination of its electric circuit illustrated in Fig. 3.

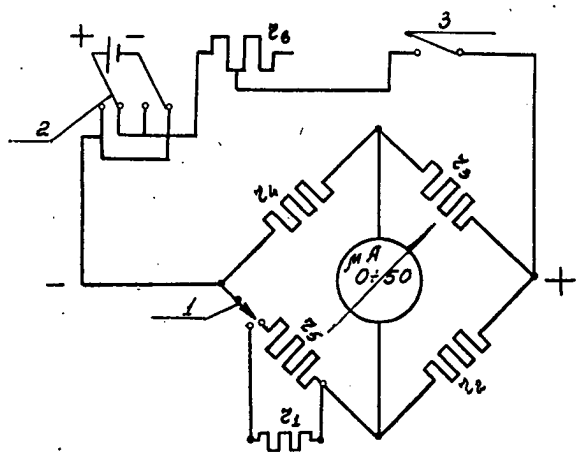

Fig. 3. The electric circuit of the semi-conductor temperature meter.

It is shown in the figure that the electric circuit of the instrument is represented by an unbalanced Wheatstone bridge.

Three arms of the bridge: τ_2, τ_3 and τ_4 are formed by constant resistance coils. The fourth arm τ_1 is a semi-conductor thermometer pickup changing its resistance in accordance with a change of the temperature of the surroundings.

For control of the voltage of the bridge peaks, the resistance may be replaced by a temporary fixed resistance τ_5 by means of the switch "I".

The resistance τ_5 is rated in such a wey that with the resistance switched into the bridge circuit the pointer of the instrument sets at the control red line of the scale.

The instrument bridge circuit has been calculated according to the method of Thevenin.

This fact causes an irregularity of the instrument scale.

Analysis have shown that for precise measurements within 0.1° C. in instruments with a range not exceeding 20° C. a sufficiently uniform scale can be obtained.

The instrument developed by the Scientific Research Institute of the Refrigerating Industry of the U.S.S.R. had to have, according to the requirements of the industry, a scale from –40° C. to 60° C. The instrument was made with two scales in order to reduce the irregularity of the scale as well as to make the measurements more precise.

Calculations have shown that the zero reading of the scale approximately coincides with 0° C.

The instrument is switched from one scale to the other by means of the switch "2" (Fig. 3). When calculating the bridge, the current in the bead-type resistances was assumed to be equal to one milliampere in accordance with the considerations mentioned in the discussion of the problem of selecting operating conditions of the circuit.

The voltage at the peaks of the bridge amounts to 1.4 V.

The semi-conductor temperature meters described above were successfully used in 1958 under industrial conditions at ice cream factories for measuring the temperature of the ice cream and other foods as well as at cold stores for measuring the temperature in cooled and frozen foods.

Approved For Release 2009/05/01 : CIA-RDP80T00246A007500340002-0

Approved For Release 2009/05/01 : CIA-RDP80T00246A007500340002-0

Several instruments that had been used under industrial conditions, were re-graduated at the end of 1958.

The characteristics of the instruments proved to be perfectly stable.

A new semi-conductor instrument with bead-type semi-conductor thermometers designed for measuring the difference of temperatures in two points was developed in 1958.

The two temperature pickups were set in this instrument in the adjoining arms of the bridge. Besides the instruments developed by the Scientific Research Institute of the Refrigerating Industry of the U.S.S.R., semi-conductor temperature meters of the KMT, KTE and other types designed at the Leningrad Scientific Research Institute of Mechanization of the Fish Industry have been used in the fisheries industry.

REFERENCES

1. VERVEY, E. Oxide semi-conductors. Collection Gosizdat, Moscow, 1954.

2. SHEFTET, I. T. Semi-conductor thermometer. The State Physical and Mathematical Literature Publishing house, Moscow, 1958.

Behrndt bogtryk, Denmark

Copyright reserved

Approved For Release 2009/05/01 : CIA-RDP80T00246A007500340002-0

Approved For Release 2009/05/01 : CIA-RDP80T00246A007500340002-0

An Attempt to Create a New Ammonia Refrigerating System for a Multi-story Refrigerated Warehouse

Essai de création d'un nouveau système frigorifique à ammoniac pour un entrepôt frigorifique à plusieurs étages.

ALEKSY TCHORZEWSKI, Graduate Engineer
ul. 20 Pazdziernika 767, Sopot, Poland

SOMMAIRE. Dans l'introduction l'A. traite d'un système frigorifique simple avec un réservoir tampon central placé sur le toit d'un entrepôt frigorifique. Ce système quelque peu démodé est cependant encore utilisé. L'A. démontre l'inefficacité de la commande manuelle, qui a pour conséquence de noyer les conduites d'aspiration des évaporateurs. D'où il résulte une élévation de la température d'évaporation. On peut pallier cet inconvénient en descendant le réservoir tampon au rez-de-chaussée, comme l'a fait l'A. dans trois grands entrepôts frigorifiques.

Il est cependant possible d'améliorer le système d'une autre façon, en établissant un nouveau système frigorifique à ammoniac. L'A démontre que lorsqu'on augmente, à l'aide de pompes, le débit de l'ammoniac liquide à travers les évaporateurs, le liquide fourni aux évaporateurs à la température du réservoir tampon est d'abord préchauffé sans évaporation, puis commence à bouillir. Un nouvel accroissement du débit de l'ammoniac liquide (avec noyage des conduites d'aspiration au niveau fixé à l'avance) entraîne un arrêt total de l'évaporation. A partir de ce moment le refroidissement ne s'effectue que par élévation de l'enthalpie du liquide. La température moyenne de l'ammoniac liquide dans les serpentins le plus proche possible de la température d'évaporation dans le réservoir tampon sera atteinte par réduction de la différence de température à l'arrivée et à la sortie des serpentins. C'est possible par suite d'une nouvelle augmentation du débit du liquide. L'A. pense que ce système frigorifique a sa valeur. Sans perte appréciable de la différence de température entre le milieu à refroidir et l'indication au manomètre d'aspiration, et sans dispositifs automatiques, cette solution permet de joindre les qualités des systèmes frigorifiques directs et des systèmes à saumure, à savoir: 1) Le réglage de l'humidité est rendu possible par réduction manuelle du débit du liquide, 2) Le dégivrage est facilité par l'utilisation d'ammoniac chaud, 3) L'ammoniac liquide est moins corrosif et a une moins grande viscosité, et 4) L'ammoniac liquide des serpentins a une plus grande inertie thermique que l'ammoniac en ébullition.

Many multi-story refrigerated warehouses up until now use a refrigerating system as shown in principle in Fig. 1. It is a direct ammonia expansion system with a central surge tank on the roof of the warehouse.

It requires an adequate ammonia feeding control for evaporators. Otherwise they may be overflooded, and the liquid ammonia will be pulled to a considerable height up in the vertical suction pipe. The liquid ammonia will partially fill up the pipe. The flow of ammonia vapour will induce violant gurgitation of this liquid. The phenomenon is similar to that in an ammonia coil of a flooded evaporator.

It is difficult to deduce the relationship of the static head from many factors, as we have to do here with a flow of a two-phase liquid. The static head in the vertical suction pipe involves a rise of evaporating temperature in the evaporator over the temperature of the liquid in the central surge tank.

This means a loss of the output of the evaporator.

On the other hand lack of liquid ammonia may involve as great a loss in

Approved For Release 2009/05/01 : CIA-RDP80T00246A007500340002-0

Approved For Release 2009/05/01 : CIA-RDP80T00246A007500340002-0

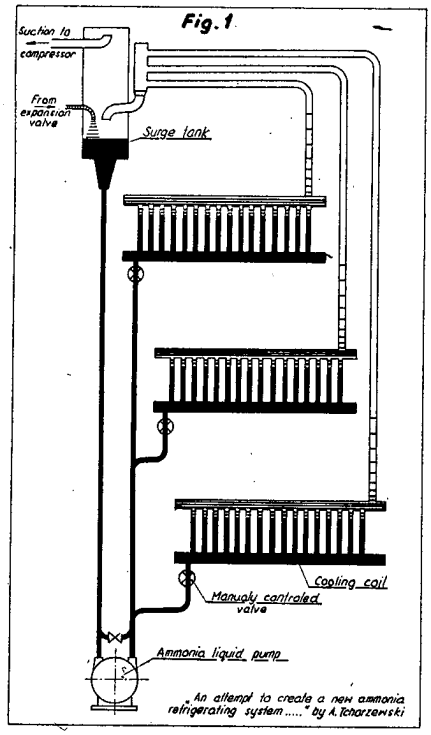

Fig. 1. A direct ammonia expansion system for a multi-story refrigerated warehouse with a surge tank on the roof.

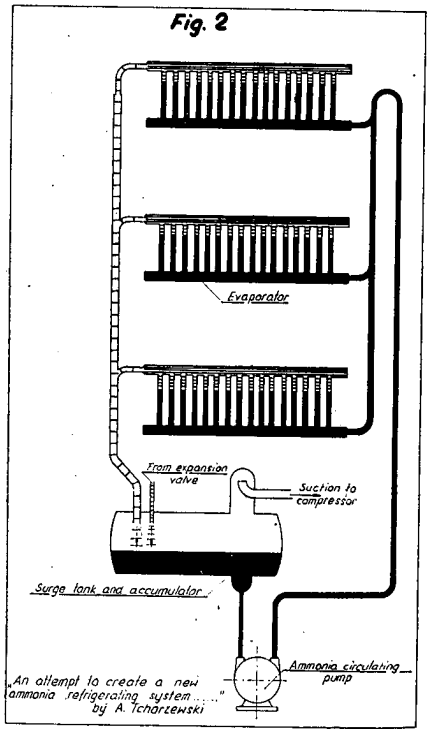

Fig. 2. A direct ammonia expansion system for a multi-story refrigerated warehouse with a surge tank and an accumulator placed in the basement.

output; this is the most frequently met in warehouses with manual liquid ammonia feed control.

To compare different refrigerating systems from the above-mentioned point of view, it is advisable to introduce a factor of the effectiveness of cooling surface of the coil of an evaporator:

$$\xi = \frac{\textit{The output of cooling coil attained}}{\text{Attainable output of cooling coil without static head and sufficient feeding with liquid ammonia.}}$$

It should be possible to solve this problem by using automatic control of liquid feeding to the evaporators instead of manual control. Though this type of automatic control is widely used in all types of refrigerating equipment, as big refrigerated warehouses are considered, their application seems to be questionable. Big refrigerated rooms, loaded almost permanently with goods, are less accessible for repairs and spare parts exchange. Control devices should be placed outside of the refrigerated space in a ventilated room. The equipment appears to be much more complicated and expensive. To be dependable such large refrigerating equipment should be as simple as possible.

To avoid these difficulties, a refrigerating system based on the principle in Fig. 2 is sometimes used. The suction pipe is conducted down vertically to prevent the rising of the static head. The surge tank is placed beneath the lowest evaporator. The feeding of the evaporators with ammonia is performed only by means of ammonia pumps. There is no problem of controlling the circulation

Approved For Release 2009/05/01 : CIA-RDP80T00246A007500340002-0

Approved For Release 2009/05/01 : CIA-RDP80T00246A007500340002-0

and distribution of liquid ammonia between separate evaporators, because the ammonia pumps used should have an overwhelming output.

The author realised this system in big warehouses with full success backed by an 8 years' experience. However it is very difficult to persuade investors of the dependability of this system, because in the event of damage to all of the ammonia pumps, there is no means for further running the equipment.

However, there is another way to avoid the difficulties induced by the static head in the suction line.

Volatile refrigerants can actuate cooling of the coil surface not only by evaporation but also by raising its sensible heat just as is done by brine.

We return to Fig. 1. As the feeding of the liquid ammonia to the coil increases, followed by an increase in the static head in the suction line and a rise of evaporating temperature, two zones in the coil of an evaporator arise.

In the lower zone the liquid ammonia is warmed up from the temperature in the surge tank to the temperature of evaporation in the coil. In the upper zone the ammonia is evaporated at a temperature corresponding to the actual static head. The lower zone is continually increasing, the upper is decreasing. Finally as the static head attains a definite value, the evaporation ceases, and the cooling of the coil proceeds further in the same way as with brine. In this system the liquid ammonia, after leaving the cooling coil, is directed through the vertical pipe towards the surge tank. In the upper part of this pipe line it begins to expand progressively as it approaches the surge tank. Evaporation in the coil is replaced by expansion in the upper portion of the suction pipe and the surge tank. The relationship between the areas of the two above-mentioned zones of a cooling coil, and the general output of the coil, on one side, and the value of ammonia circulation through the coil, on the other side, by fixed evaporating temperature in the surge tank, and air temperature in the freezing room, and fixed static head, can be expressed by the following system of two equations:

Nomenclature:

F	m^2	– Area of cooling coil
ε	dimensionless	– Ratio $\frac{\text{area of warming up liquid ammonia zone}}{\text{total area of coil}}$
k_1, k_2	$\frac{\text{kcal}}{m^2 \cdot °C. \cdot h}$	– Heat transfer coefficient for the warming up and evaporating zones, respectively
$\Delta i, \Delta i_2$	$\frac{\text{kcal}}{\text{kg}}$	– Increase of refrigerant enthalpy in warming up and evaporating zones respectively
$\Delta t_1°, \Delta t_2°$	°C.	– Mean temperature difference of air and liquid ammonia respectively of air and evaporating ammonia
G	$\frac{\text{kg}}{\text{h}}$	– Quantity of liquid ammonia fed to evaporator (liquid ammonia circulation)
Q	$\frac{\text{kcal}}{\text{h}}$	– Total output of evaporator (coil)

The following two equations can be deducted without further explanations:

$$Q_0 = \varepsilon \cdot F \cdot \Delta t_1^0 \cdot k_1 + (1 - \varepsilon) \cdot F \cdot \Delta t_2^0 \cdot k_2 = G(\Delta i_1 + \Delta i_2) \tag{1}$$

$$\frac{\Delta i_1}{\Delta i_2} = \frac{\varepsilon \cdot \Delta t_1^0 \cdot k_2}{(1 - \varepsilon) \cdot \Delta t_2^0 \cdot k_2} \tag{2}$$

Approved For Release 2009/05/01 : CIA-RDP80T00246A007500340002-0

Approved For Release 2009/05/01 : CIA-RDP80T00246A007500340002-0

From these two equations we deduce the following relationship of Q respectively ε from G:

$$Q = \varepsilon \cdot F \cdot \Delta t_1^0 \cdot k_1 + (1 - \varepsilon) \cdot \Delta t_2^0 \cdot k_2 = G \cdot \Delta i_1 \cdot \left(1 + \frac{(1-\varepsilon) \cdot \Delta t_2^0 \cdot k_2}{\varepsilon \cdot \Delta t_1^0 \cdot k_1}\right) \quad (3)$$

Fig. 3 gives a graphical interpretation of this equation for the following example:

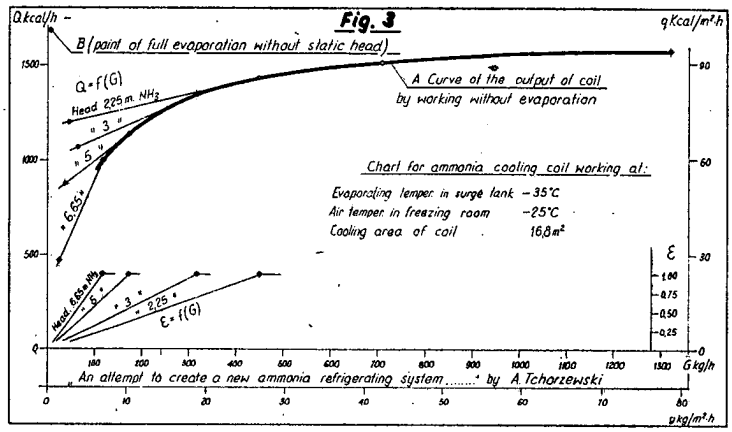

Fig. 3. The graphical interpretation of the relations between Q and ζ of the evaporative coil specified, on one side, and the ammonia circulation through the coil, on the other side.

The coil, as in Fig. 1, of an area 16,8 m², $k_1 = k_2 = 10 \frac{\text{kcal}}{\text{m}^2 \cdot °\text{C.} \cdot \text{h}}$ temperature of the air –25° C., evaporating temperature of ammonia in the surge tank –35° C. The difference of temperature, for simplification, is given as the arithmetic mean.

Fig. 3 shows a series of straights, interpreting the function Q = f (G) for different values of static head in the suction vertical pipe (isobars).

The ratio of growth of the output involved by the growth of the ammonia circulation ($\Delta Q/\Delta G$) is greater because of the increased value of the static head.

Another series of straights represents the function:

ε = f (G) for the same values of the static head. They all are produced from equation (3). With the increase of ammonia circulation, the zone of evaporation and its output decrease. When $\varepsilon = 1$, it means that when no evaporation occurs in the coil, equation (3) is simplified to:

$$Q = F \cdot \Delta t_1^0 \cdot k_1 = G \cdot \Delta i_1 \quad (4)$$

As enthalpy of liquid ammonia is practically, in the actual scope, independent from pressure, the relation:

Q = f/G/ – is now independent from static head.

In Fig. 3 equation (4) is presented by the single curve A for all values of the static head. Point B determines the highest attainable output of the coil by evaporating ammonia without the static head in the suction vertical line. By increasing the ammonia circulation through the coil at constant static head alongside the isobar, we reach first the point determined by the condition $\varepsilon = 1$ and then we proceed alongside curve A. The output of the coil is still increasing and we

Approved For Release 2009/05/01 : CIA-RDP80T00246A007500340002-0

Approved For Release 2009/05/01 : CIA-RDP80T00246A007500340002-0

are in a position to approach discretely the highest attainable output given by the ordinate of point B by a corresponding increase of the ammonia circulation. The factor of the effectiveness of the surface of the coil at a certain point on curve A is determined by the ratio of ordinates of this point and of point B.

It is obvious that the increase of G (ammonia circulation through the coil) is advantageous for the value of ξ. However we should not surpass some reasonable limit. For this limit we can accept the circulation of ammonia liquid measured in kg/1000 kcal. equal to the circulation of the brine $CaCl_2$, sp. gr. 1,28, by –30° C. and by 2° C. temperature difference, namely 785 kg/1000 kcal. Then in the example above the limit of ammonia liquid circulation will be 1320 kg NH_3/h. The corresponding output will be 1585 kcal/h by temperature difference of liquid ammonia –1,11° C. and ξ = 0,942. It does mean the loss of only 5,8% of the active surface of the coil.

Further we can deduce from the diagram, that in every refrigerating plant it would be advantageous to use only evaporative cooling in the coils, if it is possible to place the central surge tank low enough to prevent the creation of the static head in the vertical suction pipe; in a multi-story warehouse this can be done only on the upper floor by placing the central surge tank on the same floor. However, in the lower floors there are always favourable conditions for the creation of the static head because of lack of automatic liquid ammonia level control. We can work there on curve A with ammonia liquid circulation in the neighbourhood of the above-mentioned limit. It is also possible to use a mixed system: the above-described and the system in Fig. 2, by placing the central surge tank half way up the multi-story warehouse. Then all floors above the central surge tank will work on pure evaporation and below – on curve A – without evaporation.

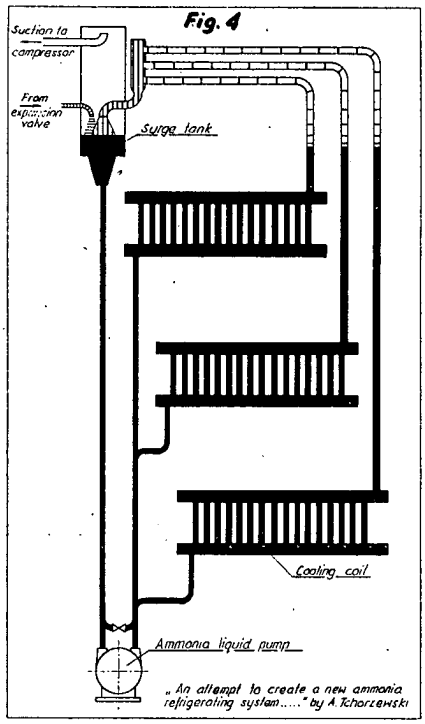

Fig. 4. A direct ammonia expansion system for a multi-story refrigerated warehouse fully flooded and operating without evaporation of liquid ammonia.

Approved For Release 2009/05/01 : CIA-RDP80T00246A007500340002-0

Approved For Release 2009/05/01 : CIA-RDP80T00246A007500340002-0

On the other hand, the author suggests that all these mixed systems, involving different conditions of work on the individual floors, complicate the refrigerating equipment and engineering of them. It is more practical to abandon some negligible gains in the value of ξ for the cooling surface and to establish unified working conditions on curve A for all floors. Such a liquid ammonia refrigerating system is presented in Fig. 4. The lay-out of this system is practically the same as for the system presented in principle in Fig. 1. Only the output of the ammonia pump and the diameter of liquid feeding pipe to coils are greater than in the system on Fig. 1.

Apart from the fact that the refrigerating system described above effectively prevents the creation of a static head in the vertical suction pipe lines, it possesses numerous advantages. Together, they combine the merits of different systems now in use and permit treating this system as a separate one. These advantages are as follows.

ADVANTAGES IN COMMON WITH THE DIRECT AMMONIA EXPANSION SYSTEM

In the recommended liquid ammonia refrigerating system, the lowest liquid ammonia temperature in the cooling coils is equal to the evaporating temperature of ammonia in the surge tank, and the highest temperature – very near the evaporative temperature as the specific heat of liquid ammonia is comparatively great (1,07 kcal/kg°C.).

This advantage is shown above in the numerical example. On the contrary, in the case of brine, its lowest temperature in the cooling coil is at least 3° C. higher than the evaporating temperature, and the temperature difference of brine 2° C. (compared to 1,11° C. in liquid ammonia in our example). The obvious thermodynamical advantage of the recommended liquid ammonia system places it in the nearest neighbourhood of the direct ammonia expansion system.

Hot ammonia presents the simplest way of defrosting cooling coils.

Ammonia is not corrosive.

The viscosity of liquid ammonia is lower than brine. In the recommended liquid ammonia system, as well in every closed brine system, the head of the circulating pump is determined chiefly by the resistance to the flow of the liquid.

With the low viscosity of liquid ammonia, the head of the ammonia pump and its power consumption should be small.

ADVANTAGES IN COMMON WITH THE BRINE SYSTEM

To stop cooling in a coil or a series of coils in the recommended liquid ammonia system, it is sufficient to use only one valve on the feeding side of the liquid ammonia. Should the solenoid valve be used, it is enough to use 1 valve, compared to 2 solenoid valves needed in the direct ammonia evaporation system. The behavior of the cooling coil full of liquid ammonia after being closed on the feeding side is different compared to the behavior of an evaporator closed on both sides. In the last case, after warming up of the liquid ammonia present in the evaporator, the cooling effect of the coils ceases abruptly. In the first case after closing the valve on the feeding side of the coil, the liquid ammonia, filling up the whole coil, will be warmed up to the temperature of boiling under the existing static head in the pipe, and then the liquid begins to boil under dimished mean temperature difference of the air and the evaporating liquid. It results ni a milder air temperature curve, during the time that the series of coils is shut.

By manual control of the ammonia liquid circulation, the level of the mean temperature of the liquid inside the coil and of the cooling surface can be changed or maintained. In this simple way the humidity of the air can be controlled.

Approved For Release 2009/05/01 : CIA-RDP80T00246A007500340002-0

Approved For Release 2009/05/01 : CIA-RDP80T00246A007500340002-0

The whole system is very simple. No automatic devices are needed for the distribution and control of the flow of the liquid ammonia.

SPECIAL ADVANTAGES

Old direct expansion systems with manual controls as in Fig. 1 can be changed without considerable costs. The author's aim in this paper is to present the principle of the liquid ammonia refrigerating system without going into details of the lay-out.

Behrndt bogtryk, Denmark

Copyright reserved

Approved For Release 2009/05/01 : CIA-RDP80T00246A007500340002-0

Approved For Release 2009/05/01 : CIA-RDP80T00246A007500340002-0

Entrepôts frigorifiques, standardisés ou individuels, polyvalents ou spéciaux

Standard or Non-standard Cold-stores; Multi-purpose or Special Plants.

GEORGES GÄNGER
Budapest, Hongrie

SUMMARY. The freezing capacity in Hungarian cold-stores was increased over the last 10 years at a ratio 1:4.5, the floor surface of the rooms at –20° C., by 1:1.65, that of spaces at 0° C. was doubled. During the next 15 years, the present capacities will be still increased at a ratio of about 1:2.30. With such rapid development, it is necessary to study accurately the problem of the most economical use of investments. Two of the most important points in this connection are discussed:

1. Must the new cold-stores have standard or non-standard design?

The greatest savings in construction costs can be obtained by extended standardization. But in a country of restricted area, it would be impossible to adopt it unreservedly without considering local requirements of production and delivery of the foodstuffs to be cooled and the purpose of some cold-stores. With such data, it seems more advisable to elaborate standard designs and to put them into effect with a slight adaptation, required by the different local conditions.

2. Must these plants be multi-purpose or special ones?

Concerning the special conditions of production of the different foodstuffs in the country, the special cold-stores of prime importance are those processing poultry, meat and those for fruit. They must be provided only if they meet severe technological requirements, for their efficiency is less than that of multi-purpose coldstores. To secure the economical efficiency of investments, it is consequently necessary to build mainly multi-purpose cold-stores.

Après la fin de la deuxième guerre mondiale, la Hongrie possédait trois entrepôts frigorifiques polyvalents à Budapest et quelques établissements spéciaux de capacité modeste en province, servant principalement au stockage de la volaille destinée à l'exportation. Les premiers – dont l'un fut à sa construction le plus grand entrepôt frigorifique de l'Europe – disposaient pour la plupart, de chambres d'une température de 0° C.; dans les salles de congélation, à capacité d'ailleurs insuffisante, la température n'était que de –8 à –10° C. Le refroidissement était effectué à l'aide d'une saumure de NaCl, utilisée comme intermédiaire frigorifique. Dans ces conditions, le développement de l'industrie frigorifique devait s'orienter vers les trois points suivants:

– il fallait d'abord augmenter considérablement la capacité totale d'entreposage et notamment la capacité de congélation ainsi que la surface servant à l'entreposage de la denrée congelée;

– il fallait ensuite généraliser la congélation à –35/–40° et le stockage à une température de –20° C. dictés par la technologie moderne;

– puis, finalement, il fallait réaliser cette augmentation de capacité par le système de détente directe du fluide frigorigène ammoniac.

Nous avons donc attaqué ces travaux de développement, il y a dix ans; au cours des années suivantes, nous avons construit plusieurs nouveaux établissements, et agrandi quelques entrepôts existants. Dans le même temps, nous avons équipé, pour les basses températures, tous nos entrepôts frigorifiques. Aussi, la capacité de congélation a-t-elle été augmentée de 350%, la surface des chambres à –20° C., de 65% et la surface des chambres à 0° C., de 100%.

Au cours de ces travaux, nous avons réalisé de nombreuses expériences con-

Approved For Release 2009/05/01 : CIA-RDP80T00246A007500340002-0

Approved For Release 2009/05/01 : CIA-RDP80T00246A007500340002-0

cernant le choix de l'emplacement, le caractère polyvalent ou spécialisé de l'entrepôt, la capacité la plus appropriée, la disposition des chambres, la juste répartition de ces chambres selon les températures, les différentes solutions techniques, etc. . . . Toutes ces expériences pourront être utilisées lors de la réalisation de nos futurs programmes.

Mais en étudiant à fond les problèmes de construction des entrepôts frigorifiques, de nombreuses questions techniques et économiques se sont également posées; leur solution est d'autant plus importante que, pendant les 15 années à venir, nous avons l'intention d'augmenter de 130% la capacité atteinte à ce jour. La nécessité d'utiliser au mieux les investissements s'impose donc. La grande difficulté est que ces problèmes ne puissent être résolus par des méthodes scientifiques à cause de leur nature même, et en raison de la diversité comme du grand nombre des facteurs exerçant une influence sur leur solution. Tout au plus peut-on les approcher, à l'aide de calculs d'économie ne considérant qu'une partie des facteurs entrant en ligne de compte. Vu ces circonstances, la décision ne peut être prise que sur la base de considérations plus ou moins subjectives de certains points de vue. A titre d'exemple, je me réfère à une seule question, discutée par tous les frigoristes qui s'occupent de la construction de nouveaux entrepôts, c'est la construction à un seul niveau ou à plusieurs étages. Ce problème, à ma connaissance, n'a pas été résolu à l'aide de méthodes scientifiques exactes, même dans des cas concrets.

Pour le moment, je voudrais seulement traiter deux questions d'importance fondamentale, à savoir:

1°) les nouveaux entrepôts frigorifiques doivent-ils être construits suivant des plans standardisés ou sur la base des projets individuels?

2°) ces établissements doivent-ils être conçus pour une exploitation polyvalente, ou dans un but spécialisé?

Selon mon opinion, ces deux questions gardent un intérêt général, étant donné que l'augmentation de la capacité de l'industrie frigorifique est un problème, non seulement pour l'Europe en général, mais pour le monde entier. Dans de nombreux pays, la construction des entrepôts frigorifiques nouveaux est réalisée sous la direction d'organisations économiques, intéressant toute l'industrie ou une partie très importante de celle-ci. Ces organisations sont en mesure d'exécuter leur programme sur la base de principes uniformes, en assurant l'utilisation la plus efficace des capitaux investis. Compte tenu de ces circonstances, il y a intérêt à étudier les questions posées, tant celle des constructions standardisées permettant une diminution des frais d'investissement, que celles du caractère polyvalent ou spécial, décisives au point de vue du régime de l'exploitation.

1°) Par projets standardisés, on entend une documentation technique englobant tous les détails du bâtiment et de l'équipement mécanique et frigorifique, sur la base desquels on peut procéder à la construction, un nombre de fois indéterminé, sans aucune modification.

La construction sur la base de projets standardisés présente des avantages considérables. Se rapportant à un seul entrepôt, les frais pour l'élaboration des projets sont sensiblement réduits; de même, le temps nécessaire à ce travail est beaucoup plus court. En général, pour les projets standardisés, les plans détaillés sont étudiés très à fond, puisqu'au cours d'exécutions répétées, les frais causés par tous ces moindres détails se trouveraient multipliés. C'est ainsi qu'on établit des plans meilleurs et plus économiques. Même l'exécution est plus économique par l'emploi étendu de la préfabrication, étant donné que le prix de certains éléments préfabriqués revient meilleur marché du fait de la quantité construite. Eventuellement, certains travaux d'assemblage peuvent être effectués en fabrique, rendant ainsi la durée des travaux à pied d'oeuvre plus courte, et causant une certaine diminution des frais de construction. Les avantages des établissements standardisés apparaissent surtout quand on les construit en grand nombre et dans un ordre de succession très rapide.

Toutefois, ces avantages exigent la stricte observation de conditions fixées et contiennent de ce fait, le germe de certains inconvénients. La moindre modification

Approved For Release 2009/05/01 : CIA-RDP80T00246A007500340002-0

Approved For Release 2009/05/01 : CIA-RDP80T00246A007500340002-0

apportée à des projets standardisés comporte le danger de réduire, ou même d'annihiler complètement les économies du coût de construction dues à des exécutions répétées.

Les conditions standard fixées rendent aussi très difficiles, voire impossibles les modifications qui pourraient être rendues nécessaires par l'étude des nécessités et des données locales du milieu d'établissement de l'entrepôt frigorifique. Même sans vouloir faire des concessions à la recherche de l'utilisation la plus favorable, on peut rarement se tenir rigidement à l'exécution des plans standardisés.

D'autre part, il est évident qu'en étudiant le développement du réseau des entrepôts frigorifiques, et en basant ce développement sur des exécutions standardisées, un critère de premier ordre est celui des possibilités de l'organisation construisant et exploitant des entrepôts frigorifiques en fonction de l'étendue du pays. On peut toutefois utiliser sans aucune crainte des projets standardisés, si les services attendus des établissements sont similaires. Mais les conditions locales des produits à traiter dans les entrepôts frigorifiques, depuis leur production jusqu'à leur distribution, rendent désirable d'avoir un choix de plans standardisés à disposition, afin de pouvoir adopter ceux correspondant le mieux aux besoins.

En considérant ces données pour un pays d'une étendue comme celle de la Hongrie, la conclusion est la suivante:

On peut admettre, sans étude approfondie, qu'il est avantageux, même nécessaire, de prévoir des entrepôts frigorifiques standardisés d'une capacité modeste de quelques centaines de tonnes, pour des municipalités dont l'approvisionnement en denrées périssables ou l'importance de leur production exigent des possibilités de réfrigération.

La question des entrepôts frigorifiques de grande capacité, à réaliser selon des projets standardisés, est beaucoup plus complexe étant donné que les avantages d'une construction standardisée ne peuvent être exploités à fond, vu le nombre relativement restreint de ces grands entrepôts frigorifiques. Il est en effet difficile de trouver plusieurs endroits présentant des données tellement similaires, que la construction d'entrepôts frigorifiques identiques y serait justifiée. Compte tenu des indications mentionnées ci-dessus, il faudrait aussi comparer les frais de l'élaboration des plans et de l'exécution d'une construction non standardisée, par rapport aux dépenses supplémentaires d'exploitation pendant des dizaines d'années, que causerait la construction d'un entrepôt standard qui ne tiendrait pas compte des exigences de l'exploitation locale.

Il semble donc préférable de construire des entrepôts frigorifiques à grande capacité, de quelques milliers de tonnes, en ne se tenant pas strictement aux projets standardisés, mais en les adaptant avec le minimum de modifications possible, tout et conservant les principes généraux et les solutions les mieux choisies.

C'est ainsi que l'on peut, par exemple, conserver les plans pour les liaisons de l'entrepôt avec l'extérieur; pour la réfrigération des chambres; pour la congélation; pour le stockage des produits congelés; pour les salles de réchauffage, les chambres de manutention et la salle des machines. De même, pour les indications concernant le choix et la pose du matériau isolant. De même encore pour le schéma de l'installation frigorifique, les plans des évaporateurs, diffuseurs d'air, etc.... la pose des portes des chambres froides, etc.

En conclusion, en ce qui concerne les grands entrepôts frigorifiques, on peut dire qu'au lieu d'établissements standardisés, on est arrivé à des types mixtes, résultant d'un compromis entre les principes rigoureux de la construction standardisée et la construction totalement indépendante. Mais, à mon avis, vouloir se tenir uniquement à la standardisation, dans les limites assez étroites de l'organisation de l'industrie frigorifique, conduirait, en négligeant les exigences locales, à des pertes qui seraient certainement beaucoup plus grandes que les économies résultant de l'application de n'importe quelle standardisation.

2°) De même faut-il construire les nouveaux entrepôts frigorifiques en établissements polyvalents ou spécialisés? Il n'est pas moins difficile de répondre à cette question. Ces deux types se distinguent par leur équipement technique, et par la température à maintenir dans les chambres frigorifiques.

Approved For Release 2009/05/01 : CIA-RDP80T00246A007500340002-0

Approved For Release 2009/05/01 : CIA-RDP80T00246A007500340002-0

Les Etablissements polyvalents doivent assurer toutes les conditions nécessaires pour la conservation à longue durée de toutes les denrées périssables. En pratique, cela signifie une température dépassant de quelques degrés le point de congélation jusqu'à –23° C. dans les chambres de stockage, et jusqu'à –40° C. dans les tunnels de congélation. Il paraît opportun d'équiper une partie des chambres frigorifiques, de manière que chacune d'elles soit capable de stockage au-dessus du point de congélation, et à basses températures, selon les besoins.

Par contre, l'équipement des établissements spécialisés ne vaut que pour le but précis pour lequel il a été prévu. Pour le stockage des fruits par exemple, une température de 0° C. suffit. Dans les établissements à congélation ultra-rapide, il n'est envisagé que des chambres d'entreposage à –20 –23° C. et des appareils de congélation. Les entrepôts frigorifiques pour la volaille doivent être équipés avec des tunnels à réfrigération, et à congélation rapide, ainsi qu'avec des chambres de stockage à basses températures. De plus, les établissements spécialisés doivent être pourvus des différents équipements nécessaires à la préparation des denrées qu'ils doivent traiter.

Les buts très différents les uns des autres et la diversité des équipements en résultant, ont des conséquences considérables quant à l'utilisation de ces établissements.

Les Entrepôts Frigorifiques polyvalents conviennent en général à tous les secteurs de la production des denrées périssables; en conséquence, leur exploitation est assez uniforme pendant les différentes saisons, permettant une répartition avantageuse des frais d'opération, d'entretien et d'amortissement.

Les Entrepôts Frigorifiques établis pour un but spécial ne sont utilisés que dans la saison productive de la marchandise qu'ils traient; par conséquent, leur exploitation est irrégulière et saisonnière. Les chambres de stockage pour fruits ne sont utilisées que pendant 6–8 mois, tandis que la saison des entrepôts à volailles est encore plus courte. La saison de congélation ultra-rapide dure pendant 4 mois environ pour les fruits et 5 mois environ pour les légumes. Le cas est identique pour les entrepôts frigorifiques d'abattoirs, bien que leur caractère saisonnier soit moins accusé. Ce sont seulement les établissements spécialisés aux industries de la pêche qui peuvent supporter la comparaison avec l'exploitation des établissements polyvalents, à cause de la constance de leur production.

Je crois qu'il est inutile d'illustrer ces constatations par des données statistiques; mais je voudrais tout de même mentionner, à titre d'exemple, qu'en Hongrie l'exploitation annuelle moyenne des entrepôts frigorifiques polyvalents – c'est-à-dire le quotient $\frac{\text{totalité des poids stockés par jour}}{365 \times \text{capacité totale}}$ atteignait en 1958 la valeur de 77,6%. A titre de comparaison, je rappelle que le coefficient d'utilisation général des entrepôts frigorifiques publics en France a atteint 47,5% en 1956. On est arrivé à cette valeur en Hongrie en utilisant pour le stockage à longue durée de la viande et des fruits presque uniquement des établissements polyvalents. Un degré d'utilisation aussi élevé serait impossible à atteindre dans des établissements spécialisés.

L'indice économique, mesuré par le degré annuel d'utilisation moyenne plaide en général en faveur de la construction d'établissements polyvalents. Mais afin d'apprécier cette question d'une manière impartiale, il faut prendre en considération certains arguments importants qui ne veulent point accepter cet indice comme décisif. Toutefois, comme il n'est pas possible d'évaluer cette question avec chiffres à l'appui, qu'il me soit possible d'évoquer le problème compliqué des entrepôts frigorifiques standardisés. Telles sont aussi certaines sujétions d'organisation industrielle et les exigences formulées par la qualité des produits. Je voudrais citer quelques exemples, à savoir: les centres de la production des fruits, ou bien d'élevage des volailles avec leurs besoins en réfrigération et en congélation, ne coïncident généralement point avec les lieux de construction des entrepôts polyvalents, dont l'établissement se justifie dans les grands centres de consommation, c'est-à-dire dans les régions industrielles et dans les villes. D'autre part

Approved For Release 2009/05/01 : CIA-RDP80T00246A007500340002-0

Approved For Release 2009/05/01 : CIA-RDP80T00246A007500340002-0

il est avantageux de soumettre au froid les produits à réfrigérer et à congeler le plus près et le plus tôt possible du lieu de production, puisque la matière première arrivera ainsi toute fraîche pour son traitement frigorifique sans avoir été éprouvée par un transport. C'est pourquoi on ne peut pas se passer des entrepôts frigorifiques spécialisés, quoique leur exploitation soit limitée par des saisons plus ou moins longues.

Considérant les circonstances particulières de production des denrées périssables en Hongrie, parmi les entrepôts frigorifiques spécialisés, la première place est occupée par les installations pour l'industrie des volailles; une grande importance doit être donnée aussi aux abattoirs. Le développement du réseau des installations pour le triage, l'emballage, la préréfrigération, la congélation ultra-rapide et le stockage dans les régions à productions fruitières, sera effectué sous peu. La proportion de la capacité entre établissements polyvalents et spécialisés est de 83 à 17.

Tout en cherchant la manière la plus économique d'investir, on arrive à la conclusion qu'il est plus avantageux de développer dans la plus grande mesure le réseau des entrepôts frigorifiques polyvalents. Ces établissements n'assurent pas seulement la meilleure possibilité d'exploitation, mais à l'unité de capacité ils peuvent être construits le plus économiquement car le nombre d'installations à construire est relativement élevé. Il est aussi recommandé de ne construire des entrepôts frigorifiques spécialisés, également indispensables, que pour des capacités strictement exigées par des buts spéciaux, rigoureusement technologiques, tel un traitement primaire par le froid avant réfrigération ou congélation, et tel un entreposage temporaire. Dans ce cas, on ne doit prévoir qu'une capacité limitée aux besoins locaux, car il est plus économique de transporter dans les entrepôts frigorifiques polyvalents les denrées à stocker, aussitôt après leur congélation.

Dans mon étude, je ne voulais indiquer que quelques facteurs à considérer lors d'une décision à prendre en réponse aux deux questions que j'ai posées.

Comme suite à cette étude, il faudrait établir une méthode pour calculer exactement l'économie résultant de l'emploi d'une solution ou de l'autre. Mais il faut bien admettre que les entrepôts frigorifiques standardisés ne peuvent remplacer, dans tous les cas, les établissements construits sur une base individuelle, de même que les établissements polyvalents ne peuvent remplacer les établissements spécialisés.

Behrndt bogtryk, Denmark

Copyright reserved

Approved For Release 2009/05/01 : CIA-RDP80T00246A007500340002-0

Approved For Release 2009/05/01 : CIA-RDP80T00246A007500340002-0

Influence of Kinds of Soils and Ground-Water Conditions on Soil Freezing Progress and Frost-heaving

Influence des natures de sols et de la présence d'eaux souterraines sur la congélation du sol et le boursouflement dû au gel.

RADZIMIR PIETKOWSKI, D. Sc., Professor
Polytechnic University, Warsaw, Poland

SOMMAIRE. L'A. à introduit quelques modifications dans l'équation de Ruckli pour le cas où il se produit une montée d'eau souterraine par capillarité pendant la congélation et il en a dérivé une équation gnérale pour le calcul de la congélation des sols à température de congélation constante. Les calculs effectués à l'aide de cette équation permettent aussi de déterminer l'étendue à prévoir au boursouflement dû au gel.

L'équation dérivée permet de tracer deux courbes de congélation extrêmes: (a pour l'eau, et (b) pour un sol saturé d'eau. Toutes les courbes intermédiaires relatives aux cas d'aspiration d'eau supplémentaire par capillarité se trouvent entre les deux courbes extrêmes.

Les phénomènes physiques qui apparaissent lorsque le niveau de congélation approche de la nappe phréatique obligent à procéder à des adaptations des calculs. On cite un exemple de calcul.

Les courbes calculées pour divers sols, températures de congélation, hauteurs d'aspiration de l'eau et perméabilités ont permis de tirer de nombreuses conclusions pratiques sur le temps de congélation, ainsi que sur la possibilité de boursouflement du sol et sur son étendue dans différentes conditions.

Le rapport comprend des conclusions résultant de nombreux calculs expérimentaux; les conclusions font ressortir les natures de sols et les conditions naturelles présentant un danger pour la construction d'entrepôts frigorifiques.

A clear understanding of phenomena in soils under floor slabs of cold stores when inner freezing acts permanently is very important for designing of these buildings. Two main problems must be solved here: the speed of frost penetration beneath the floor in various soil conditions and the consequences arising with soil freezing.

Following the priniciples and solution of R. Ruckli we can obtain the general differential equation by studying frost penetration during an infinitely small time interval dt (Fig. 1).

This equation deduced[1] by the author and varying in detail from an analogous equation of Ruckli has the following form:

$$\frac{d\xi}{dt} = \frac{A}{\xi + s} - Bv \tag{1}$$

where

$$A = -\frac{\lambda_1 \vartheta_I}{C_2 \vartheta_{II} + C\,n - \frac{1}{2}\vartheta_I C_1 - 0{,}045 n \vartheta_I C_L}$$

[1] Its deduction will be given in a special publication by the author on various cases of heat penetration in soils.

Approved For Release 2009/05/01 : CIA-RDP80T00246A007500340002-0

Approved For Release 2009/05/01 : CIA-RDP80T00246A007500340002-0

$$B = \frac{C_w\vartheta_{II} + C_t - 0{,}545\vartheta_I C_L}{C_2\vartheta_{II} + C_t n - \frac{1}{2}\vartheta_I C_1 - 0{,}045n\vartheta_I C_L}$$

Notations:
ϑ_I and ϑ_{II} – temperatures: of acting frost and initial of ground,
λ_1 – thermal conductivity of frozen soil
ξ – frost penetration depth
t – time
$s = 1{,}09\ vdt + 0{,}09n\xi$ – frost heave
n – porosity of a soil
v – velocity of upward flow of moisture in soil
C_2, C_1, C_L, C_w – heat capacities, respectively, of unfrozen soil, of frozen soil, of ice, of water
C_t – latent heat of ice fusion.

As the heat capacities of mineral components of soil and water differ approximately as 1 : 5, the frost penetration in water will proceed at a considerably slower rate than in soil even fully water-saturated. When, during frost action, the ground water will flow upward by suction, we will have a third case with intermediate freezing rate.

In the case of freezing of pure water v = 0, as the water-suction does not occur, besides n = 1, s = 0,09 and equation (1) becomes

$$\frac{d\xi}{dt} = \frac{A}{1{,}09\xi} \tag{2}$$

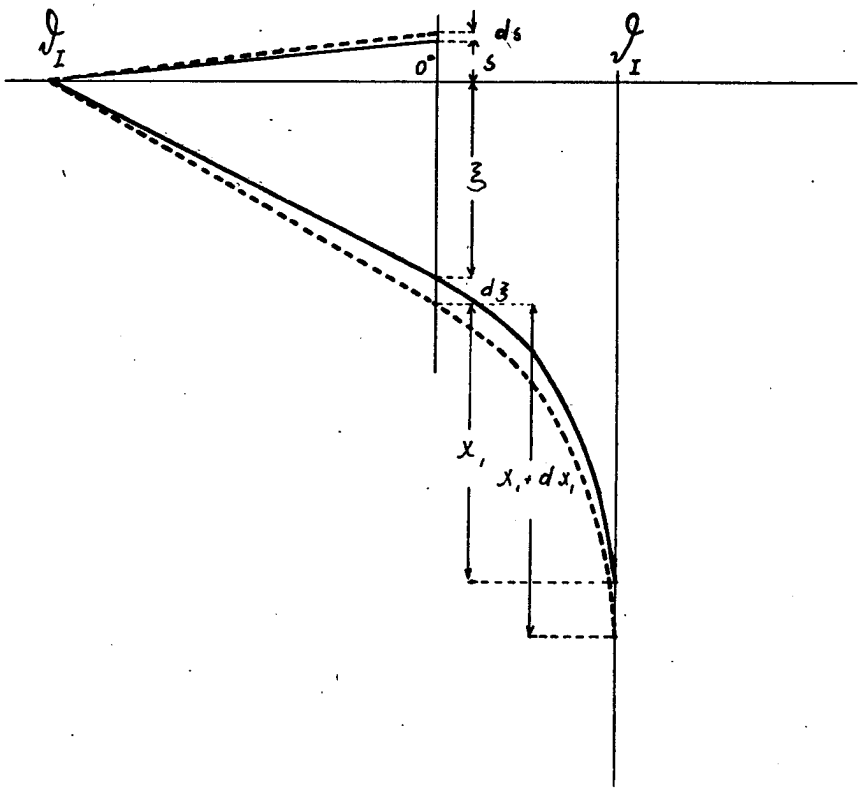

Fig. 1. Frost penetration during an infinitely small time interval.

Approved For Release 2009/05/01 : CIA-RDP80T00246A007500340002-0

Approved For Release 2009/05/01 : CIA-RDP80T00246A007500340002-0

If the frost temperature, initial temperature of water, heat conductivity of ice and heat capacities of water and ice are known, then A becomes a definite constant value:

$$A = -\frac{\lambda_1 \vartheta_I}{C_w \vartheta_{II} + C_t - 0{,}545 C_L \vartheta_I}$$

The equation (2) can be solved then as an integral:

$$\xi = \sqrt{\frac{A}{2 \cdot 1{,}09} t} \qquad (\xi \text{ in cm, } t \text{ in hours}).$$

For example, when $\vartheta_I = -10°$ C., $\vartheta_{II} = +4°$ C., $C_w = 1$, $C_L = 0{,}45$, $C_t = 80$ in cal/cm^3 · °C., $\lambda_1 = 19{,}3$ cal/cm · h°C, it is obtained A = 22,35 and

$$\xi = 2{,}02 \sqrt{t}$$

It must be added here, that rarely can we observe in nature such freezing progress, because generally snow covers the ice, to a great extent isolating it from frost penetration.

The case of freezing of pure water is a marginal case of the slowest frost penetration. On the contrary, water-saturated soils, but without any upward suction of water, present the most favourable conditions for frost penetration, compared with cases where the upward water suction arises.

If water suction does not occur, v = 0 and for A in equation (1) after introducing all respective values a definite value is obtained.

Again the solution

$$\xi = \sqrt{\frac{A}{2 \cdot 1{,}09} t}$$

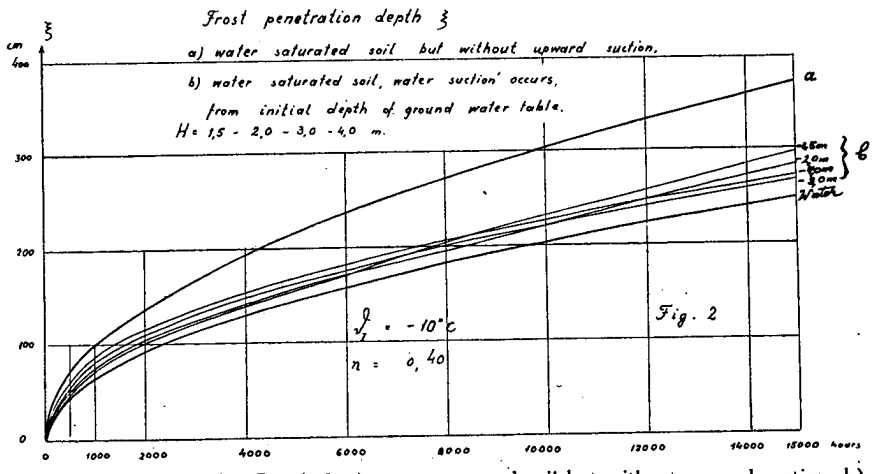

Fig. 2. Frost penetration Depth ξ. a) water saturated soil but without upward suction; b) water saturated soil, water suction occurs from initial depth of ground water table. H=1.2, 2.0, 3.0, 4.0 m.

Approved For Release 2009/05/01 : CIA-RDP80T00246A007500340002-0

Approved For Release 2009/05/01 : CIA-RDP80T00246A007500340002-0

is obtained, but the numerical value of A is another as in the case of water freezing.

For example, assuming n = 0,40, λ_1 = 19,2 cal/cmh°C., C_1 = 0,50 cal/cm³·°C., C_2 = 0,72 cal/cm³·°C, ϑ_I = –10° C., ϑ_H = +8° C., A = 4,76 and $\xi = 3{,}03\sqrt{t}$ The results of the above computations can be shown by graphs (Fig. 2).

The two margin curves illustrate the progress of freezing: a) of water (the lower curve), b) of a water saturated soil but without upward suction (upper curve). All intermediate curves relate to the cases when water suction occurred and initial depth of ground water table was respectively H = 1,50 – 2,0 – 3,0 – 4,0. It must be pointed out that in conformity with freezing progress the distance between the frost boundary and ground water table steadily decreases.

Computations illustrated in Fig. 2 were performed for a silty soil with permeability $k = 9.10^{-6}$ cm/sec.

As it is known silty soils are the most sensitive for the upward flow of the moisture and produce the biggest frost heaves. This phenomenon was reasonably explained by Gunnar Beskow.

Many computations have been made for various soils and frost temperatures and different ground water and moisture conditions. In every case the depth of frost penetration was studied for 15000 hours ≈ 21 months.

The expected frost-heave was computed by the simple formula:

$$s = 1{,}09 \int_0^t v\,dt + 0{,}09n\xi$$

A corresponding graph is shown in Fig. 3.

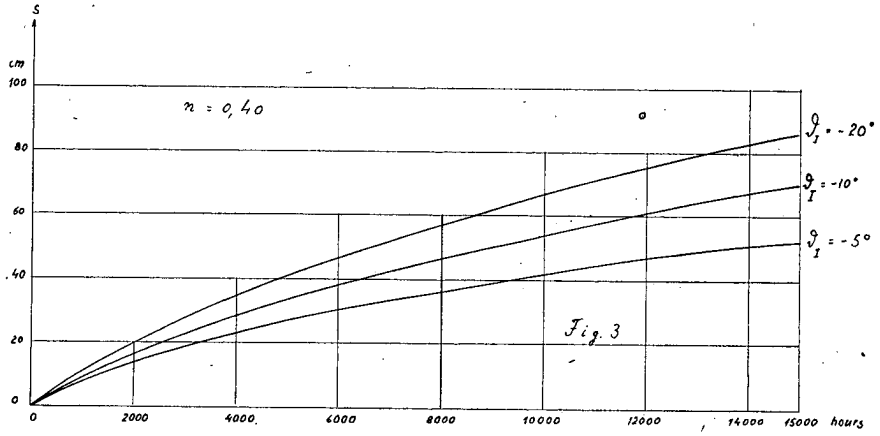

Fig. 3. Frost heaves. Water saturated soil, water suction occurs from initial depth of ground water table. H=4.0 m.

The results of many computations allow to deduce some important conclusions.

1. If suction of ground water does not occur, the rate of frost penetration and consequently the frost heaves increase considerably with decrease of temperature, approximately proportionally to the square root of temperature expressed in °C.

2. A larger water content diminishes the freezing progress but different water contents practically do not influence the rate of frost heaves.

3. The soil moisture W_n = 20 corresponding to porosity n = 0,35 can produce frost heaves 9,5 – 13,1 – 17,9 cm when steady freezing at –5° – –10° – –20° C. for 15000 hours is assumed.

These computations were done for one dimensional (vertical) heat flow. As can

Approved For Release 2009/05/01 : CIA-RDP80T00246A007500340002-0

Approved For Release 2009/05/01 : CIA-RDP80T00246A007500340002-0

be observed here, the water saturated soil, even at limited porosity, can produce dangerous consequences.

4. As ground freezing progresses, the upper frozen cover produces some isolation layer and consequently the rate of freezing decreases. This decrease is very important during the initial 2000–3000 hours, but afterwards decrease of value $\frac{d\xi}{dt}$ slackens.

5. The one dimensional heat flow can be considerably slackened if an isolating layer is introduced, but such a layer cannot stop frost penetration. Frost penetration can be cut off only by an artificial introduction of heat beneath the floor of a cold store either by electrical heating or by flow of warmed air or water. The contribution of the earth's internal heat is so small that it practically does not matter.

6. Frost penetration can be limited to definite depth in two cases: a) when freezing acts periodically with sufficient time intervals, b) when the ground floor is adequately small and the side affluent of ground heat becomes a significant value.

7. Decrease of percolation rate in cohesive soils slackens somewhat the process but does not remove the danger of frost heaves. This danger often arises in marly soils.

All these remarks lead to the conclusion that only foundations on dry soils can secure cold stores against damages caused by frost heaving.

Of course a uniform small heaving of the whole building cannot produce any harm, therefore the practical recommendations must aim either at avoiding frost-heaves at all or at admitting them small and uniformly spread. For the last solution foundations of building can be usefully designed of special stiffened construction, say, a reinforced concrete boxgrate of a height 3–3.5 m.

Another possibility of advantageous solution is presented by a stiff block of soil formed under the cold-store by using, for this purpose, the cement or chemical injections into underlying soils. Such a consolidated soil layer, has of course, to be of an appropriate thickness.

The above exposed method of computation can be helpful in elucidating the value of expected frost-heave. Of course in these computations, it can be approximately taken into account that frost does not act only in a vertical direction but its action is dissipated by reason of heat afflux from the side ground. Such adjustment can be done by a reasonable decrease of value A in formula (1).

Behrndt bogtryk, Denmark

Copyright reserved

Approved For Release 2009/05/01 : CIA-RDP80T00246A007500340002-0

Approved For Release 2009/05/01 : CIA-RDP80T00246A007500340002-0

The Design and Operation of the Air Jacket of the Moscow Cold Store No. 12

Conception et exploitation des chambres à doubles parois de l'entrepô frigorifique no. 12 de Moscou

V. Y. KOKOREV
The Ministry of Trade of the RSFSR, Moscow, U.S.S.R.

SOMMAIRE. Les fruits frais et les oeufs doivent être entreposés dans des conditions telles que la perte de poids par évaporation soit supprimée et que la température et le degré hygrométrique convenables soient strictement respectés.

De grandes quantités de viande congelée en quartiers ou en demis sont entreposées sans emballage étanche à la vapeur d'eau, et ceci demande également des conditions particulières d'entreposage pour supprimer les pertes de poids. L'entreposage des denrées alimentaires périssables dans des chambres à double paroi est une des méthodes les plus sûres pour arriver à ce résultat. La chaleur extérieure est absorbée par l'air deladouble paroi. La perte d'eau est très sensiblement diminuée, le poids et la qualité des produits alimentaires sont sauvegardés. Les dépenses de construction de chambres froides à double paroi peuvent être amorties au bout de deux ans d'exploitation de l'entrepôt frigorifique. C'est ainsi qu'à lentrepôt N° 12, à Moscou, le coût de réalisation des doubles parois représentait 3% seulement de la dépense totale de construction et était récupéré au bout de 18 mois d'exploitation grâce aux conomies réalisées sur la diminution des pertes de poids des marchandises stockées et à la meilleure préservation de leur qualité.

La présence de batteries froides dans les doubles parois permet de maintenir une température beaucoup plus uniforme. Chaque mètre de longueur de la double enveloppe est équipé de 2,5 à 3 m^2 de tubes à ailettes et, sous la terrasse, on a installé 0,6 à 0,9 m^2 de tubes à ailettes par m^2 de plafond. Les installations sont étudiées et réalisées en vue d'obtenir dans chaque chambre froide des températures différentes. La description des chambres froides à double paroi de l'entrepôt frigorifique N° 12 de Moscou ainsi que les résultats d'exploitation sont donnés dans le rapport.

BRIEF CHARACTERISTICS OF THE COLD STORE

The Moscow universal cold store no. 12 is designed for the storage of meat, butter, fish, fruits, eggs and other frozen and cooled products.

The layout, cooling system, jacket, as well as the prefabricated structural elements of the building were developed by the Giprokholod (State Institute for Designing Enterprises of the Refrigerating Industry) on the basis of suggestions made by and with the participation of I. Badylkes, Sh. Kobulashvili, U. Krylov, P. Maximov, D. Rutov, V. Safonov and N. Tkachev.

The total storage capacity of the cold store is 35,500 tons providing facilities for storing 27,240 tons of frozen foods and 8,260 tons of chilled products. Part of the rooms with a total storage capacity of 8,950 tons are convertible and may be used both for frozen and chilled foodstuffs. The freezing capacity of the freezer rooms amounts to 187 tons per day, including tunnel type quick-freezers with multiple aircooling having a 70 tons per day output.

The cold store is a 6 story building with a basement. The building is divided into 11 vertical sections with an equal temperature maintained throughout each section. The elevators and staircases are located inside the building. The warehouse has two parallel platforms: one 12 metres wide — along the railroad siding, the other one 8 m wide — for lorries. The length of each platform exceeds 150 m.

Approved For Release 2009/05/01 : CIA-RDP80T00246A007500340002-0

Approved For Release 2009/05/01 : CIA-RDP80T00246A007500340002-0

Due to the substantial dimensions of the platforms it is possible to rapidly unload RR vans and load lorries. Good operating conditions are thees also provided for electric stackers, trucks and other goods handling equipment.

The refrigeration of the storage coolers is provided by means of the single-duct air circulation air coolers with ejector distribution of the air.

The convertible chambers are equipped with combined air and coil cooling by means of air coolers and overhead coils. The latter are turned on when the room is used for storing frozen foods.

The storage freezers are equipped with overhead coils. The air coolers and overhead coils of the rooms are designed for the removal of only the internal heat gains: from the refrigerated products, lighting, opening of the door, work of the personnel, etc.

The following temperatures are maintained in the rooms:

convertible chambers	0° – -12° C
storage coolers	+4° – - 2° C
storage freezers	-18° C

In one of the sections of the warehouse the rooms are designed for storing frozen fish of particular fat species and cod liver; the temperature can be held down to -30° C.

All the coils in the rooms and air coolers are made of finned pipes.

A direct expansion ammonia system is applied in the rooms and freezers of the cold store.

The operation of the equipment of the rooms as well as of the refrigerating machinery is automated.

THE AIR JACKET

The loss of weight of the foodstuffs stored at the warehouse is in direct relation to the amount of heat penetrating into the cold rooms.

It should be born in mind that by the loss of weight (shrinkage) of the foodstuffs not only quantitative losses are caused but also the quality is impaired due to the dehydration of the surface layer of the products. This, in turn, results in a reduction of the nutritive value of the foodstuff as well as a deterioration of its appearance, especially considering that a great many products (eggs, fruits, frozen meat, etc.) are stored at cold stores without a vapourproof packing.

Each 1000 kcal of heat penetrating into the cold room is considered to cause a 150 g loss of weight of the stored products. The above considerations constituted the reason for constructing an air jacket which would absorb the heat gain from the outside before the latter penetrated into the cold rooms, while the internal heat gains (product load, operation loads, etc.) would be absorbed by the coils and aircoolers installed in the cold rooms.

Each cold room has its own jacket that provides a more uniform refrigeration of the jacket and a possibility of maintaining various temperatures in the rooms. The jacket is formed by partitions located at 0.6 m from the outer walls (Fig. 1.).

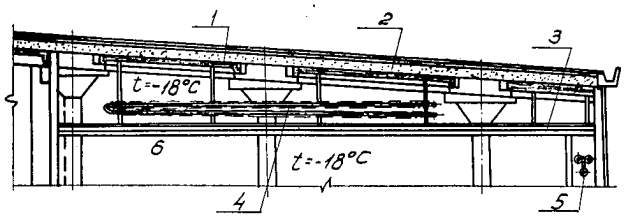

Fig. 1. The air jacket of the cold store walls.
1-floor, 2-finned wall coil, 3-outer wall panel, 4-mineral cork insulation, 5-inside wall, 6-storage room.

Approved For Release 2009/05/01 : CIA-RDP80T00246A007500340002-0

Approved For Release 2009/05/01 : CIA-RDP80T00246A007500340002-0

Overhead finned coils are mounted in the jacket for cooling the air in it down to a temperature similiar to that in the respective storage room.

The heat entering through the roof of the warehouse is absorbed by finned coils located in the floor of the garret (Fig. 2).

The surface of the overhead finned coils located along the outer walls of the cold rooms amounts to 2.5 m^2 per linear m of the jacket length and that of the garret coils to 0.6 m^2 per 1 m^2 of the cold room ceiling.

The operation of the equipment installed in the jackets and cold storage rooms is automated.

The cost of the jacket comprises approximately 3% of the cost of the structural part of the cold store.

storage rooms reached a figure of 800 million kcal. Thus the jackets of the cold According to the data for 1958 the external heat gain of the jacketed cold store, having absorbed this heat gain prevented a weight loss of 800,000 · 0.15 = 120,000 Kg of stored products.

Calculations indicate that the cost of the jacket is compensated within 18—20 months of operation.

It has also been shown by the operation of the warehouse that the jacket permits prolonging the storage time for eggs by 1.5 to 2 months, thereby ensuring a more uniform supply of eggs to the population during the year.

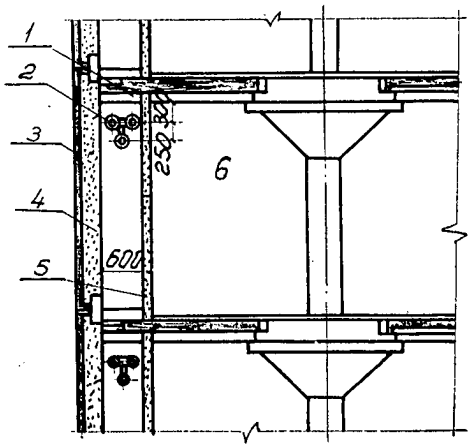

Fig. 2. Air jacket of the cold store garret.
1-central plate, 2-mineral cork insulation, 3-suspended ceiling, 4-finned coil located on the floor of the garret, 5-finned wall coil, 6-storage room.

Specialists point out that products stored in jacketed rooms have a better sales appearance.

Investigations and observations carried out by the Scientific Research Institute of the Refrigerating Industry of the USSR of the operation of a 500 m^2 control chamber (the No. 31 cold room) at -18° C. indicated the following:

1. With automatic control of the equipment a stable temperature was maintained in the room and the temperature deviations in various parts of the room did not exceed -0.5° C.

2. The relative humidity of the air averaged 97% during the entire period of the room operation.

3. The weight losses of frozen meat (327 tons of meat were stored in the room) during the storage period amounted to:

Approved For Release 2009/05/01 : CIA-RDP80T00246A007500340002-0

Approved For Release 2009/05/01 : CIA-RDP80T00246A007500340002-0

	Actual losses	Losses rated for conventional cold stores
Beef, 1st grade (stored from 29.1.1957 to 25.1.1958)	0.78%	1.67%
Beef, 2nd grade (stored from 9.11.1957 to 28.1.1958)	1.24%	2.18%
Mutton, 1st grade (stored from 29.1.1957 to 27.1.1958)	0.78%	2.02%

Many specialists considered previously that the jacket presented interest only for rooms storing frozen meat and fish. However, further investigation of this problem illustrated the expediency of the jacket for chilled egg and fruit storage rooms.

In the case of cold stores located in the southern regions of the country, the heat gain from the outside comprises 70% of the total refrigeration load and the jacket is one of the main means for improving the storage conditions for chilled eggs and fruits, frozen meat and fish.

Behrndt bogtryk, Denmark

Copyright reserved

Approved For Release 2009/05/01 : CIA-RDP80T00246A007500340002-0

Approved For Release 2009/05/01 : CIA-RDP80T00246A007500340002-0

Technical and Economic Data on Freezer and Storage Rooms of Cold Stores

Capacité d'entreposage et puissance de congélation

N. F. TKACHEV
The State Institute for Designing Enterprises of the Refrigerating Industry, Moscow, U.S.S.R.

SOMMAIRE. Les marchandises entreposées en chambres froides doivent être gerbées de manière à ne causer aucun dégât ni aux maçonneries ni à l'équipement frigorifique, tout en utilisant au maximum la capacité des salles. Les marchandises doivent également être facilement accessibles pour être surveillées en cours d'entreposage.

Ces conditions imposent quelques règles pour le chargement et l'exploitation des chambres froides. Un espace doit être rigoureusement réservé entre les parois des salles ou les appareils frigorifiques et les piles de marchandises, de même l'emplacement et la largeur des couloirs sont très importants. Les données suivantes permettent de calculer la capacité des chambres froides et des congélateurs: poids des différentes denrées au m^3 de marchandise gerbée; – disposition et charge admissible du réseau de rails aériens; – distance entre les piles de marchandises et les parois ou appareils frigorifiques à l'intérieur des chambres froides; – emplacement et largeur des couloirs dans les salles; – durée de congélation de la viande et du poisson en fonction de la température et de la vitesse de l'air; – temps de chargement et de déchargement des tunnels de congélation de viande; – hauteur admissible de gerbage dans les chambres froides.

Les types de congélateurs suivants sont très répandus désormais dans les entrepôts frigorifiques: congélateurs avec dispositifs éjecteurs pour circulation d'air froid dans la chambre froide; – tunnels de congélation avec refroidissement de l'air en plusieurs étages; – congélateurs avec refroidisseurs d'air installés dans la chambre froide; – congélateurs dans lesquels la circulation de l'air est horizontale.

Les cacactéristiques de ces appareils sont examinés de même que leur encombrement, la disposition des tuyauteries, la nature du métal employé, la consommation d'énergie, etc.

Data on the capacity of cold rooms and freezers allows food owners to use refrigerating capacity more efficiently, to correctly plan commercial operations and more exactly stipulate the quantities of various foods to be cooled, frozen and stored.

Observance of the rules given under "Determination of cold room capacity" not only promotes more effective utilization of the refrigerating capacity but also eliminates the possibility of overloading or damaging the building constructions and equipment of the cold stores.

DETERMINATION OF STORAGE ROOM CAPACITY

Storage rooms are rooms of a cold store designated for the storage of goods under definite temperature and humidity conditions. The capacity of storage rooms is expressed either in cubic metres of their total refrigerated volume, or in cubic metres of the piling volume, *i.e.* the volume directly occupied by the goods.

If it is necessary to characterize the capacity of the cold store in tons, the piling volume is to be multiplied by the weight of the goods stored in one cubic metre of this volume.

Approved For Release 2009/05/01 : CIA-RDP80T00246A007500340002-0

Approved For Release 2009/05/01 : CIA-RDP80T00246A007500340002-0

Following are the rates (tons per 1 m³ of storage room piling volume) adopted in the U.S.S.R. for various foods:

1. Beef frozen, non-standard cut	0.3
2. Beef frozen, standard cut (quarters)	0.4
3. Mutton frozen	0.3
4. Pork frozen	0.45
5. Meat and by-products frozen in blocks	0.65
6. Fish fillet frozen, in boxes	0.55
7. Fish frozen, in boxes	0.35
8. Fish frozen, in baskets	0.3
9. Fish large frozen, stacked	0.45
10. Butter in boxes (24.5 kg)	0.65
11. Butter in barrels	0.54
12. Poultry in boxes	0.35
13. Eggs in cartons or boxes	0.32
14. Egg frozen in metal cans	0.55
15. Canned food in metal cans	0.6
16. Fruits, cooled, in boxes	0.34
17. Fruits, dry frozen, in boxes	0.35
18. Fruits, frozen in syrup (cans in boxes)	0.54
19. Cheese, small, in boxes	0.35–0.38
20. Cheese, large round (stored on shelves)	0.4
21. Other cooled foods	0.3

The capacity of cold stores is rated in the U.S.S.R. also in tons (the "conventional tonnage"). This is the amount of tons of frozen meat the piling volume is capable to hold. On the average for various kinds of meat this amount corresponds to 0.35 tons per 1 m³ of the volume. The piling volume of the cold room is obtained by multiplying the piling area by the piling height. The piling area of the cold room is the area directly occupied by the foods and is equal to the total building area, less the areas occupied by the columns, equipment, passages and the distance between the stacks of goods and the building constructions and equipment of the cold room.

The piling height is the distance from the floor of the cold room to the upper level of the stack of foods.

It is recommended in the U.S.S.R. to observe the following distances between the stacks of goods and the building constructions and equipment of the cold room:

1. From cold room walls to stack	0.3 m
2. From beamless ceiling to stack	0.2 m
3. From lower part of protruding beams to the stack in the case of beam-type floors	0.2 m
4. From walls of air ducts to stack	0.3 m
5. From wall coils to stack	0.4 m
6. From overhead coils to stack	0.2 m

Passages 1.2 m wide are left in the cold rooms. When using electric fork trucks for stacking the goods the passages are 1.4 to 2.0 m wide.

Passages may be omitted in cold rooms having a capacity up to 100 tons. If the goods are to be stored in the cold rooms by the lots (grade, production of certain factories, separate owners of the goods, etc.), a 0.15 m distance is left between the stacks of separate lots.

One passage along the wall or in the centre of the cold room is provided in rooms having a width up to 18 metres. When goods are stacked in rooms more than 18 m wide passages are arranged at the rate of one passage per 15–18 m of the room width.

If the passages are located along the walls of the cold room, the distance between the stacks of goods and the equipment or walls is included in the total 1.2 m width of the passage.

Goods may be stacked directly along the walls in jacketed rooms if the walls

Approved For Release 2009/05/01 : CIA-RDP80T00246A007500340002-0

Approved For Release 2009/05/01 : CIA-RDP80T00246A007500340002-0

are rated for such loads. Racks and shields are set in this case between the stacks of goods and the wall so as not to damage the surface of the walls.

In some cases the piling volume of the cold room cannot be utilized fully as the building constructions (floors, columns, foundation) are unable to bear the weight load of the goods. Consequently, the carrying capacity of the building constructions is to be considered when determining the capacity and charge of the piling volume of cold stores. This consideration is to be taken into account especially in the case of old cold stores in which the fated load on the floors is much less.

The percentage of the area occupied by the columns, passages and the distance between the stacks of goods and the building constructions and equipment of the rooms is in small cold rooms (20–100 m^2) up to 35%, in average rooms (up to 400 m^2) about 30% and in large rooms (over 400 m^2) – up to 20% of the building area. As the piling volume amounts to 0.9 of the cold room building height, the piling height will amount on the average to $0.7 \times 0.9 = 0.63$ of the total volume of the cold rooms.

The capacity of chilled meat storage and freezing rooms is determined by the length of the overhead rails. The specific load per 1 linear metre of the rail for standard cut beef is 0.28 ton, for pork it ranges from 0.25 to 0.28 ton and for mutton it amounts to 0.25 ton. The length of the overhead rails (in metres) is to be multiplied by the specific load per 1 linear metre of rail in order to determine the capacity of such cold rooms. The height from the floor of the cold room to the overhead rail is to be not less than 3 m. The minimum distance from the extreme side overhead rail to the wall and other building constructions or to the equipment is to be 0.4 m. The distance between the centre lines of the overhead rails is to be not less than 0.8 m.

Quick chilling and other auxiliary rooms are not included in the capacity of the cold store though they may be used for storing goods when not utilized for their particular destination. The capacity of these rooms is in this case rated in the same manner as when determining the capacity of ordinary storage rooms.

Several units are applied at present in various countries for the determination of the capacity of cold stores. For example, in England and the U.S.A. the capacity of cold stores is rated in cubic feet, in France and Italy in cubic metres. In the U.S.S.R. the conventional tonnage is used, in the GDR and the FRG the m^2 of the piling area, etc.

Conversion factors for the capacities of cold stores expressed in various units are tabulated below.

TABLE 1. CONVERSION TABLE

Unit to be converted	Conversion factors				
	Into conventional tons	Into piling volume m^3	Into piling volume cu.ft.	Into piling area, m^2	
				multi story cold stores	single story cold stores
Conventional ton	1.00	2.86	101	0.95	0.5
Piling volume, m^3	0.35	1.00	35.35	0.33	0.18
Piling volume, cu.ft.	0.0099	0.028	1.00	0.0094	0.005
Piling area, m^2 multi-story cold stores	1.05	3.00	106	1.00	0.53
Piling area, m^2 single story cold stores	2.00	5.72	202	1.9	1.00

The capacity expressed in the required units is obtained by multiplying the capacity in the initial units by the corresponding factor.

CHARACTERISTICS OF FREEZER ROOMS

Freezer rooms are used at cold stores for freezing meat in halves and quarters, by-products, fish, poultry and other foods.

Approved For Release 2009/05/01 : CIA-RDP80T00246A007500340002-0

Approved For Release 2009/05/01 : CIA-RDP80T00246A007500340002-0

The freezing capacity of freezer rooms is characterized by the amount of foods frozen per day and is expressed in ton/day. The holding capacity of freezer rooms is rated by the amount of meat simultaneously suspended from the overhead rails and is expressed in tons.

The freezing cycle includes the time required for loading, freezing and unloading the food.

The term "loading time" usually includes also the time required for defrosting the coils and cleaning up the room. The daily freezing capacity C of freezer room is determined according to the formula

$$C = \frac{L \cdot 24}{T}$$

where L is the holding capacity of freezer in tons (the weight of the food simultaneously loaded into the freezer).

T the duration of the freezing cycle, in hours.

It takes from 2 to 2.5 hours to load and unload freezers having a capacity from 5 to 10 tons, and from 3 to 3.5 hours in the case of 15 to 20 ton freezers.

The following freezer rooms are widespread at present in cold stores.

a) *Tunnel freezers with multiple cooling of the air.* These are rooms with intensive movement of the air and vertical blowing over of the meat at multiple cooling of the air during its subsequent flow through sections. The sections are formed by vertical partitions equipped with finned coils which are simultaneously applied as screens for intensive radiation upon the foods being frozen. Each section is provided with overhead rails.

The movement of the –30 to –32° C. air in the sections at a velocity of from 3 to 4 m/sec as well as radiation heat-exchange and maintenance of constant temperatures in the freezer allow to freeze meat quarters in 17–19 hours.

b) *Freezers with ejecting devices.* The air, cooled in air coolers, is supplied in such freezers into the space between the main and false ceilings and then through nozzles into the freezing space where it is circulated over the meat suspended from overhead rails. The nozzles are arranged along the entire length of each line of overhead rails.

From the freezing space the air is returned to the air cooler whereafter it is recirculated. The air coolers are installed in a separate room or in the freezing space proper.

The meat is frozen in 20 to 22 hours as it is located in the active zone of circulation of air at 2.5 to 3.0 m/sec velocity and a temperature of –30° to –32° C.

c) *Freezers with air coolers installed inside the freezing space.* Such a freezer is usually a one bay wide room equipped with overhead rails and an air cooler installed at the wall (ordinarily between columns). Fans, mounted above the air cooler, supply air into the space formed between the ceiling and the overhead rails. Thence the air flows down and, passing over the meat, affects its freezing. The air is then fed to the air cooler and recirculated. Each bay of the freezer room is provided with a separate air cooler.

It takes 22 to 24 hours to freeze meat quarters in such freezers at a 1 m/sec. velocity of –30° C. air.

d) *Freezers with a horizontal air flow.* The freezer consists of a freezing space equipped with overhead rails, and a room for the air cooler.

Air, supplied by the fans into the freezing space, flows over the meat along the overhead rails and freezes it. After this the air is returned to the air cooler and is recirculated.

Meat quarters are frozen in 18 to 20 hours at a velocity of the air from 3 to 3.5 m/sec at –30 to –33° C.

The data given in the paper may be partially included in the Cold Storage Guide being compiled by Commission 5 of the International Institute of Refrigeration.

Behrndt bogtryk, Denmark

Copyright reserved

Approved For Release 2009/05/01 : CIA-RDP80T00246A007500340002-0

Approved For Release 2009/05/01 : CIA-RDP80T00246A007500340002-0

Storing Chestnuts in Polyethylene Film Box Liners

Entreposage de chataignes en caisses sous pellicule de polyethylene

J. LIPOVEC,
Chief of Fruit Department Agricultural Station Maribor, Yugoslavia.

SOMMAIRE. L'entreposage de châtaignes fraîches en caisses sous pellicule de polyéthylène de 0 à –1° C., a été entrepris avec succès. Les fruits restent sains, frais et de bon goût. Le stockage à plus haute température, par exemple à 4° C. ou plus, sous polyéthylène est risqué et peut entraîner la dépréciation de tout le lot. De même la conservation en boîtes ou en cageots sans enveloppe de polyéthylène entraîne une dessiccation rapide et la dépréciation.

INTRODUCTION

Chestnuts *(Castanea sotiva L.)* are well extended over a wide area in Southern Europe and are considered as an Atlantic-Mediterranean species. Their production is important also in Yugoslavia, where there are some nut plantations, and in addition particular chestnut forests, or chestnut trees are grown with other trees up to 1000 m above sea-level.

Fresh broiled nuts are very popular food widely consumed with wine mainly in October. Because chestnuts are highly perishable, they must be stored accordingly. Their consumption season is only one month. It would be useful to find out an acceptable method to store fresh nuts in order to prolong their storage life.

METHODS OF STORING

It is reported that under suitable conditions nuts can be stored from the time of harvesting to late April, which is necessary or desirable only in he case of the production of seedling trees. Such nuts could be placed in friction or slip-top metal cans after curing and stored at 30° to 32° F. [1]. During the last few years American scientists have introduced successful commercial packaging for more varieties of pears, apples, sweet-cherries and, under special conditions, also bananas and grapes with polyethylene film liners and cooling at suitable temperatures [2].

At Maribor Station we succeeded in developing a new storage method for fresh chestnuts. Selected nuts (with 1 % spoilage) at time of harvest were packed with 2-mil polyethylene film box liner, which were not tied up, but left with an opening for a small amount of circulation of air. Packages were kept in cold storage at temperatures of 0 to –1° C., and also in the cellar, where in autumn the temperature began at 13° C. and in winter it remained at 4° C. For comparison we stored also unlined nuts.

RESULTS

After storage for 4 months we ascertained that cooled nuts in polyethylene film box liners at temperatures of 0 to –1° C. were sound, fresh and tasty. Spoilage increased from the initial 1 % to only 4 %. Nuts stored in polyethylene box liners in the cellar quickly began to be moldy and the spreading of decay did not stop at the temperature of 4° C. After cooking we found only 17 % sound, 10 % germinated and 73 % spoiled nuts. Nuts in the unlined boxes either in cold storage or in the cellar were dried out and bony, and spoiled. It also was found that the temperature of –3° C. did not influence the quality of nuts in polyethylene liners.

Approved For Release 2009/05/01 : CIA-RDP80T00246A007500340002-0

Approved For Release 2009/05/01 : CIA-RDP80T00246A007500340002-0

DISCUSSION

The chestnuts packed with polyethylene box liners successfully kept back the moisture, reduced the rate of respiration and reached suitable percentage af CO_2 concentration, which contributes to maintaining the quality. The loss of weight of lined nuts is about ten times less than of unlined nuts. Therefore it seems that the use of polyethylene liners combined with cooling is a successful means for storing chestnuts. More experimental work is needed in that field. It is recommended that cooling plants try the use of polyethylene box liners.

REFERENCES

1. Harvesting, Treating, Storing, and Marketing Chestnuts. USDA, Beltsville, Maryland, 1951.

2. HARDENBURG, R. E., SCHOMER, H. A. and UOTA, M. Polyethylene Film for Fruit. *Modern Packaging,* February 1958.

Behrndt bogtryk, Denmark

Copyright reserved

Approved For Release 2009/05/01 : CIA-RDP80T00246A007500340002-0

Approved For Release 2009/05/01 : CIA-RDP80T00246A007500340002-0

Physio-Chemical Properties of Boned Frozen Beef, Stored in –16° C.

Propriétés physico-chimiques du boeuf congelé conservé à –14° C.

W. PEZACKI, B. CYBULKO, ST. NAWROCKI
Wyzsaz Szkola Rolnicza, Katedra Technologii Miesa, Poznan, Poland

SOMMAIRE. L'objet de ce rapport est de déterminer quelle sorte de boeuf désossé, haché, congelé et conservé à –14° C. convient le mieux à la fabrication de saucisses ébouillantées non stabilisées. – L'aptitude technologique a été jugée d'après les critères suivants: pertes de poids, variations du pH, absorption d'eau, digestibilité par la pepsine in vitro, et degré de dissociation de Ca^{++}, K^{+}, Na^{+}. Conclusion: La viande maigre et la viande grasse d'animaux bien en chair sont le plus appropriées à la congélation sous forme de viande désossée, hachée, constituée en blocs. La teneur en K. de l'exsudat est l'indice le plus sensible des variations se produisant au cours de l'entreposage. La viande ne convient plus à ce propos au moment où le niveau de K. atteint une valeur d'environ 0,07 à 0,08 mg.

Economical and technological reasons created a conception of freezing and storing of boneless meat, ground and shaped into blocks. As the biochemical composition of this material is differentiated, and as freezing and storage at low temperatures cause secondary changes in it, and as the criteria of usefulness for producing sausages are quite precisely defined, the meat technologist should, first of all, be interested in the question: Is every kind of meat suitable for freezing in blocks?

As in other cases, the reply to this question can be obtained only on the basis of observations of physio-chemical changes in meat of different qualities during freezing, storage at low temperature, and thawing.

In order to be able to direct the processing of frozen meat into, e. g., non-stable, cooked sausages, and to organize processing scientifically, the technologist must know:

1. What are the differences in bio-physio-chemistry of freezing, storage and thawing of meat, depending on the degree of fattening, age, sex and similar factors, which can be determined by an examination *in vivo*.
2. Does the meat from different parts of the same carcass react to the above mentioned processes in the same way?

The questions thus formulated are the working hypothesis of the experiments described. These experiments refer in a way to the reports of literature.

The meat of 9–11 year old cows was analysed. The animals chosen for slaughter were divided into three groups: a) fattened, b) well-fleshed not fattened, and c) lean. The carcasses were chilled and stored at 6 to 7° C., relative humidity about 90%. The chilled carcasses were then boned and divided into non-tendinous, tendinous and fat meat, which were then frozen separately. In order to facilitate chemical analysis and examination of the anatomic-histological structure, only some muscles, or groups of muscles were frozen, namely:

for non-tendinous meat – the gluteus muscle,
for tendinous meat – the sub-scapular muscle,
for fat meat – the oblique, transversal and conical muscles of the abdomen.

The whole experimental material was thus divided into nine quality classes. The meat of every class was then ground, pressed through 4 mm mesh net, formed into cylinders of identical dimensions, frozen for 24 hours at –22° C., and then stored for 9 months at –16° C. The physio-chemical changes in the meat were investigated after 2, 4, 6 and 9 months' storage, and compared with analyses performed before freezing. The samples were then thawed in air at +18° C.

Approved For Release 2009/05/01 : CIA-RDP80T00246A007500340002-0

Approved For Release 2009/05/01 : CIA-RDP80T00246A007500340002-0

Analysis of the bio-physio-chemical changes occurring in beef during 9 months' storage has shown that these changes depend not only on the storage period, but also on the initial biochemical structure. The general direction and quality of these changes are defined by the process of freezing and storage, and the quantitative deviations, their intensity, occurring in the identical technological conditions define the quality of the meat. In the analysed criteria the following deviations, connected with the chemical compositions and its physio-chemical state have been stated.

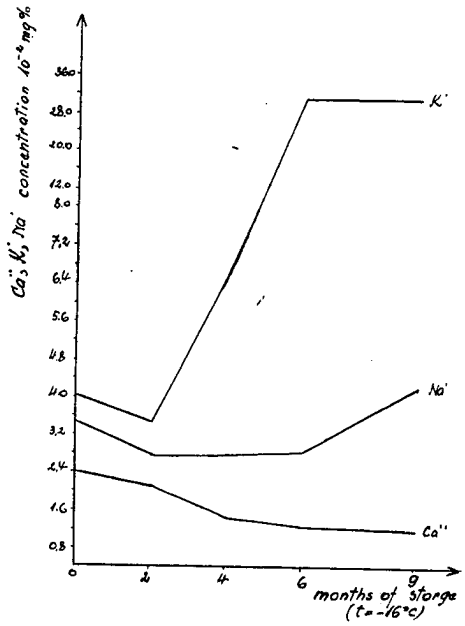

Fig. 1. Kations in the heat treatment drip.

1. *Losses of weight caused by drying* in the frozen meat during storage depend not only on the total water content, but also on the way it is chemically bound. The water is least stable in the meat of animals, whose fattening has not been finished, that it was more stable in lean animals, and most stable in well-fattened and well-fleshed animals. Taking into account that fattening raises the level of protoplasmatic proteins to the physiological norm, one must state, that it is the hydrophily of globular proteins, that plays the most important role in regulating the losses of weight caused by drying during storage at –16° C. Only in cases, where the protein content is lowered, the water bound electro-statically by sclero-proteins plays a more important role.

2. *Losses of weight during thawing* are another component of the total loss of weight of frozen meat. The smallest losses of weight, caused by de-freezing occurred in the meat of well-fattened animals. The de-freezing losses depend primarily on the total water content, which is lowest in fat meat, and highest in lean meat. These losses do change during storage. In our experiments they decreased after 4 months' storage.

The changes of quantity of thaw drip are accompanied by changes of its chemical components. The greater its general stability, and the more proteins not soluble in water, the less nitrogen compounds, practically mainly proteins, are contained in the drip. The amount of nitrogen compounds, diffusing into the thaw drip decreases with time during 9 months storage.

Approved For Release 2009/05/01 : CIA-RDP80T00246A007500340002-0

Approved For Release 2009/05/01 : CIA-RDP80T00246A007500340002-0

TABLE 1. CHEMICAL COMPOSITION OF EXPERIMENTAL MATERIAL

Cows before slaughter	Chemical component	Meat		
		Non-tendinous	Tendinous	Fat
Fattened	w	74.01	69.62	66.29
Well-fleshed	b	21.95	20.48	17.68
	s	6.46	7.92	4.74
Medium-fleshed	w	74.73	70.40	68.03
	b	20.32	19.71	20.88
	s	8.62	11.46	11.94
Lean	w	76.61	77.61	74.06
	b	19.38	18.69	18.41
	s	8.30	8.87	10.02

W – % of moisture; b – % of protein; s – % of protein not digested by pepsine.

3. *The hydrophily of meat* as a result of freezing, decreases, and never recovers the level characteristic for the meat before freezing. The initial capacity of absorbing and binding water is best preserved in the meat of fat animals, and it is worst in that of lean ones. The lowest hydrophily was stated after 2 to 6 months' storage, depending on the quality of the meat.

4. *Chemical reaction* is the criterion, which explains a number of changes, discussed above. In all cases frozen meat becomes acidified at the beginning, and then again its reaction changed to alkaline. The transitory period of the change of reaction and its stability show, however, great differences. These differences prove that the intensity of autolysis depends on the condition of the animals prior to slaughter and on local chemical changes. Again, the meat of animals killed after fattening has been completed shows the highest stability, while it is lowest in that of middle-fleshed, but not fattened animals. The higher content of connective tissue does not only rise the initial pH value, but also stabilizes the medium. In the meat containing most muscle tissue, the reaction is the least stable. It becomes acidified in the shortest time, and the low pH values persist for a long time. On the other hand, in the meat containing more fatty tissue, acidification is the slowest and the slightest, but its alkalization is fast.

The differences in the changes of reaction discussed above which occur during storage in meat of different classes are undoubtedly connected, first of all, with the initial glycogen stock in separate tissues of meat, and with its buffer capacity.

The differences discussed in the thaw drip and hydrophily of meat of different classes can be explained by the changes of reaction, and its shifting towards the isoelectric point. In general, one may state, that e. g. hydrophily of meat increases, as the pH changes towards alkaline after long storage.

5. *Ability to be digested by pepsine.* The analysis of results of ability to be digested by pepsine shows that this structure undergoes a considerable change during storage. The initial increase of the amount of proteins not digestible by this enzyme and subsequent increase of the proteins, digestible by it, are a result of these changes. Tendinous meat is characterized by an especially considerable decrease of digestibility. The digestibility of the meat of animals, whose fattening was not completed may, after longer storage at –16° C., pass the index of usefulness of this meat before freezing.

6. *Drip caused by heat treatment.* The losses of weight during heat treatment, caused by dripping of water together with chemical compounds dissolved in it, vary, depending on the initial quality of meat and on storage time. The longer the storage, the more scanty the drip, caused by heat treatment. The decrease

Approved For Release 2009/05/01 : CIA-RDP80T00246A007500340002-0

Approved For Release 2009/05/01 : CIA-RDP80T00246A007500340002-0

TABLE 2. THE CRITERIA OF THE CHANGES OF FROZEN BEEF OCCURING DURING 9 MONTHS STORAGE AT –16° C.

	Meat	Cows before slaughter			Average
		well-fleshed	medium fleshed	lean	
Per cent of total losses of water	n	3.0	5.7	4.7	4.5
	t	3.7	4.3	4.1	3.0
	f	4.2	5.8	4.7	4.9
Average de-freezing losses of weight. Per cent of the weight of frozen meat	n	10.1	12.2	11.8	11.4
	t	7.6	9.2	11.8	9.5
	f	3.8	6.7	7.3	5.9
Average nitrogen Compounds Content in the de-freezing drip. Per cent of total content of nitrogen comp. in meat	n	4.3	5.4	4.1	4.6
	t	2.9	3.4	4.0	3.4
	f	1.3	1.8	2.7	1.9
Total pH changes of the water extract	n	–0.35	–0.52	–0.42	–0.43
	t	–0.22	–0.38	–0.23	–0.28
	f	–0.17	–0.29	–0.15	–0.20
The average content of protein not digested with pepsine. Per cent of weight of meat	n	9.5	9.0	10.8	9.8
	t	10.7	11.0	11.5	11.1
	f	8.4	12.3	10.9	10.5
Heat losses of weight of meat after freezing storage. 100 = heat losses of weight before freezing	n	98.7	108.0	108.3	105.0
	t	107.0	107.0	100.3	102.9
	f	91.0	97.0	102.4	96.8
Content of Nitrogen Compounds in the heat-treatment drip. Per cent of the total content of Nitrogen Compounds of meat	n	1.64	1.86	1.67	1.71
	t	1.66	1.81	1.70	1.82
	f	1.28	1.64	1.80	1.65

n = non-tendinous meat; t = tendinous meat; f = fat meat; – = decrease and + = increase of pH value in comparison with the precedent measurement.

in the amount of drip is particularly noticeable in meat containing more connective tissue. Because of that, losses of weight during heat treatment of tendinous meat may be lower after some period of storage than before freezing. The character of these variations shows that, after a longer storage at –16° C., the sclero-proteins of meat are more readily thermo-hydrolized. Thermohydrolysis of collagen, etc., of proteins is generally known to be a phenomenon connected with lowering of the diffusion to the phase of dispersion, so it contributes to lowering the losses of weight of heat-treated meat.

The analysis of the changes of nitrogen compounds content in the heat-treatment drip indicates the increase of the solubility of meat proteins after a longer storage. The longer the storage, and the higher the sclero-protein content, the more of these substances diffuse from the meat into the heat-treatment drip. These changes

Approved For Release 2009/05/01 : CIA-RDP80T00246A007500340002-0

Approved For Release 2009/05/01 : CIA-RDP80T00246A007500340002-0

are parallel to the increase of pepsine digestibility and the shifting of reaction towards alkaline, i. e. to the increase of differences in pH values.

7. *Dissociation of Ca, K and Na compounds* proves also that considerable physio-chemical changes occur in meat during storage. One can measure this dissociation by the content of these three kations in the heat-treatment drip. This content varied for every one of them quite independently, and no greater differences, depending on the physiologic state of animals, or on the chemical composition of the meat, have been observed.

The content of $C^{"}$ proved the most stable. After 9 months' storage it reached a level equal to 50% of concentration before freezing.

The concentration of $Na^{'}$ in the heat-treatment drip is always higher than that of $Ca^{"}$. It is more or less stable in the meat of fattened animals during the first 6 months of storage. After that time the $N^{'}$ concentration in the heat-treatment drip starts to increase, and during the next 3 months it reaches the level of about 50%.

The $K^{'}$ concentration, however, does not change only during a comparatively short storage – in the present experiments this was only 2 months. Between the 2nd and the 6th month of storage, one may observe the rapid growth of this kation to a level 7 times higher than that for the meat, before freezing. During further storage the concentration of $K^{'}$ in the heat-treatment drip again remains the same.

The decrease of $Ca^{"}$ in the heat-treatment drip during storage proves that the dissociation of its compounds decreases. Also the increased mobility and weaker binding af $Na^{'}$ and $K^{'}$ in the meat proteins are not surprising.

CONCLUSIONS

1. All physio-chemical changes occurring in meat as a result of freezing and storage show considerable quantitative differences connected with the chemical compounds and with the bio-physio-chemical structure, stated *in vivo*.

2. The deviations of physio-chemical changes during storage at –16° C. prove that the usefulness of meat of certain qualities for production of non-stable cooked sausages is limited. The ground and boned meat of well-fleshed animals, killed after the fattening was concluded, is the best for freezing in blocks, especially, when it contains some % of fat. The meat of medium-fleshed animals, whose fattening has been concluded, is the least useful. The non-tendinous meat after thawing is the least suitable for producing cooked sausages, independent of the degree of fattening, for it undergoes the greatest deteriorative changes during storage at –16° C.

3. The $K^{'}$ content in the heat-treatment drip seems to be one of the most sensitive criteria of changes, occurring during storage at –16° C. At the moment, when this kation reaches a level of 0,28–0,32 mg% the meat enters the stage of undesirable autolytic deterioration.

Behrndt bogtryk, Denmark

Copyright reserved

Approved For Release 2009/05/01 : CIA-RDP80T00246A007500340002-0

Approved For Release 2009/05/01 : CIA-RDP80T00246A007500340002-0

Les modifications du poids de la viande congelée au cours de sa sortie du frigorifique

Changes in Weight of Frozen Meat on Removal from the Cold Store

Inz. WACLAW BYSZEWSKI
50 Wawolnicka 14 m. 30, Warsaw, Poland.

SUMMARY. On removal from freezing and cold storage, frozen meat becomes covered with frost, resulting in an increase in weight. As the occurence and disappearence of frost occurs during the delivery of the meat, its weight may change.

Sometimes the increase or decrease in weight exceeds the weight of separate carcasses in certain shipments, altering the appearance of the cargo and may cause disagreement between the dealer, the consignee and the carrier.

The problem is all the more complicated as:

1. *During freezing and storage dehydration occurred (shrinkage)*
2. *The occurrence of frost on the meat begins when the latter is removed from the freezing room and increases during storage (increase)*
3. *Thawing causes:*
   a) Sublimation of frost and loss of thawed frost (loss)
   b) Absorption by dehydrated meat of frost thawing-water (increase).

As the weight of frozen meat is variable, it is insufficient to observe only the principal technological conditions during the storage of frozen meat, but also to attempt to restrict every outside deleterious influence and to consider not only the weight, but also the number of units.

C'est un phénomène bien connu, qu'un corps placé dans l'atmophère, se couvre d'une couche de rosée, qui condense sur sa surface, si sa température dépasse le point de rosée de l'air ambiant. Si la température du dit corps est suffisamment au dessous du point de gelée, l'eau se dépose sous forme de givre sur la surface du corps.

C'est la règle à la sortie de la viande congelée des chambres d'entreposage, vu que la viande congelée sortant de la chambre d'entreposage a une température beaucoup plus basse, que celle des corridors et autres emplacements où a lieu toute manipulation, pesage et chargement inclus.

Si cette manutention se fait dans un temps suffisamment court et que les emplacements où elle a lieu ont des températures suffisamment basses, si enfin, ce qui devrait être bien la règle, les moyens de transports sont étanches et réfrigérés, ou tout au moins suffisamment isolés, la quantité de givre se déposant sur la surface de la viande ne devrait pas être trop importante et ne devrait pas modifier, au moins pas d'une façon grave, le poids de la livraison.

Comme malheureusement les conditions idéales ne sont pas toujours strictement observées et quelquefois les conditions réelles en sont bien éloignées, il peut y avoir des cas où le processus de changement de poids de la viande congelée causé par l'ammoncellement du givre sur sa surface et ensuite par la disparition (sublimation où la fondaison) de celui-ci, peut être assez important.

D'après les essais faits par l'Industrie de la Viande en Pologne, des surcroîts de poids de viande congelée jusque 2,4% ont été constatés causés par le givre se déposant sur la viande congelée après sa sortie de la chambre d'entreposage.

Naturellement tout ce processus a lieu en fonction de plusieurs variables, comme la température d'ambiance, le degré d'humidité de l'air, la température

Approved For Release 2009/05/01 : CIA-RDP80T00246A007500340002-0

Approved For Release 2009/05/01 : CIA-RDP80T00246A007500340002-0

initiale de la viande, le mouvement d'air etc. Il est aussi une fonction du temps pendant lequel un déposement de givre a lieu.

Après une certaine période d'équilibre thermique où il n'y a pas d'accroissement de givre ni de poids, le givre commence à fondre et le poids de la viande commence à diminuer.

Il est donc clair, que ce qui a paru comme surcroît du poids de viande peut devenir aussi bien une perte (de même en fonction du temps), il s'agit seulement du moment pris pour initial.

Si nous prenons donc le poids de la viande pure, absolument sans givre pour 100, ce poids variera en fonction du temps, dès le moment de la sortie de la chambre d'entreposage, d'une façon démontrée par la courbe sur le graphique.

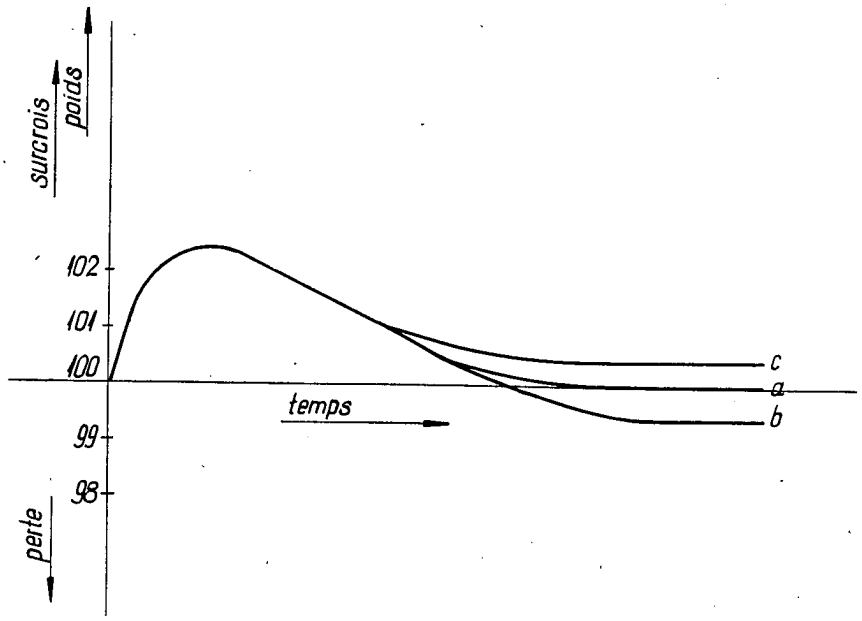

Fig.1. Variation du poids en fonction du temps

Dans ce cas le poids final devrait être le même, que l'initial (Courbe a).

En réalité ce n'est pas absolument indispensable.

Il est notamment possible, que la viande dans la chambre d'entreposage même était couverte d'une certaine quantité de givre et qu'alors le poids de la viande contenait déja le poids du givre; après la fondaison du givre la pesée diminuera d'une façon plus ou moins importante (Courbe b).

Au contraire, il peut y avoir une certaine dessication de la viande au cours de sa congélation, ainsi que pendant son entreposage.

Si une telle dessication a eu lieu, les tissus desséchés de la viande peuvent absorber l'eau, qui condensa sur la surface ou qui fond du givre et s'écoule sur la surface de la viande, ce qui donnera un surcroît durable (Courbe c).

De tels surcroîts durables ont été constatés pendant les essais fait par l'Industrie de la Viande en Pologne.

Par contre, si un desséchement important n'a pas eu lieu, une résorption d'eau ne peut pas s'extérioriser. Si enfin la viande était desséchée et en outre couverte de givre, l'eau du givre qui fond, peut être résorbée et il ne peut pas y avoir de changement de poids.

Les écoulements des jus de la viande, qui peuvent aussi avoir lieu et influencer

Approved For Release 2009/05/01 : CIA-RDP80T00246A007500340002-0

Approved For Release 2009/05/01 : CIA-RDP80T00246A007500340002-0

ainsi le poids final de la viande, n'ont pas été pris en regard dans cette dissertation.

Si le pesage de la viande était exécuté immédiatement après sa sortie de la chambre froide et que la viande ne subit pas de décongélation pendant le transport, l'acroissement de poids causé par le givre peut être considérable, et si elle a subi auparavent une dessication, l'accroissement de poids peut être durable.

Si au contraire la viande était couverte de givre, ou si le pesage de la viande était exécuté un certain temps après sa sortie de la chambre froide, le poids constaté de la "viande" contient aussi le poids du givre, qui a eu le temps de se déposer sur la surface de la viande.

Dans les cas extrêmes où le pesage serait exécuté au sommet de la courbe il ne pourrait, en conséquent y avoir que des pertes de poids.

Ce n'est naturellement pas très correct, mais si on pèse toute une cargaison à la fois, par exemple un camion de 6, 10, ou de 15 tonnes la viande, qui était chargée en premier, peut bien se trouver au moment du pesage au point sommet de la courbe (graphique).

Si le pesage d'un transport a été exécuté de telle façon et, qu'au point de destination, la viande était tout à fait ou même partiellement décongelée, il peut y avoir des pertes de poids considérables.

La situation se complique, si au cours de ce processus, la viande change de propriétaire ou de personel responsable de la marchandise et que la marchandise même n'est pas suffisamment assurée.

Dans ce cas on pourrait croire, que le convoyeur acausé le manque du poids ou tout au moins ne l'a pas gardé soigneusement. D'abord la livraison pourrait vraiment être diminuée, au cours du transport, sans que cela puisse être remarqué ou constaté. Ce serait toujours possible dans les parties où le poids des pièces particulières est plus petit, que les différences de poids causées par le givre. Comme l'accroissement du poids peut bien dépasser 2 %, dans une partie de 10 t l'accroissement de poids peut dépasser 200 kg, tandis, que les moitiés de porcs sont de 45 kg environ, de façon qu'une différence de 4 à 5 pièces ne serait pas à constater déaprès le poids.

Comme il n'est pas possible de constater courament d'une façon précise et dans des conditions spécifiques changeantes, si le givre a subi un accroissement ou une perte, il est absolutement nécessaire de baser la comptabilité et le contrôle des parties particulières, là où c'est indispensable, sur le nombre de pièces, qui est une grandeur stable et non seulement sur le poids, qui a été identifié comme une grandeur variable.

Ainsi le contrôle par pièces des parties transportées se montre seul infaillible et élimine les fautes et toutes confusions.

Il peut être intéressant de remarquer, que les considérations que voici, étaient provoquées par des cas concrets, qui pouvaient avoir des conséquences assez importantes pour les intéressés.

Il y a d'ailleurs différentes opinions sur le sujet des pertes de poids de la viande congelée sortant du frigorifique.

Ainsi les prescriptions de la Direction Centrale de l'Industrie de la Viande en Pologne, prévoient des pertes de 0.01 jusque 0.03 % suivant les distances et les saisons.

Les prescriptions de la USSR admettaient d'après un article de l'ingénieur Kontchakow dans le Nr 2 de la Holodilnaja Tehnika de 1958 «sur les pertes de poids de la viande congelée au cours de sa sortie de frigorifique et son transport», des pertes de 0.71% jusque 1.15%.

Par contre l'auteur cité Kontchakow a constaté à base d'essais, épreuve et expérimentations, qu'au cours de la sortie de la viande congelée du Frigorifique Nr. 9 à Moscou et durant un entreposage à court terme au magasin de distribution, des pertes de poids de la viande congelée n'ont pas eu lieu, tout au contraire, il y a même des accroissements de poids de 0.5 jusque 1.37%.

Il est d'ailleurs bien naturel, qu'il faut tâcher d'exclure, ou au moins de limiter toutes influences défavorables pendant la congélation, l'entreposage et le transport,

Approved For Release 2009/05/01 : CIA-RDP80T00246A007500340002-0

Approved For Release 2009/05/01 : CIA-RDP80T00246A007500340002-0

qui pourraient changer le poids de la marchandise et qu'il faut toujour tâcher de garantir les conditions technilogiques régulières.

Si tout de même, dans des circonstances spéciales, le trafic normal pouvait décevoir, il faut dans ces cas là se confier au contrôle par nombre et non seulement par poids, et surtout s'abstenir de tirer des conclusions bâties sur des manques apparents. Toutes évaluations sur ce sujet étant des grandeurs relatives à des cas spéciaux ne se laissent pas appliquer à la lettre à d'autres conditions, qui ne sont jamais identiques avec celles, qui servaient de base pour le relevé des grandeurs premières.

Behrndt bogtryk, Denmark

Copyright reserved

Approved For Release 2009/05/01 : CIA-RDP80T00246A007500340002-0

Approved For Release 2009/05/01 : CIA-RDP80T00246A007500340002-0

Investigation and Application of Freeze-Drying of Foods

Etude et application de la cryo-dessiccation des aliments

G. B. TCHIGEOV
The Leningrad Technological Institute of the Refrigerating Industry,
Leningrad, U.S.S.R.

SOMMAIRE. On utilise actuellement la lyophilisation dans l'industrie alimentaire soviétique pour la déshydratation de la viande et du poisson pour la production d'aliments concentrés. On l'utilise sur une moins grande échelle pour la déshydratation des fruits et des baies, des jus de fruits, de la levure de boulanger et de certains autres produits.

Les recherches effectuées au cours des dernières années ont été consacrées à la physique de la sublimation et de la désublimation à basses pressions, ainsi qu'au transfert de vapeur d'eau dans ces conditions. On utilise actuellement les résultats de ces recherches pour l'établissement de méthodes permettant d'évaluer les modes et le matériel de déshydratation, pour l'amélioration de la conception ainsi que pour la détermination des conditions de déshydratation optima.

En se basant sur les travaux des physiciens et des techniciens on a établi les conditions techniques assurant la qualité des aliments et l'on a élaboré des recommandations pour le choix des conditions de déshydratation. Certains types de matériel de déshydratation ont été conçus et reconnus les plus appropriés.

La lyophilisation des aliments se fait généralement à une pression de 0,5 à 1 mm de Hg, à une température de sublimation de –3° à –27° C. et à une température de désublimation de –25° à –78° C. La désublimation se fait dans un appareil à plaques froides avec dégivrage périodique. On n'utilise pas de nettoyage mecanique, ni d'absorbants d'humidité chimiques. Le vide est assuré dans les déshydrateurs par des pompes à huile rotatives. La température et la pression de déshydratation sont reglées en divers points du déshydrateur, on utilise des compteurs thermo-électriques à distance pour les mesures. L'imperméabilité est vérifiée à l'aide de spectromètres de masse à hélium.

In 1921, a patent was issued in the U.S.S.R. for the method of drying foods in a frozen state [12, 15]. However, there was neither a great need nor technical means for the industrial application of the new technique at that time.

Extensive theoretical and laboratory investigations of the freeze-drying process were carried out during the last 15 years and its application for industrial dehydration of various materials including foodstuffs has been started. The leading role in the investigation of freeze-drying in the U.S.S.R. belongs to academician A. V. Lykov and his school [9, 10, 11, 12, etc.].

According to notions based upon investigations, the entire freeze-drying process may be divided into three periods essentially differing from each other [1, 6, 9, 12, 15].

The first period, the period of vacuum freezing, starts as soon as the food to be dried is placed in the sublimator. A quick evacuation of the air from the sublimator results in intensive evaporation from the surface of the food and in its freezing. The duration of the first period constitutes 4 to 6 % of the total time of drying, and 10 to 20 % of the total moisture is evaporated.

With the required vacuum attained and the product completely frozen, the second period starts, i. e. the drying process proper begins. Outside heat is supplied to the food being dried and a sublimation of ice occurs. The second period lasts for about 50 to 60 % of the total drying time, while 40 to 50 % of the total moisture content is removed.

Approved For Release 2009/05/01 : CIA-RDP80T00246A007500340002-0

Approved For Release 2009/05/01 : CIA-RDP80T00246A007500340002-0

Thereafter, the supply of heat is increased and the temperature of the food being dried is raised up to 40 – 45° C. Thus, the third period of drying begins, and the remaining moisture is removed. The temperature increase during this period does not impair the product as it is comparatively short and the moisture content of the product is by this time small. The duration of the third period constitutes 30 to 40% of the total time of the process and the moisture removed amounts to 20 to 30 % of the original content.

The period of vacuum freezing is characterized by a gradual pressure drop in the sublimator and the temperature decrease in the food being dried. Under such conditions, the heat exchange as well as the mass exchange are not stationary and the operating parameters of these processes are changing in time. Analytical calculations of vacuum freezing are therefore quite complex [16, 17].

The role of vacuum freezing in the general process of freeze-drying is quite considerable as the intensity of evaporation occuring in this period without any supply of external heat is great. It should be noted also that the distribution of the ice crystals and the possibility of preserving the structure of the food depend to a large extent upon the conditions of vacuum freezing [12, 18, 19, etc.].

The total pressure, the water-vapour pressure and the temperature in the freeze-drier are sufficiently high at the beginning of the vacuum-freezing period and the water-vapour transfer corresponds to the viscous flow (diffusion).

It is generally assumed that the food being dried should be reduced at the end of the vacuum freezing period to the cryohydrate temperature. This assumption is hardly correct. It can only be asserted that the more labile the food is biologically speaking, the lower should its drying temperature be.

The intensity of drying increases with an increment of the temperature difference between the evaporation (or sublimation) and condensation surface. Therefore, the higher the sublimation temperature, the greater the drying rate. Good results are attained for an overwhelming majority of foods with drying temperatures ranging from –5° C. to –20° C. i. e. considerably above the cryohydrate temperature of these foods [4, 6, 13, 14, 18].

During the period of vacuum freezing the pressure and the temperature of the water-vapour in the food being dried is gradually reduced to such an extent that the length of the free path of the vapour molecules becomes commensurable with the dimensions of the pores in the material. The motion of the water-vapour in the pores is then subject to the laws of the molecular-viscous (effusive-diffusive) flow. Finally, if the total pressure in the freeze-drier during the second and third periods is sufficiently low (usually below 1 mm Hg), the water-vapour flow becomes purely molecular (effusive).

This was why A. B. Lykov suggested terming the process of drying at low pressures and low temperatures molecular drying; this term is often used in Soviet engineering literature of later years [3, 12, 15].

During the second period of the freeze-drying process a gradual deepening of the evaporation zone takes place, the temperature and pressure remaining constant. Due to a sharp increase of volume occuring when ice sublimates in a vacuum, a violent and chaotic movement of the water-vapour is created from the surface of the ice in the food to the branch line. The mass-exchange in this case completely determines the heat-exchange and is decisive for the hydrodynamic conditions of the process [5, 11].

The intensity of sublimation depends under practical conditions not only upon the rate of heat supply but also upon the rate of the water-vapour evacuation, the latter depending as well on the resistance in the pipelines and of the entire system.

In case the intensity of sublimation exceeds the actual rate of the water-vapour evacuation, the pressure in the sublimator rises and the general drying conditions are disturbed. Therefore, it is recommended that the pipelines and condensers of the freeze-dryer be arranged in such a manner that they may operate reliably at the highest drying load corresponding usually to the vacuum freezing period [13, 14, 15, 19].

With the sublimation and condensation temperatures as well as the composition

Approved For Release 2009/05/01 : CIA-RDP80T00246A007500340002-0

Approved For Release 2009/05/01 : CIA-RDP80T00246A007500340002-0

of the air-water-vapour mixture being constant, the intensity of sublimation is in direct proportion to the total pressure in the sublimator, within the range of 0.3 to 2.0 mm Hg. Within the above pressure range there is also a direct proportion between the film coefficient of heat transfer at condensation and the total pressure of the air-water-vapour mixture in the condenser [20, 21, 24].

These facts may be explained by an intense agitation of the air-vapour mixture by ricocheting gas molecules as well as by the intensification of the heat exchange resulted thereby in the case of a comparatively low concentration of molecules of non-condensable gases in the vapour-gas mixture.

Recent thorough experiments have shown that the intensity of condensation is influenced not only by the total pressure but also by the composition of the vapour-gas mixture. With an increase of the partial pressure of the vapour in the mixture, its condensation is intensified to a somewhat higher degree than in the case of an increase in the partial pressure of the gas.

The fact that the role of the condenser in the freeze-drying installation is confined to the evacuation of water-vapour generated from the substance being dried made it possible to elaborate a method of calculating a condenser as an evacuating device, though the physical nature of the evacuation action is based on the removal of heat from the condensing vapour [20].

Roentgenoscopic examinations have been carried out on the formation of ice on the cold surface of the condenser-freezer. The influence of the pressure of the water-vapour-gas mixture, of the condensing temperature and of the gas component properties upon the distribution of ice on the surface of the condenser have been thus determined. This allowed the elaboration of a method for calculating the effective condensation surface for various operating conditions depending upon the shape and dimensions of the condenser [21, 23, 24].

The investigations of the ice formed at very low pressures, corresponding to effusive flow conditions have shown that its density and thermal conductivity are greater than in the case of ice formation under pressures, corresponding to the conditions of the diffusive movement of the water-vapour [22].

The freeze-drying method is used in the Soviet Union mainly for the dehydration of cut and ground meat and fish in the production of concentrated foods. A technique has been elaborated for drying fruits and berries, fruit juices, bread yeast as well as certain other foods. A higher stability during storage and a better reconstitution of freeze-dried foods than those of heat dried foods have been proved experimentally [4, 6, 7, 12, 13, 15, 18]. Certain standards have been set for dried foods. For example, freeze-dried ground meat and fish have to comply with the following requirements [13, 14, 15]:

TABLE 1. REQUIREMENTS FOR FREEZE-DRIED GROUND MEAT AND FISH

	Ground meat	Ground fish
Minimum swelling coefficient	3.0	3.5
Maximum soft-boiling time (minutes)	20	5.0
Maximum moisture content (%)	10	10
Minimum extractivity (% in relation to dry substance)	15.0	20.0
Maximum fat content (% in relation to dry substance)	15.0	6.5

Freeze-dried ground meat or fish can be stored in nitrogen filled or evacuated glass or tin containers for 12 months if loosely packed and for 24 months if pressed.

The following table presents the freeze-drying conditions for certain foods elaborated and applied in practice [12, 13, 14, 15]:

Approved For Release 2009/05/01 : CIA-RDP80T00246A007500340002-0

Approved For Release 2009/05/01 : CIA-RDP80T00246A007500340002-0

TABLE 2. FREEZE-DRYING CONDITION FOR CERTAIN FOODS

Nos	Kind of food	Moisture content (%)		Temperature (°C.)				Pressure (mm Hg)	Drying time (hrs.)
		Initial	Final	Sublimation		Condensation			
1.	Ground meat	75–77	4–6	–5	–17	–25	–30	1.2–2.5	10–11
2.	Meat cuts 10–12 mm thick	75–77	4–6	–3	–15	–25	–30	1.2–2.2	27–30
3.	Ground fish	82–83	4–5	–5	–17	–25	–30	1.6–2.2	11–13
4.	Fish cuts 10–12 mm thick	82–83	4–5	–5	–15	–25	–30	1.5–2.2	22–24
5.	Strawberries	88.6	9.6	–3	–12	–25	–30	0.9–1.8	21
6.	Tomatopuree	85.0	10	–5	–17	–25	–30	0.5–1.8	20
7.	Orange and lemon juice (thickness of layer – 5 mm)	89.0	3.8	–25		–78		0.1–0.25	3–4

A number of freeze-drying units and installations have been designed in accordance with the accepted technique of the process. Calculation methods for the above equipment have been established [2, 3, 12, 13, 14, 20, 25].

The high stability of foods dried in the frozen state, the quick and almost complete recovery of their natural properties with water added make such foodstuffs especially valuable in all the cases when transportability, good keeping quality and easy cooking properties are of importance.

All the above characteristics contribute to the attraction of attention to the freeze-drying of foods and promote the expansion of the production of foods dehydrated in a frozen state.

REFERENCES

1. VERBA, M. Drying Foods by Sublimation. Collection *Drying in the Food Industry.* Profizdat, Moscow, 1958.

2. GRYAZNOV, A. Principles of Calculating and Designing Industrial Freeze-drying Installations. Collection No. 16. Institute of Chemical Machine Building, Moscow, 1956.

3. GRYAZNOV, A. Principles of Calculating and Designing Molecular drying Installations. Collection *Drying in the Food Industry.* Profizdat, Moscow, 1958.

4. GUIGO, E. and GULYAEVA, A. Freeze-drying of casein. *Molochnaya Promyshlennost,* (8), 1950.

5. GUKHMAN, A. and ERMAKOVA, K. Fundamentals of Heat-exchange at the Sublimation of Ice Under a Vacuum. *Journal of Technical Physics of U.S.S.R.,* (8), 1953.

6. KAUKHCHESHVILI, E. Drying Foods at Low Temperatures. *Myasnaya Industriya S.S.S.R.,* (1), 1950.

7. KAUKHCHESVILI, E. and TIMOFEYEVA, L. The Recoverability of Meat Dehydrated at a Low Temperature. *Myasnaya Industriya S.S.S.R.,* (5), 1951.

8. KAUKHCHESHVILI, E. Drying Foods at Low Temperatures. Collection *Drying in the Food Industry.* Profizdat, *Moscow, 1958.*

9. LYKOV, A. The Theory of Drying. Gosenergoizdat, Moscow, 1950.

10. LYKOV, A. Migration Phenomena in Capillary-porous Bodies. Gostekhizdat, Moscow, 1954.

11. LYKOV, A. Heat- and mass-exchange in the drying processes. Gosenergoizdat, Moscow, 1956.

12. LYKOV, A. and GRYAZNOV, A. Molecular drying. Pishchepromizdat, Moscow, 1956.

13. OLEINIKOV, F. and SINITSIN, A. Experience on Industrial Operation of a Food Freeze-drying Installation. Scientific-technical Society of the Food Industry, Rostov-on-Don, 1958.

14. POPOVSKY, V. Experimental Industrial Plant for Freeze-drying of Foods at the *Smichka* Enterprise. Collection *Drying in the Food Industry.* Profizdat, Moscow, 1958.

Approved For Release 2009/05/01 : CIA-RDP80T00246A007500340002-0

Approved For Release 2009/05/01 : CIA-RDP80T00246A007500340002-0

15. POPOVSKY, V. Production Experience in the Molecular Drying of Foods. *Technical Progress,* Bulletin of Scientific-Technical Committee of Moldavian S.S.R., Kishinev, 1957.

16. RYZHOVA, E. Self-freezing Under a Vacuum. *Works of Leningrad Refrigerating Institute,* **10**. Pishchepromizdat, Moscow, 1956.

17. RYZHOVA, E. Investigations of Freezing and Drying in a Vacuum. *Works of the Moscow Food Institute,* (6). Pishchepromizdat, Moscow, 1956.

18. TITOV, N. The technology of the Production of Dehydrated Biological Preparations. Selkhozgiz, Moscow, 1945.

19. TCHIGEOV, G. The Physical Basis of Drying Biological Materials by Freezing. *Kholodilnaya Tekhnika,* (4), 1948.

20. SHUMSKY, K. Principles of Calculating Sublimation Condensers. *Kholodilnaya Tekhnika,* (2), 1958.

21. SHUMSKY, K. The Mechanism of Condensing Vapour into a Solid State. Collection No. 24. Institute of Chemical Machine-Building, Moscow, 1958.

22. SHUMSKY, K. Thermo-physical Characteristics at the Condensation of Water-vapour in a Rarified Medium. Collection No. 24. Institute of Chemical Machine-Building, Moscow, 1958.

23. SHUMSKY, K. Specific Features in the Investigation of the Process of Condensing Vapour Into a Solid State Under a Vacuum. Collection No. 24. Institute of Chemical Machine-Building, Moscow, 1958.

24. SHUMSKY, K. The Condensation of Water-vapour in Freeze-drying Installation. Collection *Drying in the Food Industry.* Profizdat, Moscow, 1958.

25. SHUMSKY, K. and BALSHIN, R. Continuous Unit for Drying Frozen Materials Under a Vacuum. Collection *Drying in the Food Industry.* Profizdat, Moscow, 1958.

Behrndt bogtryk, Denmark

Copyright reserved

Approved For Release 2009/05/01 : CIA-RDP80T00246A007500340002-0

Approved For Release 2009/05/01 : CIA-RDP80T00246A007500340002-0

The Storage Conditions and Weight Loss of Frozen Meat in Jacketed Cold Storage Rooms

Les conditions d'entreposage et les pertes de poids de la viande congelée conservée dans des chambres froides à doubles-parois

D. G. RUTOV and P. A. ALEKSEYEV
The Scientific Research Institute of the Refrigerating Industry of the U.S.S.R., Moscow, U.S.S.R.

SOMMAIRE. Des expériences ont été effectuées en 1956–57 sur l'entreposage de la viande congelée dans une chambre froide à doubles-parois à l'Entrepôt Frigorifique n° 12 à Moscou. La température de l'air était maintenue automatiquement à – 18° C. dans la chambre et à – 18°, – 19° C. entre les parois. L'humidité relative s'élevait à 97–100 %. Le lot de viande témoin était pesé tous les mois.

Il été établi que les pertes de poids de la viande étaient à peu près proportionnelles à la quantité de chaleur pénétrant dans la chambre, cette dernière variant en fonction de la température des chambres des étages voisins. Aux périodes où les pertes de chaleur sont pratiquement nulles, les pertes de poids de la viande deviennent insignifiantes. Au cours des 12 mois, les pertes de poids totales de la viande congelée étaient de 0,78 %, soit 2 à 2,5 fois moins élevées que dans les chambres froides ordinaires, sans doubles-parois. Les pertes de poids réelles dues à l'évaporation correspondaient bien aux chiffres théoriques obtenus d'après les formules proposées par D. RUTOV en 1954–1955.

Il a été prouvé par des calculs théoriques et par des expériences que pour réduire les pertes au minimum et pour obtenir une stabilité maximum de la température et de l'humidité de l'air dans la chambre froide, la cloison de séparation entre la chambre et la double paroi doit être très imperméable à la vapeur et doit être isolée thermiquement. Dans les entrepôts frigorifiques à plusieurs étages il faut aussi prévoir une isolation thermique pour les planchers.

Two experiments on prolonged storage of frozen meat in an air-jacketed storage room of the Moscow Cold Store No 12 were carried out in 1956 end 1957 to deter-
room of the Moscow Cold Store No 12 were carried out in 1956 and 1957 to deter-
rooms.

The jacket in the form of a 60 cm wide corridor surrounds the outside walls of the rooms of the second to sixth story and the ceiling of the sixth story of the warehouse [1, 2]. The jacket is cooled by finned ammonia coils under natural air circulation.

The experiments were carried out in room No. 31 located on the third floor. The room had a floor area of 22.6 × 22.6 m and was 3.2 m in height, the useful area being 500 m².

1956 EXPERIMENTS[1]

Frozen meat was loaded in the room in 8 stacks (Fig. 1). One stack of beef (No. 6, 9550 kg in weight) was loaded directly onto the platform of ten ton truck scales mounted in the room and was weighed each month without being taken apart. The meat in the other stacks was weighed only twice, at the beginning and end of the storage period.

The loss in weight of the meat during the storage period is given in Table 1.

[1] The experiments were carried out with the participation of Y. Olenev and L. Rossovsky (Laboratory of Refrigerating Technology, VNIKhI).

Approved For Release 2009/05/01 : CIA-RDP80T00246A007500340002-0

Approved For Release 2009/05/01 : CIA-RDP80T00246A007500340002-0

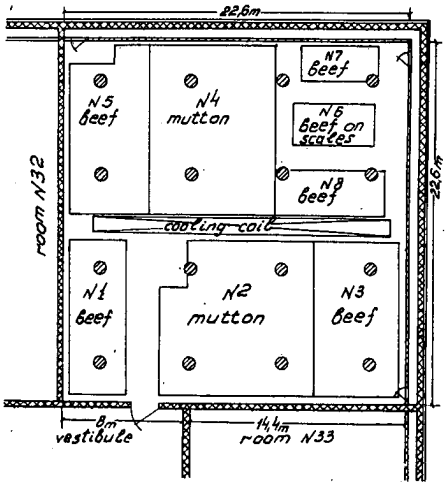

Fig. 1. Layout of room no. 31 and arrangement of the experimental stacks of frozen meat.

TABLE 1. LOSS IN WEIGHT OF MEAT IN STORAGE

Kind of meat	Weight of meat at beginning of storage, kg	Loss in weight during storage	
		kg	%
Beef, first grade	194,010	1187.9	0.61
Mutton, first grade	125,090	888.9	0.71
Total	319,100	2076.8	0.65

The mean room temperature during the storage period was –18.1° C., and the mean relative air humidity 96.1 %.

Under the operating conditions of the warehouse the temperature of the adjacent upper and lower rooms was somewhat higher most of the time than that of the experimental room, varying from –15 to –19° C., with a mean of –16.5° C. Owing to variations in the temperature differences, the heat inflow into the room through the uninsulated floors and ceilings was subjected to considerable fluctuations, enabling assessment of its influence on the shrinkage rate of the stored

TABLE 2. STORAGE CONDITIONS AND SHRINKAGE OF FROZEN MEAT 1956 EXPERIMENTS

Period	Number of days	Temperature °C.	Relative humidity %	Heat inflow Thou. kcal.	Total shrinkage kg
18.4 – 23.5	35	–18.5	96.0	3,095	–
24.5 – 21.6	29	–18.0	95.2	2,429	–
22.6 – 23.7	32	–18.4	94.3	3,996	–
24.7 – 23.8	31	–17.7	97.5	3,192	–
24.8 – 20.9	28	–18.1	97.9	–546	–
	155	–18.1	96.1	12,166	2076.8

Approved For Release 2009/05/01 : CIA-RDP80T00246A007500340002-0

Approved For Release 2009/05/01 : CIA-RDP80T00246A007500340002-0

frozen meat. The heat inflow into the room was absorbed by the cooling coil over the central aisle, the coil being turned off and on automatically.

The value of the heat inflow into room No. 31 was calculated from experimental data on the overall heat transfer coefficients of the room enclosures, their surface areas and the temperatures of the room and of all adjacent compartments.

The storage conditions and heat inflow values for each of the between weighing periods of the control stack are given in Table 2.

Since the initial and the final dates of storage for the control stack did not coincide with the mean dates its shrinkage is given in a separate table (Table 3). The total percentage of shrinkage for the control stack (0.79 %) was somewhat higher than for the others, which may be explained by the small size of the former.

TABLE 3. SHRINKAGE OF CONTROL STACK
1956 EXPERIMENTS

Period	Number of days	Heat inflow Thou. kcal.	Shrinkage of control stack %
23.4 – 23.5	30	2,653	0.14
24.5 – 21.6	29	2,429	0.13
22.6 – 23.7	32	2,996	0.26
24.7 – 23.8	31	3,192	0.21
24.8 – 17.9	25	–487	0.05
	147	10,783	0.79

1957 EXPERIMENTS[2]

In 1957 the experiments were carried out for almost the entire year. One of the stacks was kept on the platform of the truck scales and weighed monthly.

The results of the meat storage are given in Table 4:

TABLE 4. LOSS IN WEIGHT OF MEAT DURING STORAGE

Kind of meat	Weight at beginning of storage, kg	Shrinkage on storage kg	%
Beef, first grade	183,768	1,438.5	0.78
Beef, second grade	56,571	702.7	1.24
Mutton, first grade	86,530	678.7	0.78
Total	326,869	2,819.9	0.86

The mean temperature in the room during the storage period was –17° and the mean relative humidity 97 %. As in the 1956 experiments considerable heat inflow from the adjacent rooms was observed, highly varying in time especially from the rooms nos. 41 and 21 where the mean temperatures were –15.6° and –16.3° C. respectively.

In table 5 data are presented on the storage conditions and heat inflow of room no. 31 for each of the periods between weighings of the control stack and also on the weight losses in the latter.

[2] The experiments were carried out with the participation of O. Vysotskaya (Laboratory of Refrigerating Technology, VNIKhI).

Approved For Release 2009/05/01 : CIA-RDP80T00246A007500340002-0

Approved For Release 2009/05/01 : CIA-RDP80T00246A007500340002-0

TABLE 5. STORAGE CONDITIONS AND SHRINKAGE OF FROZEN MEAT
1957 EXPERIMENTS

Period	Number of days	Temperature °C.	Relative humidity %	Heat inflow Thou.kcal.	Overall shrinkage kg	Shrinkage of control stack %
9.2 – 28.2	19	–17.0	97.1	749	–	–
1.3 – 31.3	31	–14.0	96.8	1,223	–	0.06
1.4 – 30.4	30	–15.9	96.8	558	–	0.05
1.5 – 31.5	31	–17.9	95.1	2,765	–	0.13
1.6 – 30.6	30	–16.8	95.3	4,497	–	0.24
1.7 – 31.7	31	–16.6	96.0	4,275	–	0.22
1.8 – 31.8	31	–17.8	96.5	1,446	–	0.07
1.9 – 30.9	30	–17.5	97.0	–162	–	0.03
1.10 – 31.10	31	–17.3	97.5	872	–	0.07
1.11 – 30.11	30	–17.7	98.2	449	–	0.04
1.12 – 31.12	31	–17.7	98.7	–594	–	0.01
1.1 – 25.1	25	–17.6	98.5	273	–	0.02
	350	–17.0	97.0	16,351	2,819.9	0.94

In ordinary unjacketed cold store rooms the shrinkage of frozen meat calculated according to the norms adopted in the U.S.S.R. are considerably higher than those obtained for the experimental storage in the jacketed room (Table 6).

TABLE 6. SHRINKAGE OF FROZEN MEAT ACCORDING TO NORMS FOR ORDINARY COLD STORES AND IN JACKETED ROOMS

Kind of meat	Shrinkage in accordance with norms for ordinary cold stores %	Shrinkage in jacketed rooms %
1956 experiments:		
Beef, first grade	1.11	0.61
Mutton, first grade	1.33	0.71
1957 experiments:		
Beef, first grade	1.67	0.78
Beef, second grade	2.18	1.24
Mutton, first grade	2.02	0.78

Thus, despite the considerable heat influx from the adjacent rooms the jacketed room showed, on an average, a twofold decrease in shrinkage as compared with the norms for ordinary cold stores.

THE SHRINKAGE RATE OF FROZEN MEAT AS A FUNCTION OF THE HEAT INFLOW

A plot (Fig. 2) of the experimental data presented in Tables 3 and 5 confirms the close to linear dependence of the shrinkage rate on the heat inflow previously established on theoretical grounds [3]. It is characteristic that for small heat inflows (positive and negative) the shrinkage rate fluctuates around the value 0.03 % per month. This is due to the presence of transit heat flows in the room, practically unavoidable and difficult to account for, that cause frost deposits on the somewhat colder sites of the room enclosures with corresponding dessication of

Approved For Release 2009/05/01 : CIA-RDP80T00246A007500340002-0

Approved For Release 2009/05/01 : CIA-RDP80T00246A007500340002-0

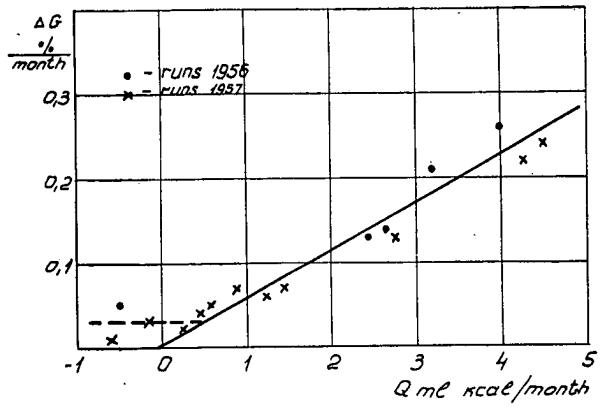

Fig. 2. Dependence of frozen meat shrinkage ΔG in the control stacks on the heat inflow rate Q into the cold storage room.

the products. Evidently 0.03 % per month is the lowest attainable shrinkage rate for frozen products in jacketed multi-story cold stores.

COMPARISON OF EXPERIMENTAL AND CALCULATED VALUES FOR SHRINKAGE RATE AND AIR HUMIDITY

Inasmuch as in the experiments account was made of all factors influencing the rate of shrinkage and the relative humidity in the room, one could compare the experimental values of these quantities with those obtained from calculation with the aid of the formulae proposed by D. Rutov in 1954–55 [3, 4].

Bearing in mind that no additional sources of moisture inflow into the room were present, calculation of the shrinkage rate was made according to the formula:

$$\Delta G = \frac{Q(p' - p_0')}{m\left(1 + \frac{\alpha_z}{\alpha_c}\right)(t - t_0) + r(p' - p_0') + \frac{QM}{\beta F}} \quad (1)$$

and the relative humidity according to

$$1 - \varphi = \frac{p' - p_0'}{p'} \cdot \frac{1}{1 + \frac{\beta F}{QM}\left[m\left(1 + \frac{\alpha_z}{\alpha_c}\right)(t - t_0) + r(p' - p_0')\right]} \quad (2)$$

In the calculation it was taken into account that the difference $t-t_0$ averaged 10° C.

Resultsof the calculation are given in Table 7.

TABLE 7. CALCULATED AND EXPERIMENTAL SHRINKAGE RATES IN FROZEN MEAT

	F m²	Q kcal/hr	ΔG g/hr experim.	ΔG g/hr calc.	Φ % experim.	Φ % calc.
1956 experiments	4,830	3270	558	585	96,1	96,5
1957 experiments	4,614	1947	336	388	97,0	97,8

Approved For Release 2009/05/01 : CIA-RDP80T00246A007500340002-0

Approved For Release 2009/05/01 : CIA-RDP80T00246A007500340002-0

Since the experiments were carried out under practical conditions the coincidence of calculated and experimental values may be considered to be quite satisfactory.

THE STATE OF THE AIR IN THE JACKET

In the 1956 experiments the mean air temperature in the jacket was –18.6° C. The turning on and off of the cooling coils caused a change in temperature of ±1.5° C. The temperature difference between the room and jacket was small and no frost deposit on the partition was observed from the side facing the room.

In the 1957 experiments the temperature in the jacket was –18.5° with a mean room temperature of –17°. This temperature difference of 1.5° already caused deposition of frost on the partition despite a layer of thermal insulation on the latter. Calculation indicates that frost deposition would occur on an uninsulated partition at a temperature difference of only 0.5° C.

In summer the relative air humidity was 15 % lower in the jacket than in the room. Consequently in constructing a jacket a good vapour seal must be provided for between the former and the room.

INSULATION BETWEEN REFRIGERATED ROOMS ENCLOSED WITHIN A COMMON JACKET

In multi-room refrigerated warehouses, particularly of the multistory type the installation of a jacket along the outside walls of the structure does not yet solve the problem of a sharp decrease in shrinkage rate. In a case of a considerable heat flow from one room to another through partitions of floors, shrinkage may attain high values even in the presence of a jacket.

Since in practice temperature fluctuations of the order of 1–2° are not excluded, the floors separating rooms with nominally the same temperature conditions should be insulated, providing for an overall heat transfer coefficient of the flooring of about 0.4 kcal/m² hr °C. The same may be said of the partitions between rooms.

CONCLUSION

A test of a jacketed room in the Moscow Cold Store No 12 showed that this method of diminishing weight losses of stored products has justified itself under practical conditions and deserves widespread application, especially in the southern parts of the country. Losses of frozen meat during storage were two times lower than in the case of ordinary cold stores. There is possibility for further decrease in shrinkage to a level of 0.03 % per month.

Cold store rooms included in a common air jacket should be separated by thermally insulated walls and floors to lower the internal heat flows. The partitions separating the rooms from the jacket should also have a layer of thermal insulation.

The temperatures in the rooms and in the jacket should be maintained as constant as possible, using reliable automatic controls. The temperature of any site in the jacket should not be below that of the room by more than 1° C.

REFERENCES

1. BADYLKES, I., SAFONOV, V. and TKACHEV, N. Automated Refrigerated Warehouse with Thermal Protective Air Jacket. *Kholodilnaya Tekhnika,* (4), 45, 1954.

2. TKACHEV, N. The Construction of Large-size refrigerated Warehouses in the U.S.S.R. Proc. of the IX International Congress of Refrigeration, Vol. II, 5 029, 1955.

3. RUTOV, D. The Diminishing of Weight Losses in Frozen Meat During Storage. Proc. of the IX International Congress of Refrigeration, Vol. II. 4 153, 1955.

4. RUTOV, D. Moisture Exchange in Rooms for the Storage of Frozen Products. *Kholodilnaya Tekhnika,* (3), 38, 1954.

Behrndt bogtryk, Denmark

Copyright reserved

Approved For Release 2009/05/01 : CIA-RDP80T00246A007500340002-0

Approved For Release 2009/05/01 : CIA-RDP80T00246A007500340002-0

The Application of Glazing and Low Temperatures in the Storage of Frozen Sprat (Clupea Harengus Membras Linné)

Emploi du givrage et des basses temperatures pour la conservation du sprat congelé

A. I. PISKAREV, A. K. KAMINARSKAYA and L. G. LUKYANITSA
The Scientific Research Institute of the Refrigerating Industry of the U.S.S.R., Moscow, U.S.S.R.

SOMMAIRE. Un des problèmes importants de l'industrie du poisson est l'emploi de poisson congelé pour la fabrication de conserves diverses. Des essais de laboratoire et des expériences industrielles ont été entreprises par le VNIKhI, sur la conservation de blocs de sprats congelés et givrés (Clupea harengus membras Linné), à –35°, –25°, et –18° C., en vue d'une transformation ultérieure en conserves.

Des essais ont été faits en additionnant l'eau destinée au givrage d'un antioxydant, l'acide ascorbique. La qualité du poisson a été évaluée, pendant l'entreposage, par les modifications des peroxydes et aussi par des tests organoleptiques. Les résultats de cette recherche ont montré l'influence du givrage et des basses températures d'entrepossage sur le poisson gras comme le hareng. L'emploi d'acide ascorbique produit une action inhibitrice notable sur la formation des peroxydes. Cependant, on a noté une saveur inhabituelle au poisson sur des échantillons traités avec l'acide ascorbique. Les conserves, obtenues à partir de sprats congelés conservés trois mois à –18° C., ont été considérées comme satisfaisantes.

Les durées d'entreposage ci-après précisées, pour des blocs de sprats congelés et givrés, destinés à la mise en conserve, peuvent être recommandées d'après les résultats des essais: à –18° C.: 2 mois; à –25° C.: 3 mois; à –35° C.: 4–5 mois.

On congèle de grandes quantités de sprats dans des installations de traitement de poisson de la côte balte. Le sprat congelé sert à la fabrication de conserves de sardines et de sprats, en dehors des saisons de pêche.

The use of frozen fish as raw material in the production of various types of canned foods is a highly important problem in the fishery industry, since the duration of the fishing season is very limited for many fishing grounds.

The solution of this problem would mean considerable increase in the production of the higher grades of canned foods and prolongation of the working season of canneries.

Of considerable interest to the fisheries industry of the Baltic Republics of the U.S.S.R. is the use of frozen sprat *(Clupea harengus membras, Linné)* for canning. Sprat constitutes about 50% of the total catch in these republics and about 80% of it is caught in the spring season (1–1.5 months). This naturally presents great difficulties for the rational utilization of sprat, in particular for canning purposes.

In respect of its chemical composition (up to 10% fat and 20% protein content) and biochemical characteristics this fish is a valuable raw material for the production of high quality canned foods of the sprat and sardine type.

However, owing to its biological properties (content of highly active enzymes) sprat begins to spoil quickly in the cooled state. Therefore, the possibility of preserving this fish in the frozen state for subsequent packing in the canneries is a question of considerable importance.

In the Baltic Sea fishing grounds two sizes of sprat are caught, large and small. The small fish serve as raw material for the production of canned sprats and sardines, the large for the production of a canned product known as "sprat in oil".

In the present report results are reported of experiments on the effect of low temperatures and glazing (with and without antioxidant) on the keeping quality

Approved For Release 2009/05/01 : CIA-RDP80T00246A007500340002-0

Approved For Release 2009/05/01 : CIA-RDP80T00246A007500340002-0

of frozen sprat as well as data on the practical utilization for the production of canned products.

Laboratory experiments on this problem were carried out at VNIKhI and field experiments in a fish plant in the Latvian SSR.

Sprat was frozen in 3.5–4.0 kg blocks in a tunnel freezer with a strong air blast at –30° C. The frozen fish were stored at temperatures of –18°, –25° and –35° C. Unglazed blocks, as well as blocks glazed in ordinary water and in a 0,8% aqueous solution of ascorbic acid were kept at each temperature. The glazing constituted 5–6% of the weight of the fish.

Quality evaluations of the fish during storage were made with respect to changes in fats, proteins and organoleptic characteristics.

The quality of the fat was determined by its peroxide content (according to the iodometric method, using chloroform for extraction of fat), that of the protein by the amounts of total and coagulable protein and of myosin (extraction with 5% sodium chloride solution). Sensory tests were made of cooked fish and of the final product (sprats and sardines).

The effect of glazing and of temperature on the change in peroxide numbers during storage of the sprat is shown in Fig. 1. The analytical results demonstrate the important part played by the glaze and the low temperatures in retarding the development of oxidative processes during the holding of the fish.

Unglazed specimens were subject to oxidation at all the storage temperatures investigated already during the first month. In the first month oxidative processes were observed in the glazed product only at –18° C., no peroxide formation being noted during that time at the other temperatures. At –25° C. peroxides began to appear in glazed sprat after a month's storage, and at –35° C. after 3 months' storage.

The peroxide values for the glazed fish at –18° C. were the same after three months as for the unglazed fish at –35° C.

A significant inhibiting action on the oxidation process in the fish fat was exerted by the ascorbic acid (Fig. 2).

For example, in storage at –25° C. the formation of peroxides in the fat of fish glazed with 0.8% ascorbic acid ice began a month later than in fish with glaze of ordinary ice.

Ascorbic acid plays a more important part in the retardation of oxidation at higher than at lower temperatures.

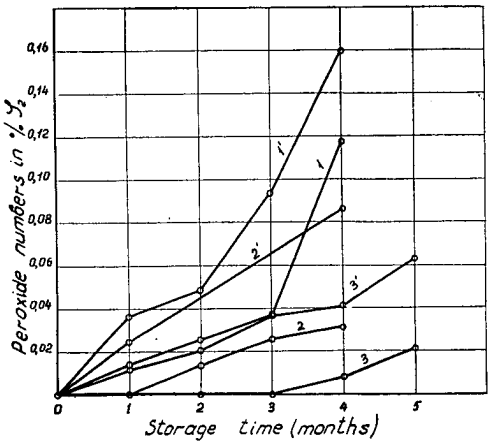

Fig. 1. The influence of glazing and temperature upon the change of peroxide numbers during the storage of sprat.
1. glazed at –18° C., 1'unglazed at –18° C. – 2. glazed at –25° C., 2' unglazed at –25° C. – 3. glazed at –35° C., 3' unglazed at –35° C.

Approved For Release 2009/05/01 : CIA-RDP80T00246A007500340002-0

Approved For Release 2009/05/01 : CIA-RDP80T00246A007500340002-0

Although ascorbic acid noticeably retarded peroxide formation, in the sensory evaluation of the ascorbic acid fish specimens the presence was marked of a foreign taste and odour in the fish.

The results of these investigations agree with the conclusions of Banks [1] and Perepletchik [2] as to the antioxidant properties of ascorbic acid and with those of Banks as to the influence of ascorbic acid on the organoleptic evaluation of fish.

The use of low storage temperatures for sprat markedly improves the keeping qualities of the fat. Moreover, at lower temperatures the sublimation of the glaze is considerably diminished, preventing the fish surface from dessication.

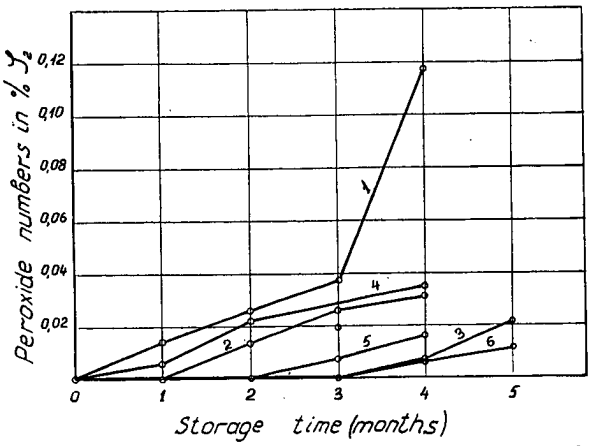

Fig. 2. The influence of ascorbic acid and temperature upon the change of peroxide numbers during the storage of sprat.
1. glazed at –18° C. – 2. glazed at –25° C., – 3. glazed at –35° C. – 4. glazed with ascorbic acid at –18° C. – 5. glazed with ascorbic acid at –25° C. – 6. glazed with ascorbid acid at –35° C.

In the studies on the protein solubility changes, no marked differences were revealed for the various storage temperatures and methods of processing of the sprat. This is evidently connected with the fattiness of the fish, because the solubility of protein, and particularly of its major fraction, myosin, depends upon the presence of lipoids, free fatty acids and other compounds in the fish.

It is known from the experiments of Dyer [3] that, other conditions (temperature and time) being equal, the denaturation of the protein of fatty fish develops slower than in nonfatty varieties. Hence, changes in the protein of the tissues will be less noticeable on storage of frozen sprat than changes in the fat. For utilization of frozen fish for canning, it is of practical importance to prevent changes in the protein of the skin layer which, owing to dessication, is particularly likely to become denaturate. In this respect glaze and low temperatures, hindering dessication of the surface, are important not only from the point of view of safeguarding against fat oxidation, but also as a means of retarding denaturation of protein.

Canned products (of the sardine and sprat type) were prepared from the experimental lot of sprat immediately after freezing and after 3 months' storage at –18° C.

Thawing the fish for this purpose was carried out in water at a temperature of 10–12° C. The thawed fish had a good appearance and firm texture. There was not a single case of belly barns[1].

On smoking the fish prior to canning the heat treatment in the oven is of prime importance. The quality of this intermediate product to a considerable extent determines that of the finished canned goods. In smoking, the skin of the fish may

[1] Fish with the intestinal tract burst open.

Approved For Release 2009/05/01 : CIA-RDP80T00246A007500340002-0

Approved For Release 2009/05/01 : CIA-RDP80T00246A007500340002-0

be impaired, making the fish unsuitable for canning. Frozen sprat is less resistant in this respect than the unfrozen product.

In processing the experimental lot of sprat for canning, 91% of the intermediate product was suited for further treatment.

The main characteristic for appraising the loss in quality of the smoked fish is impairment of the skin during the smoking operation. The origin of this defect may be traced back to both the conditions of the cold storage of the frozen fish as well as the smoking process itself. The effect of cold storage is manifested in denaturation of the skin protein. Since denaturation causes loss of firmness and elasticity of the skin the latter becomes more subject to mechanical damage during the heat treatment.

The preservation of the skin depends both on the method and conditions of smoking. Practical experience has shown that a short steaming of the fish in the smoking kiln results in a stronger skin.

On the basis of organoleptic tests it was established that canned sprats and sardines prepared from frozen sprat which had not been subjected to further storage, had a good texture, appearance and flavour and were comparable to canned products from unfrozen fish.

No significant difference has been found between canned fish prepared from frozen glazed sprat after 3 months' storage at –18° C. and that prepared from frozen non-stored specimens. Only in a few cases were impairments in the skin observed.

The advantages of the glazed sprat came to the fore during the organoleptic evaluation of fish cooked after storage at different temperatures. The taste panel recorded the considerable part played by glazing and by low storage temperature not only in preserving the fat, but also in preventing denaturative changes in the protein. Thus after a month's storage at –18° C. "dryness" was marked in both glazed and unglazed specimens, but the defect was more noticeable with the former than the latter. Dryness was also found with unglazed specimens kept at –25° C., but did not appear with the glazed ones stored at the same temperature. Note was made of the succulency of the fish stored at –35° C., there being hardly any difference in quality between the glazed and unglazed fish.

According to the sensory tests after 2.5 months' storage sprat kept at –18° C. without glazing already had a slightly oxidized fat and a faintly bitter taste. Bitterness was not noted in specimens stored at the other temperatures (–25 and –35° C.). Further development of dryness was noted in specimens stored at –18° and in unglazed fish stored at –25° C.

Our data on the importance of glazing during the cold storage of sprat are in accord with the findings of E. Nikkila and R. Linko [4].

Based on the results of the chemical and sensory analysis in the process of treatment of the fish and of the finished product the following limits in storage time for frozen fish to be used for canning have been established:

at –18° C. unglazed	1 month
at –18° C. glazed	2 months
at –25° C. unglazed	1.5 months
at –25° C. glazed	3 months
at –35° C. unglazed	3–4 months
at –35° C. glazed	4–5 months

In conformity with the technology developed, in the fish packing plants of the Baltic coast considerable quantities of sprat are frozen during the main catching period and are subsequently packed as canned sprats and sardines between seasons or during stormy weather. Such extension of the operating time of the canneries makes for better utilization of the raw fishery products.

REFERENCES

1. BANKS, J. *Sci. Food and Agric.*, **3**, 250, 1952.
2. PEREPLETCHIK, R. G. *Ribnoye Khozaistvo*, (10), 1956.
3. DYER, W. J. *Food Research*, **16**, 522, 1951.
4. NIKKILA, E. and LINKO, R. *Food Research*, **21**, 1956.

Behrndt bogtryk, Denmark

Copyright reserved

Approved For Release 2009/05/01 : CIA-RDP80T00246A007500340002-0

Approved For Release 2009/05/01 : CIA-RDP80T00246A007500340002-0

Ultra-violet Irradiation as a Factor Prolonging the Storage Life of Foods

L'utilisation des rayons ultra-violets pour la prolongation de la durée de conservation des aliments.

N. A. GOLOVKIN
The Leningrad Technological Institute of the Refrigerating Industry,
Leningrad, U. S. S. R.

SOMMAIRE. Les rayons ultra-violets sont plus efficaces aux basses températures au-dessus de 0° C. qu'au-dessous. L'effet léthal des rayons ultra-violets sur les micro-organismes est plus intense pendant les premiers stades de leur développement. Un abaissement de la température ambiante retarde leur développement et contribue ainsi à l'efficacité de l'irradiation. L'action des radiations est cumulative, ce qui permet une large application à la prolongation de la durée de conservation des aliments. Un certain nombre de chercheurs a trouvé que les bactéries se stabilisaient à la surface des aliments par suite de l'irradiation. Cet effet permet de simplifier les techniques d'irradiation aux ultra-violets et de les rendre plus sûres. Les recherches théoriques et l'expérience pratique sur l'application des rayons ultra-violets ont révélé la commodité de l'irradiation pour la prolongation des périodes de conservation de diverses denrées périssables. L'effet demandé peut être obtenu par stérilisation directe de l'air, de l'emballage et des aliments par les rayons ultra-violets. La durée d'irradiation ou la dose léthale de radiations ne dépendent pas seulement de la source d'irradiation, mais aussi des conditions d'entreposage, de la nature des aliments entreposés, de leur contamination, etc... Grâce à l'application de l'irradiation il est possible d'améliorer nettement des conditions sanitaires de préparation des aliments fabriqués dans les ateliers artisanaux et les installations industrielles.

The germicidal properties of ultra-violet rays have been discovered 80 years ago but only recently did UV irradiation attain wide industrial application for improving the storage conditions and prolonging the storage life of perishables.

Research has been carried out in this field in various countries of the world. A number of scientific research institutes in the Soviet Union are investigating the problem from various viewpoints [1-4]. A permanent committee has been set up under the Scientific Council of the Institute of Biochemistry of the U.S.S.R. Academy of Sciences to coordinate and summarize various works dealing with ultra-violet irradiation.

The present paper briefly reviews some of the investigations carried out by the Leningrad Technological Institute of the Refrigerating Industry [–12].

Experimental investigations on pure cultures of moulds have shown that the efficiency of ultra-violet irradiation increases when combined with low temperatures. The destruction of microorganisms is augmented in this case by 15-18%.

The changes which occur in the cell proper and in its surroundings at a low positive (above 0° C.) temperature probably form the basis of an increase in sensitivity of the living organism to ultra-violet rays under the influence of cold.

Investigations have revealed that irradiation of mould cultures at sub-zero temperatures are considerably less effective than at positive temperatures; this phenomenon is explained by a retardation of the photochemical and especially chemical processes occuring in the cells. By raising the temperature of mould spores from sub-zero to above zero before irradiation, the degree of destruction of the spores under the influence of ultra-violet rays is sharply increased.

A more effective action of radiant energy on warmed spores in the above case is explained, apparently, by the fact that certain essential irreversible processes

Approved For Release 2009/05/01 : CIA-RDP80T00246A007500340002-0

Approved For Release 2009/05/01 : CIA-RDP80T00246A007500340002-0

harmful to the vitality of the cells have occurred in the mould spores at sub-zero temperatures before the irradiation process.

The cited investigations have definite practical implications. In particular, it follows from them that the use of ultra-violet irradiation at sub-zero temperatures is inexpedient.

It has been established that the effect of ultra-violet rays is of a cumulative nature, i. e. the effect of a number of brief exposures is the same as that of one prolonged exposure [13].

We have found that ultra-violet irradiation creates a bacteriastatic effect in some foodstuffs. The delay in growth of the microorganisms on the irradiated food at optimal conditions of their development amounted in this case to two days. About 65 % of colonies grew on the surface of preliminarily irradiated foodstuff and they were smaller in size than on non-irradiated food. The bacteriastatic effect, as found by observations, depends upon the amount of germicidal irradiation, and upon the state of the surrounding medium as well. An extended duration of the bacteriastatic effect at lower air temperatures is caused not only by the direct temperature influence on the development of the microorganisms, but also by the greater stability of the substances formed due to chemical and physicocolloidal changes of the irradiated foodstuff surface.

Special investigations connected with the study of the changes in the chemical composition of the surface of the irradiated foodstuff, are required to determine the mechanism and nature of the bacteriastatic effect.

Wide application of ultra-violet rays is made possible by special germicidal lamps of various types manufactured by the Soviet industry: BUV-15, BUV-30 and BUV-30P, BUV-60P. The first two types of lamps, having a nominal wattage of 15 and 30 W, are designed for operation at a 10 to 25° C. ambient temperature; BUV-30P and BUV-60P, with a nominal wattage of 30 and 60 W and increased current density, are designed for operation at a 5 to 25° C. ambient temperature. Eighty per cent of the radiant flow radiated by the germicidal lamp has a wavelength of 253.7 mμ while the remaining twenty Æper cent comprise 297, 313, 365, 405, 436, 546, 577 mμ, etc. wavelengths.

It has been suggested to express the germicidal flow of the lamp sources by a unit of the germicidal flow-Bakt. A Bakt is the radiation flow with a wavelength of 254 mμ and a power of 1 W. If the radiation flow is related to 1 m^2, germicidal irradiation will be equal to one Bakt per 1 m^2 $\frac{B}{m^2}$ It is more convenient for practical measurements to apply a unit smaller by a thousand times – millibakt per 1 m^2, $\frac{mB}{m^2}$. The amount of germicidal irradiation is the product of germicidal irradiation by the time of the action of the ultra-violet ray source $\frac{mB\ min}{m^2}$ [14].

In the processing and storage of foods the greatest danger of contamination is offered by microorganisms present in the air in suspension. Investigations on the sterilizations of air by means of ultra-violet rays confirm the effectiveness of irradiation and allow to develop technical requirements of utilizing UV lamps.

Irradiation of air may be performed in the presence or absence of people. If workers or the servicing personnel are present, measures should be taken to provide a maximum limitation of the germicidal flow and the rated power should not exceed 0.7 – 1 W per 1 m^3 of the room.

Germicidal irradiation should not exceed 5 $\frac{mB}{m^2}$ in zones where people are present in the case of periodic irradiation, and 1 $\frac{mB}{m^2}$ if the lamps are on continuously. In the case of no people present, the air may be sterilized at a higher wattage, namely, up to 2-2.5 W per 1 m^3 of the room. If the lamp sources are not screened, they are

Approved For Release 2009/05/01 : CIA-RDP80T00246A007500340002-0

Approved For Release 2009/05/01 : CIA-RDP80T00246A007500340002-0

used mainly at night, during the intervals in work or in periods specially assigned for this purpose.

The utilization of recirculating devices of various design and the use of the existing air ducts as well as other ventilating means with lamp sources installed inside, whereby the direct action of the rays on the people present is eliminated, may be considered the most successful version of applying ultra-violet sterilization of the air in the presence of people.

Sterilization of air is successfully used in the U.S.S.R. various refrigerating and food processing enterprises, for instance, in the shipping rooms, grading rooms, chilled food storage rooms, etc.

Ultra-violet irradiation is applied also for the sterilization of water used for technological purposes.

The working places, equipment and the packaging means are sometimes also sterilized by ultra-violet irradiation. Portable devices with one or several lamps (depending upon the particular purpose) are best for such use.

There are diverse applications of ultra-violet rays for direct sterilization of foods. Many foodstuffs spoil from the surface, and consequently a cessation of the development of the surface microflora may result in a considerable increase in their storage life. Periodically irradiated chilled meat was preserved for longer periods than non-irradiated (2-2.5 times longer). It was possible in this case to raise the temperature and relative humidity of the air in the cold rooms which in its turn caused an acceleration of the meat aging process.

Irradiation during or before chilling imparts bacteriastatic properties to the surface of meat carcasses. This allows considerably increasing the storage life of meat and eliminating the necessity of its periodic irradiation during storage. The maximum amount of germicidal irradiation of meat is within 25 and 50 $\frac{B \text{ min}}{m^2}$.

Due to the comparatively high drying temperature and the high relative humidity used in the production of semi-smoked sausage, sausages sometimes grow mouldy in the drying chamber, especially in summertime. This essential production fault is easily eliminated by means of preliminary irradiation of the sausage before drying.

It should be considered when applying preliminary irradiation of any foodstuff that the duration of the germicidal effect is prolonged in case of the further storage of the foodstuff at low positive temperatures.

Experimental irradiation of cheese has led to good results. No mould appeared on cheeses preliminarily irradiated before storage in the course of 6 months' storage at 3-4° C., while non-irradiated cheese grew mouldy during the 4th month.

Positive results have been attained also by irradiating citrus fruits stored from one to one and a half months after being harvested.

Experiments on the irradiation of chicken eggs before breaking them for freezing justifies recommendation of this method for the disinfection of eggs.

The irradiation of milk in a thin layer for several seconds makes it possible to sharply retard its going sour. For instance, at 5° C. the acidity of non-irradiated milk increased during 72 hours of storage by 7.8° T, while in the case of irradiated milk the increase of acidity amounted to only 1-1.5° T and the milk had no deviations from the standard.

Thus, the application of ultra-violet rays in a number of branches of the food industry, including the refrigerating industry, already provides positive results for the storage of raw and processed foodstuffs.

However, vast investigations are still required on the irradiating process and especially a study of the action of ultra-violet rays on foodstuffs which are in all respects complex objects.

REFERENCES

1. Works of Academy of Sciences of the U.S.S.R. and Academy of Medical Sciences. Academy of Medical Sciences of the U.S.S.R., Moscow, 1950.

Approved For Release 2009/05/01 : CIA-RDP80T00246A007500340002-0

Approved For Release 2009/05/01 : CIA-RDP80T00246A007500340002-0

2. Works of Scientific Session Dedicated to the Achievements and Problems of Soviet Biophysics in Agriculture. Academy of Sciences of the U.S.S.R., Moscow, 1956.

3. NEISHTADT, Y. E. Germicidal ultra-violet irradiation. Medgiz, Moscow, 1955.

4. SOKOLOV, V. F. Sterilization of water by means of germicidal rays. Ministry of Municipal Economy, Moscow, 1954.

5. GOLOVKIN, N. A. The Action of Ultra-violet Rays on Moulds. *Kholodilnaya Tekhnika,* (2 and 4), 1948.

6. GOLOVKIN, N. A. The role of Ultra-violet Rays for the Preservation of Perishables. *Ibid.,* (1), 1950.

7. GOLOVKIN, N. A. The Application of Ultra-violet Rays in Processing and Storing Meat and Meat Products. *Myasnaya Industriya,* (2), 1952.

8. GOLOVKIN, N. A. The Effect of Ultra-violet Rays on Moulds. Works of the Leningrad Technological Institute of Refrigerating Industry, **9**, Leningrad, 1955.

9. GALANIN, N. F. and GOLOVKIN, N. A. The Use of Ultra-violet Rays in the Food Industry. Works of Scientific Session dedicated to the achievements and problems of Soviet biophysics in agriculture. Academy of Sciences of the U.S.S.R., Moscow, 1955; *Kholodilnaya Tekhnika,* (2), 1954; Works of the Leningrad Technological Institute of Refrigerating Industry, **10**, Leningrad, 1956.

10. GOLOVKIN, N. A. and CHERNYAK, B. I. The Use of Ultra-violet Rays for the Irradiation of Milk. Works of the Leningrad Technological Institute of Refrigerating Industry, **7**, Leningrad, 1955.

11. GOLOVKIN, N. A. and CHERNYAK, B. I. The Influence of Irradiated Milk as a Medium on the Vitality of Lactic Acid Bacteria. *Ibid.,* **13**, 1957.

12. GOLOVKIN, N. A. The Use of Ultra-violet Rays in the Food Industry. The Scientific-Technical Society of Food Industry Workers (Refrigeration Section), Leningrad, 1958.

13. NASONOV, D. N. and ALEKSANDROV, V. L. The Reaction of Living Matter to External Effect. Academy of Sciences of the U.S.S.R., Moscow, 1940.

14. Temporary Instructions on the Use of Germicidal Lamps. Academy of Sciences of the U.S.S.R., Moscow, 1956.

Behrndt bogtryk, Denmark

Copyright reserved

Approved For Release 2009/05/01 : CIA-RDP80T00246A007500340002-0

Approved For Release 2009/05/01 : CIA-RDP80T00246A007500340002-0

The Hydrature and Differential Hydrature of Foods. Changes Occuring during Cooling and Freezing

Proportions d'eau («hydrature» et «differential hydrature») dans les denrees alimentaires. Modifications intervenant pendant la refrigeration et la congelation

G. TÖRÖK and E. ALMÁSI
Institute for Research in Canning and Refrigeration, Budapest, Hungary.

SOMMAIRE. L'un des constituants les plus importants des denrées est l'eau. Son importance a été démontrée par de récentes analyses de chimie colloïdale et par l'examen des systèmes et structures macromoléculaires. Pour caractériser les états de l'eau dans les denrées (eau libre et eau liée), le terme de «hydrature» (proportion d'eau) a été crée par Walter. Il est égal à l'humidité relative d'équilibre (en %) de la substance considérée. Pour insister sur l'importance de l'eau liée, un des auteurs de ce rapport propose le terme de «differential hydrature» (qui est égal à [100-«hydrature»], en %). L'accroissement de la proportion d'eau liée correspond à un accroissement de cette «differential hydrature». La réfrigération et surtout la congélation entraînent un accroissement rapide de la «differential hydrature», lié à une diminution de la proportion d'eau libre, facteur indispensable pour les transformations chimiques et biochimiques. Le retour à la température initiale, c'est-à-dire la décongélation, rend à l'«hydrature» sa valeur initiale.

Néanmoins, l'état des denrées décongelées, après congélation ou surgélation, est plus ou moins différent de l'état initial. Aussi, on peut en déduire que les changements de la «differential hydrature», survenant pendant la congélation, entraîne des modifications permanentes de certaines propriétés de la denrée. Parmi celles-ci, des modifications d'activité des enzymes et des changements de perméabilité de la membrane cellulaire ont été étudiées.

Our foods consist mainly of plant and animal tissues or their extracts. Their constitution is quite varied, but one of the major components of most of them is water. In spite of this, its role and functions have received only little attention, possibly because it has no nutritive value. Only the study of colloid chemical and macromolecular structures and systems has pointed out the complex function of water in foods. Also, the fact that the water content of foods does not consist of water molecules of uniform state and function, has been shown only recently. The "polymolarity" of water itself, as well as its state within the system, also varies [1]. One part of the water may be assumed as more or less free water, while the other is bound in a varied manner by changing forces.

Although controversies in the question of bound or free water still exist, especially in relation to definition, determination of quantity etc., the fact itself may be considered as settled. Several reviews attempted to classify the bound proportions – suffice it here to recall the publications of Plank or Rebinder – but all authors are united in the opinion that water content alone does not define the "state of water" in food.

In our opinion, the best approach to this question has been made by Walter [2]. His definition is based on the analogy between water content and heat content. As the heat content of a material does not define the "state of heat", similarly its water content cannot indicate the "state of water". If two materials of differing "state of heat" are brought together, equalisation depends on the "state of heat" and not on the heat content. A similar situation exists between materials of differing water content. Equilibrium sets in at an identical "state of water" and not at an

Approved For Release 2009/05/01 : CIA-RDP80T00246A007500340002-0

Approved For Release 2009/05/01 : CIA-RDP80T00246A007500340002-0

identical water content. On the analogy of the word "temperature", expressing the state of heat, Walter coined the term "hydrature", characterising the state of water. The latter is measured by the relative water vapour tension or the relative humidity of the air in equilibrium with the material. Since relative vapour tension and osmotic pressure of a solution are colligative properties, hydrature may be characterised by osmotic pressure, it can be evaluated from freezing point measurements.

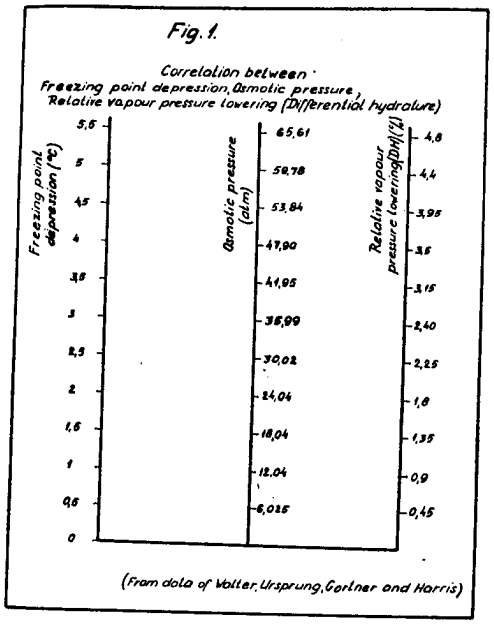

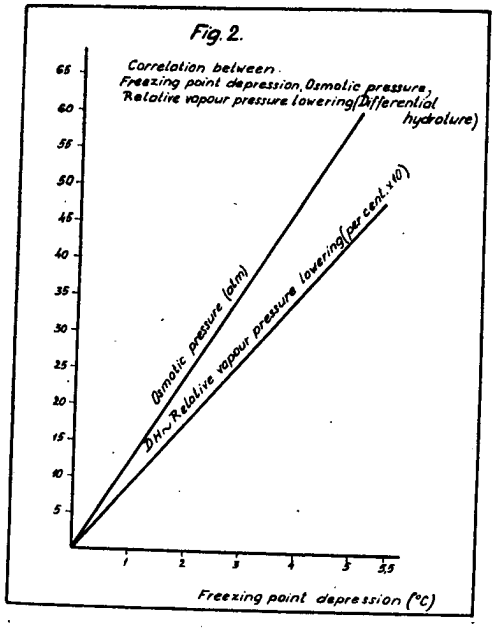

Approved For Release 2009/05/01 : CIA-RDP80T00246A007500340002-0

Approved For Release 2009/05/01 : CIA-RDP80T00246A007500340002-0

Walter's idea is essentially correct: hydrature is a readily interpretable term. As a term, it reflects the end effects of all water-binding processes.

Walter's characterisation of the state of water may be further developed by examining the situation from the angle of the bound water content, i.e. by studying the deviation of the state of water in the foodstuff from that in pure free water. Generally, in foods the role of bound water is of importance, and thus it seems to be in place to introduce a new term expressing the degree of water-binding. In this interpretation the term: "state of water" is used as the functional sum total of the fractions constituting the total water content of the food at given parameter values. Using this definition, the state of water in pure water is 0 (in contrast to Walter who uses the number 100 to characterise this state); in concentrated solutions of hydrated macromolecules, such as in foodstuffs, it has a high value. In order to differentiate our statements from Walter's values, we introduce the expression "differential hydrature" (DH). Numerically, DH values may be obtained from Walter's hydrature figures as follows:

DH = (hydrature of pure water) – (hydrature of the system examined).

Thus, DH expresses the proportion of bound water in the system and increases with increasing binding [1].

The advantage of the terms hydrature and DH is their independence of the percentual water content of the system. Thus, changes and differences in hydrated aqueous systems of fixed water content may be registered.

A further advantage of DH is that changes of all parameters – lowering of vapour tension, osmotic pressure, freezing point depression – are unidirectional and easily convertable into each other. Correlations are simple to calculate but graphical interpolation is still more convenient and the values thus obtained are sufficiently accurate in view of the accuracy of the methods of determination. (Figs. 1, 2).

Foods always contain both bound and free water. There are also water fractions of intermediate state between these extremes. The bound or free state of these is a function of temperature. Bound water, and thus DH of foods is an always changing value: the ratio of bound to free water and the amount of water of intermediate state are not fixed. The number of water layers pertaining to the hydrated components of foods is changing with temperature: in a fluid phase system, it decreases with heating, and increases with heat removal.

Generally speaking, foods are not eaten in their original state of water, not even those which are eaten raw (fruits, salads) because, in the period between plucking and consumption, DH changes: drying sets in due to the loss of free water. Changes occurring during cooling and freezing of foods are even more significant. One practice of heat removal, cooling, involves heat removal down to the temperature zone near, yet always somewhat above, the freezing point. In the course of this process, the water content of the food is in the lowest possible temperature range of the fluid phase, without suffering change in state, i.e. without ice formation. Although certain changes in DH are brought about by heat removal, this increase is not large enough to prolong the keeping time up to the level of that of preserved products. With the increase in DH caused by cooling, a decrease in the activity of enzymes of tissues and microorganisms sets in but a dormant state or a cessation of activities cannot be achieved.

Freezing of foods causes a substantial change in DH by transforming most of the free water into ice. Slow and quick freezing differ only in the velocity of the water – ice transformation and from this it follows that, at a given temperature, DH values of frozen and quick-frozen foods are identical. The reason for the usually encountered salient differences between frozen and quick-frozen foods is to be found elsewhere. This has mainly physical explanations. In a frozen system, concentrated solution always remains around the ice crystals. This solution consists of the original solute and the residues of fluid water. With slow freezing, only few but large crystals are formed. Therefore, the surface area of ice is not large. Quick-freezing brings about the formation of many small crystals and a very large "ice surface". Thus absorptive immobilisation of substances is considerably

Approved For Release 2009/05/01 : CIA-RDP80T00246A007500340002-0

Approved For Release 2009/05/01 : CIA-RDP80T00246A007500340002-0

stronger with quick-freezing and this, too many contribute to the slowing-down of enzymatic processes.

From the point of view of hydrature and DH, the beneficial effect, on keeping qualities, exerted by freezing and quick-freezing may be explained as follows. The proportion of free water, the indispensable factor of chemical and biochemical processes, is lowered accompanied by an increase in DH up to a level where biological and microbiological processes are effectively inhibited.

Since, in a given foodstuff, DH is a function of temperature, restoration of the original temperature brings about a reversible restoration of the original value of DH. From this it would follow that the state of defrosted frozen or quick-frozen

TABLE 1. ENZYMATIC ACTIVITY OF RAW GARDEN PEAS

Enzyme	Before freezing	Quick-frozen and thawed after 5 months of storage at –20° C.
Catalase	37,0	8,7
Peroxydase	1,8	1,3
Diastatic activity	250,0	370,0
Amylase	1,2	1,5

products should be identical with the original. In practice, however, one frequently encounters the opposite situation. This discrepancy may presumably be explained by irreversible changes in enzyme systems, in permeability of cell walls etc. caused by the high value of DH occurring during freezing and quick-freezing. In fact, we succeeded in detecting quite considerable changes in enzyme activity and permeability. Distortions of the functioning of enzymes were measured in frozen green peas by comparing the enzyme activity of fresh raw garden peas with that of raw, frozen peas stored at –20° C. for 5 months (Table 1).

It may be seen that the numerical values of catalase and of diastatic activity differed quite considerably in spite of the fact that both series of measurements were made at +20°C.

To observe changes in the cell wall, changes in permeability of sugar beet slices were studied. With thawed slices, previously frozen at –20 and –40°C. resp., permeability, as measured by the diffusion constant, was found to increase substantially and in proportion to the temperature lowering. The diffusion constant for sucrose and calcium was found to be higher in the product frozen at –20°C. and even more so with tissues frozen at –40°C. It is interesting to note that the increase was smaller with calcium; it is perhaps bound to compounds of higher molecular weight than sucrose (pectin) [3, 4½. (Table 2).

TABLE 2. CHANGES IN PERMEABILITY OF SUGAR BEET SLICES

Treatment of beet slices	Diffusion constant × 10^{-6} cm^2/min.	
	sucrose	calcium/Ca**/
Raw	23,6	24
Frozen at –20 °C.	96	61,5
Frozen at –40 °C.	227	83

In the case of cooling, secondary effects could not be detected (in spite of the fact that relatively small changes occur here, too). Thus restoration of the temperature causes the food to return to its original state reversibly.

Approved For Release 2009/05/01 : CIA-RDP80T00246A007500340002-0

Approved For Release 2009/05/01 : CIA-RDP80T00246A007500340002-0

All these observations point to the conclusion that the phase change water-ice, accompanying freezing and quick-freezing, brings about a substantial increase in DH, and this increase involves manifestation of secondary effects which, while considerably improving the keeping quality, may cause significant decreases in tissue reversibility.

REFERENCES

1. TÖRÖK, G. A viz szerepe élelmiszereinkben, (The Role of Water in Foods), Dissertation, 1954.

2. WALTER, H. Die Hydratur der Pflanze. Jena, 1931.

3. ALMÀSI, E. Sejtpermeabilitás vizsgálatok, (Investigations into the Permeability of Cells). Konzerv-, Hus- és Hütöipari Kutató Intézet Évkönyve 1951–52. Budapest, Élelmiszeripari Kiadó, 1953.

4. ALMÀSI, E. Enzimaktivitás változása gyorsfagyasztott zöldborsónál, (Changes in Enzyme Activities of Quick-frozen Peas). Elelmezési Ipar 7, 299, 1953.

Behrndt bogtryk, Denmark

Copyright reserved

Approved For Release 2009/05/01 : CIA-RDP80T00246A007500340002-0

Approved For Release 2009/05/01 : CIA-RDP80T00246A007500340002-0

Investigation of the Discharge Valves of a High Speed Compressor

Recherches sur les clapets de refoulement des compresseurs à grande vitesse.

B. L. TSYRLIN
The Scientific Research Institute of the Refrigerating Industry of the U.S.S.R.
Moscow, U.S.S.R.

SOMMAIRE. Des recherches expérimentales ont été réalisées à l'Institut de Recherches Scientifiques de l'Industrie Frigorifique d'U.R.S.S. sur un compresseur à ammoniac de 80 mm de course de piston et d'alésage pour 960 et 1450 t/mn. L'objet principal de ces expériences était la recherche des processus d'échange de chaleur dans le compresseur. Certaines données sur les clapets, en particulier les clapets de refoulement étaient ensuite obtenues à partir de diagrammes indicateurs provenant d'un indicateur électrique avec manomètre tensométrique.

On trouvait expérimentalement que le travail supplémentaire dû à la dépression du clapet de refoulement s'élevait à 3% pour 960 t/mn et 6,5% pour 1450 t/mn (dans des conditions de fonctionnement normales). Celle-ci non seulement augmente le travail de compression du compresseur, mais entraîne aussi une température d'aspiration plus élevée. L'élévation de température de la vapeur a pour conséquence une augmentation du travail de compression ainsi qu'une diminution du rendement pondéral du compresseur. De ces trois façons, le travail supplémentaire, dû à la dépression du clapet de refoulement entraîne une réduction de l'effet frigorifique spécifique (k_e kcal/kwh).

Avec une élévation de la vitesse de rotation de la machine, la possibilité d'éliminer la chaleur dégagée par le travail supplémentaire dû à la dépression du clapet de refoulement est réduite. Le refoulement du gaz est un phénomène compliqué et dépend beaucoup de la dynamique du mouvement du disque du clapet et de l'oscillation du ressort du clapet. Les recherches sur le diagramme indicateur ont permis de définir les coefficients de résistance du clapet de refoulement qui caractérisent la perfection du clapet pour le passage des gaz. La perte de charge $\triangle p = \xi \frac{\gamma_{mid}}{g} w^2$ *dépend beaucoup du coefficient de résistance* ξ. *Pour un clapet simple à disque du compresseur étudié cette quantité s'est révélée être* $\xi = 11{,}5$.

D'après les recherches sur les clapets à lamelles effectuées par T. Kondratyeva en établissant à travers les clapets un écoulement stationnaire, ξ *peut être réduit à 4–6, ce qui permet une augmentation sensible de la vitesse des compresseurs sans perte notable dans les soupapes.*

In the Refrigerating Machines and Appliances Laboratory of VNIKhI an experimental study was made of the operation of a uni-cast cylinder-crankcase housing ammonia compressor. The machine investigated was a serial four-cylinder model with both stroke and bore 80 mm. Tests were made at 960 and 1450 rpm.

The main object of the study was to elucidate the effect of the heat processes within the compressor on its operation. The indicator diagrams obtained also yielded data on the functioning of high speed compressor valves. The diagrams were obtained by an electric indicator assembly provided with a tensimetric pressure sensor.

The schematic diagram of the assembly developed in the Control and Measuring Instruments Laboratory of VNIKhI is shown in Fig. 1.

The pressure sensor constituted a section of a Bourdon tube with wire resistors (tensimeters) cemented to its concave and convex surfaces. Both ends of the tube

Approved For Release 2009/05/01 : CIA-RDP80T00246A007500340002-0

Approved For Release 2009/05/01 : CIA-RDP80T00246A007500340002-0

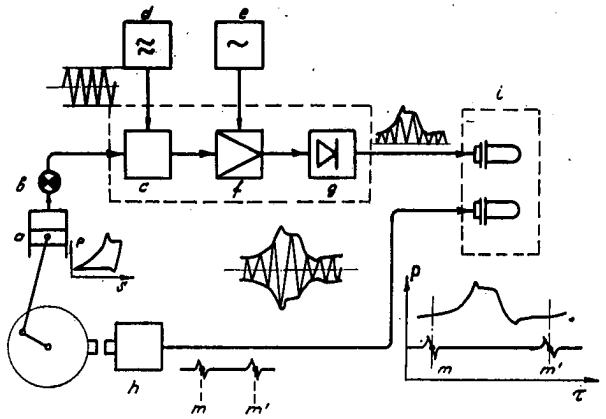

Fig. 1. Schematic diagram of indicator. *a* – compressor, *b* – pressure sensor, *c* – balancing block, *d* – electric generator of sonic frequencies, *e* – power supply, *f* – amplifier, *g* – detector, *i* – dead point recorder, *h* – oscillograph, *m* – and *m'* – dead points.

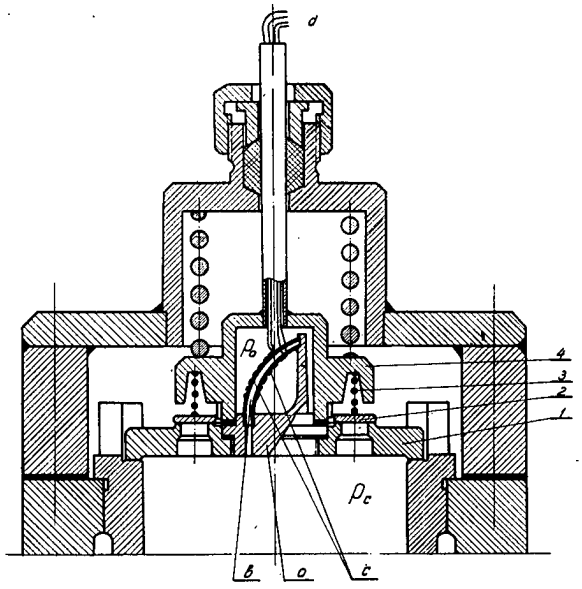

Fig. 2. Schematic diagram of sensor installation in the discharge valve. *a* – sensor casing, *b* – Bourdon tube, *c* – wire resistor sensors, *d* – terminals. 1 – valve seat, 2 – plate, 3 – spring, 4 – plate motion check. *Pc* – cylinder pressure, *Pa* – atmospheric pressure.

were rigidly fixed, one of them being sealed while the other was open, permitting entrance of gas. Fig. 2 shows the sensor mounted in the discharge valve.

Preliminary experiments showed that the position of the sensor greatly affects the accuracy of the diagrams. Initially the sensor was mounted outside the cylinder and joined to it through a three way stop-cock by a 100 mm long channel (3 mm bore). This position was found to be unsatisfactory, the diagrams obtained being distorted. In particular, considerable pulsation occurred in the suction and discharge lines, evidently due to pressure fluctuations in the connecting channel and stop cock. It should be noted that indicator diagrams with similar pulsations

Approved For Release 2009/05/01 : CIA-RDP80T00246A007500340002-0

Approved For Release 2009/05/01 : CIA-RDP80T00246A007500340002-0

have been produced in different investigations and in number of cases may also have been due to connecting line effects.

Subsequently all tests were made with the sensors mounted directly in the cylinder (*see* Fig. 2) and no pulsations appeared either in the discharge or the suction lines. Also the peaks corresponding to the moments of opening of the discharge valve at the end of the compression stroke and of the suction valve at the end of the reverse stroke stood out more clearly.

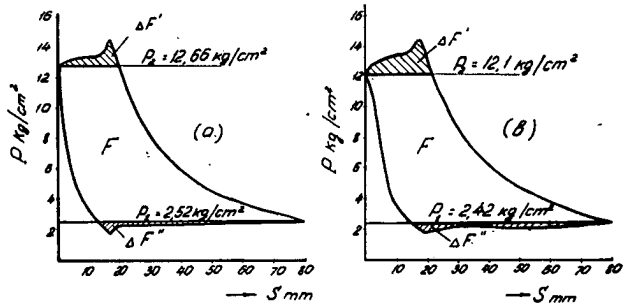

Fig. 3. Indicator diagrams *a* – 960 rpm., *b* – 1450 rpm.

In Fig. 3 typical diagrams in PV coordinates are represented, obtained for speeds of 960 and 1450 rpm. The hatched areas represent the excess work caused by the pressure losses in the suction and discharge valves.

The relative value of the energy losses due to wire drawing may be determined as the ratio between the corresponding excess area to the overall area of the diagram, $\frac{\Delta F'}{F} \cdot 100\%$, for discharge, and $\frac{\Delta F''}{F} \cdot 100\%$, for suction.

In Fig. 4 the curves show the energy losses in the discharge valve $\frac{\Delta F'}{F}$ for 1450

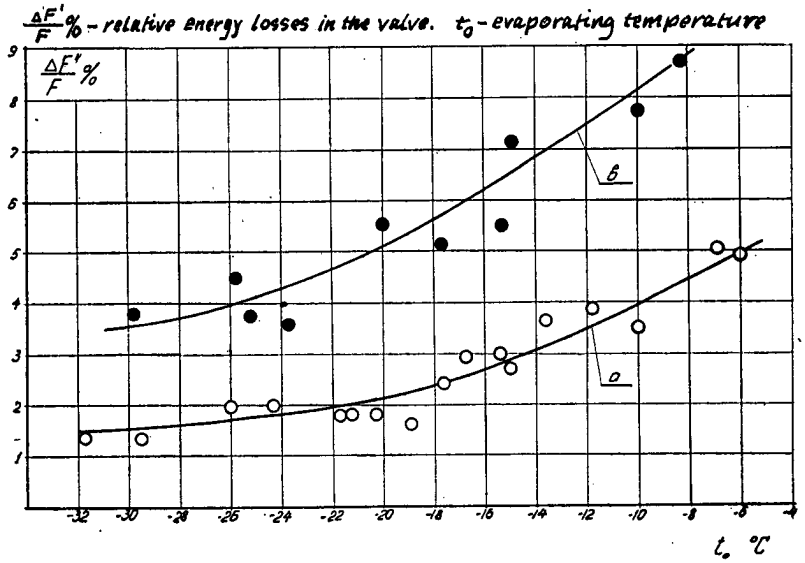

Fig. 4. Energy losses in discharge valve. *a* – 960 rpm., *b* – 1450 rpm.

Approved For Release 2009/05/01 : CIA-RDP80T00246A007500340002-0

Approved For Release 2009/05/01 : CIA-RDP80T00246A007500340002-0

and 960 rpm as a function of the evaporating temperature t_0. As can be seen, the losses due to the pressure loss increase with increase in the evaporating temperature. For standard conditions they constitute about 3% at 960 rpm and 6.5% at 1450 rpm.

Determination of the wire drawing during suction with sufficient accuracy is difficult owing to the small absolute values for the pressure losses in the suction valve. The overall pressure losses of both the discharge and suction valves under standard conditions are about 5% at 960 and about 10% at 1450 rpm.

It should be noted that actually the energy losses due to pressure loss in the valves are significantly higher than the values obtained directly from the indicator diagram. The excess work spent on overcoming the resistance in the valves not only leads to an increase in the indicator work but also to an increase in the heat evolved in the working cycle of the compressor. This increased heat evolution causes more heating up of the vapour during intake and at the beginning of compression, which in turn augments the work of compression on the one hand and lowers the weight capacity on the other. All this leads to decrease in the specific refrigerating capacity K_e (Kcal/kwh).

The compressor efficiency depends significantly upon the amount of heat removed. This, however, is relatively low in the case of water cooled cylinders. Our experiments at 1450 rpm have shown that the amount of heat removed in the jacket approaches ($\sim$ 98%) the equivalent work of friction AL_{fr} (including the work done by the oil pump) at this speed. At 960 rpm the heat removed is about 1.8 AL_{fr}.

The amount of heat removed in the cooling jacket practically did not increase on raising the number of revolutions from 960 to 1450, whereas the specific heat discharge in the jacket $\frac{Q_j}{G_a}$ decreased in proportion to increase in thecapacity G_a. Hence with increase in speed there is a diminished possibility of eliminating heat, in particular, evolved from excessive work due to pressure losses in the valves. With increased speed, energy losses in the valves grow, owing both directly to increased excessive work and to fall in heat elimination.

The indicator diagrams obtained did not reveal directly the presence of significant volumetric losses owing to the throttling of the vapour in the suction valve. However, as was shown above, pressure losses in the valves lead to decreased efficiency owing to fall in value of the heating up coefficient λ_w.

The relative value of the energy losses in the valves is a function also of the weight capacity, hence the volumetric parameters of the compressor depending prediminantly on the relative clearance volume C% is of paramount importance. One should strive to lower the clearance volume but without considerably increasing the velocities in the valves.

Not only the velocity in the various valve passages affect the magnitude of the losses, but also the valve design plays a significant part. Ordinarily in estimating the losses of various appliances use is made of the dimensionless friction coefficient ζ, determining the magnitude of the resistance in fractions of the dynamic head of the flow through the given appliance. The loss in pressure due to resistance is then expressed by the usual formula

$$\Delta p = \zeta \frac{\gamma}{2g} W^2 \qquad (1)$$

We shall assess the design qualities of the valve analogously.

The intake and discharge of gas in a cylinder is a complicated process dependent to a large extent upon the dynamics of motion of the valve plate and tension and oscillation of the valve spring. Because of the dynamic forces applied to the valve plate its flow area generally speaking does not remain constant. Hence the gas velocity in the valve and, therefore, the resistance (pressure drop) along the discharge stroke follows very complicated relationships of which the analytical expression has been derived by N. A. Dollezhal [1].

Approved For Release 2009/05/01 : CIA-RDP80T00246A007500340002-0

Approved For Release 2009/05/01 : CIA-RDP80T00246A007500340002-0

Here determination of the losses in the valves are based on results of experiments, whereas for an appraisal of the valve design we shall introduce a coefficient similar to that of equation (1).

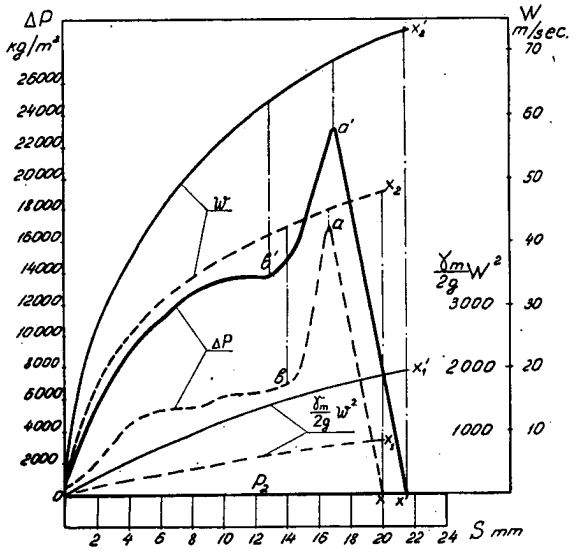

Fig. 5. Characteristics of discharge valves. - - - - - 960 rpm., ——— 1450rpm. ΔP – pressure loss in valve, S – piston stroke.

Fig. 5 shows curves for pressure changes in the discharge valves determined as the difference between the discharge pressure on the indicator diagram and the pressure P_2 in the discharge outlet after the compressor. The values for the velocities of gas in the valve openings are presented. The velocities are plotted with the assumption of full plate lift, i. e. they depend only upon the piston speed at the given point. Plots are given for speeds of both 960 and 1450 rpm.

Along the X-axis are plotted portions of the piston stroke. The upper dead point serves as coordinate origin. The segments on the lines $\triangle p = f(s)$ from x to a and from x' to a' correspond to positions of the closed valve; from a to b (a' to b') the valve is opening and from b to 0 (b' to 0) the valve is open.

The value of the energy lost by wiredrawing during the entire discharge process including the excessive work of compression in the closed valve region may be expressed as $\int_o^x \Delta p ds$

At the same time $\int_o^x \Delta p ds$ equals the area $xabox$ or area $x'a'b'ox'$. The same quantity for the energy loss may be expressed in terms of the dynamic head as $\zeta_v = \int_o^x \frac{\gamma}{2g} W^2 ds$

or, designating by γ_m the mean value for the specific weight in the discharge process

$$\zeta_v = \frac{\gamma_m}{2g} \int_o^x W^2 ds$$

Approved For Release 2009/05/01 : CIA-RDP80T00246A007500340002-0

Approved For Release 2009/05/01 : CIA-RDP80T00246A007500340002-0

The resistance coefficient of the valve then becomes

$$\zeta_v = \frac{\int_o^x \Delta p ds}{\frac{\gamma_m}{2g}\int_o^x W^2 ds}$$

The curves of the functions $\frac{\gamma_m}{2g} W^2 = f(s)$ are also given in Fig. 5.

The quantity $\frac{\gamma_m}{2g}\int_o^x W^2 ds$ is represented in Fig. 5 by the areas xx_1ox and $x'x'_1ox'$ in its corresponding scale (for the sake of clarity the latter has been enlarged as compared with that for the curves $\Delta p = f(s)$. The coefficient ζ_v, is obtained by dividing the respective areas.

Determination of the valve resistance coefficient in this way is somewhat conditional, since not only the gas dynamics characteristic of the valve but also its design features, in particular, the spring tension, are involved here. However, it has merits in that it takes into account all elements determining energy losses in the valve. As can be seen in Fig. 5, the resistance greatly depends upon the valve spring tension. This determines the pressure difference at the points a and x (a' and x') and correspondingly the area under these segments of the curves $\Delta p = f(s)$. A similar condition holds for the open valve segments ab or $a'b'$.

It should be noted that on the segments bo ($b'o$) the valve plate is not always fully lifted to the guard. Therefore, in all cases, determination of the energy loss coefficient as fraction of the pressure head, when the true values of the velocities in the valve are unknown, is conditional.

From the analysis of the indicator diagrams it was found that the quantities ζ_v for various operating conditions at both 960 and 1450 rpm were close in value (deviation not exceeding 10%). Their mean value was $\zeta_v = 12.7$.

Also of considerable interest is determination of the valve resistance under the steady state flow. Such studies have been carried out by a number of authors [2, 3]. Under steady state flow the resistance coefficient of the single ring valve tested by us had a value of $\zeta_{vs} = 7$. Considering that gas outflow from under the plate along its exterior diameter is unhampered, the value is rather high. According to the data of T. T. Kondratyeva [3] investigating the reed valve, the coefficient of resistance of the latter may be lowered to $\zeta_v = 4 \div 6$. Correspondingly the energy losses in such valves will sharply fall.

Decrease in the energy losses in the valves of particular importance for high speed machine are to be achieved both by improvement in the aerodynamic properties of the passages as well as by rational choice of spring rigidity. Judgement of the quality of different valves should be made on comparison of their resistance coefficient both in the steady state and under the actual operating conditions of the compressor.

REFERENCES

1. DOLLEZHAL, N. A. The Applied Theory of the Self-acting Valve. *Obshcheye Mashinostroyeniye*, (1), 1941.

2. SAMSONOV, N. M. Investigation of Flapper Reed Valves of a Reciprocal Compressor. Thesis, Moscow, 1958.

3. KONDRATYEVA, T. F. On the Determination of Energy Losses in Self-acting Valves of a Reciprocatnig Compressor. *Works of the Scientific Research Institute of Chemical Machine-Building* (22), 1958.

Behrndt bogtryk, Denmark

Copyright reserved

Approved For Release 2009/05/01 : CIA-RDP80T00246A007500340002-0

Approved For Release 2009/05/01 : CIA-RDP80T00246A007500340002-0

Effect of On–Off Control on Working Economy of Refrigeration Equipment

Influence du réglage par tout ou rien sur l'économie du fonctionnement du matériel frigorifique

V. POLÁK
Research Institute for Refrigeration and Food Engineering,
Prague, Czechoslovakia.

SOMMAIRE. La consommation de courant électrique du matériel frigorifique avec réglage par tout ou rien de la production frigorifique varie suivant la longueur du cycle de fonctionnement, en raison de l'influence des états transitoires. On prouve que l'économie du cycle frigorifique augmente en fonction inverse de la longueur du cycle de fonctionnement et l'on montre l'effet des constantes de temps de l'évaporation et du condenseur. On indique un certain nombre de facteurs de la conception du compresseur et dans son exploitation qui ont une influence défavorable sur l'économie de l'ensemble du système frigorifique en régime variable. Pour obtenir l'économie maximum du matériel frigorifique avec réglage par touté ou rien de la production frigorifique, le compresseur et son moteur doivent être conçus aussi du point de vue de l'économie en régime variable de façon qu'on obtienne le maximum d'économie dans le fonctionnement avec des cycles courts.

The input of refrigerating systems with on–off control of refrigeration output varies with the length of the on–off cycle. This is obviously the result of the influence of transient states. I intend to show factors to be taken into account, because the design and adjustment of this type of refrigerating system carried out with regard to these viewpoints, can contribute to a more economical operation.

Let us assume a single-evaporator refrigerating system with on–off control. The refrigerating circuit is assumed to be dimensioned so that with the compressor running continuously, the evaporator removes heat $Q_{o\,max}$ from the space refrigerated, the difference between the space refrigerated T_r and evaporator temperature $T_{o\,min}$ being $\Delta_{o\,max}$.

At the same time the condenser is removing heat $Q_{k\,max}$, the difference between the condensing temperature $T_{k\,max}$ involved and the temperature T_a of surroundings through which heat is removed from the condenser, being $\Delta_{k\,max}$.

With the heat load of the space refrigerated decreased from $Q_{o\,max}$ to value Q_o, the system starts operating in cycles composed of the period during which the compressor is running and the period during which the compressor is at a standstill.

During the working period of the cycle, the evaporator temperature drops, and rises during its off period. The system works with varying evaporator temperature and the mean difference between the temperature of the space refrigerated T_r and the mean evaporator temperature T_{om} is decreased to Δ_o.

At the same time the difference between the mean condensing temperature T_{km} and the temperature T_a of the surroundings cooling down the condenser, will be decreased to Δ_k.

These conditions are shown in Fig. 1. After starting the compressor, at the moment T_1, the evaporator temperature drops from value T_{o1} until at the moment T_2 it reaches value T_{o2} at which the compressor is cut off by the thermostat or pressostat. The evaporator temperature will again start rising until at the moment T_3, at temperature T_{o1}, the compressor will be started.

The mean evaporator temperature during the compressor running period is not identical with that during its off period. Under the simplified assumption that a single-capacity system is involved, the mean evaporator temperature during the working period of the compressor will be:

Approved For Release 2009/05/01 : CIA-RDP80T00246A007500340002-0

Approved For Release 2009/05/01 : CIA-RDP80T00246A007500340002-0

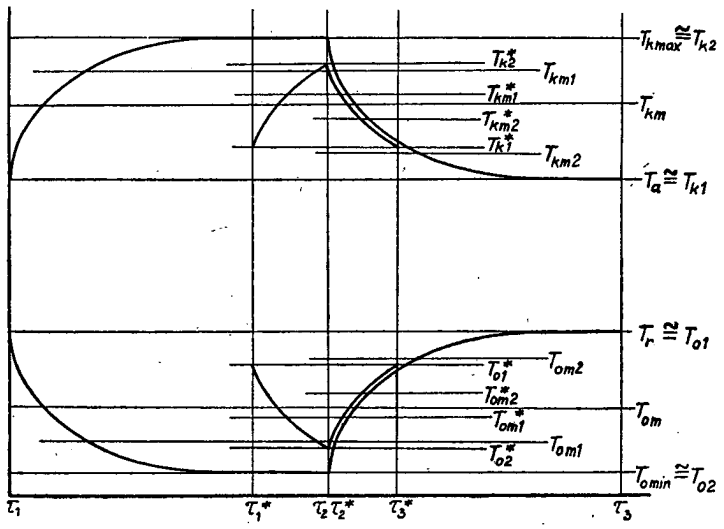

Fig. 1. Relation of condensing and evaporation temperatures to the length of on–off cycle.

$$T_{om1} = \frac{1}{\tau_2 - \tau_1} \int_{\tau_2}^{\tau_1} T_{0min} + (T_{01} - T_{0\,min})\, e^{-\frac{\tau_2 - \tau_1}{\tau_c}}\, d\tau \qquad (1)$$

Where T_C-evaporator time constant.

The mean evaporator temperature during the compressor off period is

$$T_{om2} = \frac{1}{\tau_3 - \tau_2} \int_{\tau_2}^{\tau_3} T_r - (T_r - T_{02})\, e^{-\frac{\tau_3 - \tau_2}{\tau_c}}\, d\tau \qquad (2)$$

The mean evaporator temperature during the whole cycle is

$$T_{om} = \frac{T_{om1}(\tau_2 - \tau_1) + T_{om2}(\tau_3 - \tau_2)}{\tau_3 - \tau_1} \qquad (3)$$

For evaluating the economy of the refrigerating cycle, only value T_{om1} enters the picture.

Similar equations can be written also for the mean condensing temperature during the compressor running period T_{km1}, mean condensing temperature during the off period T_{km2} and mean condensing temperature during the full cycle T_{km}.

The influence of the length of the whole on–off cycle T_3–T_1 on the size of value T_{om1} comes to prominence by substituting extreme values for T_2–T_1 and T_3–T_2 into equations (1) and (2).

If, $T_3 - T_1 \rightarrow 0$, then

$$\lim T_{o1} = \lim T_{om1} = T_{om},\ \lim T_{o2} = \lim T_{o2} = T_{om}$$

If, on the other hand, T_3–$T_1 \rightarrow \infty$ then $\lim T_{o1} = \lim T_{om2} = T_r$, $\lim T_{o2} = \lim T_{om1} = T_{o\,min}$.

By changing the length of cycle T_3–T_1 in an on–off control system it is therefore possible to change the mean evaporator temperature during the working period of cycle T_{om1} within the range of ($T_{o\,min}$, T_{om}).

Similar conditions prevail on the condenser side.

If, $T_3 - T_1 \rightarrow 0$, then

Approved For Release 2009/05/01 : CIA-RDP80T00246A007500340002-0

Approved For Release 2009/05/01 : CIA-RDP80T00246A007500340002-0

Effect of On–Off Control on Working Economy of Refrigeration Equipment

Influence du réglage par tout ou rien sur l'économie du fonctionnement du matériel frigorifique

V. POLÁK
Research Institute for Refrigeration and Food Engineering,
Prague, Czechoslovakia.

SOMMAIRE. La consommation de courant électrique du matériel frigorifique avec réglage par tout ou rien de la production frigorifique varie suivant la longueur du cycle de fonctionnement, en raison de l'influence des états transitoires. On prouve que l'économie du cycle frigorifique augmente en fonction inverse de la longueur du cycle de fonctionnement et l'on montre l'effet des constantes de temps de l'évaporation et du condenseur. On indique un certain nombre de facteurs de la conception du compresseur et dans son exploitation qui ont une influence défavorable sur l'économie de l'ensemble du système frigorifique en régime variable. Pour obtenir l'économie maximum du matériel frigorifique avec réglage par touté ou rien de la production frigorifique, le compresseur et son moteur doivent être conçus aussi du point de vue de l'économie en régime variable de façon qu'on obtienne le maximum d'économie dans le fonctionnement avec des cycles courts.

The input of refrigerating systems with on–off control of refrigeration output varies with the length of the on–off cycle. This is obviously the result of the influence of transient states. I intend to show factors to be taken into account, because the design and adjustment of this type of refrigerating system carried out with regard to these viewpoints, can contribute to a more economical operation.

Let us assume a single-evaporator refrigerating system with on–off control. The refrigerating circuit is assumed to be dimensioned so that with the compressor running continuously, the evaporator removes heat $Q_{o\,max}$ from the space refrigerated, the difference between the space refrigerated T_r and evaporator temperature $T_{o\,min}$ being $\Delta_{o\,max}$.

At the same time the condenser is removing heat $Q_{k\,max}$, the difference between the condensing temperature $T_{k\,max}$ involved and the temperature T_a of surroundings through which heat is removed from the condenser, being $\Delta_{k\,max}$.

With the heat load of the space refrigerated decreased from $Q_{o\,max}$ to value Q_o, the system starts operating in cycles composed of the period during which the compressor is running and the period during which the compressor is at a standstill.

During the working period of the cycle, the evaporator temperature drops, and rises during its off period. The system works with varying evaporator temperature and the mean difference between the temperature of the space refrigerated T_r and the mean evaporator temperature T_{om} is decreased to Δ_o.

At the same time the difference between the mean condensing temperature T_{km} and the temperature T_a of the surroundings cooling down the condenser, will be decreased to Δ_k.

These conditions are shown in Fig. 1. After starting the compressor, at the moment T_1, the evaporator temperature drops from value T_{o1} until at the moment T_2 it reaches value T_{o2} at which the compressor is cut off by the thermostat or pressostat. The evaporator temperature will again start rising until at the moment T_3, at temperature T_{o1}, the compressor will be started.

The mean evaporator temperature during the compressor running period is not identical with that during its off period. Under the simplified assumption that a single-capacity system is involved, the mean evaporator temperature during the working period of the compressor will be:

Approved For Release 2009/05/01 : CIA-RDP80T00246A007500340002-0

Approved For Release 2009/05/01 : CIA-RDP80T00246A007500340002-0

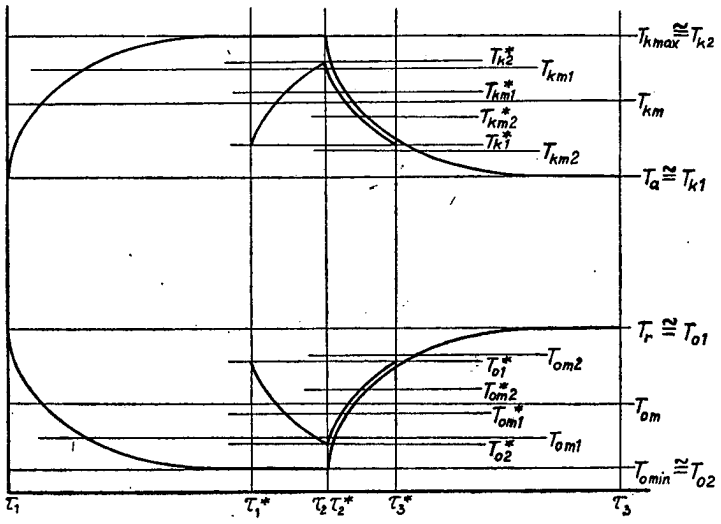

Fig. 1. Relation of condensing and evaporation temperatures to the length of on–off cycle.

$$T_{om1} = \frac{1}{\tau_2 - \tau_1} \int_{\tau_2}^{\tau_1} T_{0min} + (T_{01} - T_{0\,min})\, e^{-\frac{\tau_2 - \tau_1}{\tau_c}}\, d\tau \qquad (1)$$

Where T_C-evaporator time constant.

The mean evaporator temperature during the compressor off period is

$$T_{om2} = \frac{1}{\tau_3 - \tau_2} \int_{\tau_2}^{\tau_3} T_r - (T_r - T_{02})\, e^{-\frac{\tau_3 - \tau_2}{\tau_c}}\, d\tau \qquad (2)$$

The mean evaporator temperature during the whole cycle is

$$T_{om} = \frac{T_{om1}(\tau_2 - \tau_1) + T_{om2}(\tau_3 - \tau_2)}{\tau_3 - \tau_1} \qquad (3)$$

For evaluating the economy of the refrigerating cycle, only value T_{om1} enters the picture.

Similar equations can be written also for the mean condensing temperature during the compressor running period T_{km1}, mean condensing temperature during the off period T_{km2} and mean condensing temperature during the full cycle T_{km}.

The influence of the length of the whole on–off cycle T_3–T_1 on the size of value T_{om1} comes to prominence by substituting extreme values for T_2–T_1 and T_3–T_2 into equations (1) and (2).

If, $T_3 - T_1 \rightarrow 0$, then

$$\lim T_{o1} = \lim T_{om1} = T_{om},\ \lim T_{o2} = \lim T_{o2} = T_{om}$$

If, on the other hand, T_3–$T_1 \rightarrow \infty$ then $\lim T_{o1} = \lim T_{om2} = T_r$, $\lim T_{o2} = \lim T_{om1} = T_{o\,min}$.

By changing the length of cycle T_3–T_1 in an on–off control system it is therefore possible to change the mean evaporator temperature during the working period of cycle T_{om1} within the range of ($T_{o\,min}$, T_{om}).

Similar conditions prevail on the condenser side.

If, $T_3 - T_1 \rightarrow 0$, then

Approved For Release 2009/05/01 : CIA-RDP80T00246A007500340002-0

Approved For Release 2009/05/01 : CIA-RDP80T00246A007500340002-0

$\lim T_{k1} = \lim T_{km1} = T_{km}$, $\lim T_{k2} = \lim T_{km2} = T_{km}$
If, on the other hand, $T_3 - T_1 \rightarrow \infty$ then
$\lim T_{k1} = \lim T_{km2} = T_a$, $\lim T_{k2} = \lim T_{km1} = T_{k\,max}$.

By changing the length of cycle $T_3 - T_1$ in an on–off control system it is, therefore possible to change the mean condensing temperature during the working period of cycle T_{km1} within the limits of $(T_{km}, T_{k\,max})$.

Since the change in the evaporator temperature is taking place at the same time as the change in the condensing temperature, the value of the coefficient of performance of Carnot refrigerating cycle may reach values within the range of $(\varepsilon_{min}, \varepsilon_s)$, where

$$\varepsilon_{min} = \frac{T_{0min}}{T_{k\,max} - T_{0\,min}}$$

$$\varepsilon_s = \frac{T_{0min}}{T_{km} - T_{0m}}$$

Values T_{om} and T_{km} are changing with the relative heat load of the space refrigerated Q/Q_{max}. So under maximum heat load and with the compressor working continuously, then $T_{om} = T_{o\,min}$ and $T_{km} = T_{k\,max}$. As heat load of the space refrigerated decreases, there is a drop of the mean difference $T_r - T_{om}$ and of mean difference $T_{km} = T_a$. If $Q \rightarrow O$ then $\lim T_{om} = T_r$ and $\lim T_{km} = T_a$.

$$\varepsilon_s = \frac{T_{0min} + \left(1 - \frac{Q}{Q_{max}}\right) \Delta_{0\,max}}{T_{k\,max} - T_{0\,min} - \left(1 - \frac{Q}{Q_{max}}\right)(\Delta_{k\,max} + \Delta_{0\,max})} \qquad (6)$$

What values can be reached by relation $\varepsilon_{min}/\varepsilon_s$ are shown in diagram Fig. 2, compiled for relations $\Delta_{k\,max} = \Delta_{o\,max} = 15°$ C.; mean temperature of surroundings cooling down the condenser $T_a = 20°$ C. This diagram shows the dependence of relation $\varepsilon_{min}/\varepsilon_s$ on the relative heat load of the space refrigerated Q/Q_{max} at temperatures of the space refrigerated from –20° C. to +10° C. The influence of suction pressure on the compressor refrigeration output has not been taken into account.

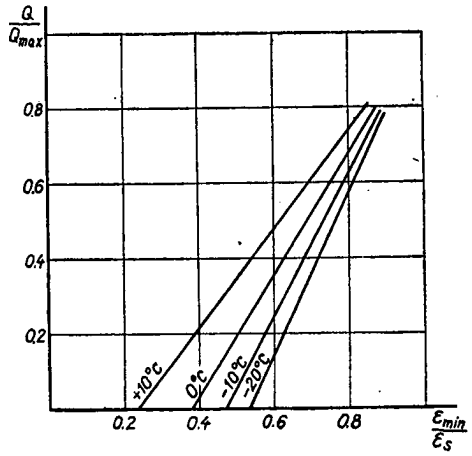

Fig. 2. Rise of the coefficient of performance of Carnot refrigeration cycle with decreasing heat load.

Approved For Release 2009/05/01 : CIA-RDP80T00246A007500340002-0

Approved For Release 2009/05/01 : CIA-RDP80T00246A007500340002-0

For example with relative heat load $Q/Q_{max} = 0,5$, a region very common in refrigerating equipment, the relation $\varepsilon_{min}/\varepsilon_s$ is about 0,7. Under these conditions it should be possible in the extreme case to reduce power consumption by as much as 30%. In reality in all cases $T_{om1} > T_{o\,min}$ and $T_{km1} < T_{k\,max}$ and also $T_{om1} < T_{om}$ and $T_{km1} > T_{km}$.

It is obvious that the coefficient of performance of Carnot refrigeration cycle will grow with increasing mean evaporating temperatures and decreasing condensing tenperatures.

From the foregoing, the extent to which the thermostat or pressostat differential will influence the length of the on–off cycle and the values of mean temperatures in the compressor running period T_{om1} and T_{km1} appears. The magnitude of the mean condensing temperature can moreover be influenced by the magnitude of the condenser and evaporator time constants. As shown in Fig. 3, large condensed time

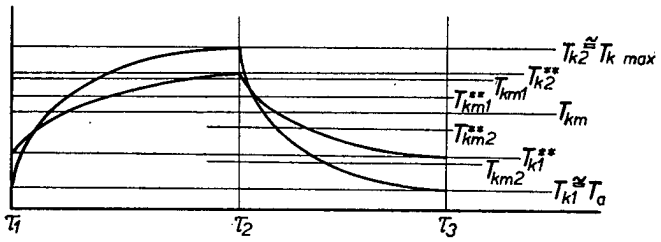

Fig. 3. Effect of condenser time constant on condensing temperature curve in transient states.

constant will reduce the mean temperature in the period of working cycle T_{km1}. Small evaporator time constant will, at equal thermostat differential, shorten time $T_2 - T_1$, thus indirectly reducing mean condensing temperature T_{km1}. Decisive for the size of the time constants are heat capacities of these exchangers and the vapor volumes of the low-pressure and high-pressure sides of the refrigeration circuit.

Heat capacity of water condenser is substantially higher than that of an air cooled one. Heat capacity can be increased by increasing the weight of material or the charge of refrigerant or water. The circuit volume can be enlarged by additional tanks.

Both these alternatives of increasing the time constant will naturally increase the investment costs, the dimensions and the weight of the equipment. It is obvious that the most effective means of reducing difference $T_{om} - T_{om1}$ and $T_{km1} - T_{km}$ is by decreasing the differential of the thermostat or pressostat. This is easily accomplished with the evaporator thermostat and the pressostat, their differentials being extensive.

The conditions of maximum economy of the whole refrigerating system are different from those of the refrigeration cycle, for the following reason: the economy of a refrigerating cycle as shown above, increases with the decrease of the differential, but on the other hand, there is an increase in the number of startings and stoppings of the compressor resulting in power losses in the compressor proper, its transmission and electric drive.

Starting and stopping will create unfavourable phenomena such as losses by piston leakage, which are very important at low speeds, and losses by friction. On the other hand, wiredrawing is smaller. Another unfavourable phenomena is high inertia of the compressor mechanism, extending the period during which these losses occur.

Exceptionally high are those losses that arise during transient states in a circuit provided with capillary tube as expansion element. After stopping the compressor there are heat losses due to noncondensed vapours entering the evaporator from the condenser.

Losses of this nature occur also after compressor starting until the moment when

Approved For Release 2009/05/01 : CIA-RDP80T00246A007500340002-0

Approved For Release 2009/05/01 : CIA-RDP80T00246A007500340002-0

$\lim T_{k1} = \lim T_{km1} = T_{km}$, $\lim T_{k2} = \lim T_{km2} = T_{km}$
If, on the other hand, $T_3 - T_1 \rightarrow \infty$ then
$\lim T_{k1} = \lim T_{km2} = T_a$, $\lim T_{k2} = \lim T_{km1} = T_{k\,max}$.

By changing the length of cycle $T_3 - T_1$ in an on–off control system it is, therefore possible to change the mean condensing temperature during the working period of cycle T_{km1} within the limits of $(T_{km}, T_{k\,max})$.

Since the change in the evaporator temperature is taking place at the same time as the change in the condensing temperature, the value of the coefficient of performance of Carnot refrigerating cycle may reach values within the range of $(\varepsilon_{min}, \varepsilon_s)$, where

$$\varepsilon_{min} = \frac{T_{0min}}{T_{k\,max} - T_{0\,min}}$$

$$\varepsilon_s = \frac{T_{0min}}{T_{km} - T_{0m}}$$

Values T_{om} and T_{km} are changing with the relative heat load of the space refrigerated Q/Q_{max}. So under maximum heat load and with the compressor working continuously, then $T_{om} = T_{0\,min}$ and $T_{km} = T_{k\,max}$. As heat load of the space refrigerated decreases, there is a drop of the mean difference $T_r - T_{om}$ and of mean difference $T_{km} = T_a$. If $Q \rightarrow O$ then $\lim T_{om} = T_r$ and $\lim T_{km} = T_a$.

$$\varepsilon_s = \frac{T_{0min} + \left(1 - \frac{Q}{Q_{max}}\right) \Delta_{0\,max}}{T_{k\,max} - T_{0\,min} - \left(1 - \frac{Q}{Q_{max}}\right)(\Delta_{k\,max} + \Delta_{0\,max})} \qquad (6)$$

What values can be reached by relation $\varepsilon_{min}/\varepsilon_s$ are shown in diagram Fig. 2, compiled for relations $\Delta_{k\,max} = \Delta_{0\,max} = 15°$ C.; mean temperature of surroundings cooling down the condenser $T_a = 20°$ C. This diagram shows the dependence of relation $\varepsilon_{min}/\varepsilon_s$ on the relative heat load of the space refrigerated Q/Q_{max} at temperatures of the space refrigerated from –20° C. to +10° C. The influence of suction pressure on the compressor refrigeration output has not been taken into account.

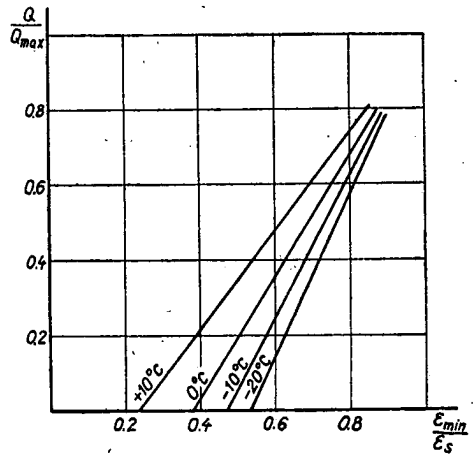

Fig. 2. Rise of the coefficient of performance of Carnot refrigeration cycle with decreasing heat load.

Approved For Release 2009/05/01 : CIA-RDP80T00246A007500340002-0

Approved For Release 2009/05/01 : CIA-RDP80T00246A007500340002-0

For example with relative heat load $Q/Q_{max} = 0,5$, a region very common in refrigerating equipment, the relation $\varepsilon_{min}/\varepsilon_s$ is about 0,7. Under these conditions it should be possible in the extreme case to reduce power consumption by as much as 30%. In reality in all cases $T_{om1} > T_{o\,min}$ and $T_{km1} < T_{k\,max}$ and also $T_{om1} < T_{om}$ and $T_{km1} > T_{km}$.

It is obvious that the coefficient of performance of Carnot refrigeration cycle will grow with increasing mean evaporating temperatures and decreasing condensing tenperatures.

From the foregoing, the extent to which the thermostat or pressostat differential will influence the length of the on–off cycle and the values of mean temperatures in the compressor running period T_{om1} and T_{km1} appears. The magnitude of the mean condensing temperature can moreover be influenced by the magnitude of the condenser and evaporator time constants. As shown in Fig. 3, large condensed time

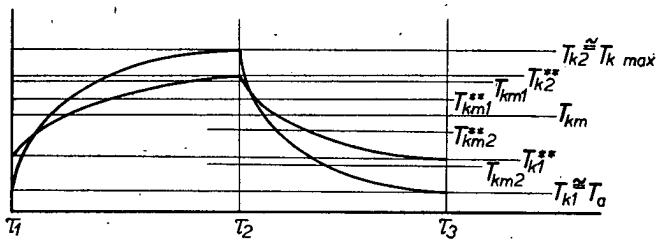

Fig. 3. Effect of condenser time constant on condensing temperature curve in transient states.

constant will reduce the mean temperature in the period of working cycle T_{km1}. Small evaporator time constant will, at equal thermostat differential, shorten time $T_2 - T_1$, thus indirectly reducing mean condensing temperature T_{km1}. Decisive for the size of the time constants are heat capacities of these exchangers and the vapor volumes of the low-pressure and high-pressure sides of the refrigeration circuit.

Heat capacity of water condenser is substantially higher than that of an air cooled one. Heat capacity can be increased by increasing the weight of material or the charge of refrigerant or water. The circuit volume can be enlarged by additional tanks.

Both these alternatives of increasing the time constant will naturally increase the investment costs, the dimensions and the weight of the equipment. It is obvious that the most effective means of reducing difference $T_{om} - T_{om1}$ and $T_{km1} - T_{km}$ is by decreasing the differential of the thermostat or pressostat. This is easily accomplished with the evaporator thermostat and the pressostat, their differentials being extensive.

The conditions of maximum economy of the whole refrigerating system are different from those of the refrigeration cycle, for the following reason: the economy of a refrigerating cycle as shown above, increases with the decrease of the differential, but on the other hand, there is an increase in the number of startings and stoppings of the compressor resulting in power losses in the compressor proper, its transmission and electric drive.

Starting and stopping will create unfavourable phenomena such as losses by piston leakage, which are very important at low speeds, and losses by friction. On the other hand, wiredrawing is smaller. Another unfavourable phenomena is high inertia of the compressor mechanism, extending the period during which these losses occur.

Exceptionally high are those losses that arise during transient states in a circuit provided with capillary tube as expansion element. After stopping the compressor there are heat losses due to noncondensed vapours entering the evaporator from the condenser.

Losses of this nature occur also after compressor starting until the moment when

Approved For Release 2009/05/01 : CIA-RDP80T00246A007500340002-0

Approved For Release 2009/05/01 : CIA-RDP80T00246A007500340002-0

the pressure in the condenser has risen to such a level that a sufficient quantity of refrigerant is condensed. Up to this point there exist also losses of energy connected with rise of pressure above that value.

At the same time heat losses are brought about by leakage of liquid refrigerant from the evaporator to the suction piping, similarly as in circuits with expansion valves.

Efficiency of the electric motor during starting is low as well, due to increased losses in the winding as well as hysteresis losses in the rotor.

It would be possible to reduce these losses at the cost of decreasing the starting torque. In most cases this will be possible at relived compressor starting only. Here as well the high inertia of the motor rotor has unfavourable effects in extending the uneconomical operation during transient state. The reduced starting torque will naturally extend starting time.

We can see, therefore, that for determining optimal conditions during starting, several contradictory requirements have to be taken into account.

What has been said in the foregoing can be recapitulated as follows: The controller differential with temperature on–off control exerts a considerable effect on the economy of operation. The economy of a refrigeration cycle rises with decrease of differential.

There is, however, a number of factors to be found under transient states, which move the economical optimum towards higher differentials, thus deteriorating the economy of the whole refrigerating system.

For safeguarding highest economy of operation it is, therefore, necessary to give due attention to not only adjusting the controller differential for optimum economy, but also designing the refrigeration circuits and compressor drives so as to achieve their highest efficiency even under transient states.

Behrndt bogtryk, Denmark

Copyright reserved

Approved For Release 2009/05/01 : CIA-RDP80T00246A007500340002-0

Approved For Release 2009/05/01 : CIA-RDP80T00246A007500340002-0

the pressure in the condenser has risen to such a level that a sufficient quantity of refrigerant is condensed. Up to this point there exist also losses of energy connected with rise of pressure above that value.

At the same time heat losses are brought about by leakage of liquid refrigerant from the evaporator to the suction piping, similarly as in circuits with expansion valves.

Efficiency of the electric motor during starting is low as well, due to increased losses in the winding as well as hysteresis losses in the rotor.

It would be possible to reduce these losses at the cost of decreasing the starting torque. In most cases this will be possible at relived compressor starting only. Here as well the high inertia of the motor rotor has unfavourable effects in extending the uneconomical operation during transient state. The reduced starting torque will naturally extend starting time.

We can see, therefore, that for determining optimal conditions during starting, several contradictory requirements have to be taken into account.

What has been said in the foregoing can be recapitulated as follows: The controller differential with temperature on–off control exerts a considerable effect on the economy of operation. The economy of a refrigeration cycle rises with decrease of differential.

There is, however, a number of factors to be found under transient states, which move the economical optimum towards higher differentials, thus deteriorating the economy of the whole refrigerating system.

For safeguarding highest economy of operation it is, therefore, necessary to give due attention to not only adjusting the controller differential for optimum economy, but also designing the refrigeration circuits and compressor drives so as to achieve their highest efficiency even under transient states.

Behrndt bogtryk, Denmark

Copyright reserved

Approved For Release 2009/05/01 : CIA-RDP80T00246A007500340002-0

Approved For Release 2009/05/01 : CIA-RDP80T00246A007500340002-0

Thermodynamic Investigations of the Working Cycle of the Philips Machine

Recherches sur les transformations thermodynamiques dans le cycle de fonctionnement des machines frigorifiques à gaz Philips

I. I. KARAVANSKY and L. Z. MELTSER
The Odessa Technological Institute of the Food and Refrigerating Industry, Odessa, U.S.S.R.

SOMMAIRE. Le rapport étudie les conditions de fonctionnement de la machine frigorifique à gaz Philips à mouvement alternatif des pistons. On suppose que toutes les transformations de la machine sont réversibles grâce à deux sources de chaleur à température constante. A l'inverse de Codegone, les AA. basent leurs calculs sur un espace mort considérable (dans les conduits du régénérateur, du refroidisseur d'eau et du congélateur) en proportion du volume du cylindre de la machine. Une nouvelle méthode, fondée sur l'application de l'équation énergétique générale pour une quantité de gaz variable est utilisée pour l'étude du cycle.

Le but de la recherche thermodynamique est de déterminer les quantités de chaleur réellement échangées par seconde aux échangeurs de chaleur de la machine. Le problème est résolu à l'aide de l'équation caractéristique et de l'équation énergétique de la quantité de gaz variable.

L'étude fait apparaître un écart considérable des quantités de chaleur par seconde échangées à chaque appareil par rapport aux quantités calculées sur la base de l'équilibre thermique du cycle.

La déduction de Codegone suivant laquelle la chaleur provenant du régénérateur est égale à $Cp\Delta T$ ne s'est révélée exacte que lorsque les quantités de gaz à l'entrée et à la sortie du générateur sont égales à tout moment.

On donne une analyse de l'influence des principaux paramètres du cycle sur son rendement en se basant sur les relations dérivées à savoir:

1. *la relation de la puissance frigorifique par unité de volume avec l'angle directeur α. Il est possible de déterminer la valeur optimum de α pour les conditions données.*
2. *L'influence du paramètre de construction égal au rapport de la valeur maximum des volumes utiles de la machine sur la puissance frigorifique par unité de volume et le rapport des pressions limites du cycle.*

L'utilisation de la méthode proposée permet une meilleure description des caractères réels des processus non stationnaires qui se produisent dans la machine et orientent la méthode du choix des principaux paramètres de la machine.

The analysis and calculation of the cycle of the Philips machine even simplified and schematic have not as yet been completely elaborated. Köhler and Jonkers [1] give no solution of the problem of a theoretical determination of the per-second heat exchange in the working spaces of the machine and the regenerator. Investigations carried out by Codegone [2] dealt with the cycle of a machine having a null clearance volume.

The investigation to be discussed in this paper has been based on the thermodynamics of a variable amount of gas. The fundamentals of this thermodynamics have been set forth by M. A. Mamontov [3]. The application of the method allows solving the problem in a general case and giving a more complete illustration of the processes occurring in the machine.

Fig. 1 illustrates our diagram with the clearance and the volumes of the heat exchangers allowed for. The sinusoidal motion of the pistons, close to actual conditions, was accepted for approximate calculation in all the investigations.

All the mechanical and thermal processes of the cycle of the machine are

Approved For Release 2009/05/01 : CIA-RDP80T00246A007500340002-0

Approved For Release 2009/05/01 : CIA-RDP80T00246A007500340002-0

supposed to be reversible. Due to the fact that only two external heat sources participate in the process with the temperatures T_C and T_E, it follows that the theoretical coefficients of performance is to be equal to the Carnot coefficient, i. e.

$$\varepsilon = \frac{T_E}{T_C - T_E}.$$

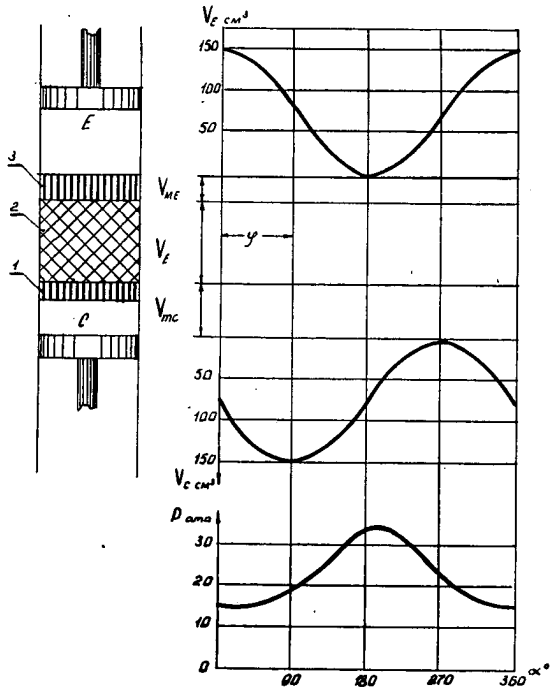

Fig. 1. Diagram of the Philips machine and piston motion. 1-water heat exchanger; 2-regenerator; 3-refrigerator.

The following nomenclature is used in the analysis:

V_C – operating volume of the warm space;
V_E – operating volume of the cold space;
W – ratio of the maximum operating volume of the warm space $V_{C\,max}$ to that of the cold space $V_{E\,max}$;
φ – the lead angle of the maximum volume $V_{C\,max}$ in relation to the volume $V_{E\,max}$;
V_{mC} – the total volume of the warm space clearance and of the water heat exchanger;
V_{mE} – the total volume of the cold space clearance volume and of the refrigerator;
V_R – the volume of the refrigerant in the regenerator;
G_C; G_E; G_R – the weight of the refrigerant in the warm and cold spaces and in the regenerator respectively;
T_R – the mean temperature of the refrigerant in the regenerator;
T_C – the mean temperature of the refrigerant in the warm space;
T_E – the mean temperature of the refrigerant in the cold space.

The following is derived on working out the equation of state for each space and regenerator separately and having summed them up by terms:

Approved For Release 2009/05/01 : CIA-RDP80T00246A007500340002-0

Approved For Release 2009/05/01 : CIA-RDP80T00246A007500340002-0

$$PV_{zed} = GRT_E \tag{1}$$

where $V_{zed} = V_E + V_C \frac{T_E}{T_C} + V_m$ – is the volume of the machine reduced to the temperature T_E,

$V_m = V_{mE} + V_R \frac{T_E}{T_R} + V_{mc} \frac{T_E}{T_C}$ – the clearance volume of the machine reduced to the temperature T_E,

$G = G_c + G_E + G_R$ – the total weight of the refrigerant.

In case of the refrigerant being distributed along the length of the refrigerator in compliance with a linear law the mean temperature of the refrigerant T_R is determined according to the following formula:

$$T_R = \frac{T_c - T_E}{\ln \frac{T_C}{T_E}} \tag{2}$$

The equation (1) allows defining the pressure of the refrigerant by the set motion of the pistons.

The initial figures in the performed calculations have been chosen close to those obtained in the Philips machine and namely:

$$T_C = 300^0\ K, \quad T_E = 75^0\ K, \quad V_{C\,max} + V_{E\,max} = 300\ cm^3,$$
$$V_{mc} = 70\ cm^3, \quad V_{mE} = 35\ cm^3, \quad V_R = 105\ cm^3,$$

the speed of the crankshaft n = 1500 rpm.

These data were used in all subsequent approximate calculations. The values of φ and W were assumed to be W = 1; $\varphi = 90°$.

Let us consider now the heat balance of the machine. We shall use equation of the first law of thermodynamics for a variable amount of gas (3).

$$dQ + \pi dG = dU + Ad\alpha + \pi_K dG_K \tag{3}$$

where dQ – is the heat exchange of the gas with the walls;
π – the energy of 1 kg of entering gas;
π_K – the energy of 1 kg of leaving gas;
dG – the weight rate of entering gas;
dG_K – the weight rate of leaving gas;
dU – the change of the total intrinsic energy of the gas;
$Ad\alpha$ – the external work of expansion.

The energy of 1 kg of the escaping gas π_K is equal to the enthalpy of the escaping gas, while the energy of 1 kg of entering gas π is equal to the enthalpy of the entering gas only in the case of the heat transfer in the gas supply duct amounting to nought.

Let us make up an equation of the first law for the refrigerant of the warm space during the period of one cycle:

$$Q_c + \varphi i_c dG = \varphi dU + \varphi P dV_c + \varphi i_c dG_k,$$

where: Q_C – is the amount of heat removed from the refrigerant in the warm space during one cycle.

It is evident that at the stable working conditions of the machine the amount of refrigerant entering the warm space and that leaving it in the course of one cycle are equal

Approved For Release 2009/05/01 : CIA-RDP80T00246A007500340002-0

Approved For Release 2009/05/01 : CIA-RDP80T00246A007500340002-0

$$\varphi dG = \varphi dG_K$$

and the intrinsic energy of the refrigerant in the warm space is not changed after a single cycle:

$$\varphi dU = O.$$

The equation will thus acquire a more simple shape:

$$Q_c = A\varphi P dV_c. \tag{4}$$

Having made up the equation of the first law for the refrigerant in the cold space in the course of one cycle, we receive:

$$Q_E = A\varphi P dV_E, \tag{5}$$

where: Q_E – is the amount of heat supplied to the refrigerant in the cold space during one cycle.

The coefficient of performance of the cycle being investigated (no matter what the character of the piston motion) is to be equal to the coefficient of the reverse Carnot cycle.

let us analyse the expression $Q_E + \frac{T_E}{T_C} Q_C$.

The following will be received by using formulae (4) and (5):

$$Q_E + \frac{T_E}{T_C} Q_c = A\varphi P / dV_E + \frac{T_E}{T_C} dV_c /.$$

And if we consider that $dV_E + \frac{T_E}{T_C} dV_c = dV_{zed}$, and P may be determined from (1), then finally:

$$Q_E + \frac{T_E}{T_C} Q_C = AGRT_E \varphi \frac{dV_{zed}}{V_{zed}} = O \tag{6}$$

$$\text{i.e.} \quad \frac{Q_E}{Q_c - Q_E} = \frac{T_E}{T_c - T_E},$$

In the case, when the pistons have a sinusoidal motion (*see* Fig. 1). the equation (5) acquires, after integration, the following shape:

$$Q_E = AGRT_E \frac{2\pi\tau W \sin\varphi}{c^2} \Big/ \frac{a}{\sqrt{a^2 - c^2}} - 1 \Big/, \tag{7}$$

where: $\tau = \frac{T_E}{T_C}$, $a = 1 + \tau W + \frac{2V_m}{V_{mE}}$, $c^2 = 1 + 2\tau W \cos\varphi + \tau^2 W^2$.

For the determination of Q_C it is best to use the relation (6).

Due to the fact that the heat flows in the spaces are non-stationary, the values Q_E and Q_C do not provide a complete characteristics of the heat exchange taking place in the apparatus of the machine. An analysis of the heat exchange intensity in each space separately may help to fill up this blank.

With the equation of the first law for the cold space made up, the following expression may be derived after a number of transformations:

Approved For Release 2009/05/01 : CIA-RDP80T00246A007500340002-0

Approved For Release 2009/05/01 : CIA-RDP80T00246A007500340002-0

$$\frac{dQ_E}{dt} = AP \cdot \frac{V_E + V_{mE}}{V_{zed}} \cdot \frac{dV_{zed}}{dt}. \tag{8}$$

And analogous for the warm space:

$$\frac{dQ_c}{dt} = AP \cdot \frac{V_c + V_{mc}}{V_{zed}} \cdot \frac{dV_{zed}}{dt}. \tag{9}$$

(t – the time in seconds).

Fig. 2 illustrates the graphs of dependence of the space heat exchange intensity for two cycles with various values of W. It follows from the graphs that there is a change in the direction of the heat flows in the spaces in the course of one cycle. It is worth noting that with W = 1 the refrigerating capacity of the cycle Q_E is only 26% of the total amount of heat supplied to the refrigerant in the cold space (area abc in Fig. 2). The greater part of this heat is removed from the refrigerant during the second period of the cycle. For greater clearness the values of Q_E and Q_C at W = 1 are represented in Fig. 2 by shaded rectangles.

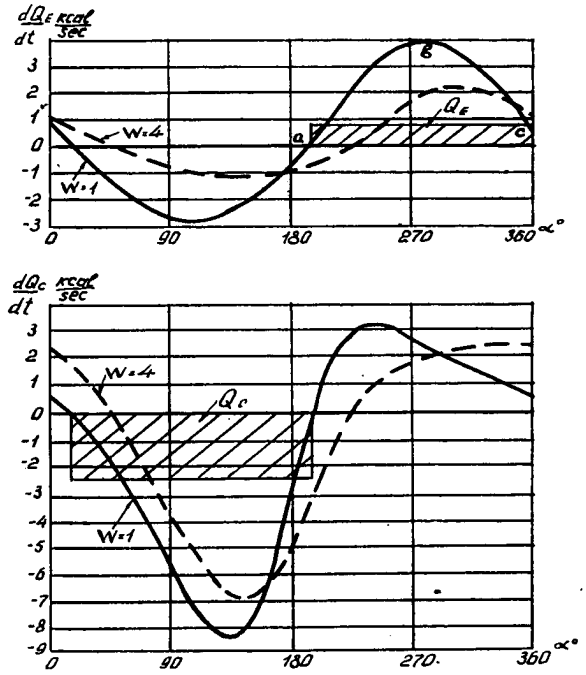

Fig. 2. Intensity of heat exchange during one cycle.

The per second rates of flow $\frac{dG_C}{dt}$ and $\frac{dG_E}{dt}$ may be determined by differentiating the equations of state for the respective space.

For the warm space:

$$\frac{dG_c}{dt} = \frac{T_E}{T_C} \cdot \frac{G}{V_{zed}^2} \left[V_{zed} \frac{dV_c}{dt} - \left| V_c + V_{mc} \right| \frac{dV_{zed}}{dt} \right]. \tag{10}$$

Approved For Release 2009/05/01 : CIA-RDP80T00246A007500340002-0

Approved For Release 2009/05/01 : CIA-RDP80T00246A007500340002-0

For the cold space:

$$\frac{dG_E}{dt} = \frac{G}{V_{zed}}\left[V_{zed}\frac{dV_E}{dt} - \left/ V_E + V_{mE}\right/ \frac{dV_{zed}}{dt}\right]. \qquad (11)$$

The equation of the first law is to be worked out for the refrigerant in the regenerator in order to determine the per-second heat load of this apparatus. With a number of transformations made the following expression is obtained:

$$\frac{dQ_R}{dt} = \left/ i_c - U_p\right/ \frac{dG_C}{dt} + \left/ i_E - U_p\right/ \frac{dG_E}{dt}. \qquad (12)$$

Some comparative calculations have been done to determine the influence of separate parameters of the machine upon its operating characteristics.

The influence of the lead angle φ was investigated first.

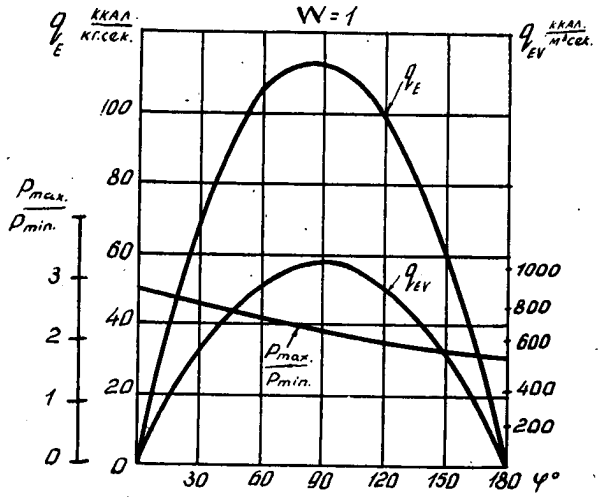

Fig. 3. Refrigerating capacity depending upon lead angle S.

Fig. 3 illustrates the graph of dependence of the refrigerating capacity of 1 kg of refrigerant q_E upon the angle φ. Besides, the value of the refrigerating capacity q_{EV}, related to the total of the maximum operating volumes of both warm and cold spaces at equal values of the clearance and of the maximum pressure of the cycle were defined.

$$q_{EV} = \frac{Q_E}{V_{Cmax}+V_{Emax}}$$

The graph of the dependence of the pressure ratio $\frac{P_{max}}{P_{min}}$ upon the lead angle φ is also given in the figure. It follows from the graph that with an increase of φ the pressure ratio $\frac{P_{max}}{P_{min}}$ drops, and consequently, the compression and expansion losses are lessened likewise. In order to obtain the maximum value of q_{EV} with minimum compression and expansion losses, the values of φ ranging from 90° to 110° are to be recommended.

For the determination of the influence of W the values of q_E; q_{EV} and $\frac{P_{max}}{P_{min}}$

Approved For Release 2009/05/01 : CIA-RDP80T00246A007500340002-0

Approved For Release 2009/05/01 : CIA-RDP80T00246A007500340002-0

were found at various values of W. A change of W was regarded as a redistribution of the same total of operating volumes $V_{C\,max} + V_{E\,max}$ between the warm and cold spaces, the other parameters of the machine remaining constant.

Graphs were drawn of the intensity of heat exchange between the spaces for various values of W. An examination of these graphs indicates that with an increase of W the exchange in the warm space is subject to insignificant changes, and that of the cold space is reduced significantly due to a decrease of regeneration. The latter must have a favourable effect upon the losses of the machine.

Graphs for $W = 1$ and $W = 4$ are given in Fig.2.

REFERENCES

1. KÖHLER, J. W. L. and JONKERS, C. O. Fundamentals of the gas refrigerating machine Philips. *Technical Review,* **16**, (3), 1954.

2. CODEGONE, K. The Philips Refrigerating cycle. *Proceedings* of IX International Congress of Refrigeration, 1955.

3. MAMONTOV, M. A. Some cases of gas flow. *Oborongiz,* 1951.

Behrndt bogtryk, Denmark

Copyright reserved

Approved For Release 2009/05/01 : CIA-RDP80T00246A007500340002-0

Approved For Release 2009/05/01 : CIA-RDP80T00246A007500340002-0

On the Energy Efficiency of Thermoelectrical Refrigeration

Caractéristiques de l'énergie du refroidissement electro-thermique

V. S. MARTYNOVSKY and V. A. NAER
The Odessa Technological Institute of the Food and Refrigerating Industry, Odessa, U.S.S.R.

SOMMAIRE. La relation entre le coefficient de rendement des machines frigorifiques à compression et à absorption, leur puissance et la température des sources de chaleur est étudié d'après les données des expériences et des calculs. On propose une méthode précise pour le calcul des systèmes électro-thermique permettant d'évaluer le coefficient de rendement du système. Cette méthode tient compte de la relation entre la température des jonctions des thermoéléments et du courrant qui les traversee (c'est-à-dire la relation entre les températures des jonctions et l'importance des fleux de chaleur).

Des essais effectués avec une installation électro-thermique d'évaporation à semiconducteur confirme les formules établies et permet des comparaisons avec les systèmes exitants à compression, à absorption et à éjection. Les expériences ont été effectuées sur une installation de pompe à chaleur d'évaporation à semi-conducteur il était possible de réduire la consommation de courant électrique de 4 à 5 fois pour $\Delta T = 10°$ C et avec une température d'évaporation de 100° C par rapport au chauffage électrique direct.

Le rapport présente aussi les domaines rationnels d'application de l'effet électric-thermique pour les installations frigorifiques et les installations de pompes à chaleur.

Dans le cas de matériaux semi-conducteurs un tel domaine d'application rationnel (du point de vue de la consommation de courant) pour les générateurs frigorifiques s'étendrait entre quelques dizaines de kcal/h seulement pour une différence de température ne dépassant pas 30 à 40° C.

Les installations électric-thermiques de pompes à chaleur sont commodes aussi pour les puissances élevées. En utilisant le chauffage électro-thermique au lieu du chauffage électrique direct on peut réaliser une économie de courant électrique importante. Cependant l'application de l'effet électro-thermique n'est guère justifié avec une différense de température dépassant 40 à 50° C.

GENERAL PRINCIPLES, COMPARISON WITH THE USUAL REFRIGERATING METHODS

Introduction of thermoelectrical refrigeration into practice requires preliminary study of its advantages and disadvantages as compared with ordinary refrigeration. Thermoelectrical installations are absolutely noiseless. They are devoid of moving parts, have no need for special refrigerating agents, are easy to control and may, with extraordinary ease, be transformed from refrigerating installations into heat pumps. The ease of conversion to a heat pump opens up a promising field for the use of thermoelectrical refrigeration in various types of installations requiring maintenance of temperature on a given level (above or below the ambient). However, although the power efficiency of thermoelectrical cooling has greatly increased with the transition from metals to semi-conductors, it is still far behind mechanical and absorption units (the latter in the case of heat but not electrical energy consumption).

At this time energy consumption is the predominant factor in the choice of a refrigeration system. For very small capacities of the order of a few score kcal/hr the energy consumption no longer plays a major part and other factors as, for instance, initial cost, portability, reliable operation, convenience in control, etc. characteristic of semi-conductor arrangements come to the fore.

Approved For Release 2009/05/01 : CIA-RDP80T00246A007500340002-0

Approved For Release 2009/05/01 : CIA-RDP80T00246A007500340002-0

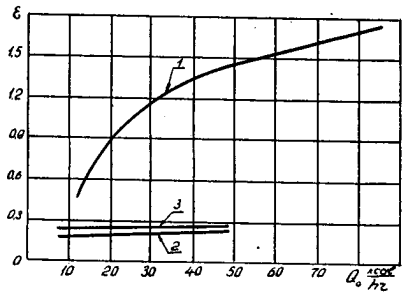

Fig. 1. Efficiency of various refrigerating systems for domestic cabinets. 1 – mechanical, 2 – absorption, 3 – thermoelectrical.

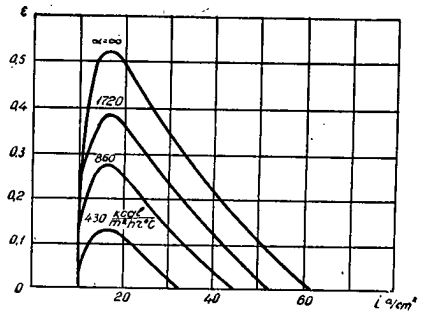

Fig. 2. The effect of heat exchange on the energy characteristics of semi-conductor thermal batteries.

We made comparative calculations based on test data for a large number of domestic refrigerators with mechanical and absorption systems. Fig. 1 shows the relation between the real coefficient of prformance and the refrigerating capacity Q_0 (of refrigerator without load), the real coefficient of performance for the semi-conductor refrigerator being obtained by calculation, using the semi-conductor materials we obtained from the Institute of Semiconductors of the Academy of Sciences of the U.S.S.R.

The value of Z for a semi-conductor thermocouple is related to the thermoelectric forces (e), specific thermal conductivities (λ) and specific resistances (ϱ) of the arms as follows:

$$Z = \frac{(e_1 + e_2)^2}{(\sqrt{\varrho_1 \lambda_1} + \sqrt{\varrho_2 \lambda_2})^2} \qquad (1)$$

The analysis led to the following conclusions. The present semi-conductor refrigerator will consume several times as much energy as the mechanical type. With regard to its energy characteristics it is approximately on a level with an absorption refrigerator with electrical heating. The latter is about three times lower in efficiency than absorption systems utilizing heat energy.

Obviously for large capacity refrigerators (and still more for industrial plants), semi-conductor units are as yet unable to compete with mechanical and absorption types. The energy characteristics of semi-conductor systems may be improved on employing them as heat pumps, particularly for evaporating plants. This is due to two factors: the relatively small temperature difference and the higher temperature of the low temperature heat source in heat pumps than in refrigerating plants. Owing to these two factors, thermoelectric losses diminish and the energy efficiency rises.

Naturally, the search for new semi-conductor materials with high Z values assumes paramount significance.

It should be noted that the existing method of calculating semi-conductor thermal batteries for refrigerating plants and heat pumps requires further development taking into account the influence of the heat exchange of the thermocouple junctions with the surrounding medium. To determine the heat and energy characteristics of a semi-conductor evaporating plant and to check the rating formulae, a test was made of a small model of up to 150 kcal/hr capacity.

CORRECTED METHOD FOR CALCULATING SEMI-CONDUCTOR BATTERIES

The classical theory of thermoelectrical cooling and heating gives formulae for calculation based upon the temperatures of the junctions T and T_0. However,

Approved For Release 2009/05/01 : CIA-RDP80T00246A007500340002-0

Approved For Release 2009/05/01 : CIA-RDP80T00246A007500340002-0

these temperatures do not remain constant on change of the heat flow in the thermocouple. In designing refrigerating and heat pump plants the temperatures of the media supplying and receiving heat (T_0' and T') and the heat transfer coefficients (α_0 and α) are usually known. Therefore, of practical interest are rating formulae depending upon these quantities.

The densities of the heat flows at the cold and hot thermocouple junctions are determined by the following formulae

$$2q_0 = eT_0 i - \frac{1}{2} i^2 \varrho l - \frac{\lambda}{l}(T - T_0) \tag{2}$$

$$2q = eTi + \tfrac{1}{2} i^2 \varrho l - \frac{\lambda}{l}(T - T_0) \tag{3}$$

The temperatures of the thermocouple junctions may be determined from the general equation for heat transmission:

$$q_0 = \alpha_0 (T_0^1 - T_0), \tag{4}$$

$$q = \alpha (T - T^1) \tag{5}$$

Solving the systems of equations (2, 3, 4, 5) and taking into account that the coefficient of performance equals

$$\varepsilon = \frac{q_0}{q - q_0}, \tag{6}$$

we obtain

$$\frac{1}{\varepsilon} = \frac{\left(\varepsilon^1 + 1\right)\left(1 + \frac{ei}{2\alpha_0}\right) + \frac{\lambda}{2l\alpha_0}}{\varepsilon^1\left(1 - \frac{ei}{2\alpha}\right) - \frac{\lambda}{2l\alpha}} \tag{7}$$

In these formulae l is the length of the thermocouple and i the density of the current passing through it.

The quantity ε' is determined from expression (6), T' and T'_0 being substituted for T and T_0 in the formulae for q_0 and q.

It should be noted that for $\alpha_0 \to \infty$ and $\alpha \to \infty$ the formula for ε coincides with the corresponding formula in the theory of thermoelectrical cooling and heating. In that case $\varepsilon \to \varepsilon'$.

Calculations show that in order to obtain ε values sufficiently approaching ε' the heat transfer coefficients should be high. For instance, for a semi-conductor thermocouple 1 cm in length operating under the temperature conditions of a domestic refrigerator, the value of α and α_0 should be measured in thousands of kcal/m²hr°C. Such values of heat transfer coefficients under conditions of natural convection are made possible only by extensive finning of the thermocouple junctions. In experimental semi-conductor refrigerators the finning coefficient attained the enormous values of 400 to 600!

In Fig. 2 the relation is shown between the performance coefficient of the thermobattery and the heat exchange conditions for the case when $\alpha = \alpha_0$, l = 1 cm, T_0' = 273° K

$$T^1 = 303\,^0K, \quad Z = 1{,}85 \cdot 10^{-3}\,\frac{1}{^0K}$$

Characteristic is the fact that the optimum current density is independent of α and α_0.

Approved For Release 2009/05/01 : CIA-RDP80T00246A007500340002-0

Approved For Release 2009/05/01 : CIA-RDP80T00246A007500340002-0

The heat flow densities diminish with increase in thermocouple length, improving the conditions for heat exchange. For constant heat transfer coefficients

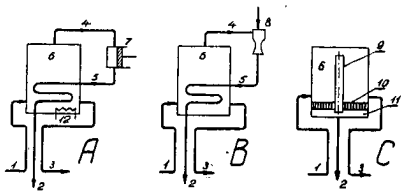

Fig. 3. Schematic diagram of heat pump evaporating plants. A – mechanical, B – ejector, C – semi-conductor. 1 – liquid inlet, 2 – condensate outlet, 3 – excess liquid outlet, 4 – vapour outlet, 5 – compressed vapour, 6 – evaporator, 7 – compressor, 8 – ejector, 9 – vapour outlet tube, 10 – thermobattery, 11 – condenser, 12 – starting electrical heater.

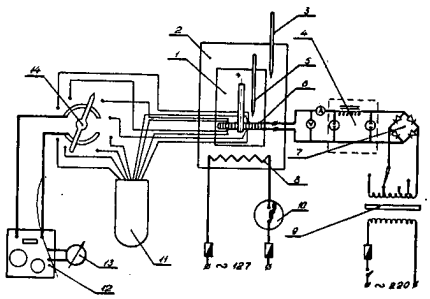

Fig. 4. Electrical measurement circuit of experimental plant. 1 – boiler, 2 – thermostat, 3, 5 – thermometers, 4 – electrical filter, 6 – thermobattery, 7 – rectifier, 8 – thermostat heater, 9 – transformer, 10 – temperature relay, 11 – Dewar flask, 12 –potentiometer, 13 – exterior galvanometer, 14 – switch.

the increase in length of a thermocouple, operating in a refrigerating unit, increases the value of the coefficient of performance.

It should be borne in mind in the calculations that under conditions of natural convection the effect of the heat flows upon the values of α and α_0 may be neglected while on boiling and condensation these relations may be easily determined with the aid of the usual heat transfer formulae.

For small current densities and intensive heat exchange the quantities $\frac{ei}{2\alpha}$ and $\frac{ei}{2\alpha_0}$ are negligible. Formula (7) in that case is considerably simplified. Then the optimum current density corresponding to ε_{max} is determined by the formula:

$$i_{opt} = \frac{e\left(T^1 - T_0^1\right)}{\left(\sqrt{1 + \frac{T^1 + T_0^1}{2} Z} - 1\right) pl} \tag{8}$$

In the particular case of calculations for an evaporator plant, when $T' = T'_0$ extreme values for ε are absent altogether. The basic principles of this method of calculation were checked experimentally in a study of the thermoelectrical evaporator plant.

EXPERIMENTAL THERMOELECTRICAL EVAPORATOR PLANT

In heat pump evaporator plants the secondary vapour is compressed in the compressor or ejector (Fig. 3). The condensation temperature of the secondary vapour then increases and the heat of condensation may be used as heat source for vaporizing the liquid in the evaporator.

Mechanical evaporator plants have high conversion coefficients (φ), but they are complicated as regards both equipment and operation. Ejector plants possessing somewhat inferior energy characteristics require vapour of comparatively high parameters.

Approved For Release 2009/05/01 : CIA-RDP80T00246A007500340002-0

Approved For Release 2009/05/01 : CIA-RDP80T00246A007500340002-0

The substitution of a compressor or ejector by a semi-conductor battery makes it possible to construct a plant outstanding in the simplicity of its design, noise-free operation, compactness and flexibility of control. Moreover, the semi-conductor thermocompressor allows change in temperature of the secondary vapour without change in pressure. In this case as heat source, use is made of the heat of condensation of the evaporating liquid, permitting considerable elevation in the temperature of the cold junctions of the thermocouples and maintenance of this temperature on a level close to that of the condensing vapour at the corresponding pressure.

The schematic diagram of the experimental thermoelectrical evaporator plant is given in Fig. 3 and the electrical measurement circuits in Fig. 4.

The evaporating liquid, heated to the boiling temperature in the regenerator enters the evaporator where it boils, taking up the heat from the hot junctions of the thermobattery. The vapour formed passes through a vapour outlet to the condenser where it condenses on the cold junctions. In the exchanger heat exchange takes place between the outflowing condensate and the entering liquid.

The effect of scale formation was studied by coating the hot junctions of the thermobattery with layers of different thickness of a cement and determining the thermal resistance $\frac{\delta}{\lambda}$

In Fig. 5 are produced the energy characteristics representing the dependence of the conversion coefficient φ on the current density i (heat load) and the thermal resistance $\frac{\delta}{\lambda}$.

The curves show that the conversion coefficient of a thermoelectrical evaporating plant increases continuously with fall in load exhibiting no extremes. The rise in φ is due to decrease in temperature difference between the junctions of the thermobattery on fall in current density.

Scale formation markedly impairs the energy characteristics of the plant. For example, at $i = 16$ a/cm² the formation of scale with a thermal resistance $\frac{\delta}{\lambda}$

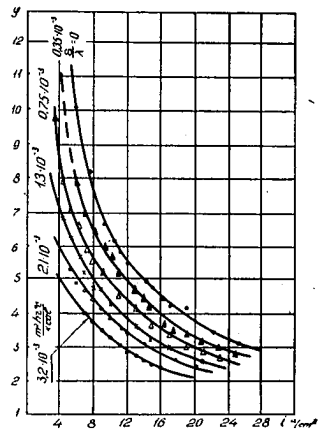

Fig. 5. Energy characteristics of thermoelectrical evaporating plant.

$= 0.75 \cdot 10^{-3}$ m²hr°C./kcal leads to a fall in φ from 4.5 at $\frac{\delta}{\lambda} = 0$ to 3.5 i.e. by 22%. The relative influence of the scale increases with decrease in load. At

Approved For Release 2009/05/01 : CIA-RDP80T00246A007500340002-0

Approved For Release 2009/05/01 : CIA-RDP80T00246A007500340002-0

$i = 7$ a/cm² an increase in $\frac{\delta}{\lambda}$ from 0 to 0.75 · 10^{-3}m²hr°C./kcal lowers φ by 30%.

The energy characteristics of a thermoelectrical evaporating plant are given by the approximate equation derived from formula (7) on neglecting the terms $\frac{ei}{2\alpha}$ and $\frac{ei}{2\alpha}$

$$\varphi = \frac{\varphi^1 + \frac{\lambda}{2l\alpha_0}}{1 + \frac{\lambda}{2l}\left(\frac{1}{\alpha} + \frac{1}{\alpha_0}\right)} \tag{9}$$

Here

$$\varphi^1 = \frac{eT}{\varrho l i} + \frac{1}{2} \tag{10}$$

Both calculation and experiment show the absence in evaporating plants of extremes for φ with respect to the current density i.

The circumstance bars the choice of optimum current density and hence of optimum heat capacity of the plant on the basis of only the energy characteristics.

To solve this question one must also possess data concerning the dependence of heat capacity on the current. Moreover, the technological and economic aspects of the plant have to be taken into account.

Computation showed that, *e. g.*, for $\frac{\delta}{\lambda} = 0.75 \cdot 10^{-3}$m²hr°C./kcal the optimum value of φ is $\varphi_{opt} = 5$, i_{opt} being 10 a/cm² and $\triangle T_{opt} = 10°$ C.

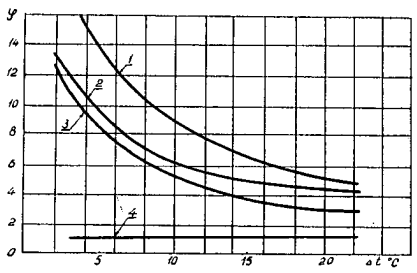

Fig. 6. Coefficient of transformation of various types of evaporating plants. 1 – mechanical, 2 – ejector, 3 – thermoelectrical, 4 – with electrical heater.

Fig. 6 shows the comparative energy characteristics of various types of evaporating apparatuses. An examination of the curves shows that in this aspect the semiconductor evaporating plant is still below compressor or ejector installations. For all values of $\triangle T$ the conversion coefficient φ of mechanical units is ca. 40% higher than for semiconductor installations. For ejector units the value of φ exceeds the semiconductor type only by 11% for $\triangle T = 5°$ C. and by 20% for $\triangle T = 15°$ C.

As compared with direct electrical heating the semiconductor evaporating unit gives considerable power economy. For example, at $\triangle T = 10°$ C. the energy consumption decreases five-fold and at $\triangle T = 7°$ C. seven-fold.

Behrndt bogtryk, Denmark

Copyright reserved

Approved For Release 2009/05/01 : CIA-RDP80T00246A007500340002-0

Approved For Release 2009/05/01 : CIA-RDP80T00246A007500340002-0

The Volumetric Efficiencies of Medium Capacity Refrigerating Compressors

Le rendement volumétrique de compresseurs frigorifiques de diverses puissances

V. F. CHAIKOVSKY, A. A. SHMIGLYA, K. I. SAVKOV,
The Odessa Technological Institute of the Food and Refrigerating Industry, Odessa, U.S.S.R.

SOMMAIRE. Le rendement volumétrique d'un compresseur frigorifique dépend de sa conception, du fluide frigorigène utilisé, du cycle de fonctionnement et de la puissance de la machine. Des recherches poussées effectuées sur divers compresseurs ont permis de déterminer certaines constantes dans la variation de la valeur du rendement volumétrique et ses éléments.

Des expériences réalisées par V.V. Lavrova (Institut de Recherches Scientifiques de l'Industrie Frigorifique d'U.R.S.S.) ont prouvé que le volume de l'espace nuisible, qui est représenté par le facteur λ_c, est de la plus haute importance dans les compresseurs à ammoniac à grande vitesse modernes, avec une vitesse de déplacement de la soupape ne dépassant pas 40 m/sec.

Des recherches expérimentales sur des compresseurs à Fréon de puissance moyenne (alé sage 100 mm et course 80 mm) ont montré qu'à 970 t mn les pertes volumétriques. incluses dans le facteur λ_l et provoquées par étranglement, chauffage et fuites, prennent la plus grande importance. Les échanges de chaleur ne doivent pas être négligés, même à de grande vitesses, où la période diminue, le fluide frigorigène est en contact avec les parois du cylindre, ce qui n'est pas le cas pour les petits cylindres où le poids du fluide frigorigène par unité de surface de la paroi est très faible. Dans les compresseurs à ammoniac refroidis par air de 100 × 100 mm et de 960 t/mn, la température au début de la compression est voisine de la température de condensation et pour des valeurs élevées de P_c, P_o est encore plus élevé.

Avec un accroissement de la vitesse de rotation du compresseur, les pertes volumétriques dues à l'étranglement de la vapeur dans les soupapes sont élevées, en particulier dans les compresseurs à Fréon. En raison du perfectionnement de la conception des soupapes de compresseurs frigorifiques et de la réduction du rôle de l'espace nuisible, l'influence de λ_l devient de plus importante.

Par exemple, dans un compresseur à Fréon de 100 × 80 mm, l'espace nuisible avec les nouvelles soupapes utilisées est de C = 1,94%. Avec la température d'évaporation $t_o = -15°$ C., la température de condensation $t_c = 30°$ C. et la température des vapeurs surchauffées $t_s = 20°$ C., on atteint les valeurs suivantes $\lambda = 0.790$, $\lambda_c = 0.930$ et $\lambda_l = 0.849$.

D'après les résultats des recherches, l'augmentation du rendement volumétrique $\lambda = \lambda_c \cdot \lambda_l$ dans les compresseurs à Fréon de puissance moyenne doit être obtenue surtout par une augmentation de λ_l.

The volumetric losses of reciprocating compressors are evaluated by the volumetric efficiency λ which may be expressed as

$$\lambda = \lambda_c \cdot \lambda_l$$

where λ_c – is the clearance volumetric efficiency;
λ_l – the factor considering the losses in the compressor due to vapour throttling in the valves, to heat exchange between the vapour and cylinder walls and to leaks.

Approved For Release 2009/05/01 : CIA-RDP80T00246A007500340002-0

Approved For Release 2009/05/01 : CIA-RDP80T00246A007500340002-0

Results of experiments on the volumetric efficiencies of two medium capacity reciprocating Freon–12 compressors are given below.

The following compressors were tested: FV–12 (100×80 mm, 980 rpm.) – a vertical, monoblock, two-cylinder, uniflow machine; FU-8 (67.5 ×150 mm, 1300 rpm.) – a V-type, four-cylinder, non-uniflow machine with two removable blocks, the angle between the cylinder centre lines being 90°.

A diagram of the experimental installation is given in Fig. 1.

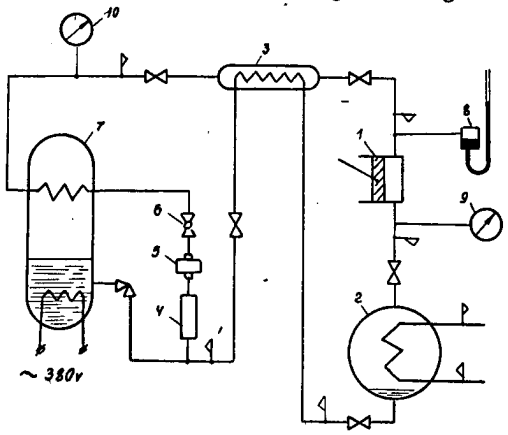

Fig. 1. Schematic diagram of the test installation. 1. Compressor; 2. Condenser; 3. Heat-exchanger; 4. Liquid strainer; 5. Peep hole; 6. Expansion valve; 7. Electric calorimeter.

The refrigerating capacity was determined by means of an electric calorimeter with a secondary medium. The tests were carried out in accordance with existing rules. Measurements were made with very precise instruments.

The FV–12 compressor was tested at a condensing temperature of $t_c = +30°$ C., evaporating temperature of $t_o = -15°$ C., a superheat of the vapour on the low side $\triangle t_s = 20°$ C. and at various values of the clearance volume (from 5.8 to 1.94%). Variations of the clearance volume were obtained by using compressor valves of various design.

Besides, tests were carried out on a FV–12 compressor, having a 1.94% clearance volume at $t_c = +35°$ C. and various evaporating temperatures.

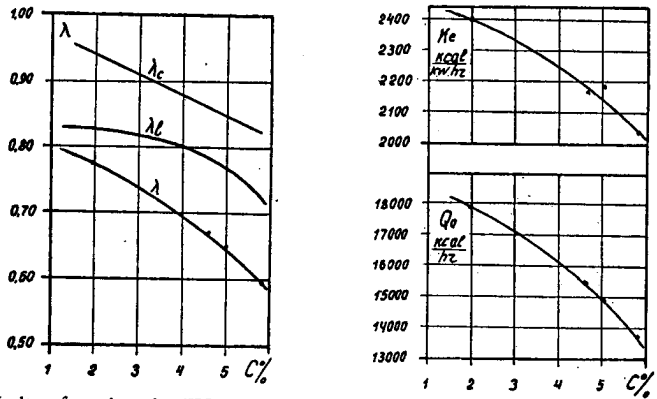

Fig. 2. Results of testing the FV–12 compressor at various values of the clearance volume C% and at $t_o = -15°$ C., $t_c = +30°$ C. and $\triangle t_s = 20°$ C.

a) Values of the volumetric coefficients.

b) The refrigerating capacity Q_o and specific refrigerating effect K_s.

Approved For Release 2009/05/01 : CIA-RDP80T00246A007500340002-0

Approved For Release 2009/05/01 : CIA-RDP80T00246A007500340002-0

The FU–8 compressor was tested at various evaporating temperatures and t_c = +50° C. The clearance volume of the compressor was equal to 4.66%.

The clearance volumetric efficiency λ_c was obtained by calculation. The exponent of the polytropic reexpansion curve m was assumed approximately equal to unity.

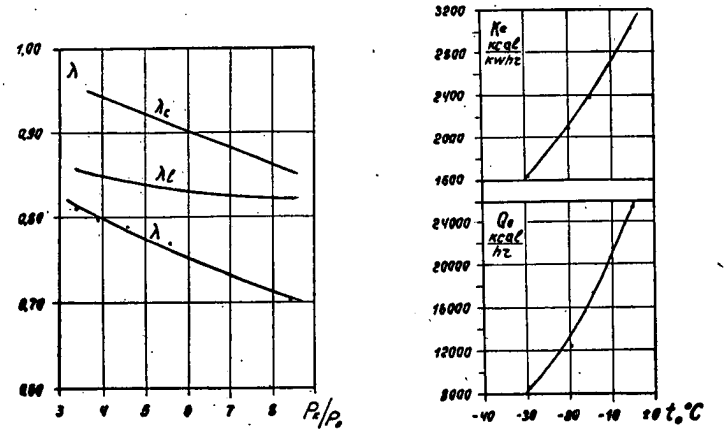

Fig. 3. Results of testing the FV–12 compressor at t_c = 35° C. and C = 1.94%.
a) Values of volumetric coefficients.
b) The refrigerating capacity Q_0 and specific refrigerating effect K_s.

As is known, at a low (up to 20° C.) superheat of the vapour sucked by the compressor the volumetric efficiency is considerably affected by the evaporation of the freon from the oil returned into the compressor, as well as by the cyclic solubility of freon in the oil deposited upon the internal surfaces of the cylinder, and also by the possible condensation of freon on the walls having a temperature below the dew point.

The superheat of the vapour on suction in the tests was not less than 20° C. The influence of the evaporation of freon from the oil on the volumetric efficiency could not be essential under these conditions. The other factors are combined in λ_1 due to the difficulties in their quantitative account.

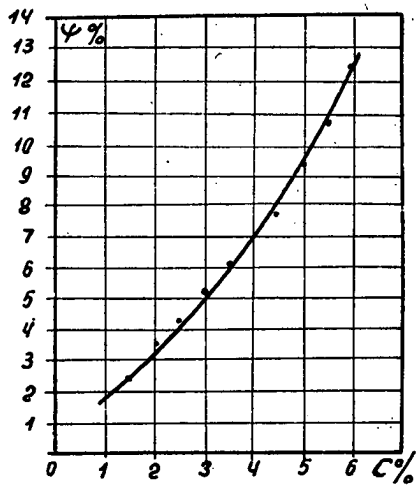

Fig. 4. The value Ψ for the FV–12 compressor at t_0 = –15° C., t_c = + 30° C. and Δt_s = 20° C.

Approved For Release 2009/05/01 : CIA-RDP80T00246A007500340002-0

Approved For Release 2009/05/01 : CIA-RDP80T00246A007500340002-0

The results of testing the FV–12 compressor are given in Figs. 2 and 3. Fig. 2 shows that with an increase of the clearance volume of the compressor, the clearance volumetric efficiency λ_c as well as λ_l are reduced. The capacity of the compressor depends largely upon the value of λ_l.

Figs. 2 and 3 illustrate that tthe values of λ_c are higher than those of λ_l. The value of the volumetric losses λ_l especially increases with the utilization of modern valves having small clearance volumes. To determine the influence of the clearance volume on the volumetric efficiency of the compressor, the change of the value Ψ (Fig. 4) has been investigated.

$$\Psi = \frac{1}{\lambda} \cdot \frac{d\lambda}{dc} \cdot 100. \quad {}^{0}/_{0}$$

The graph (Fig. 2) demonstrates that the specific (per one per cent of clearance volume) change of the volumetric efficiency depends upon the value of the clearance volume.

For example, an increase of the clearance volume from 2 to 3 % causes a decrease of the volumetric efficiency by approximately 0.04 of its value, while with the clearance volume increased from 5 to 6 % the value of λ – is lessened by nearly 0.11 of its value.

Fig. 2 shows that the values of the specific refrigerating effect K_s kcal/kw-hr reduce at an increase of the clearance volume. This is explained by the fact that at a decrease of the indicated work with a larger clearance volume, the relative value of the indicator losses of the compressor and of the friction losses is raised. An increase in the absolute value of the indicator losses is caused in this case by the irreversibility of the processes of compression and expansion of the refrigerant in the clearance volume.

During the tests the compressor was operated with group disc-plate valves with 1.94 % clearance volume the linear clearance included. The area of these valves was equal to that of 4.5 % clearance valves. The suction valve had flanges entering the apertures in the seat of the discharge valve when in the upper end point.

The linear clearance of the FV–12 compressor is 0.5 – 0.8 mm

When assuming that the FV–12 compressor has only a 0.8 mm linear clearance, the minimum value of the clearance volume would amount to 1%.

An attempt to reduce the clearance volume of the compressor from 2 to 1 % would cause an insignificant increase of the volumetric efficiency while the designing of valves with quite a small clearance volume entails great difficulties.

It should also be taken into consideration that the presence of the clearance volume has a positive influence upon the dynamic characteristics of the compressor which is especially important for high-speed machines.

All this makes it possible to conclude that no significant advantages can be achieved in medium capacity compressors by a decrease of the clearance volume below 2%.

Fig. 2 illustrates that at a small clearance volume the curves of the volumetric coefficients of the compressor as a function of the relation P_c/P_o run more steeply than in the case of large clearance volumes.

Valves with small clearance volumes are especially advantageous at large values of the pressure relation.

Results of testing the FU–8 compressor are illustrated in Fig. 5. As it was in the case of testing the FV–12 compressor, the values of λ_e are lower than of λ_c.

The present paper deals with the investigation of the clearance volumetric efficiencies of freon compressors. It is though interesting to compare the results obtained with those of testing ammonia compressors of medium capacity.

Tests of the ammonia monoblock, two-cylinder, uniflow, air-cooled compressor (80 × 80 mm, 720 and 980 rpm.) have also shown that the value of λ_l is lower than that of λ_c.

For example, at $P_c/P_o = 3.44$ and n = 980 rpm., $\lambda = 0.718$, $\lambda_c = 0.867$, and $\lambda_l = 0.828$.

At $t_o = -15°$ C, $t_c = +25°$ C. and n = 980 rpm. the volumetric efficiency

Approved For Release 2009/05/01 : CIA-RDP80T00246A007500340002-0

Approved For Release 2009/05/01 : CIA-RDP80T00246A007500340002-0

$\lambda = 0.672$, and $\lambda_w = 0.847$ – heating up coefficient, The low values of λ_l for this compressor are explained first of all by the active heat exchange inside the cylinder.

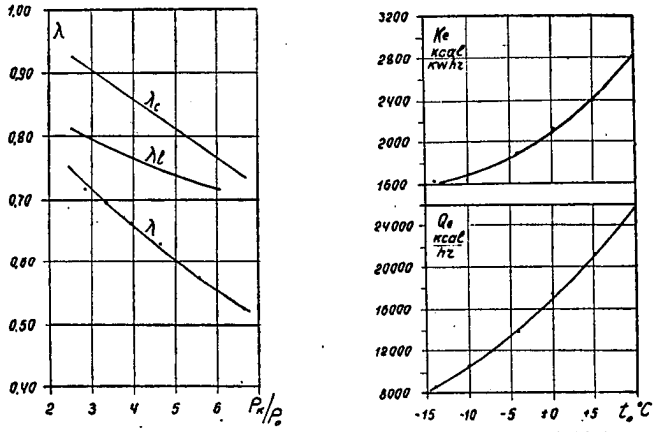

Fig. 5. Results of testing the FU–8 compressor at $t_c = 50°$ C. C = 4.66%.
a) Values of the volumetric coefficients.
b) The refrigerating capacity Q_0 and specific refrigerating effect K_s.

The availability of intensive heat exchange is proved also by the values of the cylinder wall temperatures.

Table 1 presents data on the wall temperatures measured at three points on the cylinder (n = 720 rpm.).

TABLE 1. WALL TEMPERATURES MEASURED AT 3 POINTS ON THE CYLINDER (n = 720 rpm.)

Parameters	Evaporating temperature °C. −10.0	−20.0
Temperature in the compressor suction pipe, °C.	2.0	−7.8
Temperature in the compressor discharge pipe, °C.	86.9	103.9
Mean temperature of cylinder wall:		
in upper point of cylinder, °C.	74.8	96.3
at point corresponding to half-stroke of piston, °C.	58.3	74.9
in lower point of cylinder, °C.	42.3	55.8

The temperature of the cylinder walls greatly depends upon the friction. At idle running of the compressor the temperature of the cylinder walls was by 30° C. higher than that of the surroundings.

At the same time experimental data obtained by a number of authors show that in water-cooled medium capacity ammonia compressors the volue of λ_l is higher than λ_c.

The following conclusions may be drawn from the experimental data:

1. In medium capacity air-cooled Freon and ammonia compressors the values of λ_c are higher than those of λ_l.

2. The decrease of the volumetric efficiency of medium capacity Freon compressors at an increase of the clearance volume is non-uniform. The larger the absolute value of the clearance volume, the greater its relative influence upon the volumetric efficiency.

3. In the case of medium capacity Freon machines a decrease of the clearance volume below 2 per cent is inexpedient. Such a decrease may be useful only in the case of low evaporating temperatures obtained at single stage compression.

Behrndt bogtryk, Denmark
Copyright reserved

Approved For Release 2009/05/01 : CIA-RDP80T00246A007500340002-0

Approved For Release 2009/05/01 : CIA-RDP80T00246A007500340002-0

Appareil pour la détection et la télésignalisation des fuites d'ammoniac dans les chambres frigorifiques

Device for Detection and Telesignalling af Ammonia Leaks in Cold Rooms.

V. BERCESCU, A. CIOBANU et C. MIHAILOPOL,
Institut de Recherches Alimentaires, Bucarest, Roumanie

SUMMARY. The greater use of direct expansion refrigeration requires more efficient measures to protect the products stored against damage from ammonia leaks. A device based on colour change in presence of traces of ammonia in a filter-paper strip soaked in an indicator was constructed for detecting ammonia leaks. The colour change acts on a photoelectric cell, then an electronic apparatus amplifies the variation of the photoelectric current and transmits the impulse to a visual or sound signalling device in a machine room. In automatic plants, the detector may block the automatic valve supplying ammonia from refrigerating units.

Les aliments entreposés dans les chambres frigorifiques peuvent être dépréciés en raison des fuites éventuelles d'ammoniac provenant des éléments réfrigérants, ce qui nécessite leur détection immédiate.

La littérature technique indique des appareils électroniques sensibles aux transformations de la résistance électrique de l'air qui se produit en présence des composés hallogènes (freons, chlorure de méthyle).

L'appareil que nous présentons dans cette note, a comme principe le changement de couleur d'une surface imbibée par une solution indicatrice très sensible aux modifications du pH du milieu.

Le changement de couleur agit sur une cellule photoélectrique, dont le courant est ensuite amplifié par un appareil électronique qui transmet l'impulsion à un dispositif de signalisation optique ou acoustique, placé dans la salle des machines.

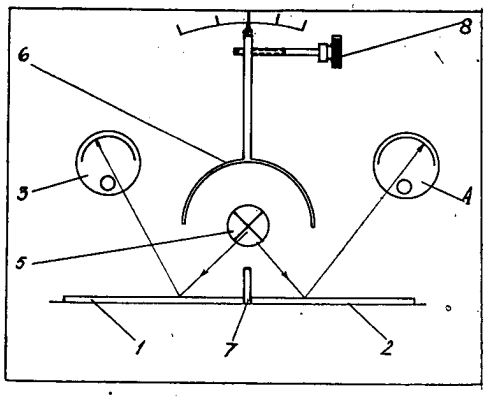

Fig. 1. Le principe du fonctionnement de l'appareil. 1. Bande de papier-filtre avec indicateur, imprégnée de chlorure de calcium $CaCl_2$. 2. Surface étalon. 3–4. Cellules photoélectriques. 5. Source de lumière. 6. Écran réflecteur. 7. Écran séparateur qui empêche l'influence des surfaces comparées sur les cellules voisines. 8. Dispositif de réglage pour la mise de l'appareil au point «zéro».

Approved For Release 2009/05/01 : CIA-RDP80T00246A007500340002-0

Approved For Release 2009/05/01 : CIA-RDP80T00246A007500340002-0

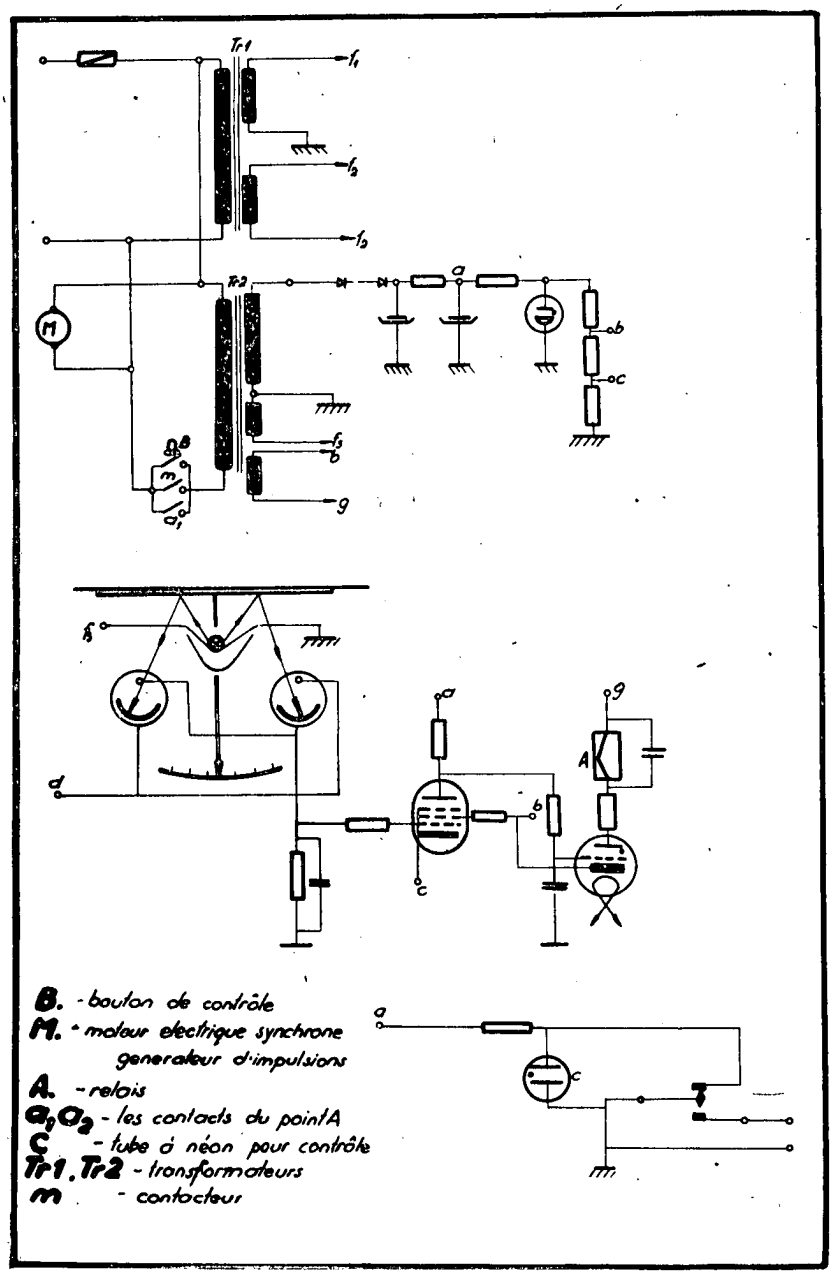

Fig. 2. Schéma électrique du principe de l'appareil.

DESCRIPTION ET FONCTIONNEMENT DE L'APPAREIL

La bande sensible 1 est en papier-filtre et est imbibée d'une solution indicatrice de bromophénol bleu ou de rouge de phénol. Ensuite, elle est imprégnée de chlorure de calcium, qui, grâce à sa propriété hygroscopique, absorbe l'humidité atmosphérique et favorise la dissolution des vapeurs d'ammoniac.

Approved For Release 2009/05/01 : CIA-RDP80T00246A007500340002-0

Approved For Release 2009/05/01 : CIA-RDP80T00246A007500340002-0

La lumière fournie par la source 5 est réfléchie par la bande sensible 1 vers la cellule photoélectrique 3, et par la surface étalon 2, vers la cellule photoélectrique 4.

Dans l'absence des traces d'ammoniac, les courants photoélectriques résultants sont égaux et de sens contraire, c'est-à-dire que leur somme est nulle. Pour mettre l'appareil au point «zéro», on emploie le bouton de réglage 8 qui, agissant sur l'écran réflecteur 6 change l'illumination des surfaces comparées, de manière que les courants résultants dans les deux cellules photoélectriques soient égaux et de sens contraire.

Lorsqu'il existe dans l'atmosphère des vapeurs d'ammoniac, la bande 1 change de couleur et détermine la modification du courant dans la cellule 3. Par suite, la résultante des courants des deux cellules photoélectriques, aura cette fois-ci une valeur déterminée, différente de zéro, par rapport à la concentration de l'ammoniac situé dans l'atmosphère.

En amplifiant le courant qui résulte, on peut actionner un relais qui transmet à distance (dans la salle des machines) les signalisations d'alarme optiques et acoustiques; dans les installations automatiques, le courant peut actionner directement les vannes automatiques qui fermeront l'accès de l'ammoniac à la chambre frigorifique.

Pour prolonger la durée de l'utilisation des cellules photoélectriques, l'appareil est pourvu d'un moteur synchrone générateur d'impulsions, qui détermine le fonctionnement périodique et à des intervalles égaux du transformateur d'alimentation de la source lumineuse 5 et des anodes.

A la réception de chaque nouvelle impulsion, la transmission d'un signal optique dans la salle des machines indique le fonctionnement de l'appareil. Le signal cesse peu de temps après s'il n'y a pas d'ammoniac dans l'atmosphère, mais il reste accouplé dans le cas contraire.

Le schéma électrique du principe de l'appareil est montré à la Fig. 2.

Les expériences ont démontré que l'appareil a une sensibilité de l'ordre de 0,0000066 vol. NH_3%.

En résumé, on peut conclure que cet appareil présente les avantages suivants:

– il empêche la dépréciation des aliments entreposés dans les chambres frigorifiques;

– il réduit les pertes d'ammoniac dans les installations frigorifiques;

– il assure un contrôle automatique permanent de l'atmosphère sous l'aspect de la sécurité du travail dans les entrepôts frigorifiques et aussi dans les autres industries qui produisent ou utilisent de l'ammoniac.

Behrndt bogtryk, Denmark

Copyright reserved

Approved For Release 2009/05/01 : CIA-RDP80T00246A007500340002-0

Approved For Release 2009/05/01 : CIA-RDP80T00246A007500340002-0

The Reason for the Invalidity of the Lewis Ratio in the Case of Air Washers

Raison de l'inapplicabilité du rapport de Lewis dans le cas des laveurs d'air

A. A. GOGOLIN
The Scientific Research Institute of the Refrigerating Industry of the U.S.S.R.
Moscow, U.S.S.R.

SOMMAIRE. Le rapport du coefficient d'échange de chaleur sèche par convection au coefficient d'échange d'humidité, connu Æsous le nom de rapport de Lewis, est très important du point de vue de la théorie de l'échange de chaleur entre l'eau et l'air sur laquelle reposent les principes du conditionnement d'air. De nombreuses recherches ont montré que dans les conditionneurs à écoulement et à pulvérisation le rapport de Lewis est très supérieur à la valeur théorique. On a exprimé à plusieurs reprises l'idée que le rapport n'est généralement pas valable pour les laveurs d'air.

Des expériences effectuées par l'A. sur divers types de laveurs d'air (à écoulement ou à pulvérisation) montrent que la valeur la plus élevée du rapport de Lewis est due à une valeur supérieure à la valeur théorique de la teneur en humidité de l'air s'écoulant à l'extérieur. Cette différence est causée par l'humidification supplémentaire des endroits arrosés seulement de façon sporadique et de la surface de petites gouttes qui se sont réchauffées à la température bulbe humide de l'air.

La preuve en est donnée dans la dépendance établie entre le rapport de Lewis et la différence de température psychrométrique à la fin de la variation théorique de l'état de l'air dans les conditionneurs à contre-courant.

L'augmentation de la dispersion des gouttes entraîne une élévation du rapport de Lewis. Cela prouve que le rôle le plus important est joué ici par l'humidité supplémentaire plutôt que par la différence entre la température superficielle des gouttelettes et la température moyenne de l'eau qui est plus importante pour une vaporisation de plus grosses gouttelettes.

Le rapport de Lewis est spécialement élevé pour de faibles coefficients de condensation d'humidité $\left(\xi = \frac{Q\ totale}{Q\ sèche}\right)$ *pour lesquels le coefficient d'échange d'humidité total diminue en raison de l'existance de deux phénomènes inverses: la déshydratation et l'humidification de l'air. Pour les coefficients de condensation élevés* (ξ = *1,5 – 2) le rapport de Lewis prend la valeur théorique.*

The ratio of the coefficient of convective heat exchange α kcal/m²hr°C. to the moisture exchange coefficient b kg/m²hr, known as the Lewis ratio, is highly important for the theory of joint heat and moisture exchange which is the basis of the entire system of air conditioning calculations.

Lewis [1] obtained in 1922 the following equation based upon theoretical premises:

$$\frac{\alpha}{b} = C_p' \text{ kcal/kg°C}$$

where: C'_p – is the specific heat of moist air at constant pressure.

Merkel [2] developed a theory of calculating joint heat and moisture exchange on the basis of the Lewis equation and was the first to check experimentally this equation in a small stream cooling tower. However, the ratio of $\frac{\alpha}{b}$ obtained in these experiments amounted to 0.3 ÷ 1 which considerably exceeded the ordinary

Approved For Release 2009/05/01 : CIA-RDP80T00246A007500340002-0

Approved For Release 2009/05/01 : CIA-RDP80T00246A007500340002-0

value of $C'_p = 0.24 \div 0.25$ kcal/kg°C. This divergence is explained by the fact that the wetted surface in the apparatus used by Merkel in his experiments consisted of metal Raschig rings. Due to the high thermal conductivity of the metal convective, heat exchange took place also on the unwetted part of the rings, *i. e.* on an area exceeding the area of moisture exchange. This caused higher sensible heat exchange as compared with moisture exchange, and enlarged values of the ratio. $\frac{\alpha}{b}$

However, this ratio $\frac{\alpha}{b}$ considerably exceeded its theoretical value also in the subsequent experiments [3, 6] carried out with both spray and stream air coolers with a packing of a low thermal conductivity.

Thus an opinion arose that the Lewis equation was not valid in air washers on account of the absence of analogy between the heat and mass-exchange due to the additional heat flow at the diffusion of water vapour, thermal diffusion etc.

The influence of all these factors makes the Lewis equation approximate. Its validity must be checked by experiments carried out on real size apparatus with the hydraulic and climatic operating conditions of the experimental unit varied in a wide range. Such experiments were run some time ago by the author at the Scientific Research Institute of the Refrigerating Industry of the U.S.S.R. Tests [3] were carried out on various stream and spray type vertical air flow counter current air coolers packed with porcelain Rashig rings. A conventional spray type horizontal air flow air washer with several rows of spray nozzles was also investigated [4]. All the tested air coolers were quite large with an air flow area from 1.7 to 2.4 m².

The counter flow air washers were tested on air cooling and dehumidityfying. In the conventional type spray air washer experiments were carried out under the operation conditions characteristic of cooling, dehumidification, humidification or heating of air.

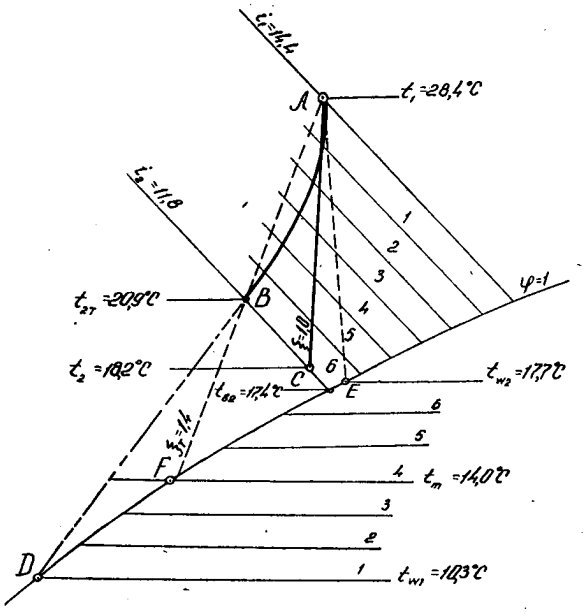

Fig 1. The change of the state of the air in a counter current air washer with Rashig ring packing. t_{w1}, t_{w2} and t_m – water temperature initial, final and mean values, °C; t_1 and t_2 – initial and final temperatures of air, °C; i_1 and i_2 – initial and final enthalpy of air, kcal/kg; t_{h2} – final wet-bulb temperature of air, °C.

Approved For Release 2009/05/01 : CIA-RDP80T00246A007500340002-0

Approved For Release 2009/05/01 : CIA-RDP80T00246A007500340002-0

On analysing the results of the tests it was noticed that an increased value of the ratio $\frac{\alpha}{b}$ was observed in air cooling and dehumidifying tests in the case of the state of the escaping air considerably deviating towards a higher specific humidity. An illustration of such a deviation is given in Fig. 1. Fig. 1 also shows the stepped plotting of the theoretical process of the air state variation which may be made for a counter current air-cooler considering the Lewis equation true.

With such a process the point corresponding to the state of the leaving air in counter current air coolers is approximately on the straight line connecting on the enthalpy – specific humidity diagram point A of the initial state of the air with point F on the saturation line. In this case the temperature at point F is equal to the mean temperature of the water t_m.

The deviation of the process from the line AF observed in the experiments was explained by two reasons. It was supposed [5] that this deviation resulted from the difference between the temperature at the surface of the droplets and the mean temperature of the water after leaving the air washer. There certainly is such a temperature difference but it cannot be the sole cause of all phenomena observed during the experiments, which is discussed below.

According to another explanation given by the author, the reason for the deviation observed is in the fact that there ordinarily are two different moisture exchange processes in air washers: dehumidification of the air on the main surface of the water and its humidification on the part of surface heated by the air flow to the wet-bulb temperature.

In stream air washers provided with Rashig rings humidification occurs on a part of the surface of the rings only sporadically wetted by water splashes. The thin water film wetting this surface is quickly heated up to the wet-bulb temperature and, while evaporating, it humidifies the air. The droplets precipitating on the surface of the moisture eliminator act in an analogous manner.

In spray air washers the air is humidified on the surface of fine droplets heated to the wet-bulb temperature, and on the wetted surface of the eliminators.

The humidifying surface is usually located at the end of the air passage (the upper surface of the wetted Rashig rings, minor droplets carried by the air flow to the end of the apparatus, eliminators).

Therefore, the process of treating air in an air washer may be conventionally divided into two: air cooling and dehumidification (line A–B, Fig. 1) and air humidification running approximately along the isoenthalpic line (B–C). Certainly, this division is somewhat schematic and on a certain part of the surface both processes go on practically simultaneously. If such an assumption is true the degree of deviation of the state of the escaping air towards a higher specific humidity and the corresponding increase in the value of the ratio $\frac{\alpha}{b}$ should depend upon the psychrometric temperature difference at the end of the first process (point B in Fig. 1) which determines the intensity of the subsequent humidification process. Such a dependence was obtained on the basis of the results of the experiments with counter current spray type air coolers (Fig. 2). At minor psychrometric temperature difference the ratio $\frac{\alpha}{b}$ approaches the theoretical value ($\sim$ 0.245) while at greater temperature differences it increases up to 0.35–0.4.

An analogous dependence was obtained also for air coolers with the Rashig rings.

The curves in Fig. 2 show that the ratio $\frac{\alpha}{b}$ increases with a rise of the pressure, *i. e.* at a finer dispersion of the water.

This is also a proof of the fact that the deviation of the state of the air towards an increase in the specific humidity is resulted by its humidification which is higher at a finer dispersion of the water. The influence of the difference between the surface temperature of the droplets and their mean temperature is, apparently,

Approved For Release 2009/05/01 : CIA-RDP80T00246A007500340002-0

Approved For Release 2009/05/01 : CIA-RDP80T00246A007500340002-0

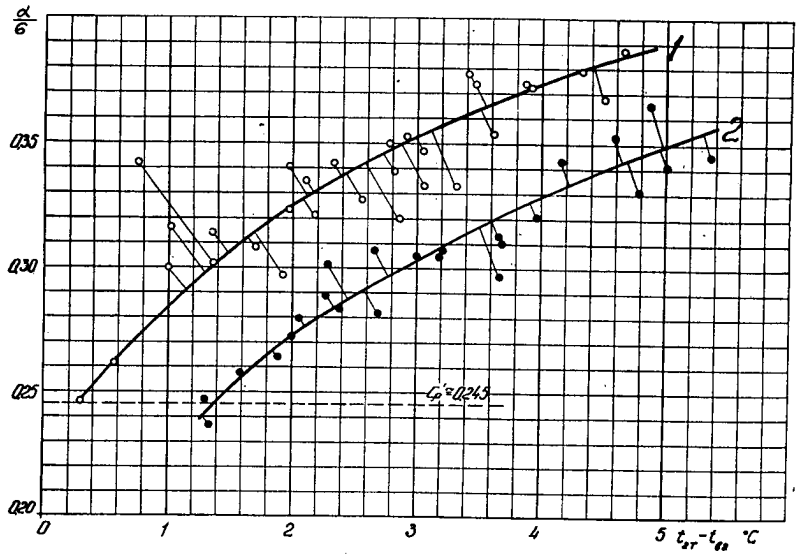

Fig. 2. The dependence of the Lewis ratio upon the psychrometric temperature difference at the end of the theoretical process for counter current spray type air washers. Water pressure before nozzles: 1–1.2–1.8 atm; 2–0.3–0.6 atm.

insignificant. Otherwise, the finer the spray, the lower would be the value of $\frac{\alpha}{b}$ which is not the case. Besides, the ratio should in this case depend upon the cha of the water temperature, but attempts to detect such a dependence were a failure. It is interesting that the coefficient of moisture exchange, calculated on base of the mean logarithmic difference of enthalpy, does not depend upon the climatic conditions. What concerns the heat exchange coefficient is that it increases with the growth of the ratio $\frac{\alpha}{b}$ as there is in this case an additional convective heat exchange occuring without any change of the enthalpy of the air (line *B–C,* Fig. 1). The relation of $\frac{d}{\delta}$ and the moisture condensation coefficient ξ (total-sensible heat ratio) was also determined in the experiments.

The ratio $\frac{\alpha}{b}$ is at its largest value at small moisture condensation coefficients when the humidification process is more intensive owing to higher temperatures of the water.

Vice versa, with moisture condensation coefficients amounting to ca. 2, when the process of the change in the state of air approaches the line $\varphi = 1$ at a very small angle, the ratio is close to its theoretical value of 0.24–0.25. A corresponding dependence for a conventional spray type horizontal air flow air washer is given in Fig. 3 which illustrates the value of $\frac{\alpha}{b}$ not only for cooling and humidification ($\xi > 1$) but also for cooling and humidification of air ($0 < \xi < 1$), as well as equilibrium humidification along the constant wet-bulb temperature line ($\xi \cong 0$) and results of several experiments at heating and humidifying air.

Given in Fig. 3 are also results of experiments carried out at the Scientific Research Institute of Water Supply and Heating Installations (NIIST) of the Academy of Architecture by E. E. Karpis and M. L. Zusmanowich at $\xi = 2.2 \div 3$. It is seen from Fig. 3 that $\xi = 0$ and $\xi = 2 \div 3$ the ratio $\frac{\alpha}{b}$ coincides almost ex-

Approved For Release 2009/05/01 : CIA-RDP80T00246A007500340002-0

Approved For Release 2009/05/01 : CIA-RDP80T00246A007500340002-0

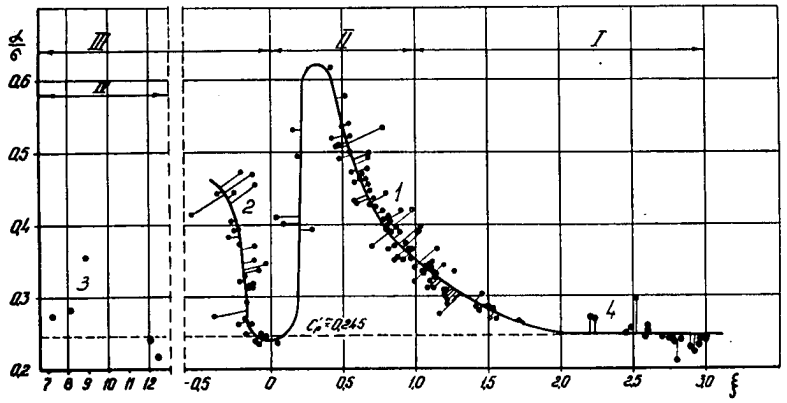

Fig. 3. The dependence of the Lewis ratio upon the moisture condensation coefficient in conventional spray type air washers. I. Cooling and dehumidification of air. II. Cooling and humidification of air. III. Increase of enthalpy of air and its humidification. IV. Increase of air temperature and its humidification. 1– experiments by the author on cooling air; 2 – experiments by the author on humidifying air; 3 – experiments by the author on heating and humidifying air; 4 – experiments by Karpis and Zusmanovich (NIIST).

actly with the theoretical value cited by Lewis. Close to the theoretical value is $\frac{\alpha}{b}$ also in the process of heating and humidification of the air.

Characteristic of all these ranges is the absence of duality of the moisture exchange processes. At equilibrium humidification of air (ξ 0) the temperature of the water temperature cannot change the incline of the line of the air process air flow. The process represented in the enthalpy-specific humidity diagram by the line of constant wet bulb temperature goes on in all points of the water surface.

In the case of cooling and dehumidification the air at high coefficients of moisture condensation ($\xi = 2 \div 3$) as well as at heating and humidification, the temperature of the water is certainly not constant.

However, as the line of the change in state of the air in the enthalpy-specific humidity diagram approaches the saturation line at a very small angle, a variation of the wter temperature can not change the incline of the line of the air process in the apparatus. Therefore, the surface of the water may conditionally be assumed as 'isothermal' in the sense of its temperature not exerting any influence upon the direction of the air state variation. Thus we may consider the validity of the Lewis equation in air washers proved in cases when a certain moisture exchange process takes place throughout the entire water surface.

The process with high coefficients of moisture condensation is typical in the air conditioning of mines.

Hewever, most of the air washers operate with joint dehumidification and humidification of the air in which case the Lewis equation is not valid. Hence these air washers should be calculated on the basis of empirical coefficients directly giving the final state of the air and the direction of its change.

The above analysis of the validity of the Lewis equation in the case of air washers is highly important for the theory of their calculation.

With high moisture condensation coefficients the flow of condensed moisture coincides with the direction of the heat flow and has the highest value practically met with in air coolers. At $\xi = 0$ the direction of the flow of evaporating moisture is opposite to the direction of the heat flow.

The validity of the Lewis equation for both above processes proves the presence of analogy between heat and moisture exchange at various directions of the heat and moisture flows for comparatively small temperature drops and specific humidity variations usual in air coolers. It is obvious that the influence of various

Approved For Release 2009/05/01 : CIA-RDP80T00246A007500340002-0

Approved For Release 2009/05/01 : CIA-RDP80T00246A007500340002-0

supplementary heat and moisture exchange processes distorting the Lewis equation in air coolers is comparatively low. This conclusion coincides with the theoretical analysis of this problem made by Prof. Berman [7].

All above considerations make it possible to conclude that the Lewis equation is valid for cooling and dehumidifying air by means of finned surfaces in which case there are no possibilities for additional humidification.

REFERENCES

1. LEWIS, W. K. The Evaporation of a Liquid into a Gas. *Mech. Eng.*, **44**, 445, 1922.

2. MERKEL, F. Verdunstungskühlung. *Vorschungsheft VDI* No. 275, Berlin, 1925.

3. GOGOLIN, A. A. and RUDOMETKIN, F. I. Heat Transfer in Air Washers for Air Conditioning. Cellection of Works of the Mechanical Section of VNIKhI, Pishchepromizdat, 1940.

4. GOGOLIN, A. A. The Calculation of Spray Type Air Conditioners. *Kholodilnaya Tekhnika,* (4), 1957.

5. KURILEV, E. S. Some Specific Features in the Process of Heat Exchange Between Droplets and Air in Spray Type Air Conditioners. Works of the Leningrad Technological Institute of the Refrigerating Industry, Vol. IV, Pishchepromizdat, 1953.

6. KARPIS, E. E. and ZUSMANOVICH, L. M. The Investigation of Air Cooling and Dehumidification in Spray Type Air Conditioners. Report of NIIST, Academy of Architecture, Moscow, 1957.

7. BERMAN, L. D. On the Analogy Between Heat- and Mass-exchange. *Teploenergetica,* (8), 1955.

Behrndt bogtryk, Denmark

Copyright reserved

Approved For Release 2009/05/01 : CIA-RDP80T00246A007500340002-0

Approved For Release 2009/05/01 : CIA-RDP80T00246A007500340002-0

Natural Convection in Air with Temperature Differences

Convection náturelle de l'air avec faibles différences de température.

K. BRODOWICZ, Dr. Eng.
Technical University in Warsaw
Nowowiejska 25, Warsaw, Poland

SOMMAIRE. La répartition de la température était effectuée autour de tuyau horizontal et à proximité de la surface de la plaque verticale. La différence de températures entre les surfaces du tuyau et de la plaque et celle de l'air était connue et le coefficient de transmission de chaleur était déterminé.

L'expérience a été réalisée pour une différence de températures de 0,5° C. Le coefficient de transmission de chaleur par convection naturelle diminue en fonction de la différence de températures. Il existe quelques équations empiriques pour le calcul de la transmission de chaleur pour une très faible valeur de Gr Pr (telle que $10^{-2} - 10^{-4}$), mais on ne peut pas les établir pour la convection de Gr Pr (telle que et elles n'ont si pas la même signification qu'une faible différence de températures.

L'expérience a été effectuée par l'A. pour confronter les résultats du calcul de la transmission de chaleur et les formules établies par d'autres auteurs. Les courbes ont été établies d'après les calculs effectuées á partir des formules. La conclusion est qu'elles sont voisines l'une de l'autre. L'A. a adopté l'interféromètre Mach-Zhenders pour mesurer la répartition de températures à proximité des surfaces.

NOMENCLATURE

The following nomenclature is used in this paper:

q	– heat stream, kcal/m²h	h	– distance from origin plate, mm
α	– heat transfer coefficient, kcal/m² °C h	Ψ	– angle from vertical
		λ	– thermal conductivity kcal/m °C. h
Δt	– difference of temperature, °C. Δt x = tx-tf, Δt = tw-tf	Nu	– Nusselt number
		Gr	– Grashof number
tf	– temperature of surface, °C.	C,n	– constant
tw	– temperature of ambient, °C.	Pr	– Prandtl number
x	– distance from surface, mm		

This paper considers a free convection in air for the horizontal pipe and vertical plate with the little difference in temperature.

Determination of heat transfer coefficient "α" with a little difference in temperature is very important when the instable heat transfer is considered.

The heat transfer gets smaller when the difference of temperature between the ambient space and the surfaces gets smaller too. It is clear that heat stream changes according to the formula:

$$q = \alpha \Delta t$$

in which α changes with change of Δt. The coefficient diminishes when the difference of the density of the ambient air gets smaller until Δt reaches zero, and in that case there is no convection at all. To determine the value of α for a little Δt °C. we can use Pohlhausen's theoretical formula

$$\alpha = c \sqrt[4]{Gr}$$

Approved For Release 2009/05/01 : CIA-RDP80T00246A007500340002-0

Approved For Release 2009/05/01 : CIA-RDP80T00246A007500340002-0

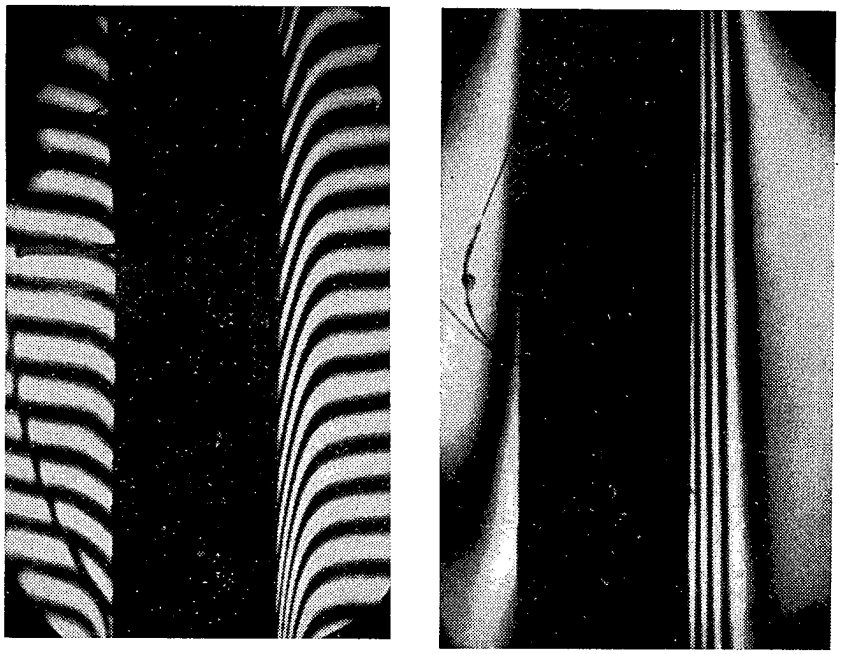

Fig. 1. a) Illustration of parallel fringes produced by difraction by the free convection in air on the vertical plate. b) Isotherm for the free convection in air on the vertical plate.

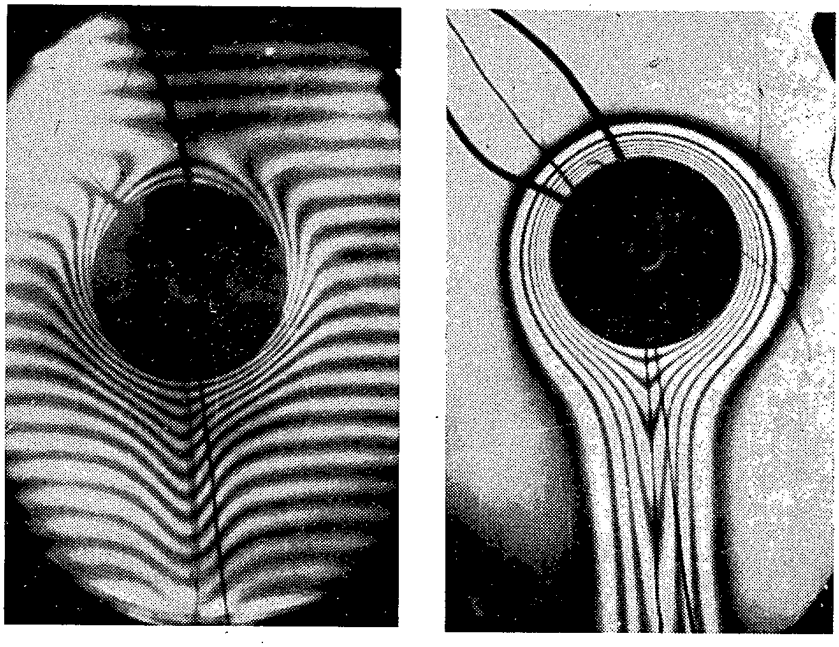

Fig. 2. a) Illustration of parallel fringes produced by difraction by the free convection in air on the horizontal pipe. b) Isotherm for the free convection in air on the horizontal pipe.

Approved For Release 2009/05/01 : CIA-RDP80T00246A007500340002-0

Approved For Release 2009/05/01 : CIA-RDP80T00246A007500340002-0

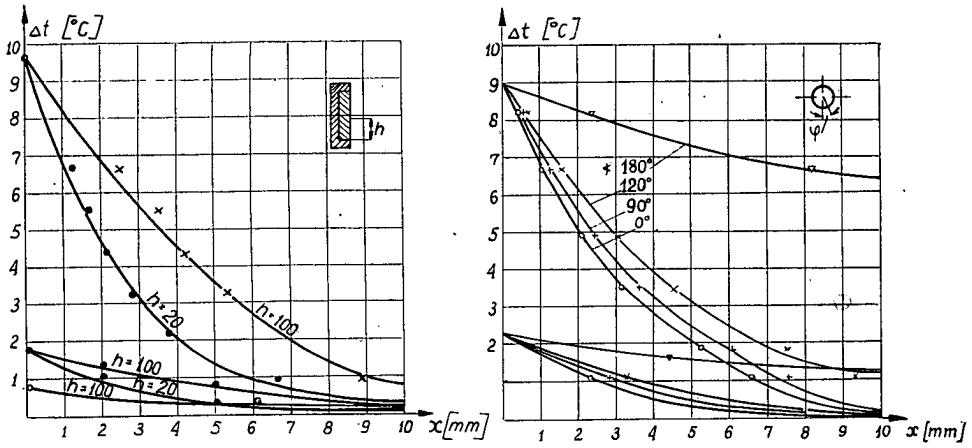

Fig. 3. Average temperature difference as a function of the distance from the surface of the plate, a. and pipe b.

or empirical formula

$$Nu = c(Gr\,Pr)^n$$

C and n are determined by experiments for large Δt °C. For a little Δt °C. c and n should be checked by experiment, this is the main subject of this paper.

Experimental method.

The visual method by using Mach-Zehnder's interferometer was adopted and

$$\left(\frac{\delta t}{\delta x}\right) x = o$$

was determined, and α was calculated from theformula:

$$\alpha \Delta t = \lambda \left(\frac{\delta t}{\delta x}\right) x = o$$

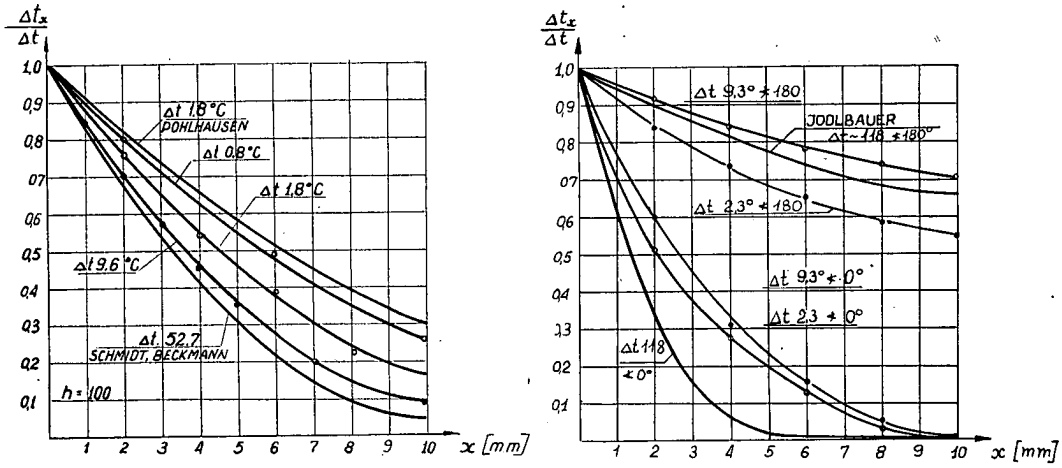

Fig. 4. Average relation $\frac{\Delta tx}{\Delta t}$ as a function of the distance from surface of plate, a. and angle from vertical of pipe b.

Approved For Release 2009/05/01 : CIA-RDP80T00246A007500340002-0

Approved For Release 2009/05/01 : CIA-RDP80T00246A007500340002-0

t was obtained by measuring. The method also allows determination of the temperature for each point in the boundary layer, which is very important, because we can compare the temperature curves with other experiments.

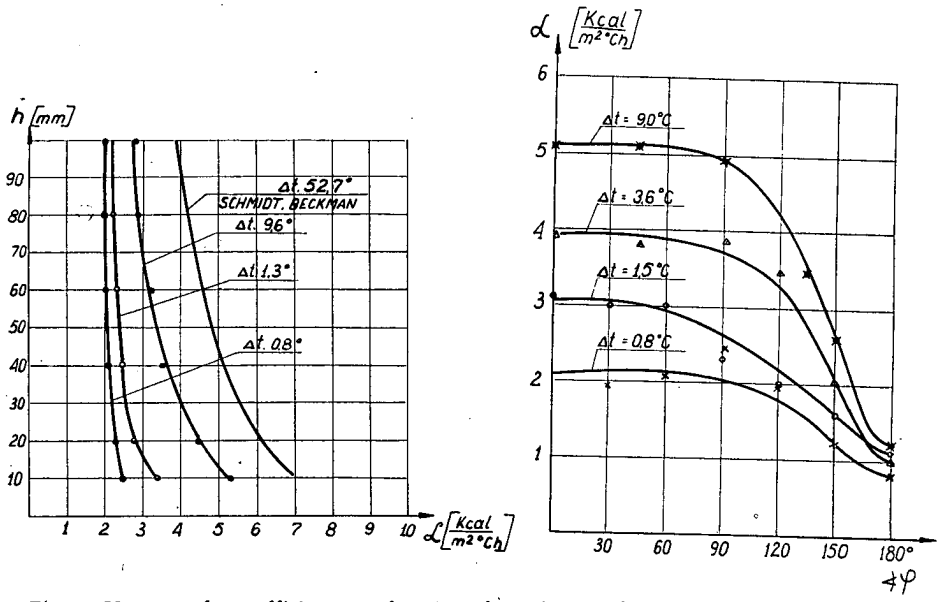

Fig. 5. Heat transfer coefficient as a function of the distance from origin of plate, a. and angle from vertical of pipe b.

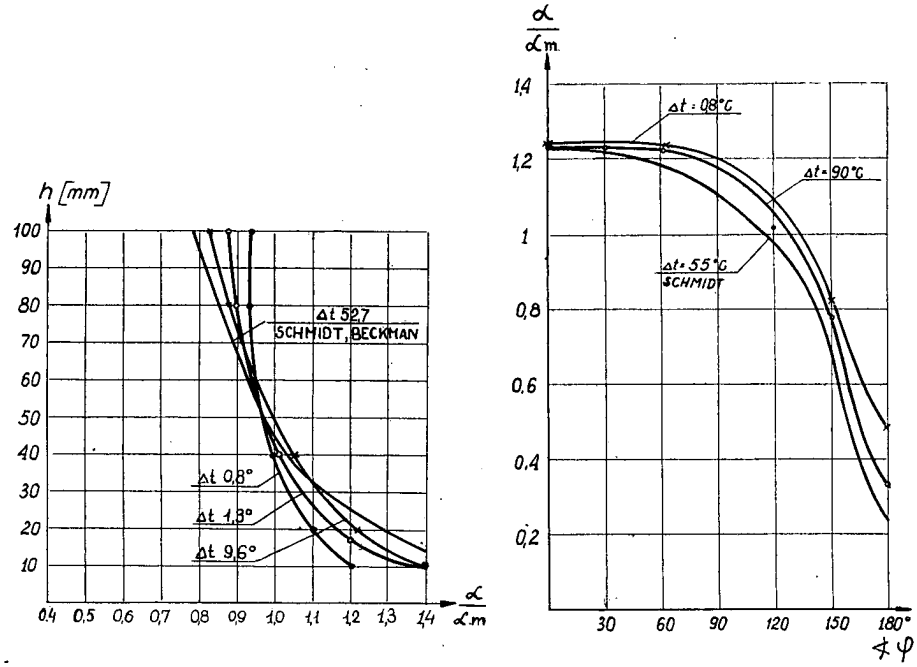

Fig. 6. Relation $\frac{a}{am}$ as a function of the distance from the origin of plate, a. and angle from the vertical of pipe b.

Approved For Release 2009/05/01 : CIA-RDP80T00246A007500340002-0

Approved For Release 2009/05/01 : CIA-RDP80T00246A007500340002-0

The experiments described in this paper were made with a copper plate which was partly insulated, only one vertical face 110 mm × 200 mm was uncoverd. The next experiments were made with copperpipe $\phi = 29$ mm and $\phi = 5$ mm 300 mm long. The pipe was placed in a horizontal position for the experiments, plate and pipe were electrically heated, and for stable thermic conditions, photographs were made. To obtain conditions $\Delta t < 0$, plate and pipe were cooled by means of ether.

The temperature difference was measured by thermocouple Cu-Konst with the use of compensation according to Lindeck's sheme.

The range of Δt °C. for the plate was –2.7° C. to +9.8° C. and the minimum was 0.8° C. and for the pipe it was –3.7 to +10 and the minimum was 0.6° C.

EXPERIMENTAL RESULTS

The results of the experiments are shown in the diagramme by the following curves: Fig. 3 – Fig. 7. We can see that the temperature curves do not change very much but when Δt diminishes, the boundary layer gets thicker, this agrees with the results obtained by calculation according to Pohlhausen's theoretical formula.

Fig. 5 a. and b. represent the change of α along the plate and around the pipe.

Fig. 6 a. and b. represent the values $\frac{\alpha}{\alpha\lambda}$ against λ or Ψ. If we compare this with the results obtained by Schmidt and Beckmann or Jodlbauer we can see that when Δt diminishes the values become more evenly distributed along the plate as well as aroud the pipe.

Fig. 7 a. and b. give average values of α against Δt°C. In addition the curves

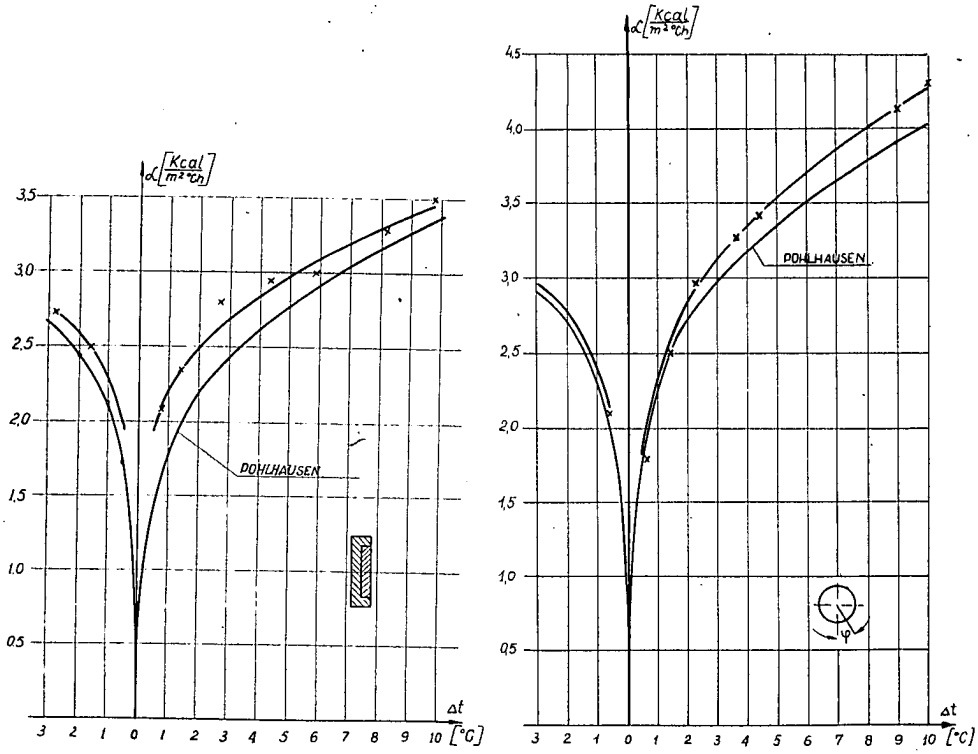

Fig. 7. Average middle heat transfer coefficient of the free convection on the vertical plate, a. and horizontal pipe, b. – as a function of the difference of temperature.

Approved For Release 2009/05/01 : CIA-RDP80T00246A007500340002-0

Approved For Release 2009/05/01 : CIA-RDP80T00246A007500340002-0

obtained by theoretical computation were drawn on the same figures; we can see that the curves obtained by experiments are higher than the theoretically calculated values.

REFERENCES

1. KRAUS, W. Messungen des Temperatur und Geschwindigkeitsfeldes bei freier konvection. Verlag G. Braun, Karlsruche, 1955.

2. SCHMIDT, E. S. Schlierenaufnahmen des Temperaturfeldes in der Nähe wärmeabgebender körper. *Forsch Ing. Wes.*, **3**, 181, 1932.

3. NUSSELT, W. Das Grungesetz des Wärmeüberganges. *Gesunh. – Ing.*, **38**, S. 477–82, 490–96, 1915.

4. JODLBAUER, K. – Das Temperatur – und Geschwindigkeitsfeld um ein geheiztes Rohr bei frier Konvektion. *Forsch. Ing. Wes.*, **4**, 157–72, 1933.

Behrndt bogtryk, Denmark

Copyright reserved

Approved For Release 2009/05/01 : CIA-RDP80T00246A007500340002-0

Approved For Release 2009/05/01 : CIA-RDP80T00246A007500340002-0

Low Temperature Expansion Turbines

Turbines à expansion à basses températures

V. I. EPIFANOVA
The U.S.S.R. Scientific Research Institute of Oxygen Machine-Building, Moscow, U.S.S.R.

SOMMAIRE. Le développement des grandes installations pour la production d'oxygène gazeux est inséparablement lié à la construction d'une turbine à expansion sûre et simple travaillant à basses températures. Une turbine à expansion réactive du type centripète dont le rendement adiabatique était de 80% fut développée en 1939 sous la direction de l'académicien P. L. Kapitza. La différence principale entre ce nouveau type de turbine à expansion et la turbine à expansion de Linde du type actif est quoique la grille de l'"impeller" du premier est du type "confusor", que l'expansion du gaz a lieu dans l'"impeller" grâce au gradient de pression considerable crée par l'action des forces centrifuges dans le "long blade impeller". Des expériences ont montré que les exigences principales pour atteindre un haut coefficient de performance consistent en la "confusional mode" du courant de gaz dans l'"impeller", les vitesses basses absolues du gaz quittant l'"impeller", l'usage correcte du gradient de pression formé par l'action des forces centrifuges et la création de conditions pour lesquelles la vitesse du courant du gaz venant des "guide vanes" ne dépasse pas la valeur critique d'une façon importante. Des projets pour des turbines à expansion réactives à basses températures ont été faites pour des capacités de 500 à 20.000 Nm^3/hr d'air. Le rendement adiabatique de grandes machines peut aller jusqu'à 82–83%. Les résultats des recherches démontrent la possibilité d'augmenter encore le rendement. Les turbines sont à un étage, avec soit un "impeller" bilatéral monté sur un axe flexible amorti, soit un "impeller" unilatéral cantilever monté sur un axe rigide. Plusieurs projets de turbines à expansion sont discutés dans cette communication et des recommandations sont données en ce qui concerne les relations et paramètres optimaux.

The last decade has been characterized by the extensive application of gaseous oxygen and other products of air separation in different fields of industry in many countries. This trend is accompanied, of course, by the development of new equipment for large-scale low temperature air-separation plants.

Big modern air-separation plants for obtaining gaseous products operate on low-pressure air refrigeration cycles using compressors and expansion engines of the rotary type. Work on low-pressure air-separation installations was started in the U.S.S.R. under P. L. Kapitza on the basis of his new expansion turbine. The high isentropic efficiency peculiar to this new expansion engine which, in the low-pressure air-separation installation, is the only source for refrigeration, ensured the development of large-scale oxygen production in big and economical air-separation plants. Installations producing up to 15,000 nm^3 oxygen per hour per unit, working continuously for two years, are being successfully run in the U.S.S.R. They have low temperature inward radial flow reaction turbines developed on the basis of that proposed by P. L. Kapitza. At present expansion turbines of this type have been developed in various countries. J. Wucherer pointed out in a communication at the Congress that such expansion turbines are reliable in operation and notable for their high efficiency.

The experience acquired in designing, investigating and operating expansion turbines at low temperatures enables us to put forward a contribution on this subject. We hope that discussion on the design and construction of expansion turbines will be of great use and favour their further development.

Approved For Release 2009/05/01 : CIA-RDP80T00246A007500340002-0

Approved For Release 2009/05/01 : CIA-RDP80T00246A007500340002-0

Unlike the turboexpanders of the impulse type developed formerly by the Linde Company, in the inward radial flow reaction turbine the air is expanded not only in the stationary nozzles but also in the channels of the wheel at a constant or accelerated channel velocity. This is achieved by using wheels with "long blades", *i. e.* with a small ratio of exit to entrance diameter of the wheel $\frac{d_2}{d_1}$, which creates a substantial pressure gradient due to the effect of the centrifugal forces. Under the operating conditions of the low-temperature expansion turbine designed in air-separation units for a comparatively small enthalpy drop (about 25 kcal/mole), such a construction made it possible to lower considerably the energy losses due to the flowing of the gas stream across the turbine. Thus it was possible to keep the gas discharge velocity from the stationary nozzles about the sonic and to employ simple nozzles. Accordingly the energy losses in the nozzles and in the radial clearance between the nozzle box and the wheel were reduced. Thanks to the small diameter ratio $\frac{d_2}{d_1}$ the change in the direction of the gas stream is smooth and not very large. This, together with the small relative velocities of the gas stream at the inlet and in the course of its usually accelerated passage along the channels of the wheel, led to a reduction of losses across the wheel. The gas stream leaves the blades at a comparatively small velocity due to the small ratio of $\frac{d_2}{d_1}$; this consequently cuts down the losses dependent on the exit velocity. These are the principal features which made it possible to obtain the high isentropic efficiency peculiar to the inward radial flow reaction expansion turbines. However, as compared with the impulse turbines, the losses due to the disk friction and flowing of the gas past the blades are considerably higher in reaction turbines where the pressure drop across the wheel is substantial and the gas in the space between the wheel and the casing has a higher pressure.

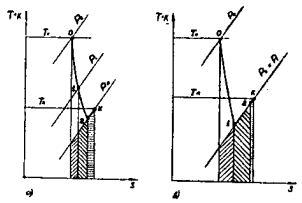

Fig. 1. T-S diagram of the gas expansion process. a) reaction expansion turbine. b) impulse turbine. Refrigerative losses: I. in the stationary nozzles, II. across the wheel and the discharge velocity, III. due to leakage through the inner labyrinth glands.

Fig. 1 shows the T-S diagram of the process for the reaction expansion turbine and impulse turbine; the main refrigerative losses are indicated respectively. Refrigerative losses are energy losses determined at the terminal expansion pressure by the product of the entropy increase and corresponding mean temperature. The different states of the gas are indicated as follows: 0 – the initial state, 1 – before the wheel, 2 – behind the wheel, K – the terminal state taking into account the changes in the state of the gas caused by contact with the part of the gas which had passed through the inner labyrinth glands.

If the design and construction ratios are selected properly the total refrigerative losses are considerably smaller in the inward radial flow reaction turbines than in impulse turbines.

Low-temperature expansion turbines are being operated in the U.S.S.R. handling from 500 to 20,000 nm^3 air per hour. The isentropic efficiency at liquefying temperatures is 82–83%. J. Wucherer reported even higher efficiencies. It should be mentioned, however, that in evaluating the efficiency of expansion turbines

Approved For Release 2009/05/01 : CIA-RDP80T00246A007500340002-0

Approved For Release 2009/05/01 : CIA-RDP80T00246A007500340002-0

which operate at a discharge gas temperature close to boiling point and at small enthalpy drop, the accuracy in determining the efficiency depends on the state diagrams used and even on the method of calculating the enthalpy by means of these diagrams. The calculation of efficiency is also affected by the method of determining the experimental data, *i. e.* the pressure and, particularly, temperature of the gas which changes considerably in time due to the switching over of the regenerators.

As a result of investigations and experience in running expansion turbines the following optimal design data for low-temperature single-stage expansion turbines have been found:

Exit to entrance diameter ratio	$\frac{d_2}{d_1} = 0.38 \div 0.45$
Dimensionless wheel inlet width	$\frac{b_1}{d_1} = 0.025 \div 0.03$
Ratio of the peripheral wheel speed to the theoretical spouting velocity which corresponds to the total isentropic enthalpy drop	$\frac{U_1}{C_0} = 0.62 - 0.67$
Reaction, i. e. the relation of the isentropic enthalpy drop across the wheel to the total enthalpy drop	$\varrho = 0.35 \div 0.42$

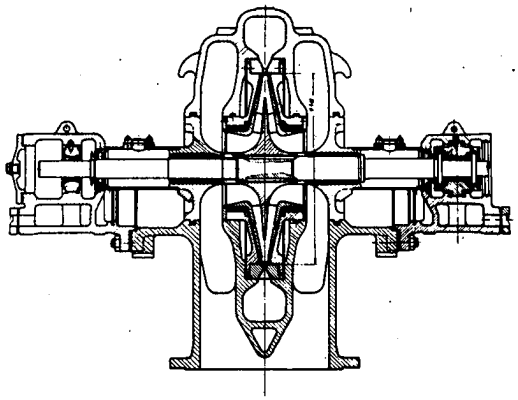

Fig. 2. Inward radial flow reaction turbine with a two-exits-wheel.

In Fig. 2 and 3 two types of reaction expansion turbines for air-separation units are shown. These turbines are single-stage, quite reliable engines, simple in design. These two types differ in the design of their wheels. Figure 2 shows an expansion turbine which has a wheel with two exits on a flexible shaft. Fig. 3 shows one which has a cantilever wheel with one exit on a rigid shaft. In the first case it is possible to design wheels of smaller diameter and consequently slightly lower the losses due to disk friction and leakage of gas through the labyrinth glands, as well as to obtain a more favourable dimensionless wheel inlet width and have the rotor free from the influence of axial forces. However, in this case the employment of an elastic damping device is required. As experience in running air-separation units has shown, in expansion turbines on a flexible shaft without a special elastic bearing the dynamic steadiness of the rotor is not ensured in cases of disturbances when the liquid air might get into the turbine.

Approved For Release 2009/05/01 : CIA-RDP80T00246A007500340002-0

Approved For Release 2009/05/01 : CIA-RDP80T00246A007500340002-0

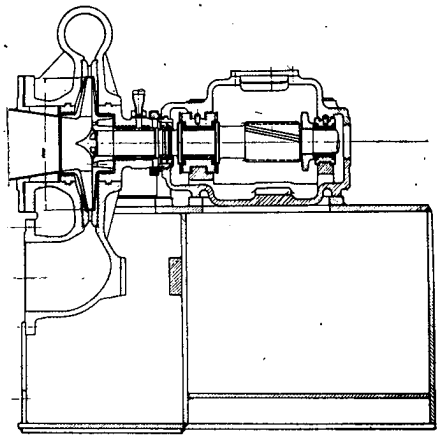

Fig. 3. Inward radial flow reaction turbine with a one-exit-wheel.

A bearing with a damping device as it is shown in Fig. 4, secures the dynamic steadiness of the turbine rotor.

The expansion turbine with a wheel which has one exit is simpler. The bearing arrangement of the high-speed shaft of the gear box gives cantilever support of the turbine wheel. To balance the axial forces, the labyrinth glands are usually located on both sides of the wheel at about the same diameter, and several drillings bored through the main wheel disk close to the hub.

Labyrinth glands with sufficiently numerous combs are employed to reduce to 3–4% the refrigerative losses due to the flowing of the gas past the blades. The leakage of cold gas through the labyrinth glands on the shaft is usually less than 1%.

Comparing these two construction types one might have expected the isentropic efficiency of the turbine with a two-exits-wheel to be higher than of that with a one-exit-wheel designed for the same conditions. As experience has shown this difference is not very essential. Thus the manufacture of expansion turbines with a one-exit-wheel is fully justified because of their notable simplicity in construction and reliability in operation.

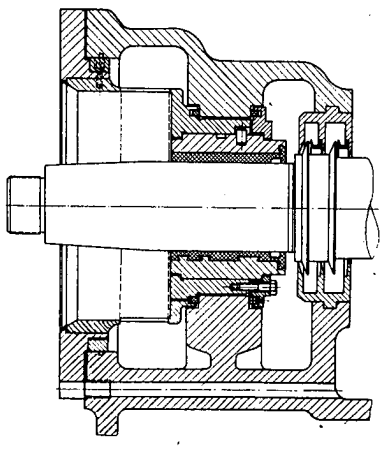

Fig. 4. Elastic damping bearing.

Approved For Release 2009/05/01 : CIA-RDP80T00246A007500340002-0

Approved For Release 2009/05/01 : CIA-RDP80T00246A007500340002-0

The blade arrangement may be of numerous thin blades (in which case half of them are shortened and located only at the entrance) as in our first engines, or it may be of the inverse centrifugal compressor type, and then the blades are not so numerous. The first blade arrangement has a relative pitch, i. e. the ratio of the blade pitch at the wheel entrance to the radial length of the blade $t_1 = \frac{t_1}{r_1 - r_2}$, about $t_1 = 0.12$, the second has a relative pitch about $t_1 = 0.6$.

As to the efficiency both arrangements, as experience has shown, are of equal value, however, from the standpoint of construction, arrangements with less numerous blades are more convenient. In addition theoretical considerations imply that the number of blades of the inward flow expander wheel may be less than that recommended for a centrifugal compressor wheel. That is why at present we produce wheels with a blade pitch of about $t_1 = 0.6$.

The investigations performed have shown that in most cases the least energy losses are peculiar to those constructions where the inlet angle of the wheel blade is 90°.

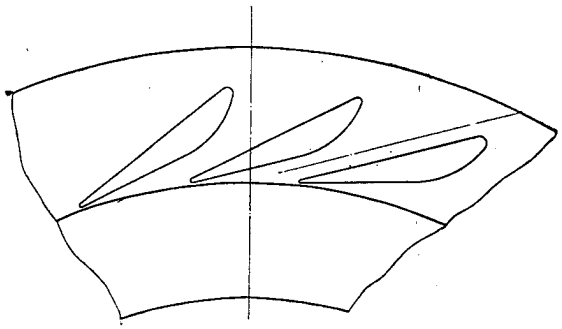

Fig. 5. Nozzle arrangement.

The stationary nozzles are shaped approximately like those shown in Fig. 5. The nozzle angle is usually 14–20°. The velocity factor for nozzles of this type, that is the ratio of the actual discharge velocity C_1 to the isentropic discharge velocity is $\Phi = 0.96 - 0.975$ if the discharge velocity is close to the sonic, i. e. at $\frac{C_1}{a_{cr.}} = 1$. If the $\frac{C_1}{a_{cr.}}$ ratio decreases Φ is lowered, that means that the losses through the nozzles increase. The negative influence of the section in the nozzles may chiefly account for this.

Calculating the stationary nozzles for a low-temperature expansion turbine one should take into account the deviations of real gas from the ideal gas laws by introducing the factor for the supercompressibility of gases $Z = \frac{PV}{RT}$. This factor is considered to be constant in the course of expansion of the gas in the nozzles.

Reaction expansion turbines have no devices to control the capacity. Therefore the oxygen plants have two identical turbines. During the starting period both of them are in operation. At liquefying conditions one of them operates and the other remains in reserve. Sometimes it is necessary to change the nozzle box, for instance, one set is designed for winter conditions and the other for summer. However, the design of a controllable reaction expansion turbine is also possible. Preliminary experimental data have shown that it is possible to control the capacity over a relatively wide range, the efficiency being lowered comparatively little.

Besides the design of controllable turbines, our task is to develop radial expansion turbines with two or even more expansion stages.

Behrndt bogtryk, Denmark

Copyright reserved

Approved For Release 2009/05/01 : CIA-RDP80T00246A007500340002-0

Approved For Release 2009/05/01 : CIA-RDP80T00246A007500340002-0

The Main Trend in the Designing of Large Gaseous Oxygen Plants

Les tendances principales dans la construction de grandes installations pour oxygène gazeux

G. M. BARANOV, Director
The U.S.S.R. Scientific Research Institute of Oxygen Machine-Building, Moscow. U.S.S.R.

SOMMAIRE. Les grandes installations modernes pour la production d'oxygène gazeux sont toutes basées sur le principe de basse pression en utilisant des turbomachines. Le travail sur le développement d'appareils pour la rectification de l'air fut commencé dans l'Union soviétique après 1940 sous la direction de l'Académicien P. L. Kapitsa en se basant sur sa turbine à expansion hautement effective.

A la suite de vastes recherches et du travail expérimental exécuté à VNIIKiMash un certain nombre d'installations furent construites dont les capacités variaient entre 3600 et 15000 m³/hr d'oxygène gazeux.

Dans le rapport le circuit de telles installations est examiné et des solutions concrètes sont présentées en ce qui concerne les problèmes techniques qui se posent à la suite de la nouveauté des projets et des grandes dimensions des installations.

La construction des colonnes de rectification et des évaporateurs-condenseurs à long tube est montrée. La solution des principaux problèmes de construction se rapportant au drainage de l'air de vapeur d'eau et d'anhydride carbonique est discutée. Le gel du régénérateur est empêché par un régénérateur d'azote supplémentaire avec bourrage ordinaire. La méthode pour dégeler des unités à basse pression est décrite.

L'expérience acquise pendant l'opération des installations à grande échelle a démontré que la construction proposée assure leur opération sans devoir dégeler pendant des périodes allant jusque deux ans.

The main current trend in the development of technological processes for the production of gaseous oxygen rests on the low pressure principle utilizing turbomachines.

All relatively large plants were built until late on a two-pressure cycle. The introduction of high pressure made it possible to remove from the regenerators by a reverse flow the moisture and carbon dioxide that remained on the packing after the direct air flow. The high pressure provided also the production of the greater part of refrigeration. The so-called rectification process reserves available in these plants were also used for the production of refrigeration by expanding in the expansion turbine a part of the nitrogen taken from under the condenser cover.

Plants, operating in two-pressure cycle, are sufficiently reliable and maneuvrable but complex in their equipment and in operation due to the presence of high pressure air, piston compressors, equipment for the chemical purification of air of carbon dioxide and an ammonia refrigerating system.

To eliminate the high pressure and to operate with only low pressures it was necessary to design a highly efficient expansion turbine that would allow to compensate refrigeration losses with a minimum worsening of the rectification process. It was also necessaryto develop a system of heat exchanging devices for freezing out the moisture and carbon dioxide present in the air and their subsequent complete removal by a reverse flow.

P. L. Kapitsa suggested in 1939–1940 a new highly efficient type of expansion turbine – a reactive radial type turbine. The new machine proved to be reliable in opetation and to have an efficiency of over 80%.

Approved For Release 2009/05/01 : CIA-RDP80T00246A007500340002-0

Approved For Release 2009/05/01 : CIA-RDP80T00246A007500340002-0

Work was started simultaneously under the guidance of P. L. Kapitsa on the development of the first air separating plants operating only with low presssures. This work actually laid the foundation for modern methods of producing large amounts of gaseous oxygen. However, no method was found at that time able to provide continuous operation of the plants for a long period.

Heat-exchange devices, designed in the USA in the form of regenerators – recuperators with an unbalanced flow, are very complex to manufacture and not efficient enough (due to a large resistance and a high temperature difference on the warm end of the regenerator).

Further investigations resulted in the development of a more simple in design and reliable method of purifying air of water vapour and carbon dioxide with clogging of the regenerators eliminated. The problem was solved by including an additional nitrogen regenerator with ordinary packing in the layout.

The essence of this solution can be demonstrated by comparing it with the method providing non-clogging of the regenerators in two-pressure plants.

Conditions providing prolonged operation of the regenerators of two-pressure installations without being clogged with carbon dioxide are created, as is known, due to a surplus (by 3 to 4%) amount of the reverse flow. This part of the reverse flow is provided by high pressure air purified of carbon dioxide and water vapour in special apparatus. Thus, in regenerators, packed with discs of corrugated aluminium band heat-exchange conditions are obtained providing, during the period of cold blowing, a complete sublimation of all the admixtures remaining on the packing after the air has passed and their removal from the regenerators.

A surplus reverse flow is also used in oxygen regenerators of low-pressure plants. In nitrogen regenerators the relation of the reverse flow to the direct one becomes in this case even less than unity. The conditions of heat-exchange in nitrogen regenerators under which the air is cooled to a state of dry saturated vapour with the accumulation of carbon dioxide in the ports of the packing eliminated are created by providing an unbalanced so-called "loop" flow. This flow allows transfer of part of the heat load of the nitrogen regenerators to the nitrogen subcooler and heater thus reducing the temperature difference at the cold end of the regenerators and facilitating the sublimation of the carbon dioxide remaining on the packing after the warm flow and its removal by the nitrogen.

A specific feature of this solution, as it has been mentioned, is the unbalanced flow provided by the installation of a third nitrogen regenerator.

The sequence of the flows through each nitrogen regenerators is as follows:

1. air is passed in a direct flow and cooled while the moisture and carbon dioxide, present in the air, precipitate on the cold packing;
2. nitrogen is passed cooling the packing and removing the deposited impurities;
3. a flow of air (a "loop" flow) is passed in the same direction as nitrogen and additionally cools the packing in the lower (cold) part of the regenerator and

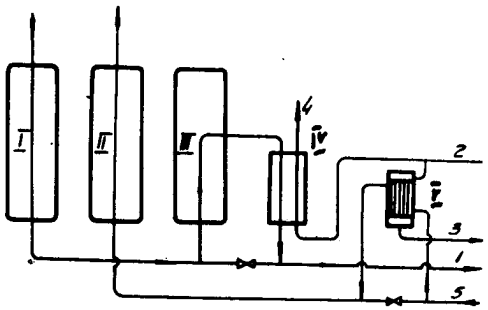

Fig. 1. Diagram of unbalanced flow provision system. I, II, III-nitrogen regenerators; IV-heat exchanger for air passing to turbine; V-nitrogen heater. Direction of flows – 1. Air to lower column; 2. Air from lower column; 3. Liquid air to lower column; 4. Air to expansion turbine; 5. Nitrogen from subcooler.

Approved For Release 2009/05/01 : CIA-RDP80T00246A007500340002-0

Approved For Release 2009/05/01 : CIA-RDP80T00246A007500340002-0

is then dicharged at 160–180°K through special valves from the middle part of the regenerator.

The flows are passed through the other nitrogen regenerators in the same succession and while a direct flow of air passes through the first (Fig. 1) regenerator, nitrogen flows through the second and the "loop" air flow is run through the third one.

The mean temperature difference at the cold end of the regenerators is maintained within 5 to 6°C by changing the heat load of the nitrogen heater as well as the amount of "loop" air.

Thus the purification of the entire amount of air, supplied for separation, of moisture and carbon dioxide is performed in the regenerators.

An additional purification of the unbalanced flow, which is required in the case of a disturbance of temperature conditions in the regenerators, is performed as this flow is cooled in a heat-exchanger by means of a heat exchange with the air passing from the lower column to the turbine.

The detaining of the carbon dioxide crystals carried along by the air from the regenerators or heat-exchanger as well as the reduction of acetylene content in the air flow passing through the expansion turbine is provided by washing the air on three washing plates arranged in the lower part of the lower column.

By applying the above new solutions on the expansion turbine design and the prevention of clogging of the regenerators, a technological process was elaborated which constituted the basis of a number of low pressure air separating units with capacities of from 3,600 to 12,500 – 15,000 norm. m^3/hr of gaseous oxygen. The largest air separating unit with a nominal capacity of 12,500 norm. m^3/hr of tonnage oxygen is manufactured on a serial scale. The first experimental unit has been in operation since 1956 and worked for the first two years without stopping.

According to the data of tests the specific power consumption was from 0.43 to 0.45 kW·hr per norm. m^3 of oxygen at a nominal capacity of 12,500 norm. m^3/hr (at 20°C and 760 mm Hg) when operating without the krypton and pure oxygen block and at a value of isothermal efficiency of the turbo-compressor amounting to 60%.

The schematic technological diagram of the part of this unit connected with the production of tonnage oxygen is given in Fig. 2.

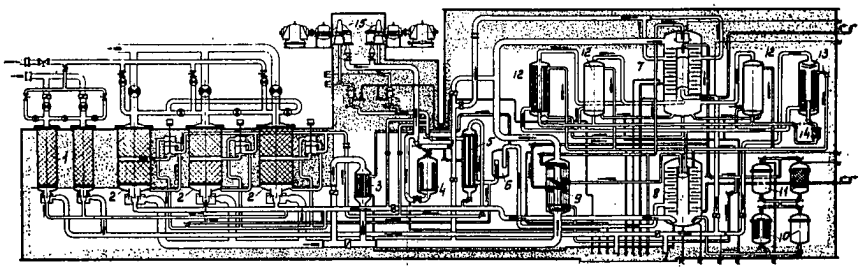

Fig. 2. Flow diagram of a 12,500 m^3/hr oxygen plant. 1. Oxygen regenerator; 2. Nitrogen regenerator; 3. Heat exchanger – nitrogen heater; 4. Acetylene adsorber; 5. Heat exchanger for air passing to turbine; 6. Liquid separator; 7. Upper rectification column; 8. Lower rectification column; 9. Liquid nitrogen and air subcooler; 10. Carbon dioxide filter; 11. Acetylene adsorber; 12. Condenser; 13. Condenser-evaporator of produce oxygen; 14. Acetylene adsorber; 15. Expansion turbine unit.

The main air separation block may be equipped, if necessary, with additional equipment for the production of primary krypton concentrate and the required amount of pure oxygen (99.5% O_2). Fig. 3 illustrates the flow diagram for obtaining these products of air separation.

Additional equipment is installed in some cases for the production of a certain amount of pure nitrogen.

Approved For Release 2009/05/01 : CIA-RDP80T00246A007500340002-0

Approved For Release 2009/05/01 : CIA-RDP80T00246A007500340002-0

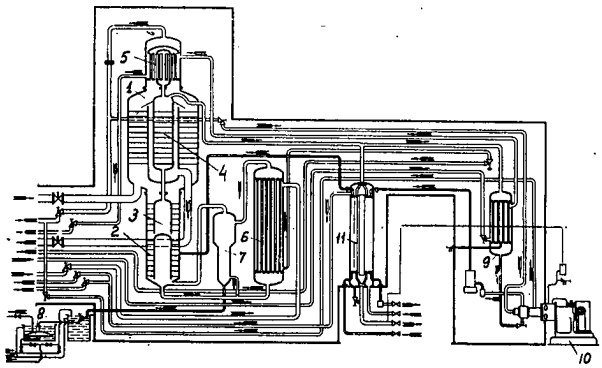

Fig. 3. Flow diagram of additional equipment for the production of krypton and pure oxygen. 1. Concentration part of krypton column; 2. Distilling part of krypton column; 3. Pure oxygen column; 4. Column for washing pure oxygen of krypton; 5. Krypton column upper condenser; 6. Condenser-evaporator; 7. Liquid separator; 8. Krypton concentrate evaporator; 9. Pure oxygen condenser-subcooler; 10. Liquid oxygen pump; 11. Pure oxygen heat exchanger.

A respective amount of air is taken from the upper part of the regenerator during the "loop" flow of air for heat exchange with the primary krypton concentrate and pure oxygen or nitrogen.

In designing a plant of a capacity mentioned above, new engineering solutions were required for the condensers, rectification column, insulation and other elements of the unit as the existing solutions were unfit or caused serious complications in operation.

As a result of investigating various models, a condenser was selected with the oxygen boiling inside the pipes and nitrogen condensing in the interpipe space. The application of this type of condenser made it possible to use considerably longer (up to 3 metres) pipes without any essential increase of the hydrostatic temperature depression and to provide the necessary surface with a considerably smaller number of pipes at a relatively small diameter of the shell. A change of the character of the load on the tube sheet caused by the transfer of the oxygen boiling process inside the pipes, made it possible to reduce the thickness of the tube sheet by three times and to simplify the construction of the condenser in general.

One of the main factors limiting the possibility of having the upper and lower columns each as a single apparatus was too large a load upon the drain device. After experimental investigations of the hydraulics of the plates, a double-drain meshed circular plate was developed which considerably reduced the load upon the drain device. This type of plates allowed to increase by 1.5 times the velocity of the vapour flow in the columns almost without any increase of resistance and, consequently, to considerably reduce the dimensions and weight of the apparatus per unit of processed air as well as to design the columns in the form of one apparatus each.

A decrease of the load upon the drain device allowed to provide also reliable and efficient operation of the rectification columns within a wide range of capacity variations (the ratio of the maximum capacity to the minimum amounting to 2).

Unlike the ordinary method of insulating apparatus located inside a shell by filling the entire inner space with insulating material, large units were made jacketed with insulating material only between the walls of the jacket. This method of insulation reduces the insulating material requirements and the apparatus and lines become accessible for assembly, repairs and inspection without the removal of the slag wool. Besides, the duration of the starting period is reduced. This is why the above method of insulation was considered most rational for large units notwithstanding the somewhat greater losses into the surrounding medium.

Approved For Release 2009/05/01 : CIA-RDP80T00246A007500340002-0

Approved For Release 2009/05/01 : CIA-RDP80T00246A007500340002-0

With the flow of high pressure air purified of moisture and carbon dioxide excluded from the layout a new defrosting system of the plant was required. The plant is defrosted by air that had been passed through the regenerators and heated up to 20 –30° C. in a special heater. The heated air is distributed among the apparatus of the separation block to be defrosted and then passed in a reverse flow through the regenerators. With such an arrangement of the flows the regenerators are the coldest apparatus throughout the entire defrostation time. Thus, during this process all impurities accumulated in the apparatus in the course of their operation are removed.

An increase in the size of the plants required a new solution of the problem of control. For most efficient operation the plants are equipped with recording control and measuring instruments and remote control devices. The latter are mounted on all the main pipelines thereby allowing more convenient arrangement of the apparatus and simplification of the lines. The remote control is performed from the central panel.

A system of automatic devices is being introduced at present that will make it possible to automatically maintain preset operating conditions without any interference of an operator.

A complex automatic system is being developed for the solution of a larger problem of automatically setting and maintaining the operating conditions in accordance with the load.

The main engineering solutions described above and tested on plants already manufactured are used as the basis for developing still larger oxygen plants and units for complex separation of air.

Behrndt bogtryk, Denmark

Copyright reserved

Approved For Release 2009/05/01 : CIA-RDP80T00246A007500340002-0